# Effects of human disturbance and human-made barriers on the behaviour, physiology, and genetic structure of painted turtle populations

Audrey Turcotte

Supervisors: Gabriel Blouin-Demers and Dany Garant

Committee Members: Vincent Careau and Lenore Fahrig

Examiners: Julien Martin (Internal) and Stéphanie Doucet (External)

Thesis submitted in partial fulfillment of the requirements

for the Doctorate in Philosophy degree in the

Ottawa-Carleton Institute of Biology

Department of Biology

Faculty of Science

University of Ottawa

*«Je suis tanné d'être un adulte, je suis pas bon, comme»*

- Tom Noël (Guillaume Lambert), L'âge adulte


*«YODO»*

- Françoise Doyon-Morin

# Abstract

Human activities, such as urban expansion, have led to an increase in contacts between humans and wildlife and have resulted in the loss and isolation of suitable habitats for animal populations. These human-induced pressures threaten the persistence of animal populations and understanding how animals respond to them is crucial for conservation. A multidisciplinary approach that includes different biological components of a species, such as behaviour, physiology, and population genetic structure, is necessary to obtain a comprehensive insight into the impact of human activities on wildlife. Turtle populations are particularly vulnerable to human disturbance due to their life-histories, but there is limited information available on how human-induced perturbations affect different components of their biology. In this context, my thesis aims to evaluate the impact of human disturbance and human-made barriers on the behaviour, physiology, and genetic structure of painted turtles (*Chrysemys picta*) in the Rideau Canal, Ontario, Canada. In chapter one, I evaluate the relationship between risk-taking behaviours and human disturbance levels. In chapter two, I assess the impact of human disturbance on the relationships between risk-taking behaviours, physiological response, and colouration. Finally, in chapter three I characterize the genetic structure of painted turtles in the Rideau Canal and assess the impact of human-made barriers, such as locks, on the genetic substructuring occurring in the system. Overall, I show that human activities and human-made barriers have several impacts on painted turtle biology, from influencing their risk-taking behaviours to inducing physiological changes and causing genetic discontinuities among groups. More specifically, in chapter one, I show that painted turtles are consistent in their risk-taking behaviour and that turtles located in areas with more boat activities are more prone to take risks, suggesting that being risk-prone may be associated with a greater tolerance to human disturbance. I also show that painted turtles exhibit a lower physiological response when human activity is limited, indicating that human activities may induce physiological costs on wildlife. In

addition, I report variations in physiological responsiveness according to the propensity of turtles to take risks, where risk-prone males have higher physiological responses than risk-averse males, highlighting the importance to use different disciplines to better understand the consequences of human activities and how the different biological components interact together under human-induced pressures. Finally, I found genetic substructuring among groups of turtles within the Rideau Canal, which seems to be partly caused by locks, especially when they are numerous and clustered in space. My results provide a better understanding of the impact of human disturbance on animal populations as well as information that could be used to better guide management decisions that are relevant to species vulnerable to human activities, such as turtles. Monitoring animal behaviour alongside physiological biomarkers and genetic populational trends can aid in the development of better adapted conservation strategies.

# Résumé

Les activités humaines, telle que l'expansion urbaine, ont entraîné une augmentation des contacts entre les humains et la faune, ainsi que la perte et l'isolement d'habitats naturels pour les populations animales. Ces pressions induites par les humains menacent la persistance des populations animales et il est donc essentiel pour la conservation de comprendre comment les animaux réagissent à ces pressions. Une approche multidisciplinaire incluant différentes composantes biologiques d'une espèce, telles que le comportement, la physiologie et la structure génétique des populations, est nécessaire pour obtenir un aperçu global de l'impact des activités humaines sur la faune. Les populations de tortues sont particulièrement vulnérables aux perturbations humaines en raison de leurs traits d'histoire de vie, mais il existe peu d'informations sur la façon dont les perturbations humaines affectent les différentes composantes de leur biologie. Dans ce contexte, ma thèse vise à évaluer l'impact des perturbations et infrastructures humaines sur le comportement, la physiologie et la structure génétique des populations de tortues peintes (*Chrysemys picta*) dans le canal Rideau, Ontario, Canada. Dans le premier chapitre, j'évalue la relation entre les comportements associés à la prise de risque et la variation spatiale des activités humaines. Dans le deuxième chapitre, j'évalue l'impact des perturbations humaines sur les relations entre les comportements associés à la prise de risque, la réponse physiologique et la coloration. Dans le chapitre trois, je caractérise la structure génétique des groupes de tortues peintes du canal Rideau et évalue l'impact des barrières artificielles, telles que les écluses, sur la sous-structuration génétique présente dans le système. Dans cette thèse, je montre que les activités humaines et les barrières construites par les humains ont un impact sur la biologie des tortues peintes, en influençant leurs comportements associés à la prise de risque, en induisant des changements physiologiques et en provoquant de la sous-structuration génétique entre les groupes de tortues. Plus précisément, dans le premier chapitre, je montre que les tortues peintes sont cohérentes dans leur capacité à prendre des

risques: les tortues situées dans des zones où les activités nautiques sont plus importantes prennent plus de risques, ce qui suggère que le fait d'être enclin à prendre des risques peut possiblement aider à mieux tolérer les perturbations humaines. Je montre également que les tortues peintes présentent une réponse physiologique plus faible lorsque l'activité humaine est limitée, ce qui indique que l'activité humaine peut infliger des pressions physiologiques sur la faune. De plus, j'observe des variations de la réactivité physiologique en fonction de la propension des tortues à prendre des risques, les mâles prenant plus de risques ont des réponses physiologiques plus élevées que les mâles qui en prennent moins, ce qui souligne l'importance d'utiliser différentes disciplines pour mieux comprendre l'impact des activités humaines sur la faune et d'identifier comment les différentes composantes biologiques interagissent ensemble sous pression humaine. Enfin, j'ai montré de la sous-structuration génétique entre les groupes de tortues du canal Rideau qui semble être principalement causée par le nombre d'écluses, en particulier lorsqu'elles sont nombreuses et regroupées dans l'espace. Mes résultats amènent une meilleure compréhension de l'impact des perturbations humaines sur les populations animales, ainsi que des informations qui pourraient être utilisées afin de mieux orienter les décisions de gestion concernant les espèces vulnérables à l'activité humaine, telles que les tortues. Le suivi du comportement des animaux, de biomarqueurs physiologiques et des tendances génétiques des populations peut aider au développement de stratégies de conservation mieux adaptées.

# Preface

My thesis consists of three stand-alone manuscripts that are already published, or will be submitted soon, in peer-reviewed journals. Each chapter represents my own work, which means that I led the conceptualization, conducted the data collection and statistical analyses, interpreted the results, created all figures and tables, and wrote the content. However, all manuscripts were prepared in collaboration with other researchers whose contribution was sufficient to merit authorship with their guidance, support, and advice. Thus, I used the term "We" instead of "I" throughout the chapters to consider their contribution as it was employed in the published versions. I slightly modified each manuscript to uniformize the thesis and to better integrate figures, tables, and all supporting documents. However, slight variations in the format can occur among chapters given that they follow the criteria of the journal where they were or will be published. Publication details are available at the beginning of each chapter for the manuscripts already published.

During my PhD studies, I also led and contributed to the peer-reviewed publication of two manuscripts that are not directly related to my thesis:

Bergman, J. N., Beaudoin, C., Mistry, I., **Turcotte, A.**, Vis, C., Minelga, V., Neigel, K. L., Lin, H.-Y., Bennett, J. R., Young, N., Rennie, C., Trottier, L. L., Abrams, A. E. I., Beaupre, P., Glassman, D., Blouin-Demers, G., Garant, D., Donaldson, L., Vermaire, J., … Cooke, S. J. (2021). Historical, contemporary, and future perspectives on a coupled social-ecological system in a changing world: Canada's historic Rideau Canal. *Environmental Reviews*, *16*, 1–16. https://doi.org/10.1139/er-2021-0026

**Turcotte, A.**, Kermany, N., Foster, S., Proctor, C. A., Gilmour, S. M., Doria, M., Sebes, J., Whitton, J., Cooke, S. J., & Bennett, J. R. (2021). Fixing the Canadian Species at Risk Act: Identifying major

issues and recommendations for increasing accountability and efficiency. *FACETS*, *6*, 1474–1494.

https://doi.org/10.1139/facets-2020-0064

# Acknowledgements

Le doctorat est un long périple sinueux composé de nombreuses vallées et de sommets. De nombreuses personnes, au cours de cette aventure qui marque une vie, m'ont aidée à rendre cette expédition beaucoup plus agréable et à atteindre le point d'arrivée sans trop d'embuches. Je voudrais tout d'abord remercier mes deux superviseurs, Gabriel Blouin-Demers et Dany Garant, pour leur soutien inestimable, leur supervision tout en douceur et leur disponibilité presque 24/7. Dany, c'est en grande partie grâce à toi et aux nombreuses opportunités que tu as mises sur mon chemin que je suis la scientifique que je suis aujourd'hui. C'est 10 ans plus tard que je quitte le laboratoire Garant après avoir eu la chance d'y faire un stage COOP dans le cadre de mon baccalauréat en 2013. Ta vision et rigueur scientifique me suivront dans mon parcours professionnel. C'est maintenant le temps de voler de mes propres ailes, comme les grands sages disent, mais ta présence va me manquer sans aucun doute! Gabriel, je ne serais pas mieux tombée avec toi comme superviseur pour cette folie qu'est le doctorat. Tu es une grande source d'inspiration pour moi avec ta capacité de maintenir un bel équilibre de vie tout en produisant de la recherche de qualité et en étant grandement disponible pour tes étudiants. J'ai développé au cours des dernières années de nombreuses compétences que je ne pense pas que j'aurais développées sous la supervision de quiconque. En espérant que le futur nous réserve quelques cafés à Chelsea! Je voudrais aussi remercier les membres de mon comité, Lenore Fahrig et Vincent Careau qui m'ont fait de nombreux commentaires constructifs tout au long de mon parcours.

Je ne pourrai jamais assez remercier Carolyne Houle qui m'a aidée et soutenue dans plusieurs aspects de ma thèse allant de l'optimisation des analyses génétiques, à l'analyse des photos pour la coloration (je vais encore te remercier sur mon lit de mort pour ça), et l'aide avec la collecte de données. Un moteur brisé sans toi ce n'est pas la même chose! Un énorme merci à Dominique Lavoie, Max Henry-Adams, Raphaël Siegel, Amélie Lessard et Manon Veselovsky qui m'ont endurée et aidée lors

de la collecte de données, mais particulièrement à Catherine Čapkun-Huot qui m'a été d'un soutien inestimable lors de ma première année de terrain: je n'aurais pas voulu soulever une chaloupe à bout de bras sous la pluie et prendre de mauvaises décisions avec personne d'autre. Je me considère très chanceuse d'avoir une personne aussi brillante dans ma vie (et merci d'avoir mis Jérôme Gosselin-Tapp sur mon chemin, une des personnes qui me fait le plus rire sur la Terre!) Merci à la station biologique de Queen's University et ses employés pour le support logistique lors de tous les travaux de terrain effectués à leurs installations.

Je voudrais remercier tous mes amis et partenaires de laboratoire qui ont été là de proche ou de loin à quelconques moments de mon parcours. Un merci particulier aux étudiants du laboratoire Garant qui m'ont toujours fait sentir incluse et comme à la maison. Un immense merci à ma deuxième famille, Françoise Doyon-Morin, Nicolas Vigneau-Roy et Whisky qui m'ont accueilli chez eux lorsque je faisais mes analyses de laboratoire à l'Université de Sherbrooke. Les séjours au domaine de la Mont-Plaisant font partie des plus beaux moments de mon doctorat. Merci à Julien F. Guertin qui est toujours à mes côtés en me comprenant comme s'il m'avait tricotée, et ce, depuis qu'il est en couche-culotte! La dernière année du doctorat n'aurait pas été aussi facile sans la présence de Maxime Fraser Franco et Marie-Ève Labonté-Dupras qui ont toujours été partants pour faire des séances de travail. Les congrès ne sont pas que des opportunités de partage scientifique, mais aussi de belles rencontres qui marquent une vie! Je tiens aussi à remercier ma famille qui m'a toujours encouragée à foncer dans les projets qui me tiennent à cœur, mais surtout, à Laurent Fafard-Couture, mon copain qui a été mon pilier tout le long de mon doctorat. Sans ton soutien inestimable, je n'aurais possiblement pas eu le courage de me lancer dans cette aventure.

La réalisation de ce projet n'aurait pas été possible sans l'aide financière du Conseil de recherches en sciences naturelles et en génie du Canada, Parcs Canada et Ottawa Field-Naturalists. Un merci

# Table of Contents

# List of Tables

# List of Figures

# General Introduction

Over the last several decades, contacts between humans and wildlife have increased in part because of the expansion of human activities (e.g., urban expansion) (Barnosky et al., 2012; Foley et al., 2005; Kennedy et al., 2019; Larson et al., 2016; Steven et al., 2011). These activities have often led to the loss and isolation of suitable habitats for animal populations (Haddad et al., 2015; Su et al., 2021; WWF, 2022). As a result, many animals are now living in highly human-impacted landscapes and subjected to growing human-induced pressures that threaten their persistence (Dirzo et al., 2014; Kennedy et al., 2019; McCauley et al., 2015; WWF, 2022). Given that human disturbance is one of the main causes of biodiversity decline worldwide, it is becoming crucial to understand how animals are affected by and respond to these perturbations (WWF, 2022). However, understanding animal responses to human disturbance can be complex given the different types of perturbations that can vary spatially both in intensity and in predictability (Gaynor et al., 2018; Larson et al., 2016; Nickel et al., 2020; Tablado & Jenni, 2017; Tucker et al., 2018). In addition, different components of an animal's biology may interact together and may be simultaneously affected by human-induced perturbations making it difficult to have a complete overview of the consequences on wildlife (Walls & Gabor, 2019). Using a multidisciplinary approach that incorporates behaviour, physiology, and population trends (e.g., genetic dynamics) is thus needed to obtain a global insight of how human activities affect animal communities (Anthony & Blumstein, 2000; Muposhi et al., 2017; Tobias & Pigot, 2019). More specifically, identifying how animals behaviourally and physiologically respond to human disturbance can give us an overview of the short-term consequences on animal populations, while the long-term effects can be perceived on the population dynamic, which can be evaluated with landscape genetic analyses.

Animals exposed to human disturbance can, as a first response, alter their behaviours in the short term to improve their probability of surviving and reproducing (Tuomainen & Candolin, 2011).

Although individuals may have the capacity to adjust their behaviours to their environment, individuals within a population may show consistent differences in the way they perceive and respond to risky situations (Koolhaas et al., 1999; Tuomainen & Candolin, 2011). Regardless of context, some individuals are consistently more prone to take risks (i.e., proactive) while others minimize their exposure to risky situations (i.e., reactive) (Koolhaas et al., 1999; Réale et al., 2007; Sih, 2004). Over time, this consistent variability in risk-taking propensity among individuals may lead to changes in the dynamics of animal populations exposed to human disturbance (Tuomainen & Candolin, 2011; Wong & Candolin, 2015). These new environmental conditions can then i) cause plastic changes in behavioural responses (Caspi et al., 2022; Vincze et al., 2016), ii) lead individuals to preferentially select habitats according to their behaviours (Cote et al., 2010; Holtmann, Santos, et al., 2017; Jacob et al., 2015), and/or iii) alter selection pressures which could favour specific behaviours (Miranda et al., 2013; Mueller et al., 2013; Sih et al., 2011). Regardless of the mechanisms, behavioural differences should be observed among habitats varying in levels of human disturbance where risk-prone individuals should be more frequent in areas highly disturbed by human activities (Breck et al., 2019; Hardman & Dalesman, 2018; Holtmann, Santos, et al., 2017; Sprau & Dingemanse, 2017).

Human disturbance also triggers the release of stress hormones, such as glucocorticoids, causing the activation of physiological processes and allowing the mobilization of energetic resources that are necessary to maintain homeostasis and to improve immediate survival probability (Buchanan, 2000; Sapolsky et al., 2000; Wingfield et al., 1997). Since human-induced perturbations generally persist over time, they often result in chronic and maladaptive physiological responses that can alter other important biological processes (e.g., immune activities and carotenoid-based colouration). Such prolonged physiological responses can be measured using the heterophil-to-lymphocyte ratio (H/L ratio), which is generally higher in animals exposed to high levels of human activities (Davis et al., 2008). When

individuals face challenging conditions, trade-offs can occur between biological functions that rely on limited resources to operate (Stearns, 1989; Zera & Harshman, 2001). For instance, this is the case for carotenoid pigments: individuals may allocate them to essential physiological functions (e.g., immune functions and antioxidant activity) at the expense of colour signalling (Aguilera & Amat, 2007; Blount et al., 2003; Faivre et al., 2003; Mcgraw, 2005). The magnitude of these trade-offs can vary between individuals according to the way they perceive and react to stressful events (Réale et al., 2010). Human activities can thus have physiological consequences that can threaten animal survival and reproductive success, and jeopardize the persistence of populations (Acevedo-Whitehouse & Duffus, 2009; Martin, 2009).

By increasing and expanding their presence on the landscape, humans create new barriers that isolate suitable habitats for wildlife: animal populations that were previously connected are now isolated in smaller habitat fragments (Haddad et al., 2015; Su et al., 2021). By restricting animal movements and thus gene flow in the landscape, human-made barriers can result in : i) the loss of genetic diversity within isolated populations and ii) the increase of genetic differentiation among isolated populations (Schlaepfer et al., 2018; Schmidt et al., 2020). Over time, with the loss and the limited exchange of favourable alleles (Lenormand, 2002; Morjan & Rieseberg, 2004), these effects may reduce population persistence in face of environmental perturbations (Leigh et al., 2019; Reed & Frankham, 2003; Willi et al., 2006). By providing insights on the dispersal events that led to successful reproduction, genetic data can inform us about the past landscape changes that impeded or improved dispersal and, thus, inform us about the functional connectivity of the landscape (Landguth et al., 2010; Lowe & Allendorf, 2010). Landscape genetics modelling is an interesting tool that can be used in conservation to determine how genetic differentiation is related to landscape features, such as human-made structures, and to identify which barriers are related to the genetic structure observed in the populations studied

(Holderegger & Wagner, 2008; Manel et al., 2003).

Turtles are one of the most threatened taxa, with more than half of the species now facing high extinction risk (Stanford et al., 2020). Under high anthropogenic pressures, turtle resilience is limited by their life-histories (e.g., delayed maturity, high longevity, low juvenile survival) that make them more vulnerable to additional mortality induced by human activities (Brooks et al., 1991; Congdon et al., 2003; Gibbons, 1987; Midwood et al., 2015). Compared to other taxa, scant information is available on how human-induced perturbations impact turtle behaviour and physiology, as well as the genetic structure of their populations, which is surprising considering the major roles they play in terrestrial and aquatic ecosystems (e.g., bioturbation, seed dispersal, carbon storage, mineral cycling) (Lovich et al., 2018). There is thus a need for more studies documenting how human disturbance affects different aspects of turtle biology (see examples: Bennett et al., 2010; Selman et al., 2013).

My thesis aims to provide an in-depth understanding of the impact of human disturbance and human-made barriers on painted turtles (*Chrysemys picta*) by assessing i) how human activities are related to turtles' propensity to take risks; ii) how human activities influence the relationships between physiological response, carotenoid-based colouration, and risk-taking behaviours; and iii) how human-made barriers, such as locks, affect the genetic structure of painted turtles living in the Rideau Canal, Ontario, Canada. My results will provide a more global view of the effects of human activities and human-made barriers on a species especially vulnerable to human disturbance, which could help guide management decisions and develop better adapted conservation plans for this species and others facing similar threats.

The Rideau Canal is a 202-km slackwater canal system (i.e., locks built above pre-canal water levels) that connects the Ottawa River to Lake Ontario. This waterway is composed of a network of

rivers, lakes, and excavated channels that are connected by 23 lockstations (45 locks). The construction of the Rideau Canal started at the beginning of the 19th century (e.g., between 1826 and 1832) with the objective to create a military supply route to facilitate the protection of British colonies against the United States (Tulloch, 1981). Since its opening approximately 200 years ago, the canal never stopped being operated, but it was never used for its original military purpose. The canal has been mainly used for recreational activities with over 40,000 vessel crossings recorded at lockstations each year (Parks Canada, 2006). Therefore, the Rideau Canal is an excellent study system to evaluate simultaneously the impact of human activities and human-made barriers on different biological components of a species.

In chapter one, I hypothesized that risk-taking behaviours in painted turtles were related to the level of human disturbance in the environment. To test this hypothesis, I took repeated measurements of three risk-taking behaviours: i) the sum of active defensive behaviours used during handling, ii) the escape latency, and iii) the emergence of the turtle from the water after escaping. Then, I assessed i) the consistency of these behaviours within individuals and ii) how these behaviours were related to the extent of human disturbance occurring in the Rideau Canal. The level of human disturbance was quantified at each sampling site using several proxies for boat and other human activities.

In chapter two, I hypothesized that human disturbance created stressful environmental conditions that resulted in greater physiological responses in turtles exposed to these stressors and led to the mobilization of carotenoids at the expense of colouration. Also, individual turtles may have perceived and responded differently to human disturbance, which could have affected i) their physiological response and ii) their capacity to gather carotenoids and, thus, to allocate them to their colouration. To test this hypothesis, I used i) the sum of active defensive behaviours used during handling as the measurement of behavioural responsiveness to human presence, ii) the H/L ratio as the measure of the prolonged physiological response to stressors, and iii) the proportion of yellow on the turtle's head and

red on the turtle's neck as the measurements of colouration. Then, I assessed how recreational boating influenced the relationships between these different biological components with structural equation modelling.

In chapter three, I hypothesized that the construction of locks for the Rideau Canal has impeded movements of painted turtles and thus reduced gene flow between populations. I used 13 microsatellite loci to characterize the genetic diversity and genetic structure of painted turtles in the Rideau Canal. Then, I evaluated how landscape features of the Canal, especially the locks, were related to the genetic structuring occurring in the canal and I assessed if specific barriers were responsible for the genetic substructure observed.

# Chapter 1

Effects of human disturbance on risk-taking behaviour in painted turtles

This chapter is a slightly modified version of the manuscript published in *Ethology*:

Turcotte, A., Garant, D., & Blouin-Demers, G. (2023). Effects of human disturbance on risk-taking behavior in painted turtles. Ethology, 129, 406–420. https://doi.org/10.1111/eth.13377

**Abstract**

Animals are exposed to high levels of anthropogenic disturbance, which has profound consequences for population persistence. Individuals can adjust their behaviour plastically when faced with perturbations in their environment and may show consistent differences in the way they perceive and respond to risky situations. Over time, this variability among individuals in response to risk can affect the dynamics of populations exposed to human disturbance. Thus, understanding how animals cope behaviourally with human disturbance is important, especially for species vulnerable to human perturbations, such as turtles. In this context, we evaluated whether risk-taking behaviours are consistent within individual painted turtles (*Chrysemys picta*) and assessed how these behaviours are related to the extent of human disturbance along the Rideau Canal, Ontario, Canada. Specifically, we conducted repeated measurements of the number of active defensive behaviours used during handling and the time taken to escape a floating platform for a total of 730 painted turtles (1117 observations) from 22 sites varying in human disturbance along the canal. We also quantified the emergence of the turtles from the water after escaping the platform. First, individual painted turtles showed consistent differences in all risk-taking behaviours. Second, painted turtles in areas with high boat activity displayed more active defensive behaviours, while turtles from sites in proximity to more houses with access to the canal used fewer. Our study highlights the importance of studying animal behaviour to better understand the impact of human activities on animal populations.

**Introduction**

Human activities impact wildlife in most ecosystems (Barnosky et al., 2012; Ceballos et al., 2015; Foley et al., 2005). In fact, only 5 % of the Earth's terrestrial lands are still untouched (Kennedy et al., 2019). Animals are now exposed to frequent and varied anthropogenic disturbances (e.g., pedestrian/vehicle traffic, outdoor recreation, noise pollution, etc.) that can negatively affect important fitness-related activities (e.g., reproduction and foraging; Larson et al., 2016; Price, 2008; Steven et al., 2011) and thus threaten the persistence of wild populations (Dirzo et al., 2014). Therefore, the ability of animals to adjust to these perturbations is crucial to persist in human-impacted landscapes (Lowry et al., 2013).

To cope with human disturbance, the initial response of animals is often to alter their behaviour (Lowry et al., 2013; Tuomainen & Candolin, 2011; Wong & Candolin, 2015). By adjusting their behaviour to the new conditions prevailing in their environment, animals may improve their probability of surviving and reproducing in the short-term (reviewed in: Lowry et al., 2013; Tuomainen & Candolin, 2011; Wong & Candolin, 2015). For example, animals exposed to frequent human disturbance are more often in vigilance postures, at the expense of other activities (e.g., feeding and sleeping), to assess and respond better to potential threats (Ciuti et al., 2012; McBlain et al., 2020). Changes in activity and feeding patterns to avoid disturbed areas are other common behavioural modifications that help reduce animal exposure to stressful conditions (Tuomainen & Candolin, 2011). For instance, two studies conducted on over 50 species of mammals showed that they are less active, less vagile, and more nocturnal near human disturbance (Gaynor et al., 2018; Tucker et al., 2018). In contrast, some species (e.g., Peregrine falcons *Falco peregrinus*, Kettel et al., 2018; Raccoons *Procyon lotor,* Prange et al., 2003; Eastern chipmunks *Tamias striatus*, Lyons et al., 2017) often thrive in areas with high human density by benefiting from new food resources and reduced predation (Spotswood et al., 2021).

Individuals can adjust their behaviours to their environment and consistent differences in behavioural responses are often present among individuals within a single population (Dingemanse & Wolf, 2010). Many studies showed that individuals differ consistently over time and across contexts in the way they perceive and respond to risky situations by expressing different behaviours, referred to as animal personalities (McDougall et al., 2006; Réale et al., 2007; Sih, 2004). Regardless of context, some individuals are consistently more prone to take risks (i.e., bold) while others minimize their exposure to risky situations (i.e., shy; Koolhaas et al., 1999; McDougall et al., 2006; Réale et al., 2007; Sih, 2004). Therefore, behavioural consistency within individuals may affect how an individual perceives and copes with the changes in its environment (Dingemanse et al., 2004; Sih, 2004).

Among-individual variability in risk-taking propensity can affect the dynamics of populations exposed to human disturbance (Tuomainen & Candolin, 2011; Wong & Candolin, 2015). Environmental changes induced by human activities can alter selection pressures and individuals with specific behaviours can become favored in this new context, therefore shaping the population's behavioural response to human exposure (Miranda et al., 2013; Møller, 2008; Mueller et al., 2013; Sih et al., 2011). Alternatively, individuals can settle preferentially in habitats that better match their capacity to respond to risky situations, allowing them to reduce their stress level and avoid the need for behavioural adjustments (Cote et al., 2010; Holtmann, Santos, et al., 2017; Jacob et al., 2015; Martin & Réale, 2008). Over time, regardless of the underlying mechanism, an increase in interindividual differences in behaviour should be observed among habitats exposed to different intensities of perturbations (Lowry et al., 2013; Tuomainen & Candolin, 2011). Several studies showed that animals living in areas that were highly impacted by human activities differ behaviourally from their conspecifics located in less perturbed regions in that the former use more risk-taking behaviours (see Breck et al., 2019; Hardman & Dalesman, 2018; Holtmann, Santos, et al., 2017). For instance, Great tits (*Parus major*) that are

consistently more prone to take risks are more common in areas with higher human frequentation (Sprau & Dingemanse, 2017). Given that variability in behavioural types could shape population dynamics, it is important to consider interindividual differences in risk-taking propensity when studying adaptation to human disturbance (Sprau & Dingemanse, 2017).

Evidence of how animal behaviour is affected by human activities is accumulating for various taxa (reviewed in: Lowry et al., 2013; Tuomainen & Candolin, 2011; Wong & Candolin, 2015). Early studies mainly focused on mammals and birds, but there is growing interest to study animal behaviour in other taxa, such as turtles. Indeed, the propensity to take risks has been explored in turtles using various behavioural measurements. Diverse measures of latencies (e.g., latency for the head to emerge from the shell, latency to move) following a confinement or a simulated predator attack have been used as proxies for risk-taking propensity in several turtle species (Eastern box turtles *Terrapene carolina*, Carlson & Tetzlaff, 2020; Kashon & Carlson, 2018; Pich et al., 2019; Painted turtles *Chrysemys picta*, Roth et al., 2020; Carter et al., 2016; Spanish terrapins *Mauremys leprosa*, Ibáñez et al., 2013b, 2015, 2018). In particular, Pich et al. (2019) assessed risk-taking propensity in Eastern box turtles by adding the number of active defensive behaviours used during a simulated predator attack. Furthermore, the propensity to surface from the water was used by Allard et al. (2019) to evaluate risk-taking behaviour in Blanding's turtles (*Emydoidea blandingii*) exposed to a simulated predator attack. By taking repeated measurements on individuals, these previous studies established that these behaviours were consistent within individuals, but the influence of human disturbance on these behavioural responses has yet to be assessed. A few studies indicated that turtles from areas highly frequented by humans seem to take more risks (i.e., shorter flight initiation distance to human approach and lower abandonment rate of basking sites after disturbance by boats; Polich & Barazowski, 2016; Selman et al., 2013). Given that turtles were not uniquely identified and not tested multiple times, the authors were unable to determine if the

different behavioural responses expressed toward human disturbance were consistent within turtles (Polich & Barazowski, 2016; Selman et al., 2013).

The scant information on how turtles adjust behaviourally to human disturbance is surprising considering their important ecological roles and that they are among the taxa most vulnerable to human activities (Böhm et al., 2013; Buhlmann et al., 2009; Gibbons et al., 2000; Lovich et al., 2018). In Canada, six out of 10 native freshwater turtles are considered at risk by the Committee on the Status of Endangered Wildlife in Canada (COSEWIC, Species at risk public registry: www.canada.ca/en/environment-climate-change/services/species-risk-public-registry). Freshwater turtles are exposed to human perturbations both on land and in the water. On land, females can be disturbed while nesting (Moore & Seigel, 2006). In the water, recreational boating can perturb important activities, such as basking (Bulté et al., 2020; Moore & Seigel, 2006; Selman et al., 2013). Freshwater turtles can abandon nesting and basking sites for many hours after disturbance by a boat (Bulté et al., 2020; Moore & Seigel, 2006). Loss of basking opportunities can compromise thermoregulation, a critical behavioural mechanism to maintain body temperature in a range that optimizes reproductive success in turtles (Bulté & Blouin-Demers, 2010; Ernst & Lovich, 2009; Jain-Schlaepfer et al., 2017; Rollinson & Brooks, 2007).

In this study, we first determined whether risk-taking behaviours are consistent within individuals and different among individuals in painted turtles by estimating their repeatability. We took repeated measurements of three risk-taking behaviours: i) the sum of active defensive behaviours used during handling, ii) the escape latency, and iii) the emergence of the turtle from the water after escaping. Then, we assessed the relationship between these behaviours and the extent of human disturbance along the Rideau Canal, Ontario, Canada. We quantified the level of human disturbance at each sampling site with several proxies for boat and human activities. We hypothesized that risk-taking behaviours in painted

12

turtles are related to the level of human disturbance in the environment. More specifically, we predicted that individuals located in areas with higher human disturbance should be more prone to take risks. Our study was not designed to assess the mechanisms responsible for the observed relationships, but we offer plausible explanations for our findings.

**Methods**

*Study species and system*

Painted turtles occupy various aquatic habitats (e.g., swamps, marshes, rivers and lakes) and are present in human-impacted habitats (DeCatanzaro & Chow-Fraser, 2010; Ernst & Lovich, 2009). Painted turtles inhabit the Rideau Canal, a 202-km slackwater canal located in southeastern Ontario, Canada, that connects the Ottawa River to Lake Ontario (Figure 1-1a). The Rideau Canal is composed of rivers, lakes, and excavated channels connected by 23 lockstations (Figure 1-1a). The canal is used extensively for recreational boating: there were over 60,000 vessel crossings recorded at lockstations in 2019 (Figure 1-1b), without counting the boaters that used the canal without going through the locks. Therefore, painted turtles are exposed to high levels of disturbance in some sections of the canal. Painted turtles have been assessed as a species of Least Concern by the International Union for Conservation of Nature (van Dijk, 2011), but populations in southeastern Ontario are considered of Special Concern by COSEWIC given their life-history traits (e.g., late sexual maturity, low juvenile survival) that make them vulnerable to the rapid human-induced changes currently occurring in their environment (COSEWIC 2018).

*Sampling sites and turtle captures*

We captured 730 painted turtles with fyke nets from May to August in 2019 and in 2020 at 22 sampling sites distributed approximately every 10 km along the Rideau Canal (except two pairs of

sampling sites, RR3-1 and RR3-2: 1.2 km apart, RR2-2-2019 and RR2-2020: 2.2 km apart; Figure 1-1a; Supporting Information 1 – Table S1-1). We set our nets in areas suitable for painted turtles characterized by shallow water, weak currents, abundant aquatic vegetation, and presence of structures for basking (e.g., rocks, logs, and stumps). We deployed fyke nets for at least one week at each site and checked them every 24 hours. During sampling, we moved nets within a given site to increase trapping success. We visited ten sampling sites both years (Supporting Information 1 – Table S1-1). We uniquely marked painted turtles by notching their marginal scutes according to the North American coding system developed for hard-shelled turtles to identify individuals (Nagle et al., 2017). We determined the sex of each turtle based on external morphological traits (e.g., tail and claw length, cloaca position on the tail, and shape of the shell). We also measured plastron length, carapace length, height, and width (± 0.5 mm) with an aluminum caliper (Haglöf, Sweden).

*Risk-taking behaviours*

We measured three behaviours related to risk-taking propensity: sum of active defensive behaviours used, escape latency, and emergence of the turtle from the water after escaping. We repeated all behavioural measurements at each capture to obtain multiple observations per individual (mean number of observations per turtle: 1.5; range = 1 - 7 observations per turtle, see Supporting Information 1 – Table S1-2 for the number of painted turtles per number of trials). All turtles were tested individually and no visual contact with other turtles occurred during testing. The behavioural responses could be influenced by the experimenter's handling and measurement techniques, but we tried to minimize variation in handling by always performing our behavioural tests in the same way and order (i.e., sum of active defensive behaviours, escape latency, and emergence of the turtle after escaping). It was not possible to use a blinded method because our study involved behavioural measurements that required the release of focal turtles at their site of capture (see below in *Escape latency* and *Emergence of the*

14

*turtle after escaping*). The experimenter was thus aware of the identity of the turtle tested and the location of capture. We controlled statistically for variation in testing conditions (e.g., order, time and day of the trial and lab- vs. field-based tests) and individual characteristics (e.g., sex and carapace length) to minimize the possible effects of potential confounds related to the STRANGE framework (e.g., biases related to individual learning, habituation, natural behavioural changes over time; Webster & Rutz, 2020) on the relationship between human disturbance and risk-taking behaviours (see *Relationships between risk-taking behaviours and human disturbance* in the *Methods*). No information was available on individual history prior to the first capture given that turtles were captured from the wild. All turtles sampled during the study were used in the analyses (see Supporting Information 1 – Table S1-1 for more details on the sample sizes).

*Sum of active defensive behaviours used*

During measurements of the four morphological traits, we noted if the turtle used the following active defensive behaviours: i) trying to escape (movement of the legs), ii) trying to bite (the turtle closes and opens the mouth with its neck stretched), iii) hissing (gaping of the mouth when retracting the head in the shell, thus expulsing air), iv) defecating and/or urinating. We then calculated the number of active defensive behaviours used during the test ranging from 0 (no active defensive behaviours used) to 4 (all four active defensive behaviours used). Turtles were not handled prior to this test. This test was adapted from Pich et al. (2019) (see Supporting Information 2 of Chapter 1 for an example of the test). We considered that a turtle that used more active defensive behaviours was more prone to take risks. Uniquely among vertebrates, turtles have the possibility to withdraw in their shell, a passive strategy that is their main protection against predation (Greene, 1988). Thus, we considered the use of alternative active defensive behaviours to be a riskier strategy than hiding in the shell.

*Escape latency*

After the morphological measurements, we measured surface temperature ($\pm$ 1 °C) of the turtle with an infrared laser thermometer (UEi test instruments, United States) pointed at the middle of the plastron because latency behaviours in turtles are affected by plastron temperature (see Pich et al., 2019). We then put the turtle in the center of a floating platform (Figure 1-1c) and kept it under a black pail for 1 min. The floating platform consisted of a 0.6 m x 0.6 m plywood mounted on rigid polystyrene and covered with white adhesive vinyl (Figure 1-1c). The platform was held away from the boat with a 1 m wooden dowel attached to the platform with a hinge. After the 1-min wait, we lifted the pail with a stick from the boat and timed the latency to escape as the time until the turtle touched the water for a maximum of 10 min. The maximum time (i.e., 10-min latency) was recorded if a turtle did not escape. We estimated wind speed with the Beaufort scale during the platform test as wind can affect water turbulence and, thus, turtle escape behaviour. Head emergence and movement latency were also measured during the platform test, but were not kept for analyses given their strong positive correlations with escape latency (Pearson's *r* correlations > 0.60; see Supporting Information 1 – Table S1-3 for the correlation coefficients between behavioural measurements), as observed in previous studies (see Carlson & Tetzlaff, 2020). We considered that a turtle that left the platform rapidly was more prone to take risks. As suggested by Ibáñez et al. (2018), turtles that take more time to move could be considered more cautious given that they are taking more time to get visual information about their environment and to analyze risk cues. In addition, the pace-of-life syndrome hypothesis suggests that risk-averse individuals explore more thoroughly their environment compared to risk-prone individuals (Réale et al., 2010).

*Emergence of the turtle after escaping*

After the turtle escaped the platform, we surveyed the water surface around the platform for 30 sec to see if the turtle emerged from the water (No = 0, Yes = 1; Figure 1-1d). Individuals who did not escape from the platform after the 10-min period were not considered for this test. We considered that a turtle that emerged from the water after escaping was more prone to take risks than a turtle that remained submerged. We acknowledge that turtles could emerge far from the platform and several minutes after the test was performed. However, we were not interested in monitoring distant and late emergence from the platform given that we wanted to measure the level of risk-taking. Turtles that emerged close to the platform (i.e., the risky environment) were more prone to take risks than those that emerged far from the platform or much later.

*Behavioural measurements in a controlled environment*

To secure repeated behavioural measurements on several individuals, we brought 122 painted turtles (2019 = 50; 2020 = 72) to the Queen's University Biological Station (Figure 1-1a). Turtles were kept for a maximum of four days in outside tanks (940 L; 1.3 m x 1 m [diameter x depth]) filled with water from the canal in groups consisting of a maximum of 10 individuals from the same sampling site. The same three behavioural measurements described above were made every day on each turtle. The platform test, used to measure escape latency and the emergence of the turtle after escaping, was performed in the tank (Supporting Information 2 of Chapter 1). On the last day of captivity, we performed all behavioural tests one last time prior to release at the sites of capture. Sampling occurred daily in the field and newly captured turtles were brought every day at the station until we reached the end of sampling period at a given site of capture (i.e., approximatively one week). Thus, the number of days in captivity varied between turtles leading to different numbers of repeated behavioural

17

measurements per turtle (see Supporting Information 1 – Table S1-2 for the number of painted turtles per number of trials for each behavioural test in the controlled environment).

The measurements made in the controlled environment were combined with those made in the field for the analyses. We statistically controlled for the testing environment (i.e., tests performed in the field or in the controlled environment), allowing us to quantify the impact of the environment on each risk-taking behaviour. Measuring behavioural responses in both settings also allowed us to document the context-dependency of the behavioural tests by comparing repeatability estimates and estimating the correlations between lab- and field-based behavioural measurements (see *Repeatability and correlations between risk-taking behaviours and testing environments* and *Relationships between risk-taking behaviours and human disturbance* in the *Methods*).

*Ethical statement*

All protocols were approved by animal care committees at the University of Ottawa (protocol BL-3008) and Queen's University (protocol 2018-1836). All fieldwork was conducted under a Parks Canada Agency research and collection permit (number RIC-2018-29178) and Wildlife Scientific Collector's Authorizations from the Ontario Ministry of Natural Resources (numbers 1089358, 1092637 and 1095459). Prior to handling, turtles were kept under constant supervision in large containers away from direct sunlight with a small amount of lake water. Turtles that were temporarily kept in tanks at the Queen's University Biological Station had access to rocks for hiding and logs for basking. Food (e.g., lettuce and worms according to the recommendations made by the University of Ottawa Animal Care Committee) was distributed in each tank every two days and the tank water was changed 3-4 hours after feeding. The health status of each turtle was visually verified every day for the turtles in captivity and prior to their release at the capture sites.

*Repeatability and correlations between risk-taking behaviours and testing environments*

All statistical analyses were conducted with R 3.6.2 (R Core Team, 2019). We used mixed models to assess the consistency of behavioural measurements. Prior to analyses, we explored the distribution of each behavioural measurement (response variable) to select the best distribution to use for our models. We fitted the sum of active defensive behaviours with a Gaussian distribution and an identity link function, the emergence of the turtle after escaping with a Binomial distribution and a logit link function, and the escape latency with a Gaussian distribution and an identity link function, after normalizing the variable using a $\log(x+1)$ transformation. In all models, we included turtle identity as a random effect and assessed among and within-individual variance for each behavioural measurement. Individual repeatability corresponds to the proportion of phenotypic variance attributed to differences among individuals (Nakagawa & Schielzeth, 2010). A high repeatability indicates that the variance of a repeated measurement within an individual is smaller than the variance among individuals (Lessells & Boag, 1987). We only used observations from individuals tested more than once and from sampling sites with more than five individuals sampled ($N = 202$ turtles from 15 sampling sites; see Supporting Information 1 – Table S1-1, S1-2). We used the rpt function implemented in the rptR package (Stoffel et al., 2017) and adjusted our models for among-individual differences using sex, order of the trial, testing environment (i.e., made in the controlled environment or in the field), and sampling year as fixed effects. We included sampling site identity as a random effect to control for the non-independence of observations from the same location. We also fitted unadjusted models with only turtle identity as a random effect. We calculated 95 % confidence intervals (95 % CI) of repeatability estimates and raw variance components using likelihood ratio tests (LRTs) with 1,000 parametric bootstrap iterations. We also assessed repeatability separately for behavioural measurements made in the field and in the controlled environment. Finally, we calculated Pearson's and Spearman's correlations between each

pair of behaviours (and their respective p values) by using the mean values of each behaviour for each individual tested (entire dataset, N = 730) with R Hmisc packages (Harrell, 2020). We also assessed correlations between lab- and field-based measurements for each behaviour with the first measurement of each individual tested in both environments (N = 122).

*Quantifying human disturbance*

We used ArcGIS version 10.7.1 (ESRI, 2019) and Python version 2.7.16 (Python Software Foundation, 2019) to perform all spatial analyses. We used four variables to quantify the intensity of human disturbance at each sampling site: i) mean number of daily vessel crossings during the operational period of the canal, ii) shortest aquatic distance (in m) to the navigation channel, iii) number of houses with access to the canal within various buffers (see below), and iv) proportion of urban area within various buffers (see below).

We calculated the mean daily number of vessel crossings at each lockstation based on Parks Canada counts made during the operational period (i.e., May (Canadian Victoria Day) to October (Canadian Thanksgiving); see Supporting Information 1 - Table S1-4; Figure 1-1b). Given the lower frequentation and late opening of the Rideau Canal in 2020 due to the Covid-19 pandemic, we only used the number of vessel crossings from 2019 to be more representative of boat traffic during a typical year and given that we were interested in the inter-site variation in boating activity (Supporting Information 1 - Table S1-4). We used the mean daily number of vessel crossings from the upstream and downstream lockstations of each sampling site to calculate the mean daily number of vessel crossings. We considered that sampling sites in proximity to lockstations with high mean daily numbers of vessel crossings should have more boat activity.

We calculated the shortest aquatic distance of each sampling site to the navigation channel with

the *Generate near table* tool in ArcMap. The channel was digitized by Parks Canada from digital navigation charts. We considered that sampling sites closer to the navigation channel should have more boat activity.

We used ArcGIS world imagery online basemap (ESRI, 2021) to identify each house with access to the Rideau Canal (e.g., presence of a dock on the property or at least one side of the property with access to the canal). We calculated the number of houses with access to the canal using buffer distances that ranged from 100 m to 1000 m at 100-m increments with the *Spatial Join* tool in ArcMap (based on the work of Čapkun-Huot et al. (2021) and Fyson & Blouin-Demers (2021). We considered that sampling sites close to numerous houses with access to the canal should have more boat activity.

Based on the same buffer distances as above, we determined the proportion of urban area around each sampling site based on the Southern Ontario Land Resource Information System (SOLRIS) V.3 with 15-m resolution (OMNRF, 2019; Figure 1-1a). We used the *Tabulate Area 2* tool from the Spatial Analyst Supplemental Tools v1.3 in ArcMap to calculate the number of cells of each land cover class inside each buffer distance. Then, we calculated the proportion of urban area (i.e., transportation, built-up area-pervious, and built-up area-impervious land cover classes) over the total buffer area (Figure 1-1a). We considered that sampling sites in proximity to higher proportion of urban area should have more human activity.

Finally, we determined the distance at which the number of houses with access to the canal and the proportion of urban area had the maximum effect on the three behavioural measurements separately. The scale of maximum effect was attributed to the buffer distance at which the variable had the highest Pearson's correlation coefficient with each behavioural measurement (see Supporting Information 3 of Chapter 1). We only kept the scale of maximum effect for each variable for further analyses. Similar

techniques were used in other taxa to determine the scale of maximum effect of landscape variables (see Čapkun-Huot et al., 2021; Courtois et al., 2021; Fyson & Blouin-Demers, 2021; Martin et al., 2020; Wilkin et al., 2006).

*Relationships between risk-taking behaviours and human disturbance*

The same distributions and link functions described above for repeatability analyses were used here. We used (generalized) linear mixed models to assess the relationships between human disturbance and risk-taking behaviours from measurements made on 730 painted turtles (Supporting Information 1 – Table S1-1, S1-2) with the lme4 package (Bates et al., 2015). In all models, we used the behaviour as the response variable and different predictor variables to assess the variance related to testing conditions (e.g., order of the trial and lab- vs. field-based tests) and individual characteristics (e.g., sex and carapace length), as well as the variables quantifying human disturbance (see Supporting Information 1 – Table S1-5 and S1-6 for a list and description of all the variables included). All continuous predictor variables were standardized (mean zero, unit variance) before model selection (Supporting Information 1 – Table S1-6). We removed from initial models all variables that were highly correlated ($r > 0.8$) or with high generalized variance inflation factors ($GVIF^{(1/(2*df))} > 2$) to avoid multicollinearity (see Supporting Information 1 – Table S1-5 and S1-7). We simplified models with a backward selection procedure ($\alpha = 0.05$) until all remaining variables were significant and the inclusion/deletion of each variable was confirmed with a LRT (Crawley, 2007). We also included turtle and sampling site identity as random effects to respectively control for the repeated behavioural measurements on individuals and individuals from the same location. Turtle identity was significant (according to LRTs) and kept in all models, while sampling site identity was only significant in the sum of active defensive behaviours model. We visually verified model assumptions of each initial model by checking residual distributions and their relationships with fitted values. We calculated the estimates and 95 % CI for all predictor variables from

the final models fitted with restricted maximum likelihood (Zuur et al., 2009). We estimated marginal and conditional variance explained ($R^2$) by the final models with the MuMIn package (Bartoń, 2020). We generated final model predictions with the ggeffects package (Lüdecke, 2018) and built figures with the ggplot2 package (Wickham, 2016).

**Results**

*Description of risk-taking behaviours in painted turtles*

Combining tests performed in the controlled environment and in the field, we made 1117 observations of the number of active defensive behaviours used during manipulations on the 730 turtles captured. In 30 % of observations, no active defensive behaviours were used (340 observations; mean = 1.08 active defensive behaviours used, standard deviation (SD) = 0.92). Only three turtles used all four active defensive behaviours during the same trial. We made 1115 observations of escape latency and turtles escaped within 30 sec 82 % of the time (929 observations; mean = 65.74 sec, SD = 117.54). During the platform test, 23 turtles (29 observations) had not escaped after 10 min. Finally, for the 1071 observations of emergence after escaping, turtles did not emerge from the water 70 % of the time (750 observations; see Supporting Information 1 – Table S1-1 for more details on the sample sizes).

*Repeatability and correlations between risk-taking behaviours and testing environments*

We obtained repeated behavioural measurements both from the controlled environment and in the field for 202 individuals, representing 28% of the total number of turtles tested (N = 730; Supporting Information 1 – Table S1-2). We found statistically significant adjusted repeatability estimates for sum of active defensive behaviours (0.363 (95 % CI = 0.263 – 0.458)), escape latency (0.387 (95 % CI = 0.286 – 0.490)) and emergence of the turtle after escaping (0.365 (95 % CI = 0.129 – 0.630)) (Table 1-1). There were slight differences between adjusted and unadjusted

23

repeatability estimates for all behavioural measurements: when our models were adjusted with the fixed effects and sampling site identity as a random effect, repeatability estimates for escape latency and emergence of the turtle after escaping increased, while it decreased for the sum of active defensive behaviours used (Table 1-1). For all behavioural measurements, however, the 95 % CI of the unadjusted and adjusted repeatability estimates overlapped (Table 1-1). In each testing environment separately, repeatability estimates were significant for all risk-taking behaviours and similar to those we obtained with the combined dataset (Supporting Information 1 – Table S1-8). We found slightly higher repeatability estimates in the field for the sum of active defensive behaviours used and escape latency, while it was the opposite for the emergence of the turtle after escaping the platform (Supporting Information 1 – Table S1-8). However, the 95 % CI of repeatability estimates from field and controlled environment all overlapped (Supporting Information 1 – Table S1-8).

Painted turtles that used more active defensive behaviours escaped from the floating platform sooner (Pearson's $r$ correlation = -0.24, $p < 0.01$; Supporting Information 1 - Table S1-3) and emerged from the water more often after escaping ($r = 0.26$, $p < 0.01$; Supporting Information 1 - Table S1-3). Finally, turtles that took more time to escape from the platform emerged less often from the water after escaping ($r = -0.19$, $p < 0.01$; Supporting Information 1 - Table S1-3). We obtained similar results with a multivariate mixed model that included the three behavioural measurements as response variables with the MCMCglmm package (Hadfield, 2010; Supporting Information 1 – Table S1-9). Painted turtles tested in the controlled environment used fewer active defensive behaviours during handling and emerged less often from the water after escaping (Table 1-2). Lastly, for all risk-taking behaviours, we obtained significant positive correlations between measurements made in the field and those made in the controlled environment ($r$ active defensive behaviours = 0.40; $r$ escape latency = 0.39; $r$ emergence = 0.33; $p < 0.01$; Supporting Information 1 – Table S1-10).

*Relationships between risk-taking behaviours and human disturbance*

We found significant relationships between some measurements of human disturbance and the sum of active defensive behaviours used, but no relationships for escape latency and emergence of the turtle after escaping (Table 1-2). Painted turtles from sites closer to the navigation channel (Table 1-2; Figure 1-2a) and with more daily vessel crossings (Table 1-2; Figure 1-2b) used more active defensive behaviours. In contrast, painted turtles from sites with more houses with access to the canal within 200 m used fewer active defensive behaviours (Table 1-2; Figure 1-2c). Model estimates and their 95 % CI for all predictor variables included in our models are provided in Table 1-2.

## Discussion

Understanding how animals adjust behaviourally to perturbations in their environment is crucial to better evaluate the impact of human disturbance on wildlife populations, especially for species particularly vulnerable to human activities. We observed that risk-taking behaviours of painted turtles were repeatable and consistent among the different tests and the two testing environments. Painted turtles from sites with more boat activity used more active defensive behaviours, while turtles from sites in proximity to more houses with access to the canal used fewer. These findings add to the limited information currently available on the impact of human disturbance on risk-taking behaviours in turtles.

*Painted turtles show consistent differences in risk-taking behaviours*

All three risk-taking behaviours of painted turtles were repeatable, as observed in other studies (Bell et al., 2009; Holtmann, Lagisz, et al., 2017). Across taxa, approximately 40 % of the phenotypic variation of behavioural responses reflects among-individual variance, similar to our estimates (Bell et al., 2009; Holtmann, Lagisz, et al., 2017). In previous studies of turtles, repeatability estimates of risk-taking behaviours were slightly higher than ours (mean ~ 0.5; see Supporting Information 1 – Table S1-

11). In these studies, however, repeated measurements were generally only obtained in controlled environments, over short periods of time (i.e., a few hours to several weeks), and on a small number of individuals (i.e., fewer than 30 turtles; Supporting Information 1 – Table S1-11). Repeatability estimates are generally higher when measurements are made temporally close to each other and in stable conditions (Bell et al., 2009; Holtmann, Lagisz, et al., 2017). The use of only one sampling technique (i.e., fyke nets) in our study, however, could have led to more conservative repeatability estimates (see also *Possible limitations of the study*). Estimating repeatability over a longer period and from a large dataset collected in the field, as in our study, is probably more realistic and representative of the long lifespan of turtles and the environmental context in which they live. Given that risk-taking behaviours are partially consistent within individuals, it allows evaluating the effect of human disturbance on the variation observed in risk-taking behaviours.

We observed consistency among our three measures of risk-taking propensity. Painted turtles that escaped sooner from the floating platform used more active defensive behaviours and emerged more often from the water after escaping: these turtles may be considered more risk prone. Our three behavioural tests seem to measure the same underlying risk-taking propensity. Previous studies in turtles also indicated consistent boldness under alternative tests (Pich et al., 2019; Roth et al., 2020). Behavioural consistency among tests could indicate a behavioural syndrome (i.e., suite of correlated behavioural measurements) in painted turtles where individuals use different behavioural strategies (i.e., pace-of-life continuum: proactive vs. reactive individuals; Réale et al., 2010; Sih, 2004). Measurements in different contexts (e.g., simulated predation attack vs. human presence) or along other axes of behaviour (e.g., exploration, aggressivity, and sociability) are needed to confirm the presence of a behavioural syndrome in painted turtles.

Risk-taking behaviours were positively correlated between testing environments indicating

consistency across contexts. Risk-taking behaviours were also repeatable in each testing environments indicating consistency in among-individual differences regardless of the context (Rudin, Simmons, et al., 2018). These results indicate that behavioural measurements obtained in a controlled environment could predict risk-taking level in the field. On the other hand, painted turtles used fewer active defensive behaviours and emerged less often from the water after escaping in the controlled environment. Painted turtles reacted slightly differently between testing environments. In the controlled environment, turtles were not exposed to external cues and might have perceived it as a novel environment while turtles tested in the field had access to cues from their surroundings with which they were familiar (Mouchet & Dingemanse, 2021; Rudin, Simmons, et al., 2018; Rudin, Tomkins, et al., 2018). Turtles tested in the controlled environment may also have different behavioural responses to the tests given their short-term captivity. Our findings highlight the importance of performing behavioural tests in different contexts, especially in natural environments, and to control statistically for testing conditions given their potential impacts on behavioural responses. We lacked enough repeated measurements in the field to calculate correlations between contexts by partitioning among- and within-individual variances and to completely evaluate cross-context consistency, which would be useful in future analyses (Mouchet & Dingemanse, 2021).

*Painted turtles from sites with high boat activity take more risks*

Painted turtles from sites more exposed to boat activity were more prone to take risks, as indicated by their use of more active defensive behaviours, suggesting that human presence influences behavioural responses. Previous studies documented similar relationships. For instance, more risk-prone turtles (i.e., shorter flight initiation distance to human approach and lower abandonment rate of basking sites after boating disturbance) were observed in areas with more frequent human disturbance (Polich & Barazowski, 2016; Selman et al., 2013). To our knowledge, our study is the first to relate the use of

active defensive behaviours to human disturbance, making comparisons with other studies impossible. While shorter flight initiation distances and lower abandonment rates in areas with higher exposure to human activities reflect a higher tolerance toward human disturbance, the use of more active defensive behaviours suggests the opposite (Bejder et al., 2009). We need to understand how these various behaviours are related to each other and to human disturbance.

It is unclear how the use of active defensive behaviours can be advantageous in human-altered environments considering that turtles have the opportunity to withdraw in their shell, a possibly safer strategy for protection. A previous study by Kashon and Carlson (2018) found that risk-prone Eastern box turtles (i.e., low movement latencies) had more shell injuries, suggesting a higher exposure to risky situations such as predation. Thus, risk-prone turtles may use alternative active defensive behaviours (i.e., stronger antipredator behaviours) to compensate for the risks of not hiding in risky situations (Pascual & Senar, 2014; Pich et al., 2019). While risk-averse individuals (i.e., those that use fewer active defensive behaviours, greater propensity to hide) are more cautious and may have a lower mortality rate (Smith & Blumstein, 2008), they may miss many feeding, reproductive and basking opportunities compared to risk-prone individuals by avoiding areas with high human disturbance (Dugatkin & Alfieri, 2003; Dyer et al., 2009; Griffin et al., 2017; Réale et al., 2009). Risk-prone individuals resume activities more rapidly after exposure to an unknown threat, suggesting that the loss of opportunities can be limited compared to risk-averse individuals (Cole & Quinn, 2014). Therefore, the capacity to cope better with risky situations, suggested by the use of more active defensive behaviours, may allow painted turtles to coexist with boating activities in the canal and to persist in a human-altered environment.

We observed that painted turtles from sites with more houses with access to the canal used fewer active defensive behaviours. This result is unexpected because we predicted that all our proxies of human disturbance would be similarly related to risk-taking behaviour. One possible explanation is that

this relationship is simply spurious. The scale of maximum effect occurred at 200 m and the effect size was weak, at least partly because of limited variance in the predictor variable (Supporting Information 1 – Table S1-6). It is also possible that the number of houses within 200 m is a poor predictor of the level of recreational boating. The response of wildlife to human disturbance can be complex depending on the type and intensity of perturbations (Gaynor et al., 2018; Larson et al., 2016; Tablado & Jenni, 2017; Tucker et al., 2018). The behavioural response can also depend on the predictability of perturbations and, thus, the capacity of the animal to predict the risk level (Nickel et al., 2020). Therefore, risk-averse turtles (i.e., that use fewer active defensive behaviours) could avoid areas with high boat activity where risk level is less predictable, whereas the number of houses may reflect a more permanent and constant human disturbance (i.e., predictable), leading to different behavioural responses to these different proxies of human disturbance.

While our study was not designed to assess the mechanisms responsible for the observed effects, our findings still provide insights into which mechanisms may play a role in the relationship observed between human disturbance and the number of active defensive behaviours used. For instance, the use of a higher number of active defensive behaviours in larger turtles (i.e., long carapace; Table 1-2) that are likely older (Wilson et al., 2003), suggests a long-term behavioural plasticity where turtles may adapt their behaviour according to their past experiences. We cannot exclude that the behavioural responses observed in this system could be the result of multiple mechanisms. Indeed, new selection pressures could have appeared during canal construction leading to the selection of risk-prone turtles and followed by a long-term behavioural plasticity of the individuals that have persisted in these new conditions. The construction of the canal is relatively recent (e.g., between 1826 and 1832) in terms of painted turtle generation time (~ 30-45 years; COSEWIC, 2018) and it could be too short for selection to occur. Another possibility is that painted turtles, after exposure to new environmental conditions

caused by the canal construction, have dispersed and selected habitats better adapted to their behaviour at some point during their lifetime. Long-term monitoring of these populations would be necessary to achieve a better understanding of the mechanisms driving the behavioural responses of painted turtles toward human disturbance.

*Possible limitations of the study and STRANGEness of animals sampled*

We are aware of the potential lack of independence between nearby sampling sites along the canal and that risk-taking behaviours could be spatially autocorrelated. To quantify the potential presence of spatial autocorrelation, we estimated the Moran's I statistic for different distances (i.e., from 5 km to 130 km) for each risk-taking behaviour. We detected positive spatial autocorrelation for the sum of active defensive behaviours and the emergence of the turtle after escaping in the water (positive and significant Moran's I statistic respectively under 5 km and 27 km; see Supporting Information 1 – Table S1-12). Given that we did not find a significant effect of sampling site identity and human disturbance on the emergence of the turtle after escaping, it was only relevant to evaluate the effect of spatial autocorrelation on the results obtained for the sum of active defensive behaviours. We modified the variable representing sampling site identity by grouping together observations from sampling sites located less than 5 km apart (i.e., RR3-1 with RR3-2 and RR2-2-2019 with RR2-2020). By fitting a new model with this adapted version of sampling site identity that considers spatial autocorrelation as a random effect, we found that the variance explained by sampling site identity was very similar to that in the model that did not consider spatial autocorrelation (without correction for spatial autocorrelation: variance = 0.051, SD = 0.226; with the correction: variance = 0.053, SD = 0.229). We also obtained the same significant predictors in the final model after model selection (Supporting Information 1 – Table S1-13).

We only used one sampling technique (i.e., fyke nets), which may have led to the capture of turtles that are not representative of the entire population in their behaviours according to the STRANGE framework (Webster & Rutz, 2020). Nets could have been avoided by risk-averse individuals leading to the trapping of more risk-prone individuals and, thus, to the underestimation of the range of behavioural responses. Less diversity in behavioural types, however, should have led to more conservative repeatability estimates by reducing among-individual variances. It should also have reduced our capacity to identify how human disturbance is related to risk-taking behaviours, which did not appear to be the case, possibly because our high sampling effort at a large spatial scale may have minimized these biases. In addition, by combining data collected in two testing environments, we obtained a large sample size that allowed us to control statistically and quantify the effect of multiple confounding factors related to testing conditions (e.g., order of the trial and lab- vs. field-based tests) and individual characteristics (e.g., sex and carapace length; see Table 1-2 for a list of all the variables included in models and their respective effect size). By measuring behaviours in the field, however, we could not control for spatio-temporal variations in the testing environment. In addition, our ability to detect the emergence of the turtle after escaping could potentially vary between testing environments. Positive correlations and similar repeatability estimates between testing environments indicate that our behavioural tests seem appropriate to assess risk-taking level in both contexts. In addition, repeating the analyses separately for turtles tested in the controlled environment and in the field, and for turtles tested more than once, gave qualitatively similar results (see Supporting Information 1 – Table S1-14 and S1-15). Thus, we are confident that our analyses are robust, and that the results obtained reflect how human disturbance is related to risk-taking behaviours in painted turtles.

**Conclusion**

Overall, we found that painted turtles show consistent differences in risk-taking behaviours and

that their behavioural response to risky situations is influenced by the level of human disturbance in the Rideau Canal. Our study adds to the current research on turtle behaviour and is one of the first to assess how risk-taking behaviour is related to human disturbance in this group. There is a need to assess the impact of human activities on other types of behaviours and to identify the mechanisms driving the differences observed in behavioural responses according to the level of human disturbance. It would also be critical to assess how the behavioural responses are related to fitness and survival (see Allard et al., 2019; Germano et al., 2017). A better understanding of the consequences of behavioural changes would allow better management of species vulnerable to human activities through the creation of conservation plans that are better adapted to minimize the negative effects of human disturbance on wildlife.

**Data availability**

Data and R codes used for this study are available in the Zenodo Digital Repository: https://doi.org/10.5281/zenodo.7795750

**Tables**

**Table 1-1** Sources of variance ($V_G$: group-level variance; $V_R$: residual variance) and repeatability estimates (R) for three risk-taking behaviours in painted turtles (*Chrysemys picta*): sum of active defensive behaviours, escape latency, and emergence of the turtle after escaping. The unadjusted repeatability estimates only included turtle identity as random effect, while the adjusted repeatability estimates also included sex, trial order, testing environment (i.e., made in the controlled environment or in the field), and year as fixed effects, and sampling site identity as a random effect ($V_{G\text{ - site}}$ and $R_{site}$). Significance [95 % confidence intervals] of the variances and repeatability estimates were determined with likelihood ratio tests. The coefficient of determination ($R^2$) of the fixed effects included in the adjusted repeatability estimates was calculated. Sources of variances for the emergence of the turtle after escaping were estimated from the link-scale approximation and repeatability estimates from the original scale. Number of individuals tested (Nb. ID) with the total number of observations (Nb. Entries) for each behaviour are provided

| | Nb. ID (Nb. Entries) | $V_{G \text{ - individual}}$ | $V_{G \text{ - site}}$ | $V_R$ | $R_{individual}$ | $R_{site}$ | $R^2_{fixed}$ |
|---|---|---|---|---|---|---|---|
| **Sum of active defensive behaviours** | | | | | | | |
| Unadjusted | 202 (569) | 0.374 [0.275 - 0.492] | – | 0.430 [0.374 - 0.499] | 0.465 [0.371 - 0.549] | – | – |
| Adjusted | 196 (553) | 0.292 [0.206 - 0.388] | 0.103 [0.014 - 0.234] | 0.411 [0.349 - 0.473] | 0.363 [0.263 - 0.458] | 0.128 [0.020 - 0.254] | 0.06 |
| **Escape latency** | | | | | | | |
| Unadjusted | 199 (574) | 0.506 [0.338 - 0.681] | – | 0.916 [0.796 - 1.045] | 0.356 [0.258 - 0.442] | – | – |
| Adjusted | 193 (558) | 0.506 [0.352 - 0.682] | 0.081 [0.000 - 0.226] | 0.723 [0.619 - 0.817] | 0.387 [0.286 - 0.490] | 0.062 [0.000 - 0.154] | 0.10 |
| **Emergence of the turtle after escaping** | | | | | | | |
| Unadjusted | 196 (543) | 1.679 [0.521 - 2.484] | – | 4.565 [4.298 - 5.065] | 0.257 [0.107 - 0.317] | – | – |
| Adjusted | 190 (527) | 3.185 [0.813- 4.928] | 2.325 [0.226 - 4.553] | 4.576 [4.152 - 6.137] | 0.365 [0.129 - 0.630] | 0.267 [0.008 - 0.555] | 0.20 |

**Table 1-2** Summary statistics for the final (generalized) linear mixed models with risk-taking behaviours in painted turtles (*Chrysemys picta*) as the response variable: sum of active defensive behaviours used, escape latency, and emergence of the turtle after escaping. All continuous predictor variables were scaled (mean zero, unit variance) before model selection. Reference factors are in parentheses for categorical predictor variables. Turtle and sampling site identities were included as random effects in the model for sum of active defensive behaviours, while only turtle identity was included in the two other models. For each model, we provided for each significant predictor variable: the estimate, the standard error (SE), the t-value (z-value for the binomial model), the p-value, and the 95 % confidence interval (95 % CI). Statistically significant effects (p-value < 0.05) are in bold. The marginal and conditional coefficient of determination ($R^2$) are provided for each model as well as the number of unique painted turtles tested with the total number of observations in parentheses

| Variables | Estimate | SE | t-value | p-value | [95 % CI] |
|---|---|---|---|---|---|
| Sum of active defensive behaviours | 714 individuals (1091 observations); $R^2$ - marginal : 0.08; $R^2$ - conditional: 0.52 | | | | |
| Intercept | 0.853 | 0.074 | 11.544 | < 0.001 | [0.708 to 0.998] |
| **Number of houses within 200 m** | -0.134 | 0.058 | 2.316 | 0.031 | [-0.247 to -0.021] |
| **Distance to navigation channel** | -0.122 | 0.057 | 2.122 | 0.047 | [-0.234 to -0.009] |
| **Mean daily number of vessel crossings** | 0.194 | 0.065 | 2.986 | 0.008 | [0.067 to 0.321] |
| **Sex (Male)** | 0.327 | 0.070 | 4.687 | < 0.001 | [0.191 to 0.464] |
| **Testing environment (controlled setting)** | -0.218 | 0.068 | 3.228 | 0.001 | [-0.350 to -0.086] |
| **Carapace length** | 0.112 | 0.037 | 3.014 | 0.003 | [0.040 to 0.186] |
| Turtle temperature | 0.003 | 0.046 | 0.077 | 0.939 | [-0.087 to 0.094] |
| Julian Day | -0.012 | 0.061 | 0.197 | 0.845 | [-0.132 to 0.107] |
| Hour | 0.016 | 0.035 | 0.462 | 0.644 | [-0.053 to 0.086] |
| Year (2020) | 0.040 | 0.073 | 0.555 | 0.579 | [-0.102 to 0.183] |
| Order of the trial | 0.043 | 0.027 | 1.573 | 0.116 | [-0.010 to 0.096] |
| | | | | | |
| Escape latency | 596 individuals (919 observations); $R^2$ - marginal : 0.10; $R^2$ - conditional: 0.44 | | | | |
| Intercept | 3.401 | 0.044 | 76.525 | < 0.001 | [3.314 to 3.488] |
| **Order of the trial** | -0.231 | 0.036 | 6.415 | < 0.001 | [-0.302 to -0.161] |
| **Julian Day** | 0.141 | 0.053 | 2.645 | 0.008 | [0.036 to 0.245] |
| **Turtle temperature** | -0.199 | 0.047 | 4.245 | < 0.001 | [-0.291 to -0.107] |
| **Carapace length** | 0.167 | 0.042 | 4.013 | < 0.001 | [0.085 to 0.248] |
| **Wind scale (Beaufort scale)** | -0.176 | 0.036 | 4.899 | < 0.001 | [-0.246 to -0.106] |
| Sex (Male) | 0.005 | 0.093 | 0.053 | 0.958 | [-0.177 to 0.186] |
| Distance to navigation channel | 0.025 | 0.052 | 0.475 | 0.635 | [-0.077 to 0.126] |
| Number of houses within 400 m | 0.032 | 0.053 | 0.602 | 0.548 | [-0.072 to 0.137] |
| Mean daily number of vessel crossings | -0.028 | 0.041 | 0.681 | 0.496 | [-0.108 to 0.052] |
| Year (2020) | -0.087 | 0.088 | 0.995 | 0.320 | [-0.260 to 0.085] |
| Proportion of urban areas within 200 m | 0.094 | 0.060 | 1.547 | 0.123 | [-0.025 to 0.212] |
| Testing environment (controlled setting) | 0.244 | 0.144 | 1.692 | 0.091 | [-0.039 to 0.527] |
| Hour of the platform test | -0.039 | 0.039 | 0.990 | 0.322 | [-0.115 to 0.038] |

| Emergence of the turtle after escaping | 704 individuals (1071 observations); $R^2$ - marginal : 0.12; $R^2$ - conditional: 0.49 | | | | |
|---|---|---|---|---|---|
| Intercept | -1.135 | 0.208 | 5.464 | < 0.001 | [-1.543 to -0.728] |
| **Testing environment (controlled setting)** | -2.318 | 0.417 | 5.558 | < 0.001 | [-3.135 to -1.500] |
| **Julian Day** | 0.994 | 0.182 | 5.473 | < 0.001 | [0.638 to 1.350] |
| **Carapace length** | -0.323 | 0.131 | 2.473 | 0.013 | [-0.579 to -0.067] |
| Sex (Male) | -0.072 | 0.242 | -0.298 | 0.767 | [-0.545 to 0.402] |
| Turtle temperature | 0.082 | 0.135 | 0.606 | 0.545 | [-0.183 to 0.348] |
| Hour of the platform test | 0.080 | 0.128 | 0.627 | 0.531 | [-0.170 to 0.331] |
| Year (2020) | 0.299 | 0.231 | 1.293 | 0.196 | [-0.154 to 0.751] |
| Distance to navigation channel | -0.188 | 0.138 | 1.361 | 0.173 | [-0.459 to 0.083] |
| Number of houses within 300 m | -0.160 | 0.134 | 1.196 | 0.232 | [-0.423 to 0.102] |
| Mean daily number of vessel crossings | 0.196 | 0.121 | 1.620 | 0.105 | [-0.041 to 0.433] |
| Order of the trial | 0.167 | 0.107 | 1.570 | 0.116 | [-0.042 to 0.376] |

# Figures
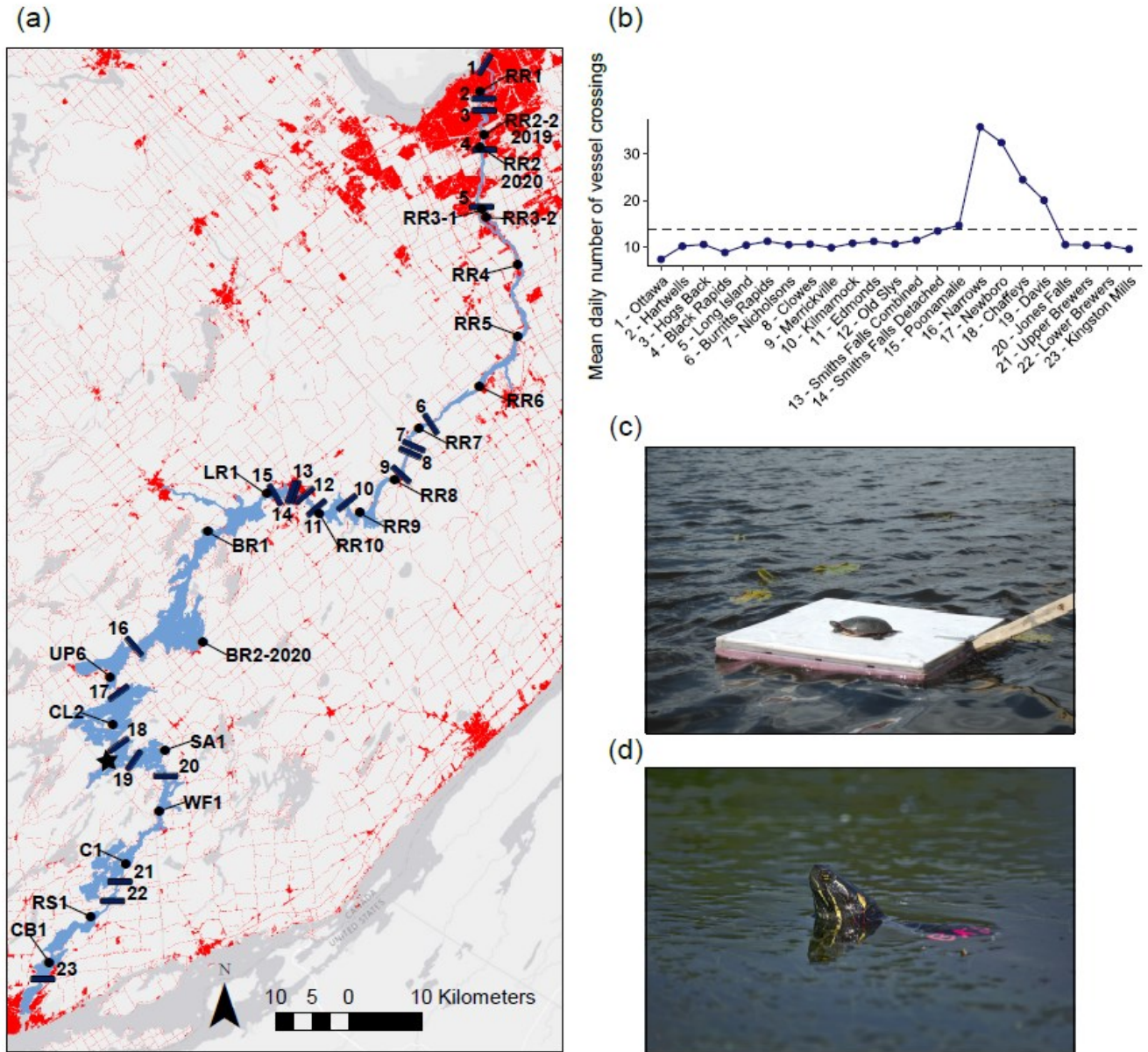


**Figure 1-1** (a) Map of the Rideau Canal Waterway, Ontario, Canada, and the 22 sites (dots labelled with site names) sampled in 2019 and 2020. Solid bars (dark blue) represent the lockstations with their respective numbers used as reference for Figure 1-1b. Urban areas (i.e., building and roads) are depicted in red (dark grey) based on the Southern Ontario Land Resource Information System (SOLRIS) V.3 (OMNRF, 2019). The star shows the location of the Queen's University Biological Station where the

behavioural measurements in a controlled environment occurred. The map was built using ArcGIS® software by ESRI (www.esri.com) (b) Mean daily number of vessel crossings at each lockstation in 2019 based on Parks Canada records. The dashed line represents the mean across all lockstations. The numbers used to identify each lockstation are the reference numbers from Figure 1-1a. (c) Image of a painted turtle (*Chrysemys picta*) on the floating platform during the platform test. (d) Image of a painted turtle that emerged from the water after escaping from the floating platform
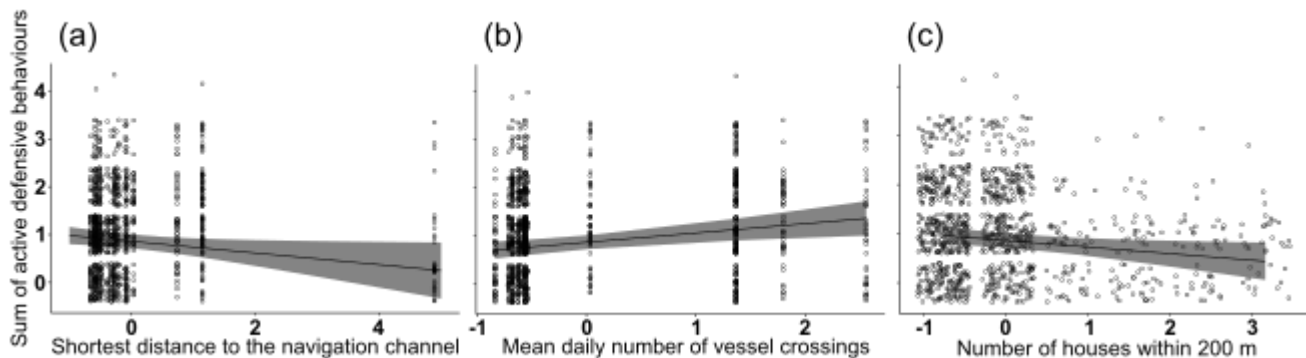


**Figure 1-2** Relationships between the number of active defensive behaviours used by painted turtles (*Chrysemys picta*) and three proxies of human disturbance in the Rideau Canal, Ontario, Canada: (a) shortest aquatic distance to the navigation channel, (b) mean daily number of vessel crossings, and (c) number of houses with access to the canal within 200 m of the sampling site. Predictor variables were standardized (mean zero, unit variance). Each dot represents an observation (N = 1091). Dots were jittered to avoid overlap. Grey areas represent 95 % confidence intervals of the model-predicted effect (black line)

**Supporting Information for Chapter 1**

*Supporting Information 1 – Table S1-1 to S1-15*

**Table S1-1** Count of observations made for the three risk-taking behaviours (Sum of active defensive behaviours, escape latency and emergence of the turtle after escaping) measured on painted turtles at 22 sampling sites across the Rideau Canal, Canada, in 2019 and 2020. Number of unique painted turtles tested are in parentheses. The total number per site correspond to the total of unique painted turtles tested: some turtles were captured between years during the entire project and, thus, are duplicated between years. [a]Sampling sites whose data have been used for repeatability analyses

| Sampling sites | Sum of active defensive behaviours | | | Escape latency | | | Emergence of the turtle after escaping | | |
|---|---|---|---|---|---|---|---|---|---|
| | 2019 | 2020 | Total | 2019 | 2020 | Total | 2019 | 2020 | Total |
| RR1[a] | 27 (21) | 35 (20) | 62 (26) | 27 (21) | 33 (19) | 60 (26) | 25 (19) | 32 (18) | 57 (24) |
| RR2-2-2019 | 15 (9) | 0 (0) | 15 (9) | 14 (8) | 0 (0) | 14 (8) | 14 (8) | 0 (0) | 14 (8) |
| RR2-2020[a] | 0 (0) | 50 (30) | 50 (30) | 0 (0) | 50 (30) | 50 (30) | 0 (0) | 50 (30) | 50 (30) |
| RR3-1[a] | 25 (17) | 0 (0) | 25 (17) | 25 (17) | 0 (0) | 25 (17) | 25 (17) | 0 (0) | 25 (17) |
| RR3-2[a] | 12 (11) | 24 (9) | 36 (16) | 12 (11) | 24 (9) | 36 (16) | 11 (11) | 24 (9) | 35 (16) |
| RR4 | 32 (32) | 0 (0) | 32 (32) | 32 (32) | 0 (0) | 32 (32) | 30 (30) | 0 (0) | 30 (30) |
| RR5 | 46 (43) | 0 (0) | 46 (43) | 45 (42) | 0 (0) | 45 (42) | 43 (40) | 0 (0) | 43 (40) |
| RR6[a] | 32 (22) | 46 (42) | 78 (61) | 31 (22) | 46 (42) | 77 (61) | 32 (22) | 44 (40) | 76 (59) |
| RR7[a] | 31 (29) | 32 (27) | 63 (54) | 25 (23) | 32 (27) | 57 (49) | 24 (22) | 31 (26) | 55 (47) |
| RR8 | 37 (35) | 0 (0) | 37 (35) | 36 (34) | 0 (0) | 36 (34) | 37 (35) | 0 (0) | 37 (35) |
| RR9[a] | 13 (13) | 27 (24) | 40 (33) | 13 (13) | 27 (24) | 40 (33) | 13 (13) | 27 (24) | 40 (33) |
| RR10 | 30 (28) | 0 (0) | 30 (28) | 30 (28) | 0 (0) | 30 (28) | 29 (27) | 0 (0) | 29 (27) |
| LR1 | 51 (47) | 0 (0) | 51 (47) | 50 (46) | 0 (0) | 50 (46) | 48 (44) | 0 (0) | 48 (44) |
| BR1[a] | 13 (13) | 105 (40) | 118 (53) | 12 (12) | 105 (40) | 117 (52) | 12 (12) | 103 (40) | 115 (52) |
| BR2-2020[a] | 0 (0) | 32 (25) | 32 (25) | 0 (0) | 32 (25) | 32 (25) | 0 (0) | 32 (25) | 32 (25) |
| UP6 | 42 (40) | 0 (0) | 42 (40) | 42 (40) | 0 (0) | 42 (40) | 42 (40) | 0 (0) | 42 (40) |
| CL2[a] | 0 (0) | 54 (21) | 54 (21) | 0 (0) | 54 (21) | 54 (21) | 0 (0) | 54 (21) | 54 (21) |
| SA1[a] | 59 (20) | 0 (0) | 59 (20) | 77 (20) | 0 (0) | 77 (20) | 57 (20) | 0 (0) | 57 (20) |
| WF1[a] | 7 (7) | 52 (29) | 59 (35) | 7 (7) | 52 (29) | 59 (35) | 6 (6) | 51 (29) | 57 (34) |
| C1[a] | 13 (12) | 27 (15) | 40 (26) | 13 (12) | 27 (15) | 40 (26) | 13 (12) | 23 (12) | 36 (23) |
| RS1[a] | 52 (16) | 22 (13) | 74 (29) | 51 (16) | 22 (13) | 73 (29) | 49 (16) | 22 (13) | 71 (29) |
| CB1[a] | 35 (16) | 39 (36) | 74 (50) | 30 (16) | 39 (36) | 69 (50) | 29 (16) | 39 (36) | 68 (50) |
| TOTAL | 572 (431) | 545 (331) | 1117 (730) | 572 (420) | 543 (330) | 1115 (720) | 539 (410) | 532 (323) | 1071 (704) |

**Table S1-2** Count of painted turtles per number of trials performed for the three risk-taking behaviours: Sum of active defensive behaviours, escape latency and emergence of the turtle after escaping. (A) Count from the dataset to calculate repeatability estimates: include only individuals with more than one observation and from sites with more than 5 unique turtles (15 sampling sites; Table S1-1). (B) Count from the dataset used for the (generalized) linear mixed models to assess the relationship between risk-taking behaviours and human disturbance. Some turtles were captured and tested between sampling years (2019 and 2020). Numbers in parentheses represent the number of painted turtles tested in the controlled setting

**(A) Repeatability**

| Number of trials | Number of turtles | | |
| --- | --- | --- | --- |
| | Active defensive behaviours | Escape latency | Emergence of the turtle |
| 2 | 92 (52) | 93 (29) | 97 (38) |
| 3 | 67 (28) | 48 (46) | 57 (31) |
| 4 | 37 (1) | 52 (1) | 37 (0) |
| 5 | 2 (0) | 2 (0) | 1 (0) |
| 6 | 2 (0) | 2 (0) | 3 (0) |
| 7 | 2 (0) | 2 (0) | 1 (0) |
| Total number of turtles | 202 (81) | 199 (76) | 196 (69) |
| Turtles tested between years | 31 (0) | 29 (0) | 28 (0) |

**(B) (Generalized) linear mixed models**

| Number of trials | Number of turtles | | |
| --- | --- | --- | --- |
| | Active defensive behaviours | Escape latency | Emergence of the turtle |
| 1 | 509 (41) | 502 (46) | 489 (50) |
| 2 | 110 (52) | 111 (29) | 115 (38) |
| 3 | 68 (28) | 49 (46) | 58 (31) |
| 4 | 37 (1) | 52 (1) | 37 (0) |
| 5 | 2 (0) | 2 (0) | 1 (0) |
| 6 | 2 (0) | 2 (0) | 3 (0) |
| 7 | 2 (0) | 2 (0) | 1 (0) |
| Total number of turtles | 730 (122) | 720 (122) | 704 (119) |
| Turtles tested between years | 32 (0) | 30 (0) | 29 (0) |

**Table S1-3** Pearson (lower panel) and Spearman (upper panel) correlation coefficients between the risk-taking behaviours measured on painted turtles. All correlations were significant (p value < 0.01). Head emergence and movement latencies were not kept in further analyses given their relatedness with escape latency (Pearson correlation coefficients over 0.6)

|  | Active defenses | HEL | ML | EL | Emergence |
|---|---|---|---|---|---|
| Sum of active defensive behaviours (Active defenses) | – | -0.31 | -0.27 | -0.24 | 0.28 |
| Head emergence latency (HEL) | -0.15 | – | 0.47 | 0.45 | -0.28 |
| Movement latency (ML) | -0.24 | 0.60 | – | 0.95 | -0.20 |
| Escape latency (EL) | -0.24 | 0.60 | 0.99 | – | -0.16 |
| Emergence of the turtle after escaping (Emergence) | 0.26 | -0.16 | -0.19 | -0.19 | – |

**Table S1-4** Mean daily number of vessel crossings of the 23 lockstations of the Rideau Canal, Canada. The count of vessel crossings was collected during the operational period (May to October) of 2019 and 2020 from the Ottawa River (Ottawa) to Lake Ontario (Kingston Mills). The mean number represents the mean between 2019 and 2020. Data were provided by Parks Canada

| Lockstations | 2019 | 2020 | Mean |
|---|---|---|---|
| 1. Locks 1-8 (Ottawa) | 7.33 | 4.41 | 5.87 |
| 2. Locks 9-10 (Hartwells) | 10.14 | 6.81 | 8.48 |
| 3. Locks 11-12 (Hogs Back) | 10.51 | 6.79 | 8.65 |
| 4. Lock 13 (Black Rapids) | 8.80 | 6.96 | 7.88 |
| 5. Locks 14-16 (Long Island) | 10.37 | 6.67 | 8.52 |
| 6. Lock 17 (Burritts Rapids) | 11.21 | 8.01 | 9.61 |
| 7. Lock 18-19 (Nicholsons) | 10.46 | 7.48 | 8.97 |
| 8. Lock 20 (Clowes) | 10.57 | 7.52 | 9.04 |
| 9. Locks 21-23 (Merrickville) | 9.82 | 6.90 | 8.36 |
| 10. Lock 24 (Kilmarnock) | 10.76 | 7.33 | 9.04 |
| 11. Lock 25 (Edmonds) | 11.18 | 7.30 | 9.24 |
| 12. Locks 26-27 (Old Slys) | 10.61 | 7.29 | 8.95 |
| 13. Lock 29a (Smiths Falls Combined) | 11.43 | 8.32 | 9.87 |
| 14. Lock 31 (Smiths Falls Detached) | 13.41 | 11.77 | 12.59 |
| 15. Lock 32 (Poonamalie) | 14.63 | 13.06 | 13.84 |
| 16. Lock 35 (Narrows) | 35.75 | 31.98 | 33.86 |
| 17. Lock 36 (Newboro) | 32.38 | 22.66 | 27.52 |
| 18. Lock 37 (Chaffeys) | 24.43 | 15.06 | 19.75 |
| 19. Lock 38 (Davis) | 19.99 | 11.60 | 15.80 |
| 20. Locks 39-42 (Jones Falls) | 10.48 | 5.98 | 8.23 |
| 21. Locks 43-44 (Upper Brewers) | 10.39 | 6.05 | 8.22 |
| 22. Lock 45 (Lower Brewers) | 10.31 | 6.04 | 8.18 |
| 23. Locks 46-49 (Kingston Mills) | 9.51 | 5.85 | 7.68 |

**Table S1-5** Pearson (lower panel) and Spearman (upper panel) correlation coefficients between continuous predictor variables included in each initial mixed model before multicollinearity tests and model selection. Coefficients > 0.80 are in bold. A table is available for each model given that the variables estimating human disturbance were adapted for each risk-taking behaviour used as response variable in models: (A) Sum of active defensive behaviours used, (B) escape latency and (C) emergence of the turtle after escaping (see the selection process for the variables quantifying human disturbance in the Supporting Information 3 of Chapter 1)

**(A) Sum of active defensive behaviours used**

| Variables | 1. | 2. | 3. | 4. | 5. | 6. | 7. | 8. | 9. |
|---|---|---|---|---|---|---|---|---|---|
| 1. Number of houses within 200 m | – | 0.45 | 0.07 | -0.32 | -0.25 | -0.10 | 0.09 | -0.20 | 0.04 |
| 2. Proportion of urban areas within 900 m | **0.80** | – | -0.13 | -0.72 | -0.29 | -0.44 | 0.16 | -0.52 | -0.35 |
| 3. Order of the trial | 0.15 | 0.10 | – | 0.23 | -0.11 | 0.01 | 0.02 | 0.24 | -0.02 |
| 4. Julian Day | -0.40 | -0.56 | 0.16 | – | 0.25 | 0.40 | -0.17 | 0.56 | 0.19 |
| 5. Hour | -0.28 | -0.28 | -0.09 | 0.31 | – | 0.06 | -0.14 | 0.28 | 0.05 |
| 6. Turtle temperature (°C) | -0.19 | -0.34 | 0.04 | 0.44 | -0.01 | – | -0.07 | 0.39 | 0.19 |
| 7. Carapace length (mm) | 0.15 | 0.22 | 0.04 | -0.17 | -0.13 | -0.06 | – | -0.11 | -0.12 |
| 8. Shortest aquatic distance to the navigation distance (m) | -0.10 | -0.22 | 0.10 | 0.10 | 0.01 | 0.25 | -0.01 | – | 0.37 |
| 9. Mean daily number of vessel crossings in 2019 | -0.11 | -0.35 | 0.02 | 0.33 | 0.13 | 0.32 | -0.08 | 0.49 | – |

**(B) Escape latency**

| Variables | 1. | 2. | 3. | 4. | 5. | 6. | 7. | 8. | 9. | 10. |
|---|---|---|---|---|---|---|---|---|---|---|
| 1. Number of houses within 400 m | – | 0.45 | 0.01 | -0.24 | -0.15 | -0.06 | 0.13 | -0.28 | 0.13 | -0.02 |
| 2. Proportion of urban areas within 200 m | 0.43 | – | 0.02 | -0.44 | -0.06 | -0.20 | 0.14 | -0.10 | -0.30 | 0.06 |
| 3. Order of the trial | -0.01 | 0.20 | – | 0.23 | -0.09 | 0.01 | 0.02 | 0.24 | -0.02 | -0.03 |
| 4. Julian Day | -0.35 | -0.39 | 0.16 | – | 0.19 | 0.40 | -0.17 | 0.56 | 0.19 | -0.27 |
| 5. Hour | -0.12 | -0.15 | -0.11 | 0.23 | – | 0.09 | -0.12 | 0.28 | < -0.01 | -0.41 |
| 6. Turtle temperature (°C) | -0.16 | -0.22 | 0.04 | 0.44 | 0.03 | – | -0.07 | 0.39 | 0.19 | 0.10 |
| 7. Carapace length (mm) | 0.17 | 0.18 | 0.04 | -0.17 | -0.12 | -0.06 | – | -0.11 | -0.12 | 0.09 |
| 8. Shortest aquatic distance to the navigation distance (m) | -0.25 | -0.06 | 0.10 | 0.10 | 0.11 | 0.25 | -0.01 | – | 0.37 | -0.27 |
| 9. Mean daily number of vessel crossings in 2019 | 0.02 | -0.21 | 0.02 | 0.33 | 0.09 | 0.32 | -0.08 | 0.49 | – | -0.09 |
| 10. Wind speed (Beaufort scale) | 0.01 | < 0.01 | 0.03 | -0.26 | -0.34 | 0.02 | 0.07 | -0.03 | -0.13 | – |

**(C) Emergence of the turtle after escaping**

| Variables | 1. | 2. | 3. | 4. | 5. | 6. | 7. | 8. | 9. |
|---|---|---|---|---|---|---|---|---|---|
| 1. Number of houses within 300 m | – | 0.64 | 0.12 | -0.22 | -0.11 | -0.15 | 0.08 | -0.12 | 0.05 |
| 2. Proportion of urban areas within 600 m | **0.82** | – | -0.11 | -0.73 | -0.23 | -0.38 | 0.19 | -0.50 | -0.10 |
| 3. Order of the trial | 0.10 | 0.12 | – | 0.23 | -0.09 | 0.01 | 0.02 | 0.24 | -0.02 |
| 4. Julian Day | -0.42 | -0.54 | 0.16 | – | 0.19 | 0.40 | -0.17 | 0.56 | 0.19 |
| 5. Hour | -0.12 | -0.19 | -0.11 | 0.23 | – | 0.09 | -0.11 | 0.28 | < -0.01 |
| 6. Turtle temperature (°C) | -0.32 | -0.32 | 0.04 | 0.44 | 0.03 | – | -0.07 | 0.39 | 0.19 |
| 7. Carapace length (mm) | 0.13 | 0.23 | 0.04 | -0.17 | -0.12 | -0.06 | – | -0.11 | -0.12 |
| 8. Shortest aquatic distance to the navigation distance (m) | -0.18 | -0.18 | 0.10 | 0.10 | 0.11 | 0.25 | -0.01 | – | 0.37 |
| 9. Mean daily number of vessel crossings in 2019 | -0.18 | -0.27 | 0.02 | 0.33 | 0.09 | 0.32 | -0.08 | 0.49 | – |

**Table S1-6** Descriptive statistics of continuous variables included in the initial mixed models as predictor variables before standardization (mean zero, unit variance). Year of the trial, sex and testing environment (i.e., made in a controlled environment or directly in the field) were included as categorical predictor variables in models

| Variables | Range | Mean | Standard deviation |
|---|---|---|---|
| Julian Day | 128-234 | 185.93 | 29.71 |
| Hour | 730-2020 | 1244.37 | 249.94 |
| Order of the trial | 1-7 | 1.60 | 0.97 |
| Carapace length (mm) | 30-188 | 138.24 | 18.69 |
| Hour of the platform test | 730-2020 | 1295.05 | 249.25 |
| Turtle temperature (°C) | 9.5-34 | 22.94 | 4.69 |
| Shortest aquatic distance to the navigation distance (m) | 15.13-6140.65 | 744.17 | 1104.15 |
| Mean daily number of vessel crossings in 2019 | 8.74-34.07 | 14.99 | 7.46 |
| Number of houses within 200 m | 0-5 | 0.97 | 1.28 |
| Number of houses within 300 m | 0-17 | 2.91 | 4.33 |
| Number of houses within 400 m | 0-28 | 6.41 | 8.41 |
| Proportion of urban areas within 200 m | 0-0.57 | 0.05 | 0.14 |
| Proportion of urban areas within 600 m | 0-0.78 | 0.14 | 0.23 |
| Proportion of urban areas within 900 m | 0-0.81 | 0.16 | 0.23 |
| Wind speed (Beaufort scale) | 0-6 | 1.91 | 1.81 |

**Table S1-7** Generalized variance inflation factors (GVIF) for the predictor variables included in the three mixed models using different risk-taking behaviours as response variable: Sum of active defensive behaviours, escape latency and emergence of the turtle after escaping. Combination of predictor variables are not the same across models. Variable with a GVIF$^{(1/(2*df))}$ > 2 were not included in the initial model before model selection (column *Before*). The GVIF of the variables after the deletion of variables with GVIF$^{(1/(2*df))}$ > 2 are available in the column After. [b]The hour for the escape latency and the emergence of the turtle after escaping are not the same as the hour for the sum of active defensive behaviours: It corresponds to the hour when the platform test was performed for escape latency and emergence of the turtle after escaping

| Variables | GVIF$^{(1/(2*df))}$ | | | | | |
| | Sum of active defensive behaviours | | Escape latency | | Emergence of the turtle after escaping | |
| | Before | After | Before | After | Before | After |
| Number of houses within 200 m | 1.84 | 1.25 | – | – | – | – |
| Number of houses within 300 m | – | – | | – | 1.86 | 1.17 |
| Number of houses within 400 m | – | – | 1.36 | – | – | – |
| Proportion of urban areas within 200 m | – | – | 1.28 | – | – | – |
| Proportion of urban areas within 600 m | – | – | – | – | **2.13** | – |
| Proportion of urban areas within 900 m | **2.08** | – | – | – | – | – |
| Shortest aquatic distance to the navigation distance (m) | 1.25 | 1.25 | 1.40 | – | 1.23 | 1.23 |
| Mean daily number of vessel crossings in 2019 | 1.28 | 1.26 | 1.40 | – | 1.23 | 1.23 |
| Order of the trial | 1.11 | 1.09 | 1.12 | – | 1.12 | 1.10 |
| Sex | 1.12 | 1.10 | 1.07 | – | 1.08 | 1.07 |
| Testing environment (controlled setting) | 1.50 | 1.50 | 1.84 | – | 1.41 | 1.40 |
| Year | 1.22 | 1.22 | 1.13 | – | 1.13 | 1.11 |
| Julian day | 1.69 | 1.64 | 1.50 | – | 1.46 | 1.40 |
| Hour[b] | 1.27 | 1.27 | 1.32 | – | 1.21 | 1.22 |
| Turtle temperature (°C) | 1.45 | 1.44 | 1.18 | – | 1.29 | 1.27 |
| Carapace length (mm) | 1.12 | 1.12 | 1.12 | – | 1.09 | 1.08 |
| Wind speed (Beaufort scale) | – | – | 1.38 | – | – | – |

**Table S1-8** Sources of variance (VG: group-level variance; VR: residual variance) and repeatability estimates (R) separately calculated for each testing environment (i.e., tests performed in the field vs. in the controlled environment) for three risk-taking behaviours in painted turtles (*Chrysemys picta*): sum of active defensive behaviours, escape latency, and emergence of the turtle after escaping. The unadjusted repeatability estimates only included turtle identity as random effect, while the adjusted repeatability estimates also included sex, trial order, and year as fixed effects, and sampling site identity as a random effect (VG - site and Rsite). Significance [95 % confidence intervals] of the variances and repeatability estimates were determined with likelihood ratio tests. The coefficient of determination (R2) of the fixed effects included in the adjusted repeatability estimates was calculated. Sources of variances for the emergence of the turtle after escaping were estimated from the link-scale approximation and repeatability estimates from the original scale. Number of individuals tested (Nb. ID) with the total number of observations (Nb. Entries) for each behaviour are provided. No information is available for the adjusted model in the controlled environment with emergence of the turtle after escaping as the response variable given that the model fail to converge

A) IN THE FIELD

| Behaviours | Nb. ID (Nb. Entries) | $V_{G\text{-individual}}$ | $V_{G\text{-site}}$ | $V_R$ | $R_{individual}$ | $R_{site}$ | $R^2_{fixed}$ |
|---|---|---|---|---|---|---|---|
| **Sum of active defensive behaviours** | | | | | | | |
| Unadjusted | 84 (218) | 0.427 [0.268 - 0.606] | – | 0.308 [0.245 - 0.383] | 0.581 [0.444 - 0.676] | – | – |
| Adjusted | 83 (215) | 0.274 [0.158 - 0.432] | 0.145 [0.000 - 0.406] | 0.295 [0.228 - 0.362] | 0.384 [0.226 - 0.564] | 0.203 [0.000 - 0.410] | 0.04 |
| **Escape latency** | | | | | | | |
| Unadjusted | 81 (211) | 0.550 [0.287 - 0.828] | – | 0.779 [0.609 - 0.978] | 0.414 [0.248 - 0.551] | – | – |
| Adjusted | 80 (208) | 0.662 [0.346 - 0.964] | 0.059 [0.000 - 0.283] | 0.644 [0.488 - 0.799] | 0.469 [0.295 - 0.618] | 0.045 [0.000 - 0.195] | 0.06 |
| **Emergence of the turtle after escaping** | | | | | | | |
| Unadjusted | 81 (210) | 4.393 [1.125 - 63.745] | – | 4.95 [4.410 - 6.747] | 0.398 [0.143 - 0.583] | – | – |
| Adjusted | 80 (207) | 3.425 [0.596 - 18.918] | 1.228 [0.000 - 3.700] | 4.907 [4.080 - 6.540] | 0.358 [0.080 - 0.766] | 0.150 [0.000 - 0.458] | 0.11 |

B) IN THE CONTROLLED ENVIRONMENT

| Behaviours | Nb. ID (Nb. Entries) | $V_{G\text{ - individual}}$ | $V_{G\text{ - site}}$ | $V_R$ | $R_{individual}$ | $R_{site}$ | $R^2{}_{fixed}$ |
|---|---|---|---|---|---|---|---|
| **Sum of active defensive behaviours** | | | | | | | |
| Unadjusted | 81 (192) | 0.280 [0.130 - 0.470] | – | 0.524 [0.394 - 0.675] | 0.349 [0.159 - 0.498] | – | – |
| Adjusted | 79 (187) | 0.202 [0.052 - 0.370] | 0.039 [0.000 - 0.190] | 0.528 [0.388 - 0.661] | 0.263 [0.091 - 0.445] | 0.051 [0.000 - 0.237] | 0.07 |
| **Escape latency** | | | | | | | |
| Unadjusted | 76 (200) | 0.560 [0.275 - 0.882] | – | 1.004 [0.770 - 1.271] | 0.358 [0.190 - 0.495] | – | – |
| Adjusted | 74 (195) | 0.508 [0.251 - 0.833 | 0.206 [0.000 - 0.823] | 0.817 [0.618 - 1.023] | 0.332 [0.170 - 0.511] | 0.134 [0.000 - 0.401] | 0.11 |
| **Emergence of the turtle after escaping** | | | | | | | |
| Unadjusted | 69 (169) | 31.54 [61.794 - 548.006] | – | 6.364 [5.272 - 11.667] | 0.577 [0.546 - 0.782] | – | – |
| Adjusted | – | – | – | – | – | – | – |

**Table S1-9** Summary statistics of the multivariate mixed model performed with the package MCMCglmm and the three risk-taking behaviours as response variables: Sum of active defensive behaviours, escape latency and emergence of the turtle after escaping. We used a log(x+1) transformation to normalize escape latency. All the values are significant according to the 95% Bayesian credibility interval. Priors used: variance V = 1 and belief parameter $\nu$ = 2.002 (inverse-Wishart priors). Iterations = 200,000; burn-in = 50,000; thinning = 500. Analyses were based on Pich et al. (2019)

**(A) G-structure (Group level)**

Variances among individuals (diagonal) and between-behaviour correlations at the among-individual level (upper panel)

| | Family | Active.defenses | EL | Emergence |
|---|---|---|---|---|
| Sum of active defensive behaviours (Active defenses) | Gaussian | 0.43 | -0.17 | 0.67 |
| Escape latency (EL) | Gaussian | – | 0.47 | -0.36 |
| Emergence of the turtle after escaping (Emergence) | Categorical | – | – | 4.24 |

**(B) R-Structure (Residual level)**

Variances within individuals (diagonal) and between-behaviour correlations at the within-individual level (upper panel)

| | Family | Active.defenses | EL | Emergence |
|---|---|---|---|---|
| Sum of active defensive behaviours (Active defenses) | Gaussian | 0.44 | -0.09 | 0.19 |
| Escape latency (EL) | Gaussian | – | 0.90 | -0.47 |
| Emergence of the turtle after escaping (Emergence) | Categorical | – | – | 1.94 |

**Table S1-10** Pearson and Spearman correlation coefficients for each risk-taking behaviour between measurements performed in the field and in the controlled environment. All correlation coefficients are significant (p value < 0.01). Numbers in parentheses represent the number of turtles with measurements in both testing environment

| Behaviours | Correlation coefficients | |
|---|---|---|
| | Pearson | Spearman |
| Sum of active defensive behaviours (N = 122) | 0.397 | 0.383 |
| Escape latency (N = 121) | 0.389 | 0.312 |
| Emergence of the turtle after escaping (N = 118) | 0.327 | 0.327 |

**Table S1-11** Compilation of the risk-taking behaviours measured in turtles from literature. We extracted data from these studies: A short description of the behaviour, the average time period between the first and the last trial made on turtles to measure the behaviour (only applies for studies that took repeated measurements), the age group as it is mentioned in the article, the number of turtles tested, the number of repeated measurements on each turtle, the repeatability estimates if applicable, and if the study assesses the relationship between human disturbance and the behaviour. [a]not the number of unique turtle tested: It is a total of observations

| Reference | Risk-taking behaviours | Time period | Age | Number | Number of repetitions | Repeatability | Linked to human disturbance |
|---|---|---|---|---|---|---|---|
| **Blanding's turtles** (*Emydoidea blandingii*) | | | | | | | |
| Allard et al. (2019) | Difference in latency to consume food (Food - Predator test) | 3 weeks | Juvenile | 23 | 3 | 0.28 (ICC) | No |
| | Difference in percent of time moving (Predator - Food test) | 3 weeks | Juvenile | 23 | 3 | 0.24 (ICC) | No |
| | Difference in the rate of surfacing (Predator - Food test) | 3 weeks | Juvenile | 23 | 3 | 0.42 (ICC) | No |
| **Desert tortoises** (*Gopherus agassizii*) | | | | | | | |
| Germano et al. (2017) | Head emergence latency | Few weeks | Juvenile | 60 | 2-3 | – | No |
| **Eastern box turtles** (*Terrapene carolina*) | | | | | | | |
| Carlson & Tetzlaff (2020) | Head emergence latency | 1-3 years | Adult | 21 | 2-4 | 0.69 [0.48-0.88] | No |
| | Movement latency | 2 years | Juvenile | 20 | 4 | 0.78 [0.36-0.94] | No |
| Kashon & Carlson (2018) | Head emergence latency | Few months | Adult | 33 | 2-7 | 0.73 [0.61-0.82] | No |
| | Movement latency | Few months | Adult | 33 | 2-7 | 0.43 [0.25-0.58] | No |
| Pich et al. (2019) | Head emergence latency - confinement test | Few weeks | Adult | 15 | 2 | 0.77 [0.42-0.92] | No |

| | | | | | | | |
|---|---|---|---|---|---|---|---|
| | Head emergence latency - predation simulation | Few weeks | Adult | 15 | 2 | 0.76 [0.44-0.92] | No |
| | Number of active defensive behaviours | Few weeks | Adult | 15 | 2 | 0.63 [0.34-0.86] | No |
| **European pond turtles** (*Emys orbicularis*) | | | | | | | |
| Ibáñez et al. (2018) | Appearance time | Few months | Adult | 22 | 3 | 0.67 [0.38-0.81] | No |
| | Righting attempts | Few months | Adult | 22 | 3 | 0.58 [0.33-0.76] | No |
| | Waiting time | Few months | Adult | 22 | 3 | 0.22 [0.00-0.45] | No |
| **Green turtles** (*Chelonia mydas*) | | | | | | | |
| Griffin et al. (2017) | Boldness index from 5 measurements: Flight initiation distance, latency to forage, abrupt burst response and flight to nearest neighbor | 1 month | Immature | 19 | 3-14 | 0.132 [0.001-0.253] | No |
| **Hermann's tortoises** (*Eurotestudo boettgeri*) | | | | | | | |
| Mafli et al. (2011) | Boldness index from 4 measurements: Immediate response to handling, latency to move towards the handed food, latency to eat and duration of eating | 2 weeks | Adult | 25 | 3 | 0.54 | No |
| **Painted turtles** (*Chrysemys picta*) | | | | | | | |
| Polich & Barazowski (2016) | Flight initiation distance | 26 days | NA | 335[a] | NA | – | Yes |
| Roth et al. (2020) | Body movement latency | Same day | Adult | 86 | 3 | 0.783 (Cronbach's alpha) | No |

| | Head movement latency | Same day | Adult | 86 | 3 | 0.760 (Cronbach's alpha) | No |
|---|---|---|---|---|---|---|---|
| **Red-eared slider turtles** (*Trachemys scripta*) | | | | | | | |
| Carter et al. (2016) | Latency to explore | 72-120h | Hatchlings | 394 | 2 | 0.13-0.43 (according to different treatments) | No |
| | Righting latency | 24-72h | Hatchlings | 394 | 2 | 0.22-0.72 (according to different treatments) | No |
| **Spanish terrapins** (*Mauremys leprosa*) | | | | | | | |
| Ibáñez et al. (2013a) | Appearance time | – | Adult | 20 | 1 | – | No |
| | Righting time | – | Adult | 20 | 1 | – | No |
| Ibáñez et al. (2015) | Appearance time | – | Adult | 20 | 1 | – | No |
| | Waiting time | – | Adult | 20 | 1 | – | No |
| Ibáñez et al. (2018) | Appearance time | Few months | Adult | 29 | 3 | 0.58 [0.37-0.74] | No |
| | Righting attempts | Few months | Adult | 29 | 3 | 0.69 [0.56-0.82] | No |
| | Waiting time | Few months | Adult | 29 | 3 | 0.14 [0.00-0.30] | No |

**Table S1-12** Moran's I correlation coefficients estimated at different distances in meters for each risk-taking behaviour measured in painted turtles: Sum of active defensive behaviours used, escape latency and emergence of the turtle after escaping. N = number of sampling site pairs compared for each distance. Significant Moran's I correlation coefficients are in bold (p value < 0.05)

| N | distance (m) | Active defensive behaviours | | Escape latency | | Emergence | |
|---|---|---|---|---|---|---|---|
| | | coefficient | p value | coefficient | p value | coefficient | p value |
| 30 | 4926 | **0.654** | **0.003** | -0.203 | 0.712 | **0.527** | **0.011** |
| 36 | 12263 | 0.052 | 0.334 | 0.085 | 0.285 | **0.427** | **0.023** |
| 42 | 19601 | -0.126 | 0.636 | 0.115 | 0.232 | **0.343** | **0.039** |
| 38 | 26938 | 0.155 | 0.187 | 0.170 | 0.168 | **0.467** | **0.012** |
| 36 | 34276 | 0.293 | 0.074 | 0.302 | 0.066 | 0.308 | 0.062 |
| 42 | 41613 | 0.181 | 0.152 | 0.007 | 0.398 | 0.306 | 0.053 |
| 38 | 48951 | -0.191 | 0.727 | -0.083 | 0.556 | -0.219 | 0.769 |
| 34 | 56288 | -0.291 | 0.834 | -0.346 | 0.890 | -0.322 | 0.868 |
| 28 | 63626 | -0.007 | 0.427 | 0.198 | 0.172 | -0.332 | 0.842 |
| 22 | 70963 | 0.020 | 0.397 | -0.244 | 0.734 | -0.104 | 0.560 |
| 22 | 78301 | 0.050 | 0.352 | -0.365 | 0.842 | -0.200 | 0.680 |
| 20 | 85638 | 0.049 | 0.327 | -0.533 | 0.905 | -0.545 | 0.919 |
| 22 | 92976 | -0.513 | 0.923 | 0.040 | 0.351 | -0.774 | 0.990 |
| 18 | 100313 | -0.700 | 0.972 | 0.208 | 0.193 | -0.707 | 0.976 |
| 12 | 107651 | -0.695 | 0.932 | -0.763 | 0.946 | -0.440 | 0.806 |
| 10 | 114989 | -0.239 | 0.590 | 0.083 | 0.291 | -0.713 | 0.901 |
| 6 | 122326 | -1.008 | 0.903 | -0.610 | 0.735 | -0.532 | 0.756 |
| 6 | 129664 | -0.804 | 0.945 | -0.282 | 0.443 | -0.582 | 0.885 |

**Table S1-13** Summary statistics for the final linear mixed models with the sum of active defensive behaviours used by painted turtles as the response variable. We fitted the model with a random variable that represent sampling site but including the effect of spatial autocorrelation. We detected a positive significant spatial autocorrelation on the sum of active defensive behaviours for sites within less than 5 km of each other (Table S1-12). We also included turtle identity as a random effect. We provided for each predictor variable of the final model after model selection: the estimate, the standard error (SE), the t-value, the p-value and the 95% confidence intervals (95% CI). REML was set as TRUE for the calculation of the model statistics and set as FALSE for model selection. All the continuous predictor variables were scaled (mean zero, unit variance) before model selection. Reference factors are in parentheses for categorical predictor variables

| Variables | Estimate | SE | t-value | p-value | 95% CI |
|---|---|---|---|---|---|
| **Sum of active defensive behaviours** | 714 individuals (1091 observations) $R^2$ - marginal: 0.07; $R^2$ - conditional: 0.52 | | | | |
| Number of houses within 200 m | -0.098 | 0.052 | -1.894 | 0.063 | [-0.199 to 0.003] |
| Distance to navigation channel | -0.122 | 0.058 | -2.103 | 0.049 | [-0.236 to -0.008] |
| Mean daily number of vessel crossings | 0.196 | 0.066 | 2.969 | 0.009 | [0.066 to 0.325] |
| Sex (Male) | 0.329 | 0.070 | 4.701 | < 0.001 | [0.192 to 0.466] |
| Testing environment (controlled setting) | -0.217 | 0.068 | -3.212 | 0.001 | [-0.350 to -0.085] |
| Carapace length | 0.113 | 0.037 | 3.027 | 0.003 | [0.040 to 0.186] |

**Table S1-14** Summary statistics for the final (generalized) linear mixed models with risk-taking behaviours in painted turtles as response variable: Sum of active defensive behaviours used, escape latency and emergence of the turtle after escaping. We performed analyses with two subsets: i) observations only made in a controlled environment, and ii) only made in the field, and compared the results obtained to those with the complete dataset. For each model, we provided for each predictor variable: the estimate, the standard error (SE), the t-value (z-value for the binomial model), the p-value and the 95% confidence intervals (95% CI). REML was set as TRUE for the calculation of the model statistics. All the continuous predictor variables were scaled (mean zero, unit variance) before model selection. Reference factors are in parentheses for categorical predictor variables. Turtle and sampling site identity were included as random effects in the model for sum of active defensive behaviours with the complete dataset and the subset with only the observations made in the field, while only turtle identity was included in the other models

| Variables | Estimate | SE | t-value | p-value | 95% CI |
|---|---|---|---|---|---|
| **Sum of active defensive behaviours** | | | | | |
| Only in the controlled environment | 117 individuals (225 observations) $R^2$ - marginal: 0.12; $R^2$ - conditional: 0.37 | | | | |
| Mean daily number of vessel crossings | 0.262 | 0.066 | 3.978 | < 0.001 | [0.133 to 0.392] |
| Sex (Male) | 0.452 | 0.141 | 3.196 | 0.002 | [0.175 to 0.730] |
| | | | | | |
| Only in the field | 714 individuals (866 observations) $R^2$ - marginal: 0.08; $R^2$ - conditional: 0.62 | | | | |
| Number of houses within 200 m | -0.145 | 0.060 | 2.416 | 0.026 | [-0.263 to -0.027] |
| Distance to navigation channel | -0.116 | 0.060 | 1.944 | 0.067 | [-0.233 to 0.001] |
| Mean daily number of vessel crossings | 0.170 | 0.068 | 2.500 | 0.023 | [0.037 to 0.303] |
| Sex (Male) | 0.321 | 0.073 | 4.395 | < 0.001 | [0.178 to 0.465] |
| Carapace length | 0.126 | 0.039 | 3.219 | 0.001 | [0.049 to 0.203] |
| | | | | | |
| Complete dataset | 714 individuals (1091 observations) $R^2$ - marginal: 0.10; $R^2$ - conditional: 0.52 | | | | |
| Number of houses within 200 m | -0.134 | 0.058 | 2.316 | 0.031 | [-0.247 to -0.021] |
| Distance to navigation channel | -0.122 | 0.057 | 2.122 | 0.047 | [-0.234 to -0.009] |
| Mean daily number of vessel crossings | 0.194 | 0.065 | 2.986 | 0.008 | [0.067 to 0.321] |
| Sex (Male) | 0.327 | 0.070 | 4.687 | < 0.001 | [0.191 to 0.464] |
| Testing environment (controlled setting) | -0.218 | 0.068 | 3.228 | 0.001 | [-0.350 to -0.086] |
| Carapace length | 0.112 | 0.037 | 3.014 | 0.003 | [0.040 to 0.186] |
| | | | | | |
| **Escape latency** | | | | | |
| Only in the controlled environment | 117 individuals (238 observations) $R^2$ - marginal: 0.22; $R^2$ - conditional: 0.50 | | | | |
| Urban areas within 200 m | 3.307 | 1.502 | 2.201 | 0.030 | [0.362 to 6.251] |
| Mean daily number of vessel crossings | -0.185 | 0.089 | 2.092 | 0.038 | [-0.359 to -0.012] |
| Order of the trial | -0.399 | 0.076 | 5.274 | < 0.001 | [-0.547 to -0.251] |
| Sex (Male) | -0.431 | 0.190 | 2.266 | 0.025 | [-0.804 to -0.058] |
| Hour of the platform test | -0.272 | 0.099 | 2.757 | 0.006 | [-0.466 to -0.079] |
| Carapace length | 0.296 | 0.101 | 2.924 | 0.004 | [0.098 to 0.495] |

| Only in the field | 580 individuals (691 observations) | | $R^2$ - marginal: 0.08; $R^2$ - conditional: 0.40 | | |
|---|---|---|---|---|---|
| Order of the trial | -0.131 | 0.040 | 3.303 | 0.001 | [-0.208 to -0.053] |
| Year (2020) | -0.239 | 0.086 | 2.766 | 0.006 | [-0.408 to -0.070] |
| Turtle temperature | -0.195 | 0.050 | 3.938 | < 0.001 | [-0.292 to -0.098] |
| Carapace length | 0.100 | 0.042 | 2.358 | 0.019 | [-0.017 to 0.183] |
| Wind scale (Beaufort scale) | -0.139 | 0.046 | 3.037 | 0.002 | [-0.229 to -0.050] |

| Complete dataset | 596 individuals (919 observations) | | $R^2$ - marginal: 0.10; $R^2$ - conditional: 0.44 | | |
|---|---|---|---|---|---|
| Order of the trial | -0.231 | 0.036 | 6.415 | < 0.001 | [-0.302 to -0.161] |
| Julian Day | 0.141 | 0.053 | 2.645 | 0.008 | [0.036 to 0.245] |
| Turtle temperature | -0.199 | 0.047 | 4.245 | < 0.001 | [-0.291 to -0.107] |
| Carapace length | 0.167 | 0.042 | 4.013 | < 0.001 | [0.085 to 0.248] |
| Wind scale (Beaufort scale) | -0.176 | 0.036 | 4.899 | < 0.001 | [-0.246 to -0.106] |

**Emergence of the turtle after escaping**

| Only in the controlled setting | 119 individuals (219 observations) | | $R^2$ - marginal: 0.00; $R^2$ - conditional: <0.001 | | |
|---|---|---|---|---|---|

*no significant variables*

| Only in the field | 701 individuals (844 observations) | | $R^2$ - marginal: 0.12; $R^2$ - conditional: 0.28 | | |
|---|---|---|---|---|---|
| Order of the trial | 0.230 | 0.091 | 2.516 | 0.012 | [0.051 to 0.408] |
| Julian Day | 0.543 | 0.136 | 3.988 | <0.001 | [0.276 to 0.810] |
| Turtle temperature | 0.257 | 0.113 | 2.268 | 0.023 | [0.035 to 0.479] |
| Carapace length | -0.273 | 0.102 | 2.683 | 0.007 | [-0.473 to -0.074] |

| Complete dataset | 704 individuals (1071 observations) | | $R^2$ - marginal: 0.12; $R^2$ - conditional: 0.49 | | |
|---|---|---|---|---|---|
| Testing environment (controlled setting) | -2.318 | 0.417 | 5.558 | < 0.001 | [-3.135 to -1.500] |
| Julian Day | 0.994 | 0.182 | 5.473 | < 0.001 | [0.638 to 1.350] |
| Carapace length | -0.323 | 0.131 | 2.473 | 0.013 | [-0.579 to -0.067] |

**Table S1-15** Summary statistics for the final (generalized) linear mixed models with risk-taking behaviours in painted turtles as response variable: Sum of active defensive behaviours used, escape latency and emergence of the turtle after escaping. We used only observations from turtles tested more than one and compared the results obtained to those with the complete dataset. For each model, we provided for each predictor variable: the estimate, the standard error (SE), the t-value (z-value for the binomial model), the p-value and the 95% confidence intervals (95% CI). REML was set as TRUE for the calculation of the model statistics. All the continuous predictor variables were scaled (mean zero, unit variance) before model selection. Reference factors are in parentheses for categorical predictor variables. Turtle and sampling site identity were included as random effects in the model for sum of active defensive behaviours with the complete dataset, while only turtle identity was included in the other models

| Variables | Estimate | SE | t-value | p-value | 95% CI |
|---|---|---|---|---|---|
| **Sum of active defensive behaviours** | | | | | |
| Turtles tested more than once | 215 individuals (561 observations) $R^2$ - marginal: 0.11; $R^2$ - conditional: 0.49 | | | | |
| Number of houses within 200 m | -0.154 | 0.049 | 3.160 | 0.002 | [-0.249 to -0.058] |
| Distance to navigation channel | -0.145 | 0.060 | 2.395 | 0.017 | [-0.263 to -0.026] |
| Mean daily number of vessel crossings | 0.184 | 0.062 | 2.983 | 0.003 | [0.063 to 0.304] |
| Order of the trial | 0.058 | 0.029 | 2.049 | 0.041 | [0.003 to 0.114] |
| Sex (Male) | 0.338 | 0.110 | 3.079 | 0.002 | [0.123 to 0.553] |
| Turtle temperature | 0.111 | 0.044 | 2.528 | 0.012 | [0.025 to 0.198] |
| Carapace length | 0.140 | 0.059 | 2.387 | 0.018 | [0.025 to 0.255] |
| | | | | | |
| Complete dataset | 714 individuals (1091 observations) $R^2$ - marginal: 0.10; $R^2$ - conditional: 0.52 | | | | |
| Number of houses within 200 m | -0.134 | 0.058 | 2.316 | 0.031 | [-0.247 to -0.021] |
| Distance to navigation channel | -0.122 | 0.057 | 2.122 | 0.047 | [-0.234 to -0.009] |
| Mean daily number of vessel crossings | 0.194 | 0.065 | 2.986 | 0.008 | [0.067 to 0.321] |
| Sex (Male) | 0.327 | 0.070 | 4.687 | < 0.001 | [0.191 to 0.464] |
| Testing environment (controlled setting) | -0.218 | 0.068 | 3.228 | 0.001 | [-0.350 to -0.086] |
| Carapace length | 0.112 | 0.037 | 3.014 | 0.003 | [0.040 to 0.186] |
| | | | | | |
| **Escape latency** | | | | | |
| Turtles tested more than once | 202 individuals (543 observations) $R^2$ - marginal: 0.15; $R^2$ - conditional: 0.46 | | | | |
| Urban areas within 200 m | 0.242 | 0.072 | 3.333 | 0.001 | [0.100 to 0.384] |
| Order of the trial | -0.269 | 0.043 | 6.184 | < 0.001 | [-0.354 to -0.184] |
| Julian Day | 0.339 | 0.086 | 3.961 | <0.001 | [0.171 to 0.507] |
| Carapace length | 0.145 | 0.063 | 2.298 | 0.023 | [0.021 to 0.270] |
| Wind scale (Beaufort scale) | -0.153 | 0.051 | 3.023 | 0.003 | [-2.253 to -0.054] |
| | | | | | |
| Complete dataset | 596 individuals (919 observations)  $R^2$ - marginal: 0.10; $R^2$ - conditional: 0.44 | | | | |
| Order of the trial | -0.231 | 0.036 | 6.415 | < 0.001 | [-0.302 to -0.161] |
| Julian Day | 0.141 | 0.053 | 2.645 | 0.008 | [0.036 to 0.245] |

| | | | | | |
|---|---|---|---|---|---|
| Turtle temperature | -0.199 | 0.047 | 4.245 | < 0.001 | [-0.291 to -0.107] |
| Carapace length | 0.167 | 0.042 | 4.013 | < 0.001 | [0.085 to 0.248] |
| Wind scale (Beaufort scale) | -0.176 | 0.036 | 4.899 | < 0.001 | [-0.246 to -0.106] |

**Emergence of the turtle after escaping**

| Turtles tested more than once | 215 individuals (582 observations) $R^2$ - marginal: 0.16; $R^2$ - conditional: 0.56 | | | | |
|---|---|---|---|---|---|
| Mean daily number of vessel crossings | 0.482 | 0.210 | 2.294 | 0.022 | [0.070 to 0.894] |
| Testing environment (controlled setting) | -2.895 | 0.421 | 6.877 | < 0.001 | [-3.719 to -2.070] |
| Julian Day | 1.013 | 0.224 | 4.515 | < 0.001 | [0.573 to 1.453] |

| Complete dataset | 704 individuals (1071 observations) $R^2$ - marginal: 0.12; $R^2$ - conditional: 0.49 | | | | |
|---|---|---|---|---|---|
| Testing environment (controlled setting) | -2.318 | 0.417 | 5.558 | < 0.001 | [-3.135 to -1.500] |
| Julian Day | 0.994 | 0.182 | 5.473 | < 0.001 | [0.638 to 1.350] |
| Carapace length | -0.323 | 0.131 | 2.473 | 0.013 | [-0.579 to -0.067] |

*Supporting Information 2 – Video of risk-taking behaviours in painted turtles*

The first part of the video (00:00 to 00:50) is an example of the test to calculate the number of active defensive behaviours used by painted turtles during the measurement of four morphological traits (i.e., plastron length, carapace length, height, and width). The second part of the video (00:50 to 02:30) shows the platform test to measure escape latency in a controlled environment at the Queen's University Biological Station. Video available at: https://youtu.be/sb6qoy_qF-A

*Supporting Information 3 – Determination of the scale of maximum effect*

For the proportion of urban area and the number of houses with access to the canal, we needed to determine at which scale their effect on the three risk-taking behaviours (sum of active defensive behaviours used, escape latency and emergence of the head after escaping) was maximal. The determination of the scale of maximum effect was done separately for each behaviour. This protocol is based on the work of Čapkun-Huot et al. (2021) and Fyson & Blouin-Demers (2021).

1. Dataset

For each individual, a mean value of all the repeated measurements was calculated for each behaviour and a table with one line per individual was created. We added columns for all the buffer distances ranging from 100 m to 1000 m in 100-m increments with the values of the human disturbance variables.

2. Calculating the correlations

We used the function rcorr from the R Hmisc package (Harrell, 2020) to calculate correlations (Pearson's correlation coefficient) between the behaviour (e.g., escape latency) and the human disturbance variables (e.g., proportion of urban area) for each buffer distance, and kept only the buffer distance at which the correlation was maximal for further analyses (Figure S1-1 and Table S1-16). This step was conducted for each behaviour and for each human disturbance variable separately.
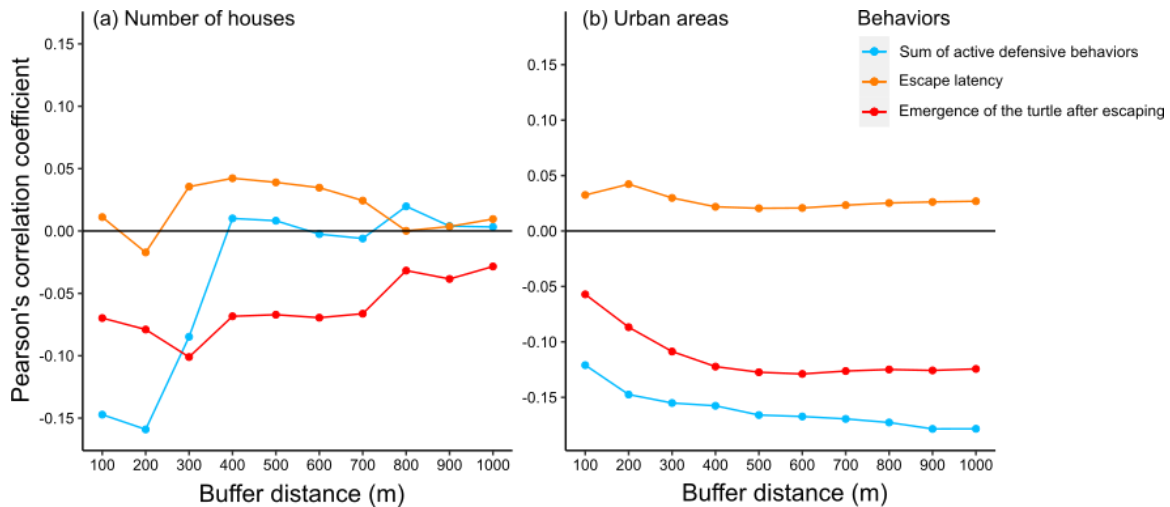
**Figure S1-1** Pearson's correlation coefficients between the human disturbance variables (a: Number of houses with access to the canal; b: Proportion of urban areas) and risk-taking behaviours (blue: sum of active defensive behaviours; orange: escape latency; red: emergence of the turtle after escaping) at buffer distances ranging from 100 m to 1000 m in 100-m increments. The buffer distance with the absolute highest correlation was kept for further analyses.

**Table S1-16** Buffer distances for the number of houses with access to the canal and proportion of urban areas with the highest absolute correlation for each behaviour: Sum of active defensive behaviours, escape latency, and emergence of the turtle after escaping.

| | Number of houses | | Urban areas | |
|---|---|---|---|---|
| Variables | Buffer size | Correlation | Buffer size | Correlation |
| Sum of active defensive behaviours | 200 | -0.159 | 900 | -0.178 |
| Escape latency | 400 | 0.042 | 200 | 0.042 |
| Emergence of the head after escaping | 300 | -0.101 | 600 | -0.129 |

68

# Chapter 2

Disentangling how human disturbance influences the relationships between colouration, physiological response, and risk-taking behaviour in painted turtles with structural equation modelling

A slightly modified version of this chapter will be submitted for publication in *Conservation Physiology*.

**Abstract**

Human activities result in fast-changing environmental conditions that often threaten persistence of animal populations. Consequences on animals include important physiological modifications that can be detrimental for them and affect other important biological processes, such as colour signalling. Individuals also vary in the way they perceive and react to these perturbations. The use of a global approach that integrates the complex interactions among different biological factors that could be affected by human disturbance is thus needed to analyze animal responses. In this context, we investigated the effect of recreational boating on the relationships between carotenoid-based colouration (i.e., proportion of yellow and red), physiological response (i.e., heterophil-to-lymphocyte (H/L) ratio) and risk-taking behaviour (i.e., use of active defensive behaviours) in painted turtles (*Chrysemys picta*). To do so we analysed data from 217 turtles collected within 18 sites varying in boat activities along the Rideau Canal, Canada, with structural equation modelling. We found that males and females differed in colouration, but that colouration was not related to physiological or behavioural traits. In addition, H/L ratios did not vary according to boat activities level, but was lower in painted turtles sampled in 2020, possibly due to restrictions related to the COVID-19 pandemic. Finally, risk-taking propensity led to higher H/L ratios in more risk-prone males, but not in females. Our findings suggest that human activities may induce physiological changes in wildlife which could depend on their propensity to take risks. Given the pace of anthropogenic changes on wildlife, our study highlights the importance of considering both behavioural and physiological components of animals' biology when creating conservation plans.

## Introduction

Human activities impact most ecosystems and expose wildlife to various anthropogenic disturbances (Barnosky et al., 2012; Foley et al., 2005; Kennedy et al., 2019; Larson et al., 2016; Steven et al., 2011). The growing anthropogenic pressures on wild populations threaten their persistence and are the main driver of the global biodiversity loss (Dirzo et al., 2014; McCauley et al., 2015; WWF, 2022). Therefore, the ability of animals to respond and adjust to human-induced environmental stressors may predict if they will persist in changing environments (Tablado & Jenni, 2017; Wong & Candolin, 2015).

To persist in changing environments, animals need to cope with frequent and often unpredictable perturbations that can destabilize their physiological state (i.e., homeostasis; Dantzer et al., 2014; Wingfield, 2013; Wingfield et al., 1997). During stressful events, stress hormones, such as glucocorticoids, are released by the organism and these hormones trigger behavioural and physiological responses to maintain homeostasis (Buchanan, 2000; Sapolsky et al., 2000; Wingfield et al., 1997). Such physiological responses mobilize energetic resources at the expense of other physiological functions (e.g., digestion, energy storage, growth) that are not essential to immediate survival (Buchanan, 2000; Sapolsky et al., 2000; Wingfield et al., 1997). Frequent human disturbance, however, may result in prolonged and maladaptive physiological responses where high basal levels of glucocorticoids are maintained (Sapolsky et al., 2000; Wingfield et al., 1997). Maladaptive physiological responses could have important fitness consequences on individuals, for instance through the reduction of other physiological functions (e.g., immune activities) that could impede the responsiveness to other stressors, such as pathogens and parasites ( i.e., allostatic overload; Acevedo-Whitehouse & Duffus, 2009; Martin, 2009).

The quantification of circulating leukocyte profile (e.g., heterophil-to-lymphocyte ratio) is commonly used to evaluate the physiological impact of anthropogenic (e.g., human activity) and natural environmental stressors (e.g., infections/parasites) on animals (Davis et al., 2008; Davis & Maney, 2018). An increase of glucocorticoids alters the circulating leukocyte profile of animals by relocating the different leukocytes where most needed to respond efficiently to a stressor (Coico & Sunshine, 2015; Davis et al., 2008; Dhabhar, 2002). This response is characterized by an influx of heterophils (i.e., primary phagocytic leukocytes in reptiles and birds) and a migration of lymphocytes (i.e., related to the regulation of the immune response and immunological memory) from the blood to other tissues (Coico & Sunshine, 2015; Davis et al., 2008; Dhabhar, 2002). Animals exposed to high human disturbance have typically higher heterophil-to-lymphocyte ratios (i.e., H/L ratios) compared to individuals from less perturbed areas (Fokidis et al., 2008; Palacios et al., 2018; Selman et al., 2013). Since it fluctuates less rapidly over long periods of time compared to glucocorticoid levels, using the leukocyte response through the H/L ratio to estimate chronic stress is a more appropriate approach than measuring glucocorticoid levels (Davis et al., 2008; Davis & Maney, 2018)

Aside from their role in the stress response, glucocorticoids mediate the expression of carotenoid-based colouration (i.e. colours ranging from yellow to red; Berg et al., 2019; Loiseau et al., 2008; Martínez-Padilla et al., 2013). Glucocorticoids can modulate how carotenoid pigments are allocated to the diverse physiological processes that require them (Berg et al., 2019; Loiseau et al., 2008; Martínez-Padilla et al., 2013). Carotenoids are limited because they cannot be synthesized; they can only be acquired through food (Goodwin, 1980, 1984; Hill, 1992). Thus, when the physiological state of an animal is disrupted by suboptimal environmental conditions, carotenoids may be used preferentially to stabilize and/or improve essential physiological functions, and this at the expense of colouration (Aguilera & Amat, 2007; Blount et al., 2003; Faivre et al., 2003; Mcgraw, 2005). For instance, Pérez-

Rodríguez and Viñuela (2008) observed that red-legged partridges (*Alectoris rufa*) with less red colouration on their eye ring had lower body condition and higher H/L ratios, highlighting the potential trade-off between displaying a carotenoid-based colouration and maintaining essential physiological processes. Red carotenoid pigments are less abundant in food than yellow pigments and, thus, red and yellow colouration may be affected differently when physiological stasis is compromised (Hill, 1996). Given that carotenoid-based colouration may be used as reliable signaling information during various social interactions, including courtship (see examples: Ibáñez et al., 2014; Polo-Cavia et al., 2013; Schweitzer et al., 2015; Sundberg, 1995; Svobodová et al., 2013), there is a need to understand how the physiological changes caused by human disturbance affect its expression.

Individuals could differ in their perception of cues across contexts and over time and, thus, consistently differ in their physiological response to human disturbance (McDougall et al., 2006; Réale et al., 2007, 2010; Sih, 2004). Risk-prone individuals (i.e., proactive) are less responsive to stressors and usually better tolerate stressful conditions by producing lower basal levels of glucocorticoids compared to risk-averse individuals (i.e., reactive) (Koolhaas et al., 1999; Réale et al., 2010). For instance, Carbillet et al. (2019) observed that proactive wild roe deer, based on their behavioural response upon capture, had lower neutrophil-to-lymphocyte ratios than reactive individuals (neutrophils replace heterophils in vertebrates other than reptiles and birds). By being less responsive to stressors, risk-prone individuals may potentially lose few foraging opportunities in disturbed environments (Cole & Quinn, 2014) and have a better access to limited resources, such as carotenoids, allowing them to allocate more resources to colouration (Biro & Stamps, 2008; Dyer et al., 2009). On the other hand, risk-averse individuals explore more thoroughly their environment (Réale et al., 2010), potentially making them better foragers than risk-prone individuals and thus allowing them to acquire more carotenoid-rich food resources. Finally, risk-prone individuals are more active than risk-averse

individuals and the higher energetic demands to perform those activities could lead to the re-allocation of carotenoids used in colouration to maintain their activity level (Anderson et al., 2015). The link between colouration and physiological responses could thus be influenced by an individual's propensity to take risks, highlighting the importance of considering behavioural variation among individuals when analysing this relationship.

In this study, we investigate the effects of human disturbance (i.e., boat activity) on the relationships between colouration (i.e., proportion of yellow and red), physiological response (i.e., H/L ratio), and risk-taking behaviour (i.e., sum of active defensive behaviours used during handing) in painted turtles (*Chrysemys picta*) of the Rideau Canal, Ontario, Canada, with structural equation modelling. Investigating the consequences of human disturbance on animals is often difficult given the direct and indirect relationships among the various behavioural and physiological factors that are differently affected by these perturbations. Structural equation modelling is a powerful statistical method that can be used to decipher complex multivariate hypotheses by considering a network of direct and indirect causal relationships among variables that could influence animal responses to human disturbance (Arhonditsis et al., 2006; Eisenhauer et al., 2015; Fan et al., 2016).

Male and female painted turtles have colourful patterns ranging from yellow to red on the majority of their body, such as the head, neck, legs and shell (Ernst & Lovich, 2009; Steffen et al., 2015). In particular, painted turtles have red and yellow stripes on their neck and chin, and a yellow spot behind each eye (Ernst & Lovich, 2009; Steffen et al., 2015). During courtship rituals, male painted turtles may repeatedly touch the female's head and neck with their front claws and make several movements (e.g., head vertical vibrations, stretching of anterior limbs; Ernst & Lovich, 2009; Liu et al., 2013; Steffen et al., 2015). Such behaviours seemingly help display their colouration, thus suggesting that carotenoid-based colouration could be a visual signal used by painted turtles for mate choice.

The sum of active defensive behaviours displayed by painted turtles during handling can be used to quantify the propensity to take risks (Turcotte et al., 2023 (Chapter 1)). In a previous study in the Rideau Canal, we showed that individual painted turtles were consistent in the use of active defensive behaviours during handling (repeatability estimate = 0.36; Turcotte et al., 2023 (Chapter 1)). In addition, the sum of active defensive behaviours was correlated with other risk-taking behaviours (i.e., by also escaping more rapidly from a floating platform and emerging more often from the water after escaping), indicating that turtles displaying more active defensive behaviours were more prone to take risks overall (Turcotte et al., 2023 (Chapter 1)). We also showed that painted turtles in areas with more boat activity used more active defensive behaviours (Turcotte et al., 2023 (Chapter 1)), making this behaviour relevant to identify how human disturbance influence its relationship with colouration and physiological response.

We hypothesized that human disturbance creates stressful environmental conditions that should elicit a physiological response in turtles exposed to these stressors and lead to the mobilization of carotenoids at the expense of colouration. Also, individual turtles may perceive and respond differently to human disturbance, which should affect i) their physiological response and ii) their capacity to gather carotenoids and, thus, to allocate them to their colouration. More specifically, we predicted that painted turtles in areas with more boat activity should have higher H/L ratios leading to lower proportions of red on their necks and yellow on their heads. We also predicted that turtles that used more active defensive behaviours during handling would have i) lower H/L ratios and ii) higher proportions of red on their necks and yellow on their heads. We expected to find stronger trade-offs i) with red colouration given that red carotenoids are more limited in the environment and ii) in males given the potential role of colouration in mate choice (Figure 2-1a illustrates how we tested these hypotheses with structural equation modelling).

**Methods**

*Study system and turtle captures*

We captured painted turtles between May and August of 2019 and 2020 with fyke nets at 18 sampling sites along the Rideau Canal, a 202-km slackwater canal located in southeastern Ontario, Canada, that connects the Ottawa River to Lake Ontario (shortest aquatic distance between sampling sites: 10.2 km; Figure 2-1b). The Rideau Canal is composed of rivers, lakes, and excavated channels connected by 23 lockstations (Figure 2-1b). The canal is used extensively for recreational boating with over 40,000 vessel crossings recorded at lockstations each year (Figure 2-1c, Supporting Information 1 – Table S1-4 (Chapter 1) and Supporting Information 2 of Chapter 2), which exclude boats travelling on the canal without going through locks. We deployed our nets in areas suitable for painted turtles characterized by shallow water, weak currents, abundant aquatic vegetation, and presence of structures for basking (e.g., rocks, logs, and stumps). We trapped turtles at each site for at least one week and checked the nets every 24 hours. We trapped at five of the 18 sites both years (Supporting Information 1 – Table S2-1). Upon capture, we measured the plastron length and the carapace length, height, and width (± 0.5 mm) of each turtle with an aluminum caliper (Haglöf, Sweden). We also sexed each turtle based on external morphological characteristics (e.g., tail and claw length, cloaca position on the tail, and shape of the shell). Lastly, we filed notches on the marginal scutes of each turtle according to the North American coding system to create unique identifications (Nagle et al., 2017).

*Blood sampling and haematological parameters*

We took a blood sample from the jugular or coccygeal vein of each turtle using a U-100 insulin syringe with a 28G × 12.7 mm microfine needle (BD Medical). We favoured blood sampling at the jugular vein to reduce the risk of haemodilution that is higher when sampling from the coccygeal vein

(66% of blood samples were obtained from the jugular vein; Perpiñán, 2017). We noted the venipuncture site for each turtle to be able to control for its potential effect on H/L ratios in our models (see *Structural equation modelling* section; Figure 2-1a). We smeared 1-2 drops of blood (~ 4 mm diameter) on a microscopy slide, air-dried them, and then stored them in the dark until further manipulation. For each turtle, we prepared two blood smears to ensure having at least one good-quality smear for cell counts. Once in the laboratory, we fixed blood smears with methanol for 1 minute and air-dried them prior to staining. We stained them with Wrigth-Giemsa solution following the rapid dipping method (Sigma-Aldrich, 2016).

We analyzed the circulating leukocyte profile of painted turtles using a compound microscope (Leitz Laborlux S, Leica) at 1000X magnification under oil immersion. We differentiated the first 200 leukocytes observed (except thrombocytes and erythrocytes) as heterophils, eosinophils, basophils, lymphocytes, or monocytes (Javanbakht et al., 2013; Kassab et al., 2009; Sanchez & Refsnider, 2017). We performed counts by following a line perpendicular to the blood smear in the two-thirds of the smear (i.e., in the monolayer section where approximately 50 % of the visible cells touched neighbours' cells; Lentfer et al., 2015). We started counts at the edge of the smear, moved towards the center, and stopped when 200 leukocytes were counted. It is important to perform the count perpendicularly to the blood smear because leukocytes can be non-randomly distributed on the smear according to morphological characteristics: heterophils and monocytes are usually more present at the edge of the smear while lymphocytes are more often found in the middle (Briggs & Bain, 2017). We calculated the H/L ratio by dividing the number of heterophils by the number of lymphocytes (within the 200 leukocytes). We also calculated the proportion of the different leukocytes observed over the total number of leukocytes counted (Supporting Information 2 of Chapter 2). In addition, we counted the total number of leukocytes at 400x magnification in 10 fields of view that were equally distributed on a new scan line (Supporting

Information 2 of Chapter 2). Lastly, we reported the presence/absence of haemoparasites (i.e., Yes: 1 or No: 0; hemogregarines and reptilian malaria) across the same 10 fields of views. Haemoparasites are common parasites infecting erythrocytes and they are transmitted by leeches and/or mosquitoes in reptilian hosts (Campbell, 2015; Heatley & Russell, 2018). The consequences of haemoparasite infections are variable ranging from being non-detrimental to life-threatening for infected hosts (Maia et al., 2014; Paterson & Blouin-Demers, 2020; Stacy et al., 2011). We statistically controlled for the potential impact of blood parasites on circulating leukocyte profiles by including the infection status in our models (see *Structural equation modelling* section; Figure 2-1a). To have complete observations for all the variables included in our structural equation models, we used haematological parameters from 217 turtles in our statistical analyses (males = 215, females = 92; Supporting Information 1 – Table S2-1). Descriptive statistics of the haematological parameters on the full dataset (N = 382) are available in Supporting Information 2 of Chapter 2.

We evaluated the reproducibility of haematological counts by assessing repeatability between the first and second set of 100 leukocytes differentiated along the same scan line and from randomly selected subsamples of blood smears that were analyzed twice by different observers. We obtained relatively high repeatability estimates (ranging from 0.65 to 0.94 according to the parameters and the subsamples used), confirming that our haematological counts had good precision (see Supporting Information 2 of Chapter 2 for more details). All haematological measurements used in statistical analyses were performed by the same observer.

*Colouration*

*Picture linearization and scaling*

We photographed the head and neck of each captured painted turtle with a Nikon digital camera

D3200 (18 – 55 mm lens). Pictures were saved in a RAW file format (i.e., NEF file). Each turtle was photographed in the field on a light background with a colour chart including a ruler (i.e., X-Rite ColorChecker Passport). We avoided direct sunlight. Reflectance values of each picture's colour channel (i.e., red, blue, and green wavelength) should linearly increase with light intensity and, if not, a correction should be applied (Stevens et al., 2007). To do so, we extracted the reflectance value of each grey scale (i.e., grey colour standard) of the colour chart (ranging from 20 % to 95 % in expected reflectance) from the first picture taken for each turtle (N = 260) in ImageJ (Abràmoff et al., 2004). Prior to correction, the observed reflectance values already appeared linearly related to expected values. The observed values were lower than expected, however. Thus, to obtain a better fit between expected and observed reflectance values, we applied a linear correction to each colour channel based on these equations:

$$Q_r = a_1 + b_1 r$$
$$Q_g = a_2 + b_2 g$$
$$Q_b = a_3 + b_3 b$$

In these linearization equations, $Q$ is the expected reflectance value of the grey colour standard, $a$ and $b$ are constants, and $r$, $g$, and $b$ represent the observed reflectance value from each colour channel (i.e., red, green, and blue). To determine the value of $a$ and $b$ for each colour channel, we fitted a linear regression using the *lm* function in R 4.2.0 (R Core Team, 2022) with the expected reflectance value of each grey scale of the colour chart as the response variable and the corresponding reflectance values extracted from Image J for each picture as the predictor. We applied these equations to all our pictures before further analyses in R (see Supporting Information 3 of Chapter 2). We also verified that the linearized reflectance values of grey colour standards were equal in each colour channel with paired t-tests (Stevens et al., 2007). Finally, we rescaled all linearized pictures from a line of known length (i.e.,

the ruler from the colour chart) in ImageJ to ensure that they were all at the same scale. The area of interest (i.e., head or neck) was cropped and placed on a 10 cm X 10 cm black background.

*Proportion of colours*

We measured the proportion of yellow on the head and of red on the neck for each turtle. To do so, we created segmented black-and-white pictures from all our linearized and scaled pictures. More specifically, we binarized our pictures by giving a score of 0 (black) to each pixel corresponding to the colour of interest (i.e., yellow or red) and a score of 1 (white) to all other pixels based on a threshold reflectance value specific to each colour. We then calculated the proportion of each colour of interest as a function of the total area (i.e., black pixel / (black + white pixels)).

We started the segmentation by extracting the colour of interest in each picture (Teasdale et al., 2013). The yellow component was isolated by subtracting the blue channel from the green channel. For the red component, we subtracted the green channel from the red channel which also allows to keep orange hues. Then, we identified a pixel in ImageJ that visually corresponds to each colour of interest on a subset of 50 pictures and extracted its reflectance value in R. Based on the values obtained, we tested a range of reflectance values as the threshold for each colour of interest and selected the optimal value (i.e., value that isolates only the colour of interest, without losing too much of it; threshold value = 0.08 for yellow and = 0.15 for red) for the binarization. The proportion of yellow on the turtle's head and red on the turtle's neck was extracted from 92 females and 215 males (one male had only a measurement for the proportion of yellow, and another one only for the red: 214 males for each colour; Supporting Information 1 – Table S2-1). We documented step-by-step our colouration analyses in the Supporting Information 3 of Chapter 2.

*Risk-taking behaviour*

We assessed the propensity to take risks in painted turtles by calculating the sum of active defensive behaviours displayed during handling (see Turcotte et al., 2023 (Chapter 1) for more details). In brief, during measurement of the four morphological traits (i.e., plastron length, carapace length, height, and width), we noted if the turtle used the following active defensive behaviours: i) try to escape (movement of the legs), ii) try to bite (the turtle closes and opens the mouth with its neck stretched), iii) hiss (gaping of the mouth when retracting the head in the shell, thus expulsing air), and/or iv) urinate/defecate. We summed the number of active defensive behaviours used by the turtle during the test which ranged from zero (i.e., no active defensive behaviours used) to four (i.e., all four active defensive behaviours used). We did not handle turtles prior to this test and only used the first behavioural measurement performed in the field for the analyses.

*Boat activity*

We quantified boat activity at each sampling site using the mean daily number of vessel crossings at each lockstation along the Rideau Canal. The canal is operated by Parks Canada who recorded all vessels crossings at each lockstation during the operating period (i.e., May (Canadian Victoria Day) to October (Canadian Thanksgiving); Figure 2-1c and Supporting Information 1 – Table S1-4 (Chapter1)). We calculated the mean daily number of vessel crossings separately for 2019 and 2020. The number of vessel crossings decreased significantly in 2020 due to restrictions related to the COVID-19 pandemic (Figure 2-1c, Supporting Information 1 – Table S1-4 (Chapter1)). To estimate boat activity at each sampling site, we calculated the mean daily number of vessel crossings using the vessel counts from the upstream and downstream lockstations for each sampling year. We considered that sampling sites located near lockstations with numerous vessel crossings should be exposed to higher boat activity.

*Habitat quality: Estimation of food resources*

In turtles, carotenoids are mainly gained by eating algae and various aquatic plants (Ernst & Lovich, 2009). Painted turtles occupy shallow, slow-moving, and well-vegetated water bodies such as wetlands (Ernst & Lovich, 2009), which are essential foraging habitats and comprised approximately 20 % of the Rideau Canal (see Figure 2-1b) (Ernst & Lovich, 2009). We considered that sampling sites with high surrounding proportion of wetlands should have more food resources available. We thus assessed the proportion of wetlands around each sampling site and used it as a proxy for the abundance of carotenoids. We used ArcGIS (version 10.7.1; ESRI, 2019) to calculate the proportion of wetlands within various buffer distances around each sampling site using the Southern Ontario Land Resource Information System (SOLRIS) V.3 with 15-m resolution (OMNRF, 2019; Figure 2-1b). First, we calculated the number of cells from each land cover class within buffer distances ranging from 100 m to 1000 m at 100-m increments. During the active period, painted turtles make relatively short daily aquatic movements up to 300 m (mean home range = 20.38 ha, mean radius = 250 m; Supporting Information 1 – Table S2-2; COSEWIC, 2018), and, thus, a maximal buffer distance of 1000 m should cover the scale at which landscape features could potentially affect daily activities. Then, we divided the number of cells representing wetland areas (i.e., treed swamp, thicket swamp, fen, bog, and marsh) by the total number of cells within each buffer area. Finally, we determined the distance at which the effect of the proportion of wetlands was maximal for our four variables of interest (i.e., proportion of yellow on head, proportion of red on neck, H/L ratio, and sum of active defensive behaviours). We also selected the distance of maximum effect separately for males and females because the scale at which landscape features influence movement patterns and space use could differ between sexes (Ernst & Lovich, 2009). We calculated Pearson's correlation coefficients between our variables of interest and the proportion of wetlands at each buffer distance, and only kept the buffer distance with the highest

value for further analyses (see Supporting Information 1 – Table S2-3 for the selected buffer distances; see Čapkun-Huot et al., 2021; Fyson & Blouin-Demers, 2021; Turcotte et al., 2023 (Chapter1)) for similar analyses).

*Structural equation modelling*

All statistical analyses were conducted in R 4.2.0 (R Core Team, 2022). We used Bayesian multivariate mixed-effect regression models to evaluate the influence of human disturbance on colouration (i.e., proportion of yellow and red on head and neck), physiological response (i.e., H/L ratio), and risk-taking behaviour (i.e., sum of active defensive behaviours), while accounting for the relationships among these variables. The models were implemented in the brms package (Bürkner, 2017) using Stan R interface (rstan package: Stan Development Team, 2023; rstanarm package: Goodrich et al., 2022). We built separate models for the proportion of red and yellow, and for males and females. We obtained complete observations for all our variables of interest for 124 males and 92 females with a single observation per turtle (see Supporting Information 1 – Table S2-1). We included sampling site identity as a random effect to control for the non-independence of observations from the same location and potential confounding variables (i.e., proportion of wetlands, sampling year, venipuncture site, presence/absence of haemoparasites, and carapace length) as predictors in models (Figure 2-1a). We applied a square-root transformation to the proportion of red and yellow colouration and a log transformation to the H/L ratio to achieve normality. We defined the sum of active defensive behaviours as a probability to use the four active defensive behaviours during handling by using a binomial distribution. We used a lognormal distribution for the mean daily number of vessel crossings. No variables were scaled prior to the analyses (Supporting Information 1 – Table S2-4). For each model, we ran four chains with 8000 iterations and 2000 warm-ups. We fitted our models with the default priors of the brms package. Finally, given that analyses were performed separately for males and females, we

83

estimated if our variables of interest (i.e., proportion of yellow and red on head and neck, H/L ratio, and sum of active defensive behaviours) differed between the sexes with univariate mixed models.

We verified sampling quality and model fit with the shinystan package (Gabry & Veen, 2022). We visually verified that the four chains converged to the same area and no parameters had an $\hat{R}$ statistic above 1.1 (Gelman et al., 2022; Muth et al., 2018). All effective posterior sample sizes (ESS) were over 1000 and no parameters had an effective sample size that was less than 10% of the total sample size. We assessed the error introduced by the Markov chain Monte Carlo (MCMC) approximation by calculating the Monte Carlo standard error (MCSE) and found that no parameters had a MCSE greater than 10% of the posterior standard deviation (Muth et al., 2018). Finally, we checked if the data simulated by our models fitted our observed data by comparing the observed distribution of our response variables to 100 simulated datasets from the posterior predictive distribution. We obtained a similar distribution between the observed and simulated data from the posterior predictive distribution for the response variables of each model (Muth et al., 2018).

## Results

Our analysis of 217 painted turtles, with complete observations for all our variables of interest, showed that lymphocytes (proportion of lymphocytes: mean ± standard deviation = 0.56 ± 0.14) and heterophils (proportion of heterophils: 0.36 ± 0.13) were the most abundant leukocytes (see Supporting Information 1 – Table S2-4). We found high variability in the H/L ratio among individuals, which ranged between 0.10 and 3.56 (0.77 ± 0.60), but found no difference between the sexes (estimate [95% credible intervals] = 0.01 [-0.16 to 0.16]). We detected that 28% of the painted turtles were infected by haemoparasites (Supporting Information 1 – Table S2-4). Painted turtles with higher proportions of red on the neck also had higher proportions of yellow on the head (Pearson's $r$ correlation = 0.23, $p < 0.01$;

$r_{male} = 0.29$, $p < 0.01$; $r_{female} = 0.36$, $p < 0.01$). Males had a higher proportion of red on the neck (0.012 [0.005 to 0.018]), but a smaller proportion of yellow on the head (-0.008 [-0.013 to -0.004]) compared to females. Males did not differ from females in the sum of their active defensive behaviour (0.20 [-0.11 to 0.51]).

We detected no relationship between the H/L ratio and the proportion of red on the neck or yellow on the head, regardless of sex (Figure 2-2, Table 2-1). We also found no relationship between the proportion of red and yellow and the number of active defensive behaviours used during handling, again regardless of sex (Figure 2-2, Table 2-1). We found that males, but not females, that used more active defensive behaviours had higher H/L ratios (Figure 2-2 and 2-3, Table 2-1). The mean daily number of vessel crossings was higher in 2019 than in 2020 (Table 2-1). However, we found no effect of the mean daily number of vessel crossings on either H/L ratio (even though painted turtles had a higher H/L ratio in 2019 compared to 2020; Figure 2-3 and Table 2-1) or on the proportion of yellow and red colouration (Figure 2-2, Table 2-1). Blood samples collected from the jugular vein had higher H/L ratio in both sexes (Figure 2-2, Table 2-1). Infection with haemoparasites was not related to the H/L ratio (Figure 2-2, Table 2-1). Finally, the proportion of wetlands was not related to any of our variable of interest, regardless of sex (Figure 2-2, Table 2-1).

**Discussion**

Here we investigated the impact of human disturbance on animals by considering the complex relationships among colouration, physiological response, and risk-taking behaviour to understand better how they cope and persist in a fast-changing world. We found that painted turtles did not seem to respond physiologically to boat activity, but lower H/L ratios were detected in 2020, which was the first year of restrictions related to the COVID-19 pandemic. Risk-prone males, but not females, were

physiologically more responsive in that they exhibited higher H/L ratios than risk-averse males. Males and females differed in colour, but their colouration was unrelated to any physiological or behavioural traits.

*Painted turtles physiologically respond to changes in human activity*

We found no relationship between H/L ratios of turtles and mean daily numbers of vessel crossings at lockstations suggesting that this measure of physiological response was not affected by spatial variation in boat activity. This result is unexpected because we predicted that higher H/L ratios should be detected in turtles exposed to higher levels of human activity, as found in many other studies (Fokidis et al., 2008; Palacios et al., 2018; Selman et al., 2013). On the other hand, our findings are consistent with other studies that also found no significant relationship between H/L ratios and human activity (Carbó-Ramírez & Zuria, 2017; Hevia et al., 2023; Walthers & Barber, 2020). The inconsistency in the relationships observed in previous studies between H/L ratios and human activity could be caused by differences in the history of exposure to perturbations, which is generally unknown in wild animals (Davis & Maney, 2018). Reflecting the long-term physiological response to challenging conditions, changes in leukocyte profiles depend on the quantity and frequency of stressful events experienced prior to capture, which could differ among turtles; some individuals could have been recently exposed to multiple stressful events while others were not, even if they are from the same area (Davis & Maney, 2018). This variation in previous experiences can modulate our measurements of H/L ratios. It is also possible that the variation in boat activity is too limited in the canal to detect a potential physiological effect (Supporting Information 1 – Table S1-4 (Chapter1)). Even if H/L ratios constitute a reliable measurement to estimate the prolonged physiological response to human activities, the use of multiple biomarkers (e.g., blood and faecal glucocorticoids levels, haematrocrit levels, measures of oxidative stress, etc.) could help better quantify variations in stress response (Dantzer et al., 2014; Davis & Maney,

2018).

Interestingly, we observed lower H/L ratios in painted turtles sampled in 2020, which may indicate a potential reduction of the physiological effect of exposure to human activities that were largely reduced in 2020 due to the COVID-19 pandemic. Movement restrictions mandated to reduce COVID-19 propagation drastically limited human outdoor activities worldwide and possibly reduced human pressures on wildlife (Montgomery et al., 2021; Rutz et al., 2020; Zellmer et al., 2020). For example, the opening of the Rideau Canal to navigation was delayed of two weeks in 2020 and aquatic recreational activities were highly discouraged which drastically reduced human activity in the canal. As a result, we observed a significant reduction in the mean daily number of vessel crossings at lockstations in 2020 compared to 2019. Even if we did not detect a significant effect of boat activity on H/L ratios, vessel crossings at lockstations are strongly intertwined with sampling year, preventing us from differentiating the effects of these two predictors. By repeating the analyses without considering sampling year in our mixed-effect regression models, we detected a significant relationship between the mean daily number of vessels crossings and H/L ratios in males, but not in females, where individuals in areas with more boat activity had higher H/L ratios (Supporting Information 1 – Table S2-5). Thus, sampling year seems to predict better changes in human activity that occurred during this period and prevails over the possible impact of spatial variation in boat activity on the physiological response. While the restrictions related to the COVID-19 pandemic provided an opportunity to quantity the impact of human-wildlife interactions on physiological state, more data would be necessary to evaluate if the reduced physiological response we observed in 2020 is truly a consequence of lower human activity.

*Physiological cost of being risk-prone in males*

We observed that male painted turtles, but not females, that used more active defensive behaviours

had higher H/L ratios. This result suggests that males, according to their behavioural types, may differently cope with stressful situations where taking risks could be physiologically costly. This result is unexpected given that risk-averse individuals usually strongly respond to stressful conditions by activating their hypothalamic-pituitary-adrenal axis (i.e., HPA axis; reviewed in: Carere et al., 2010; Réale et al., 2010) leading to a higher release of glucocorticoids and thus a higher H/L ratio compared to risk-prone individuals. However, Dantzer et al., (2014) indicated that the magnitude of the physiological response can differ between sexes, where males can exhibit more marked responses to challenging conditions. Higher H/L ratios in risk-prone males could indicate that they face more stressful conditions than risk-averse males during the sampling period, which coincides with the breeding season. In freshwater turtles, courtship and search for reproductive opportunities constitute large parts of male activity during the breeding period, which could be energetically demanding (Gibbons, 1968; Gibbons et al., 1990; Morreale et al., 1984). Freshwater turtles also use aggressive behaviours (e.g., gaping, biting, lateral displacement) to gain access to high-quality basking sites that facilitate efficient thermoregulation and thus optimize reproductive success (Lindeman, 1999; Lovich, 1988). Beside the traditional courtship behaviours, male painted turtles often employ an alternative reproductive tactic where they use aggressive and coercive behaviours toward females to increase their mating success (Moldowan et al., 2020a, 2020b). Risk-prone males could search more actively for reproductive opportunities and be involved in more agonistic interactions to secure more reproductive events and high-quality resources. Thus, considering that fitness-related activities are already energetically costly in male reptiles (Abell, 2000; Aldridge & Brown, 1995; Olsson & Madsen, 1998), it is possible that risk-prone males have additional energetic expenses compared to risk-averse males. Therefore, we show that variation in the propensity to take risks can lead to different physiological responsiveness to stressors that can be specific to each sex, thus highlighting the importance of

considering behavioural types when studying physiological responses in animals.

*Colouration differs between the sexes, but is unrelated to any physiological or behavioural response*

Male and female painted turtles differed in colouration: males had more red on their necks and less yellow on their heads compared to females, indicating sexual colour dimorphism in this species (Bulté et al., 2013). However, this variation in colouration was unrelated to any physiological or behavioural traits we measured, rendering difficult the interpretation of biological processes underlying these differences. A similar difference in colouration was observed in painted turtles by Rowe et al., (2014) where males had slightly redder forelimbs than females. As other studies suggested, colouration could be used by animals to signal information that is not directly related to fitness-related activities, but, for example, used in conspecific and/or mate recognition (Rowe et al., 2014; Wang et al., 2013). In addition, higher proportions of red than yellow in males could be advantageous by making them more cryptic in aquatic habitats when they are actively searching for reproductive opportunities (Rowe et al., 2012, 2014). In the visible spectrum, red wavelengths have the highest rate of absorption when going through water making red colouration darker and less visible than yellow in water (Clarke, 1939).

By using single predictors to represent colouration, behavioural and physiological responses in painted turtles, we were possibly limited in our capacity to uncover the potential trade-offs among them. Many studies have used spectral reflectance both in the visible and UV spectrum to measure colouration in turtles and found significant relationships with physiological state and behaviour (see Ibáñez et al., 2013b, 2014; Judson, 2021; Polo-Cavia et al., 2013). To our knowledge, no other studies have used the proportion of colours as a measure of colouration in turtles. We are aware that our colour measurements do not completely reflect how turtles perceive carotenoid-based colour patterns given that these colours can also reflect in the UV spectrum and can be detected by their tetrachromatic visual system (Steffen

et al., 2015; Ventura et al., 1999). However, the use of digital pictures is still useful to collect information on colour patterns given that it has been previously related to physiological response in other taxa (e.g., Pérez-Rodríguez & Viñuela, 2008; Svobodová et al., 2013). It is also possible that colouration is more directly related to immune functions (e.g., bactericidal competence, phytohemagglutinin response) than to the physiological stress response, highlighting the need to include multiple biomarkers to better represent the physiological response of animals. We can also not exclude that painted turtles could potentially use chemical signals and body condition as indications of physiological state, as suggested by other studies (Ibáñez et al., 2012; Polo-Cavia et al., 2013). Thus, further studies should include a combination of measurements for each variable of interest when studying the relationship of colouration with behavioural and physiological traits.

*Importance to standardize blood sampling when measuring leukocyte profiles*

We found that sampling blood at the coccygeal vein, where the risk of haemodilution is higher, led to lower H/L ratios indicating that blood sampling at different venipuncture sites can cause variation in leukocyte profiles and bias measurements. This result highlights the importance of standardizing blood sampling procedures and of following a strict protocol when measuring haematological parameters. The effect of venipuncture site on various haematological values due to haemodilution is well-known, generally leading to lower counts of the different leukocytes (Gottdenker & Jacobson, 1995; Harms et al., 2016; Perpiñán, 2017; Stewart et al., 2012). In our case, the lower H/L ratios measured from blood samples obtained at the coccygeal vein were mainly caused by a lower detection of heterophils and higher detection of lymphocytes (see post-hoc analyses in Supporting Information 1 – Table S2-6). Thus, it is crucial to be aware of how sampling and analytical methods can affect counts by reporting venipuncture site used and other possible confounding factors (e.g., observers that performed counts and needle size; Mumm et al., 2019), and by statistically controlling for their potential

effects.

## Conclusion

Our study showed the potential physiological costs that human activities can exert on painted turtles and that sex and behavioural types can influence physiological responsiveness to stressors. To our knowledge, few studies have incorporated structural equation modelling to investigate the impact of human activities on the relationships between several biological factors that can potentially impact reproduction and survival of animals. We encourage the use of a synthetic and hypothesis-driven approach when studying animal responses to human disturbance to have a more complete understanding of human consequences on wildlife. In addition, there is a need to quantify the long-term cost of the physiological responses observed in this study by integrating predictors that quantify reproductive success and survival. Considering both physiological and behavioural impacts of human disturbance on wildlife is essential to make better informed management decisions and to develop conservation plans that are better adapted to species that are already threatened by human activities.

## Tables

**Table 2-1** Posterior mean and 95% credible intervals of predictors from our structural equation modelling with proportion of colours, Heterophil-to-lymphocyte ratio (H/L ratio), sum of active defensive behaviours and mean daily number of vessel crossings as response variables in painted turtles (*Chrysemys picta*). The models were performed separately for males and females, and for the proportion of red on the turtle's neck and yellow on the turtle's head. Reference factors are in parentheses for categorical predictor variables. Residual and group-level (i.e., sampling site identity) variances are available for each response variable. Predictors for which the 95% credible intervals did not overlap with zero are in bold

| Response variables | Predictors | Male (N = 124) | | Female (N = 92) | |
|---|---|---|---|---|---|
| | | Red | Yellow | Red | Yellow |
| Proportion of colours | Intercept | -0.019 | 0.042 | 0.065 | 0.064 |
| | | [-0.063 to 0.028] | [0.011 to 0.075] | [0.023 to 0.107] | [0.029 to 0.100] |
| | H/L ratio | -0.003 | -0.004 | 0.004 | 0.002 |
| | | [-0.012 to 0.005] | [-0.010 to 0.001] | [-0.006 to 0.015] | [-0.009 to 0.012] |
| | Year (2020) | -0.004 | -0.001 | -0.008 | 0.004 |
| | | [-0.019 to 0.011] | [-0.013 to 0.010] | [-0.025 to 0.007] | [-0.009 to 0.016] |
| | Carapace length | 0.001 | 0.0001 | -0.0001 | -0.0001 |
| | | [0.0003 to 0.001] | [-0.0002 to 0.0003] | [-0.0004 to 0.0002] | [-0.0003 to 0.0002] |
| | Sum of active defensive behaviours | 0.002 | 0.001 | -0.001 | 0.0001 |
| | | [-0.004 to 0.005] | [-0.002 to 0.004] | [-0.006 to 0.003] | [-0.004 to 0.004] |
| | Proportion of wetlands | -0.012 | -0.008 | -0.017 | -0.006 |
| | | [-0.031 to 0.008] | [-0.026 to 0.008] | [-0.054 to 0.018] | [-0.025 to 0.016] |
| | Sampling site identity (Group-level) | 0.008 | 0.008 | 0.018 | 0.007 |
| | | [0.001 to 0.016] | [0.002 to 0.015] | [0.009 to 0.033] | [0.0004 to 0.017] |
| | Residuals | 0.023 | 0.015 | 0.019 | 0.019 |
| | | [0.020 to 0.026] | [0.013 to 0.018] | [0.016 to 0.023] | [0.016 to 0.022] |
| H/L ratio | Intercept | 0.090 | 0.298 | 0.147 | 0.151 |
| | | [-0.664 to 0.837] | [-0.445 to 1.127] | [-0.471 to 0.738] | [-0.443 to 0.741] |
| | Mean daily number of vessel crossings | -0.006 | -0.012 | -0.007 | -0.007 |
| | | [-0.040 to 0.028] | [-0.050 to 0.021] | [-0.032 to 0.018] | [-0.032 to 0.018] |
| | Year (2020) | **-0.978** | **-1.160** | **-0.677** | **-0.680** |
| | | **[-1.503 to -0.479]** | **[-1.710 to -0.639]** | **[-1.142 to -0.189]** | **[-1.138 to -0.204]** |
| | Venipuncture site (Jugular vein) | **0.218** | **0.249** | **0.304** | **0.306** |
| | | **[0.002 to 0.439]** | **[0.029 to 0.469]** | **[0.047 to 0.571]** | **[0.044 to 0.571]** |
| | Sum of active defensive behaviours | **0.124** | **0.105** | -0.070 | -0.071 |
| | | **[0.021 to 0.229]** | **[0.002 to 0.211]** | [-0.193 to 0.048] | [-0.187 to 0.046] |
| | Haemoparasites (Infected) | 0.115 | 0.137 | -0.028 | -0.027 |

|  |  | | | | |
| --- | --- | --- | --- | --- | --- |
|  |  | [-0.136 to 0.364] | [-0.106 to 0.390] | [-0.293 to 0.239] | [-0.291 to 0.236] |
|  | Proportion of wetlands | -0.083 | -0.060 | -0.339 | -0.333 |
|  |  | [-1.121 to 1.018] | [-1.144 to 1.106] | [-0.960 to 0.222] | [-0.898 to 0.237] |
|  | Sampling site identity (Group-level) | 0.387 | 0.402 | 0.181 | 0.176 |
|  |  | [0.177 to 0.690] | [0.192 to 0.713] | [0.009 to 0.469] | [0.010 to 0.451] |
|  | Residuals | 0.551 | 0.554 | 0.543 | 0.544 |
|  |  | [0.479 to 0.631] | [0.484 to 0.636] | [0.463 to 0.638] | [0.466 to 0.636] |
| Sum of active defensive behaviours | Intercept | -2.880 | -2.757 | -0.831 | -0.833 |
|  |  | [-5.183 to -0.612] | [-5.115 to -0.522] | [-2.972 to 1.189] | [-2.970 to 1.135] |
|  | Mean daily number of vessel crossings | 0.008 | 0.009 | 0.018 | 0.018 |
|  |  | [-0.029 to 0.050] | [-0.029 to 0.051] | [-0.024 to 0.057] | [-0.025 to 0.059] |
|  | Carapace length | 0.015 | 0.014 | -0.004 | -0.004 |
|  |  | [-0.001 to 0.031] | [-0.001 to 0.031] | [-0.017 to 0.010] | [-0.017 to 0.010] |
|  | Proportion of wetlands | -0.403 | -0.314 | 0.552 | 0.585 |
|  |  | [-1.720 to 0.941] | [-1.621 to 0.969] | [-1.227 to 2.099] | [-1.213 to 2.087] |
|  | Sampling site identity (Group-level) | 0.503 | 0.513 | 0.424 | 0.432 |
|  |  | [0.135 to 0.994] | [0.120 to 0.989] | [0.022 to 1.132] | [0.022 to 1.137] |
|  | Residuals | – | – | – | – |
| Mean daily number of vessel crossings | Intercept | 2.626 | 2.593 | 2.576 | 2.577 |
|  |  | [2.341 to 2.906] | [2.294 to 2.889] | [2.268 to 2.883] | [2.266 to 2.885] |
|  | Year (2020) | **-0.395** | **-0.347** | **-0.370** | **-0.369** |
|  |  | **[-0.436 to -0.355]** | **[-0.390 to -0.304]** | **[-0.420 to -0.319]** | **[-0.419 to -0.319]** |
|  | Sampling site identity (Group-level) | 0.568 | 0.588 | 0.582 | 0.580 |
|  |  | [0.395 to 0.847] | [0.407 to 0.877] | [0.398 to 0.879] | [0.397 to 0.873] |
|  | Residuals | 0.042 | 0.044 | 0.055 | 0.055 |
|  |  | [0.037 to 0.048] | [0.039 to 0.051] | [0.047 to 0.065] | [0.047 to 0.065] |

# Figures



**Figure 2-1** (a) The structural equation model used to investigate how human disturbance influence the relationships between colouration, physiological response, and risk-taking behaviour in painted turtles (*Chrysemys picta*) of the Rideau Canal, Ontario, Canada. More specifically, we examined i) how human disturbance indirectly influenced colouration through physiological response (light blue lines), and ii) the impact of risk-taking propensity on colouration and physiological response (dark blue lines). Predictors used as proxies for our variables are in parentheses. The expected direction of the relationship between our variables of interests (in grey boxes) are represented by the (+) and (-) symbol located on the causal links. All the other predictors were included to control for their potential effect on the variables of interest. (b) Map of the Rideau Canal Waterway (light blue), Ontario, Canada, and the 18 sites (dots labelled with site names) sampled in 2019 and 2020. Pink dots represent supplementary sites from which we only have information on haematological parameters. Solid bars represent the lockstations with their respective numbers used as reference for Figure 2-1c. Wetland areas are depicted in dark blue based on the Southern Ontario Land Resource Information System (SOLRIS) V.3

(OMNRF, 2019). The map was built using ArcGIS® software by ESRI (www.esri.com). (c) Mean daily number of vessel crossings at each lockstation in 2019 (light blue) and 2020 (dark blue) based on Parks Canada records. The dashed line represents the mean across all lockstations for both years. The numbers used to identify each lockstation are the reference numbers from Figure 2-1b
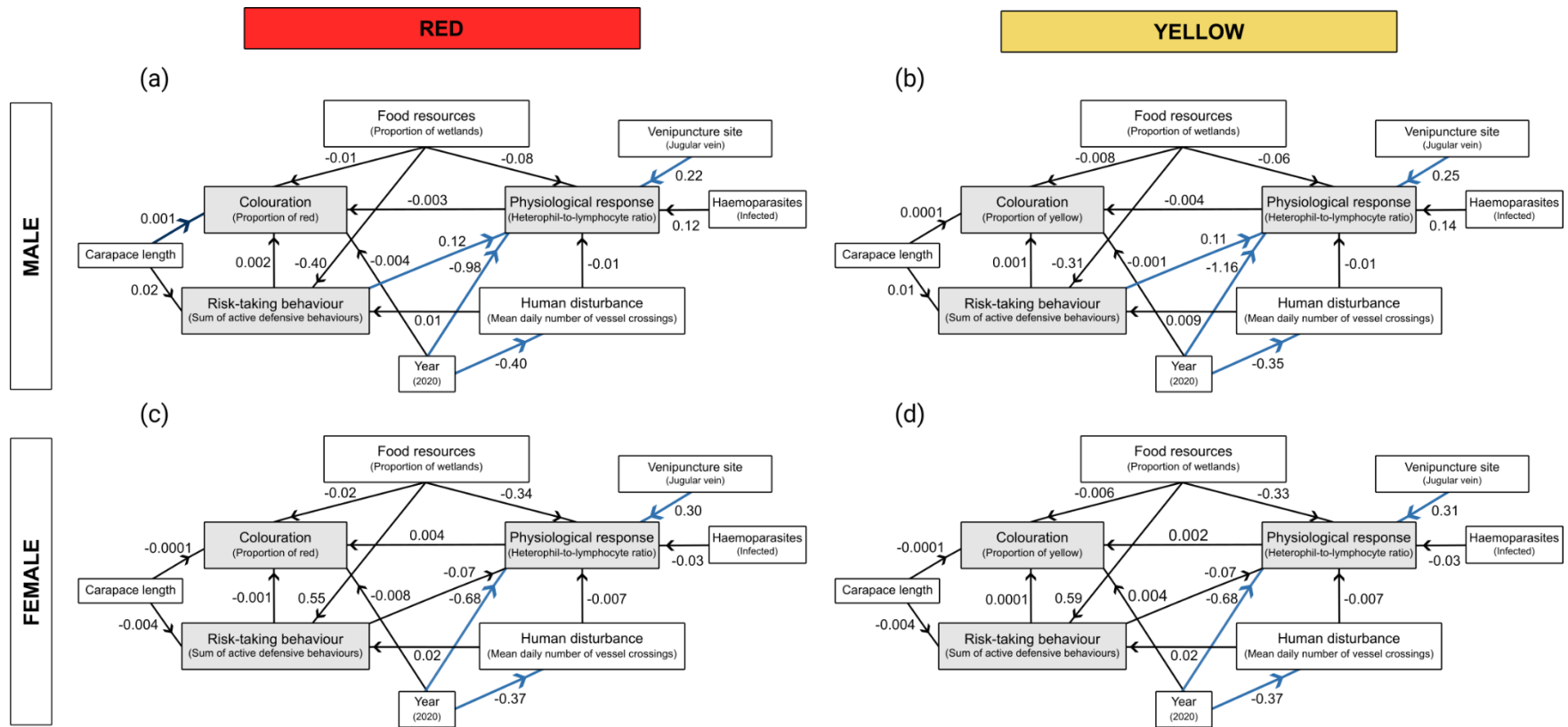
**Figure 2-2** Structural equation models used to assess the effect of human disturbance on the relationships between colouration, physiological response and risk-taking behaviour in painted turtles (*Chrysemys picta*) of the Rideau Canal, Ontario, Canada. The models were performed separately for males (a-b) and females (c-d), and for the proportion of red on the turtle's neck (a-c) and yellow on the turtle's head (b-d). The numbers correspond to the non-standardized coefficients of the causal links (lines) between variables. Light blue lines depict significant relationships for which the 95% credible intervals do not overlap zero. Variables in grey boxes represent our variables of interest according to our hypotheses. Predictors used as proxies for our variables are in parentheses, except for the categorical variables (i.e., venipuncture site, haemoparasites and year), for which it is the reference factor from the models
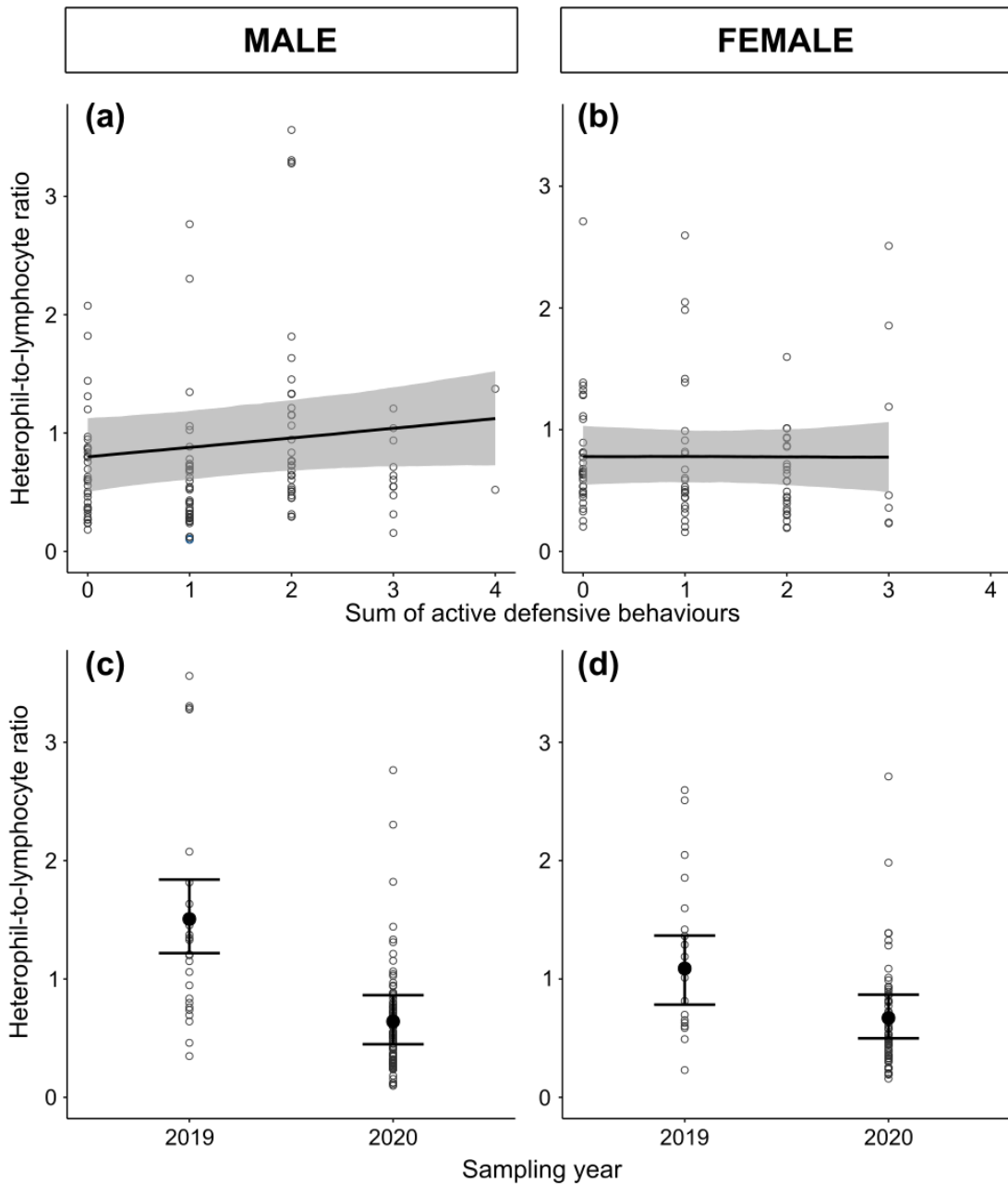
**Figure 2-3** Effects of (a-b) the sum of active defensive behaviours used by painted turtles during handling, and (c-d) the sampling year on the heterophil-to-lymphocyte ratio separately for the males (a-c) and the females (b-d). Grey dots represent observations (males = 125, females = 92). Black dots (c-d) and lines (a-b) depicted the model-predicted effect from a simplified version of our final model from which no other predictors were included, and the response variable was not log-transformed to facilitate effect visualization. Grey areas (a-b) and black bars (c-d) represent the 95% credible intervals.

# Supplementary information for Chapter 2

*Supporting Information 1 – Table S2-1 to S2-6*

**Table S2-1** Count of unique painted turtles with complete observations for all variables of interest (i.e., proportion of colours, heterophil-to-lymphocyte ratio and sum of active defensive behaviours used during handling) at 16 sampling sites across the Rideau Canal, Canada, in 2019 and 2020. The data from these turtles was used in our structural equation modelling which was performed separately for males and females, and for the proportion of yellow on turtle's head and proportion of red on turtle's neck. ¶: Sampling sites that were visited both years

| | YELLOW | | | | | | RED | | | | | |
| | MALE | | | FEMALE | | | MALE | | | FEMALE | | |
| Sites | 2019 | 2020 | Total | 2019 | 2020 | Total | 2019 | 2020 | Total | 2019 | 2020 | Total |
|---|---|---|---|---|---|---|---|---|---|---|---|---|
| RR1 | 0 | 4 | 4 | 0 | 8 | 8 | 0 | 4 | 4 | 0 | 8 | 8 |
| RR2-2020 | 0 | 9 | 9 | 0 | 13 | 13 | 0 | 9 | 9 | 0 | 13 | 13 |
| RR3-2 | 0 | 5 | 5 | 0 | 2 | 2 | 0 | 5 | 5 | 0 | 2 | 2 |
| RR6 | 0 | 25 | 25 | 0 | 14 | 14 | 0 | 25 | 25 | 0 | 14 | 14 |
| RR7 | 0 | 4 | 4 | 0 | 1 | 1 | 0 | 4 | 4 | 0 | 1 | 1 |
| RR9 | 0 | 12 | 12 | 0 | 9 | 9 | 0 | 12 | 12 | 0 | 9 | 9 |
| RR10 | 3 | 0 | 3 | 1 | 0 | 1 | 3 | 0 | 3 | 1 | 0 | 1 |
| LR1 | 1 | 0 | 1 | 2 | 0 | 2 | 1 | 0 | 1 | 2 | 0 | 2 |
| BR1¶ | 6 | 3 | 9 | 3 | 6 | 9 | 6 | 2 | 8 | 3 | 6 | 9 |
| BR2-2019 | 1 | 0 | 1 | 0 | 0 | 0 | 1 | 0 | 1 | 0 | 0 | 0 |
| BR2-2020 | 0 | 12 | 12 | 0 | 2 | 2 | 0 | 12 | 12 | 0 | 2 | 2 |
| UP6 | 9 | 0 | 9 | 7 | 0 | 7 | 9 | 0 | 9 | 7 | 0 | 7 |
| WF1¶ | 1 | 9 | 10 | 1 | 8 | 9 | 1 | 9 | 10 | 1 | 8 | 9 |
| C1¶ | 2 | 4 | 6 | 5 | 3 | 8 | 3 | 4 | 7 | 5 | 3 | 8 |
| RS1¶ | 0 | 4 | 4 | 0 | 1 | 1 | 0 | 4 | 4 | 0 | 1 | 1 |
| CB1¶ | 0 | 10 | 10 | 0 | 6 | 6 | 0 | 10 | 10 | 0 | 6 | 6 |
| TOTAL | 23 | 101 | 124 | 19 | 73 | 92 | 24 | 100 | 124 | 19 | 73 | 92 |

**Table S2-2** Compilation of home range estimates for painted turtles from the literature. N: Number of painted turtles sampled

| FEMALE | | MALE | | TOTAL | | |
|---|---|---|---|---|---|---|
| N | Home range (ha) | N | Home range (ha) | N | Home range (ha) | Source |
| 3 | 3.90 | 5 | 7.50 | 8 | 6.15 | Banning Anthonysamy (2012) |
| NA | NA | NA | NA | 10 | 89 | Jaeger & Cobb (2012) |
| NA | NA | NA | NA | 15 | 1.20 | Rowe (2003) |
| 9 | 1.80 | 4 | 2.90 | 13 | 2.14 | Rowe & Dalgarn (2010) |
| 5 | 21.60 | 3 | 8.30 | 8 | 14.95 | Saba & Spotila (2003) |
| 8 | 8.86 | NA | NA | 8 | 8.86 | Spalding (2020) |
| Mean | 9.04 | Mean | 6.23 | Mean (ha) | 20.38 | |
| | | | | Mean (in $m^2$) | 203800 | |

The majority of the data (except Spalding (2020)) come from Slavenko et al. (2016).

**Table S2-3** Buffer distances (in meters) for the proportion of wetlands with the highest absolute Pearson's correlation coefficient for each variable of interest: heterophil-to-lymphocyte ratio, proportion of colours and sum of active defensive behaviours used during handling. We determined the scale of maximum effect separately for the proportion of red and yellow, and for males and females. The buffer distance at which the correlation was maximal was included in the mixed-effect regression models

| Male - Red (N=124) | | |
|---|---|---|
| Variables | Correlation | Buffer (m) |
| Heterophil-to-lymphocyte ratio | -0.09 | 400 |
| Proportion of red on turtle's neck | -0.19 | 100 |
| Sum of active defensive behaviours | -0.10 | 200 |

| Male - Yellow (N=124) | | |
|---|---|---|
| Variables | Correlation | Buffer (m) |
| Heterophil-to-lymphocyte ratio | -0.09 | 400 |
| Proportion of yellow on turtle's head | -0.12 | 100 |
| Sum of active defensive behaviours | -0.08 | 200 |

| Female - Yellow and Red (N=92) | | |
|---|---|---|
| Variables | Correlation | Buffer (m) |
| Heterophil-to-lymphocyte ratio | -0.28 | 100 |
| Proportion of yellow on turtle's head | -0.10 | 100 |
| Proportion of red on turtle's neck | -0.12 | 100 |
| Sum of active defensive behaviours | 0.16 | 400 |

**Table S2-4** Descriptive statistics of our variables of interest and the predictors included in the mixed-effect regression models which were computed separately for the proportion of red on turtle's neck and yellow on turtle's head, and for males and females. Haemoparasites and venipuncture site were included as categorical predictors in models. SD = Standard deviation

| | TOTAL (N=217) | | | MALE (N=125) | | | FEMALE (N=92) | | |
|---|---|---|---|---|---|---|---|---|---|
| **Variables of interest** | mean | SD | range | mean | SD | range | mean | SD | range |
| Heterophil-to-lymphocyte ratio | 0.77 | 0.60 | 0.10 - 3.56 | 0.78 | 0.65 | 0.10 - 3.56 | 0.75 | 0.53 | 0.16 - 2.71 |
| Proportion of lymphocytes | 0.56 | 0.14 | 0.18 - 0.86 | 0.56 | 0.15 | 0.18 - 0.86 | 0.56 | 0.13 | 0.23 - 0.83 |
| Proportion of heterophils | 0.36 | 0.13 | 0.08 - 0.73 | 0.35 | 0.13 | 0.08 - 0.73 | 0.36 | 0.13 | 0.13 - 0.68 |
| Sum of active defensive behaviours used | 1.13 | 1.00 | 0 - 4 | 1.21 | 1.01 | 0 - 4 | 1.03 | 0.99 | 0 - 3 |
| Proportion of red on turtle's neck | 0.003 | 0.003 | 0.000 - 0.015 | 0.003 | 0.003 | 0.000 - 0.015 | 0.002 | 0.002 | 0.000 - 0.008 |
| Proportion of yellow on turtle's head | 0.003 | 0.002 | 0.000 - 0.011 | 0.002 | 0.002 | 0.000 - 0.007 | 0.003 | 0.002 | 0.000 - 0.011 |
| **Predictors** | | | | | | | | | |
| Carapace length (mm) | 140.34 | 18.46 | 93 - 188 | 134 | 14.09 | 95 - 160 | 148.95 | 20.20 | 93 - 188 |
| Mean daily number of vessel crossings | 11.76 | 8.85 | 5.61 - 34.07 | 12.02 | 8.91 | 5.61 - 34.07 | 11.41 | 8.80 | 5.61 - 34.07 |
| Proportion of wetlands within 100 m | 0.43 | 0.32 | 0.00 - 0.98 | 0.45 | 0.32 | 0.00 - 0.98 | 0.40 | 0.32 | 0.00 - 0.98 |
| Proportion of wetlands within 200 m | 0.34 | 0.28 | 0.00 - 0.76 | 0.37 | 0.28 | 0.00 - 0.76 | 0.31 | 0.28 | 0.00 - 0.76 |
| Proportion of wetlands within 400 m | 0.29 | 0.26 | 0.00 - 0.65 | 0.31 | 0.26 | 0.00 - 0.65 | 0.26 | 0.26 | 0.00 - 0.65 |
| Haemoparasites (0: uninfected; 1: infected) | 0.28 | 0.45 | 0 - 1 | 0.29 | 0.45 | 0 - 1 | 0.26 | 0.44 | 0 - 1 |
| Venipuncture site (0: coccygeal vein; 1: jugular vein) | 0.68 | 0.47 | 0 - 1 | 0.64 | 0.48 | 0 - 1 | 0.73 | 0.45 | 0 - 1 |

**Table S2-5** Posterior mean and 95% credible intervals of predictors from our structural equation modelling with proportion of colours, heterophil-to-lymphocyte ratio (H/L ratio), sum of active defensive behaviours, and the mean daily number of vessel crossings as response variables in painted turtles (*Chrysemys picta*). These models were performed to see the outcomes without sampling year as predictor and to confirm that the effect of sampling year observed in our final models cannot be distangled from the mean daily number of vessel crossings. The models were performed separately for males and females, and for the proportion of red on the turtle's neck and yellow on the turtle's head. Reference factors are in parentheses for categorical predictor variables. Residual and group-level (i.e., sampling site identity) variances are available for each response variable. Predictors for which the 95% credible intervals did not overlap with zero are in bold

| Response variables | Predictors | MALE (N = 124) | | FEMALE (N = 92) | |
| --- | --- | --- | --- | --- | --- |
| | | Red | Yellow | Red | Yellow |
| Proportion of colours | Intercept | -0.021 | 0.041 | 0.059 | 0.068 |
| | | [-0.066 to 0.024] | [0.010 to 0.071] | [0.019 to 0.100] | [0.033 to 0.103] |
| | H/L ratio | -0.002 | -0.004 | 0.005 | 0.0006 |
| | | [-0.010 to 0.005] | [-0.009 to 0.001] | [-0.006 to 0.016] | [-0.009 to 0.011] |
| | Carapace length | **0.0006** | 0.0001 | -0.0001 | -0.0001 |
| | | **[0.0002 to 0.0009]** | [-0.0002 to 0.0003] | [-0.0004 to 0.0002] | [-0.0003 to 0.0002] |
| | Sum of active defensive behaviours | 0.001 | 0.0008 | -0.001 | 0.000 |
| | | [-0.003 to 0.005] | [-0.002 to 0.004] | [-0.006 to 0.003] | [-0.004 to 0.004] |
| | Proportion of wetlands | -0.013 | -0.008 | -0.019 | -0.005 |
| | | [-0.032 to 0.007] | [-0.025 to 0.007] | [-0.053 to 0.013] | [-0.024 to 0.015] |
| | Sampling site identity (Group-level) | 0.008 | 0.007 | 0.016 | 0.007 |
| | | [0.001 to 0.016] | [0.002 to 0.015] | [0.007 to 0.029] | [0.001 to 0.017] |
| | Residuals | 0.023 | 0.015 | 0.020 | 0.019 |
| | | [0.020 to 0.026] | [0.013 to 0.018] | [0.017 to 0.023] | [0.016 to 0.022] |
| H/L ratio | Intercept | -1.035 | -1.024 | -0.474 | -0.488 |
| | | [-1.638 to -0.506] | [-1.574 to -0.510] | [-0.933 to 0.007] | [-0.952 to -0.020] |
| | Mean daily number of vessel crossings | **0.037** | **0.035** | 0.018 | 0.018 |
| | | **[0.009 to 0.071]** | **[0.008 to 0.070]** | [-0.005 to 0.044] | [-0.004 to 0.043] |
| | Venipuncture site (Jugular vein) | 0.188 | 0.218 | 0.225 | 0.232 |
| | | [-0.043 to 0.425] | [-0.018 to 0.453] | [-0.038 to 0.489] | [-0.029 to 0.502] |

| | | | | | |
|---|---|---|---|---|---|
| | Sum of active defensive behaviours | **0.139** | **0.117** | -0.062 | -0.063 |
| | | **[0.026 to 0.246]** | **[0.003 to 0.230]** | [-0.185 to 0.064] | [-0.187 to 0.062] |
| | Haemoparasites (Infected) | 0.036 | 0.091 | -0.037 | -0.033 |
| | | [-0.214 to 0.280] | [-0.176 to 0.366] | [-0.308 to 0.236] | [-0.311 to 0.235] |
| | Proportion of wetlands | -0.468 | -0.542 | **-0.688** | -0.679 |
| | | [-1.735 to 0.718] | [-1.714 to 0.536] | **[-1.386 to -0.048]** | [-1.386 to 0.006] |
| | Sampling site identity (Group-level) | 0.446 | 0.417 | 0.297 | 0.297 |
| | | [0.216 to 0.798] | [0.148 to 0.755] | [0.072 to 0.583] | [0.070 to 0.587] |
| | Residuals | 0.578 | 0.603 | 0.551 | 0.551 |
| | | [0.503 to 0.669] | [0.525 to 0.695] | [0.470 to 0.652] | [0.470 to 0.650] |
| Sum of active defensive behaviours | Intercept | -2.887 | -2.712 | -0.798 | -0.804 |
| | | [-5.155 to -0.610] | [-4.978 to -0.638] | [-2.882 to 1.207] | [-2.940 to 1.156] |
| | Mean daily number of vessel crossings | 0.008 | 0.009 | 0.019 | 0.018 |
| | | [-0.030 to 0.048] | [-0.030 to 0.053] | [-0.024 to 0.057] | [-0.023 to 0.056] |
| | Carapace length | 0.015 | 0.014 | -0.004 | -0.004 |
| | | [-0.001 to 0.032] | [-0.001 to 0.030] | [-0.018 to 0.010] | [-0.018 to 0.010] |
| | Proportion of wetlands | -0.407 | -0.304 | 0.560 | 0.585 |
| | | [-1.751 to 0.947] | [-1.679 to 1.054] | [-1.267 to 2.010] | [-1.134 to 2.056] |
| | Sampling site identity (Group-level) | 0.507 | 0.520 | 0.426 | 0.416 |
| | | [0.118 to 0.993] | [0.139 to 1.016] | [0.027 to 1.153] | [0.024 to 1.110] |
| | Residuals | – | – | – | – |
| Mean daily number of vessel crossings | Intercept | 2.359 | 2.351 | 2.308 | 2.308 |
| | | [2.009 to 2.705] | [2.012 to 2.707] | [1.949 to 2.661] | [1.958 to 2.667] |
| | Sampling site identity (Group-level) | 0.700 | 0.709 | 0.675 | 0.682 |
| | | [0.487 to 1.028] | [0.489 to 1.057] | [0.462 to 1.015] | [0.464 to 1.043] |
| | Residuals | 0.088 | 0.082 | 0.108 | 0.110 |
| | | [0.077 to 0.100] | [0.072 to 0.093] | [0.092 to 0.125] | [0.092 to 0.126] |

**Table S2-6** Posterior mean and 95% credible intervals of the effect of venipuncture site on different haematological parameters in painted turtles (*Chrysemys picta*) from mixed-effect regression models. Sampling site identity was included as random effect. We sampled blood from two venipuncture sites: the coccygeal and the jugular vein which the latest is the reference factor used in the models

| Haematological parameters | Total (N = 217) | Male (N = 125) | Female (N = 92) |
|---|---|---|---|
| Heterophil-to-lymphocyte ratio | 0.18 [0.01 to 0.36] | 0.19 [-0.06 to 0.43] | 0.21 [-0.06 to 0.48] |
| Proportion of lymphocytes | -0.05 [-0.08 to -0.01] | -0.05 [-0.10 to -0.00] | -0.05 [-0.10 to -0.00] |
| Proportion of heterophils | 0.03 [-0.00 to 0.07] | 0.03 [-0.02 to 0.08] | 0.04 [-0.02 to 0.10] |
| Total count of leukocytes | -30.28 [-67.51 to 7.30] | -1.08 [-49.68 to 45.34] | -66.19 [-126.82 to -5.41] |

*Supporting Information 2 – Description and repeatability estimation of haematological parameters*

1. Description of the haematological parameters

In this study, we were mainly interested by the heterophil-to-lymphocyte ratio (H/L ratio), which is widely used to quantify physiological response to environmental stressors in wildlife (Davis et al., 2008; Davis & Maney, 2018). However, other parameters can be measured to have a better overview of animal's physiological state (Davis et al., 2008). Indeed, infections and diseases can also be responsible for changes observed in circulating leukocyte profiles (Davis et al., 2008). Distinguishing these effects from physiological stress can be difficult when no information on animals' infection status is available (Davis et al., 2008). In addition to increase H/L ratios, infections may also lead to an increase in the number of circulating monocytes and the total count of leukocytes. On the other hand, physiological response to stressful conditions can be associated to a decrease in circulating eosinophils (Davis et al., 2008). Thus, taking into account of several haematological parameters can help us to dissociate the possible different sources of changes in circulating leukocyte profiles (Davis et al., 2008). In our case, we included the infection status by blood parasites in our models. In addition, in reptiles, descriptive statistics of haematological parameters are currently mainly available for veterinary medicine purpose leaving many wildlife species with scant information (Arikan & Çiçek, 2014; Campbell, 2015; Heatley & Russell, 2018; Nardini et al., 2013). Thus, increasing the access to haematological information for wildlife species is necessary. See Table S2-7 for a descriptive summary of the haematological parameters measured in painted turtles, Table S2-8 for the number of individuals with haematological measurements per sampling site, and Figure S2-1 for the correlation coefficients between the parameters.

**Table S2-7** Descriptive statistics of haematological parameters measured on 382 painted turtles. SD = Standard deviation. Sex was unidentified for 12 individuals. Some granulocytes (i.e., heterophils, eosinophils and basophils) were difficult to differentiate and were categorized as unidentified granulocytes

| Haematological parameters | Total (N=382) | | | Male (N=219) | | | Female (N=151) | | |
|---|---|---|---|---|---|---|---|---|---|
| | Mean | SD | Range | Mean | SD | Range | Mean | SD | Range |
| Proportion of lymphocytes | 0.57 | 0.14 | [0.18 - 0.90] | 0.56 | 0.15 | [0.18 - 0.88] | 0.58 | 0.14 | [0.22 - 0.90] |
| Proportion of heterophils | 0.35 | 0.13 | [0.05 - 0.73] | 0.35 | 0.13 | [0.06 - 0.73] | 0.35 | 0.14 | [0.06 - 0.68] |
| Proportion of eosinophils | 0.06 | 0.04 | [0.00 - 0.26] | 0.06 | 0.04 | [0.00 - 0.23] | 0.06 | 0.04 | [0.00 - 0.26] |
| Proportion of basophils | 0.01 | 0.01 | [0.00 - 0.06] | 0.01 | 0.01 | [0.00 - 0.06] | 0.00 | 0.01 | [0.00 - 0.06] |
| Proportion of monocytes | 0.01 | 0.01 | [0.00 - 0.06] | 0.01 | 0.01 | [0.00 - 0.06] | 0.01 | 0.01 | [0.00 - 0.04] |
| Proportion of unidentified granulocytes | 0.01 | 0.01 | [0.00 - 0.06] | 0.01 | 0.01 | [0.00 - 0.06] | 0.01 | 0.01 | [0.00 - 0.03] |
| Heterophil-to-lymphocyte ratio | 0.73 | 0.54 | [0.07 - 3.56] | 0.76 | 0.58 | [0.07 - 3.56] | 0.71 | 0.50 | [0.07 - 2.71] |
| Total count of leukocytes | 326.36 | 135.06 | [54 - 856] | 310.25 | 134.06 | [71 - 807] | 346.83 | 133.82 | [54 - 856] |

**Table S2-8** Number of painted turtles with haematological measurements per sampling site. Sex was not determined for 12 painted turtles. ¶ Sites sampled in 2019 and 2020

| Sampling sites | Female | Male | Not determined | Total |
|---|---|---|---|---|
| RR1 | 13 | 4 | 2 | 19 |
| RR2-2020 | 14 | 9 | 4 | 27 |
| RR3-2 | 2 | 7 | 0 | 9 |
| RR6 | 16 | 26 | 0 | 42 |
| RR7 | 6 | 17 | 0 | 23 |
| RR9 | 9 | 13 | 0 | 22 |
| RR10 | 1 | 6 | 0 | 7 |
| LR1 | 3 | 1 | 0 | 4 |
| BR1¶ | 18 | 26 | 2 | 46 |
| BR2-2019 | 0 | 1 | 1 | 2 |
| BR2-2020 | 8 | 14 | 0 | 22 |
| UP6 | 8 | 10 | 0 | 18 |
| CL2 | 5 | 11 | 1 | 17 |
| SA1 | 3 | 9 | 0 | 12 |
| WF1¶ | 10 | 16 | 2 | 28 |
| C1¶ | 10 | 10 | 0 | 20 |
| RS1¶ | 5 | 17 | 0 | 22 |
| CB1¶ | 20 | 22 | 0 | 42 |
| Total | 151 | 219 | 12 | 382 |
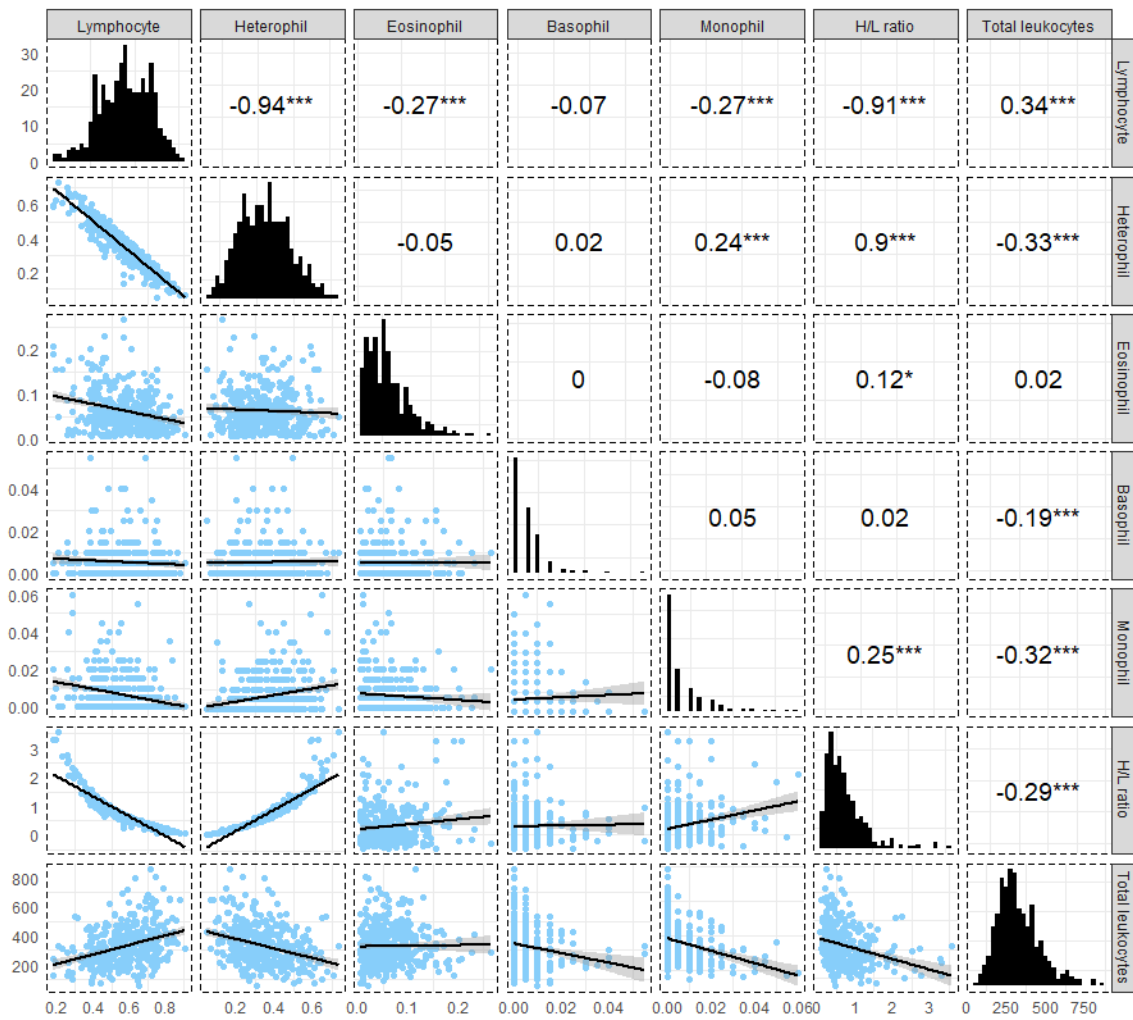
**Figure S2-1** Pearson correlation coefficients (upper panel) between haematological parameters measured on 382 painted turtles: proportion of different leukocytes (i.e., lymphocytes, heterophils, eosinophils, basophils, monocytes), heterophil-to-lymphocyte ratio (H/L ratio), and total number of leukocytes (Total leukocytes). Significance level of the correlations are represented by the number of asterisks (*** = < 0.001; ** = 0.001 – 0.01; * = 0.01 – 0.05). Distribution of each parameter is available on the diagonal. Relationships between parameters are illustrated by scatter pots with a regression line on the lower panel. Each blue dot represents an observation

## 2. Assessment of repeatability estimates

To evaluate the accuracy of our measurements, we analyzed twice randomly selected subsamples of blood smears and estimated the repeatability of our different haematological parameters: the proportion of different leukocytes (i.e., lymphocytes, heterophils and eosinophils), the H/L ratio and the total number of leukocytes. The proportion of basophils and monocytes were too low to correctly estimate repeatability (mean = 0.01, standard deviation = 0.01; Table S2-7). More specifically, we wanted i) to evaluate our capacity to obtain similar haematological measurements between two scans following different lines in the same region of the smear; ii) to assess the level of reproducibility of our counts between observers; and iii) among scans from a second observer. In addition, we wanted to evaluate the potential effect on our measurements of the non-random distribution on the smears of the different types of leukocytes. To do so, we estimated the repeatability of our measurements between the first and second set of 100 leukocytes differentiated along the same scan line from our entire dataset.

The statistical analyses were conducted with R 4.2.0 (R Core Team, 2022) using the *rpt* function implemented in the rptR package (Stoffel et al., 2017). We assessed repeatability by using mixed models which included turtle identity as a random effect to estimate among and within-individual variance for each haematological parameter. We used a Gaussian distribution for all our models, except that we applied a log or a square-root transformation prior to the analyses for some parameters (Table S2-9). The transformation that we applied is specific to each subsample we used (Table S2-9). We also adjusted our models for among-individual differences using sex, venipuncture site (i.e., jugular or coccygeal vein), order of processing (to possibly control for an effect of learning by the observer over time on the measurements), scan order (i.e., first or second scan), and sampling year (2019 or 2020) as fixed effects. The observer identity was included in the

models used to estimate repeatability between observers. We also included sampling site identity as a random effect to control for the non-independence of observations from the same location. Blood smears analyzed by the second observer were all from 2020 and scanned in a timeframe of two weeks, while those analyzed by the first and main observer were scanned over six months. Only the variables having a significant effect on the response variable (i.e., haematological parameter) were kept in the final adjusted models (Table S2-9). We estimated the 95% confidence intervals of our repeatability estimates using likelihood ratio tests (LRTs) with 1,000 parametric bootstrap iterations. See Table S2-9 for repeatability estimates and more details about the analyses.

**Table S2-9** Repeatability estimates (R) of five haematological parameters analyzed in painted turtles to evaluate the accuracy of our measurements: the proportion of lymphocytes, heterophils and eosinophils, the heterophil-to-lymphocyte ratio (H/L ratio), and the total number of leukocytes (Total leukocytes). The unadjusted repeatability estimates only included turtle identity (ID) as random effect, while the adjusted repeatability estimates also included sex, venipuncture site, order of processing, scan order, sampling year and/or observer identity as fixed effects (according to the subsample analyzed), and sampling site identity as a random effect ($R_{site}$). Only the fixed and random variables having a significant effect on the haematological parameters were included in the final models used to calculate the adjusted repeatability estimates (Final models). Significance [95 % confidence intervals] of repeatability estimates were determined with likelihood ratio tests. The coefficient of determination ($R^2$) of the fixed effects included in the adjusted repeatability estimates was calculated. Number of turtles measured (Nb.turtles) with the total number of observations (Nb.entries: two scans per turtle) for each haematological parameter are provided

**A) Repeatability between the first and second set of 100 leukocytes differentiated by the observer 1 along the same scan line**

| Parameters | Unadjusted | | Adjusted | | | | |
| --- | --- | --- | --- | --- | --- | --- | --- |
| | Nb.turtles (Nb.entries) | $R_{individual}$ | Nb.turtles (Nb.entries) | Final models | $R_{individual}$ | $R_{site}$ | $R^2_{fixed}$ |
| Lymphocytes | 379 (758) | 0.86 [0.84 - 0.89] | 379 (758) | y ~ Year + (1 \| ID) + (1\|Site) | 0.70 [0.60 - 0.79] | 0.14 [0.04 - 0.25] | 0.16 |
| Heterophils | 379 (758) | 0.86 [0.84 - 0.89] | 379 (758) | y ~ Year + (1 \| ID) + (1\|Site) | 0.73 [0.63 - 0.82] | 0.11 [0.03 - 0.22] | 0.14 |
| Eosinophils | 379 (758) | 0.65 [0.60 - 0.71] | 379 (758) | sqrt(y) ~ Year + Processing order + (1 \| ID) + (1\|Site) | 0.52 [0.44 - 0.60] | 0.08 [0.01 - 0.16] | 0.18 |
| H/L ratio | 379 (758) | 0.86 [0.83 - 0.89] | 379 (758) | sqrt(y) ~ Year + (1 \| ID) + (1\|Site) | 0.73 [0.64 - 0.80] | 0.11 [0.03 - 0.21] | 0.17 |
| Total leukocytes | – | – | – | – | – | – | – |

**B) Repeatability between two scans made by the observer 1 following different lines in the same region of the smear**

| Parameters | Unadjusted | | Adjusted | | | | |
| --- | --- | --- | --- | --- | --- | --- | --- |
| | Nb.turtles (Nb.entries) | $R_{individual}$ | Nb.turtles (Nb.entries) | Final models | $R_{individual}$ | $R_{site}$ | $R^2_{fixed}$ |
| Lymphocytes | 21 (42) | 0.80 [0.58 - 0.91] | 21 (42) | y ~ (1 \| ID) | – | – | – |
| Heterophils | 21 (42) | 0.85 [0.64 - 0.94] | 21 (42) | y ~ (1 \| ID) | – | – | – |
| Eosinophils | 21 (42) | 0.82 [0.58 - 0.92] | 21 (42) | sqrt(y) ~ Processing order + (1 \| ID) | 0.71 [0.45 - 0.87] | – | 0.37 |
| H/L ratio | 21 (42) | 0.82 [0.60 - 0.92] | 21 (42) | log(y) ~ (1 \| ID) | – | – | – |
| Total leukocytes | 21 (42) | 0.63 [0.32 - 0.84] | 21 (42) | y ~ (1 \| ID) | – | – | – |

**C) Repeatability between two scans made by the observer 2 following different lines in the same region of the smear**

| Parameters | Unadjusted | | Adjusted | | | | |
|---|---|---|---|---|---|---|---|
| | Nb.turtles (Nb.entries) | $R_{individual}$ | Nb.turtles (Nb.entries) | Final models | $R_{individual}$ | $R_{site}$ | $R^2_{fixed}$ |
| Lymphocytes | 20 (40) | 0.92 [0.82 - 0.97] | 20 (40) | y ~ (1|ID) + (1|Site) | 0.30 [0.08 - 0.84] | 0.64 [0.00 - 0.87] | – |
| Heterophils | 20 (40) | 0.94 [0.85 - 0.98] | 20 (40) | y ~ (1|ID) + (1|Site) | 0.27 [0.08 - 0.88] | 0.67 [0.00 - 0.89] | – |
| Eosinophils | 20 (40) | 0.67 [0.36 - 0.85] | 20 (40) | sqrt(y) ~ (1 | ID) | – | – | – |
| H/L ratio | 20 (40) | 0.93 [0.84 - 0.97] | 20 (40) | log(y) ~ (1|ID) + (1|Site) | 0.29 [0.08 - 0.88] | 0.65 [0.00 - 0.88] | – |
| Total leukocytes | 20 (40) | 0.60 [0.22 - 0.82] | 20 (40) | log(y) ~ scan order + (1|ID) | 0.69 [0.39 - 0.87] | – | 0.07 |

**D) Repeatability between observers**

| Parameters | Unadjusted | | Adjusted | | | | |
|---|---|---|---|---|---|---|---|
| | Nb.turtles (Nb.entries) | $R_{individual}$ | Nb.turtles (Nb.entries) | Final models | $R_{individual}$ | $R_{site}$ | $R^2_{fixed}$ |
| Lymphocytes | 20 (40) | 0.82 [0.61 - 0.92] | 18 (36) | y ~ Sex + Processing order + Observer + (1|ID) | 0.75 [0.51 - 0.91] | – | 0.48 |
| Heterophils | 20 (40) | 0.73 [0.44 - 0.88] | 18 (36) | y ~ Sex + Processing order + Observer + (1|ID) | 0.64 [0.30 - 0.87] | – | 0.57 |
| Eosinophils | 20 (40) | 0.63 [0.29 - 0.84] | 20 (40) | sqrt(y) ~ Observer + (1 | ID) | 0.69 [0.39 - 0.87] | – | 0.04 |
| H/L ratio | 20 (40) | 0.77 [0.52 - 0.90] | 18 (36) | log(y) ~ Sex + Processing order + Observer + (1|ID) | 0.68 [0.38 - 0.88] | – | 0.55 |
| Total leukocytes | 20 (40) | 0.75 [0.48 - 0.89] | 20 (40) | log(y) ~ Processing order + Observer + (1|ID) | 0.85 [0.67 - 0.94] | – | 0.25 |

*Supporting Information 3 – A step-by-step method to quantify colouration with digital photography*

**Note:** A slightly modified version of this protocol is currently under review for publication in *MethodsX*.

Abstract

Colouration is often used in biological studies, for example when studying social signaling or antipredator defense. Yet, few detailed and standardized methods are available to measure colouration using digital photography. Here we provide a step-by-step guide to help researchers quantify colouration from digital images. We first identify the do's and don'ts of taking pictures for colouration analysis. We then describe how to i) extract reflectance values with the software ImageJ; ii) fit and apply linearization equations to reflectance values; iii) scale and select the areas of interest in ImageJ; iv) standardize pictures; and v) binarize and measure the proportion of different colors in an area of interest. We apply our methodological protocol to digital pictures of painted turtles (*Chrysemys picta*), but the approach could be easily adapted to any species. More specifically, we wished to calculate the proportion of red and yellow on the neck and head of turtles. With this protocol, our main aims are to make colouration analyses with digital photography:

- more accessible to researchers without a background in photography ;

- more consistent between studies.

About

Colouration is often used in biological studies, for example when studying social signaling or antipredator defense (see Cuthill et al. (2017) for a review). Yet, few detailed standardized methods are available to measure colouration using digital photography. Here we aim to make colouration analyses: i) more accessible to researchers without a background in photography and ii) more consistent between

studies. In this tutorial, you will learn 1) the do's and don'ts of taking pictures for colouration analysis, 2) to extract reflectance values with ImageJ, 3) to create linearization equations, 4) to linearize your pictures with the equations created, 5) to scale and select the areas of interest in ImageJ, 6) to rapidly classify your pictures, 7) to standardize your pictures, and 8) to binarize the colours of the areas of interest. Make sure you thoroughly read the whole protocol before beginning your analyses. Important notes are included throughout the different sections.

You should first install the following software/packages:

- ImageJ: http://imagej.nih.gov/ij/download.html (Abràmoff et al., 2004)

- DCRaw Reader (ImageJ package to open various RAW file types): http://ij-plugins.sourceforge.net/plugins/dcraw/ (Coffin, 2015)

- R https://cran.r-project.org/ (R Core Team, 2022)

- RStudio (https://posit.co/download/rstudio-desktop/) (Posit Team, 2022)

The tutorial has been optimized for use under Windows 10. We have not verified compatibility with any other operating system and/or version, but because the software and packages we used are available for multiple platforms, it should work on all major platforms such as Mac OS and Linux.

Basic knowledge in colouration and digital photography is needed to understand well this tutorial. We also suggest reading the following papers: Paterson & Blouin-Demers, 2017; Stevens et al., 2007; Teasdale et al., 2013.

1. In the field: steps to follow

Here are some basic guidelines to consider before taking pictures:

**Tip #1**: All pictures should include a colour chart (e.g., X-Rite ColorChecker Passport) and a ruler (most colour charts already include a ruler).

**Tip #2**: Pictures should be stored as .RAW or an equivalent format (e.g., .NEF); avoid compressed files.

**Tip #3**: All pictures should be taken with identical camera settings. Avoid automatic settings. Importantly, make sure all your pictures are taken with the same ISO value.

**Tip #4:** It is more convenient if all picture elements have the same configuration: the animal and the ruler are approximately at the same place in all pictures, and they are all taken either in portrait or in landscape format.
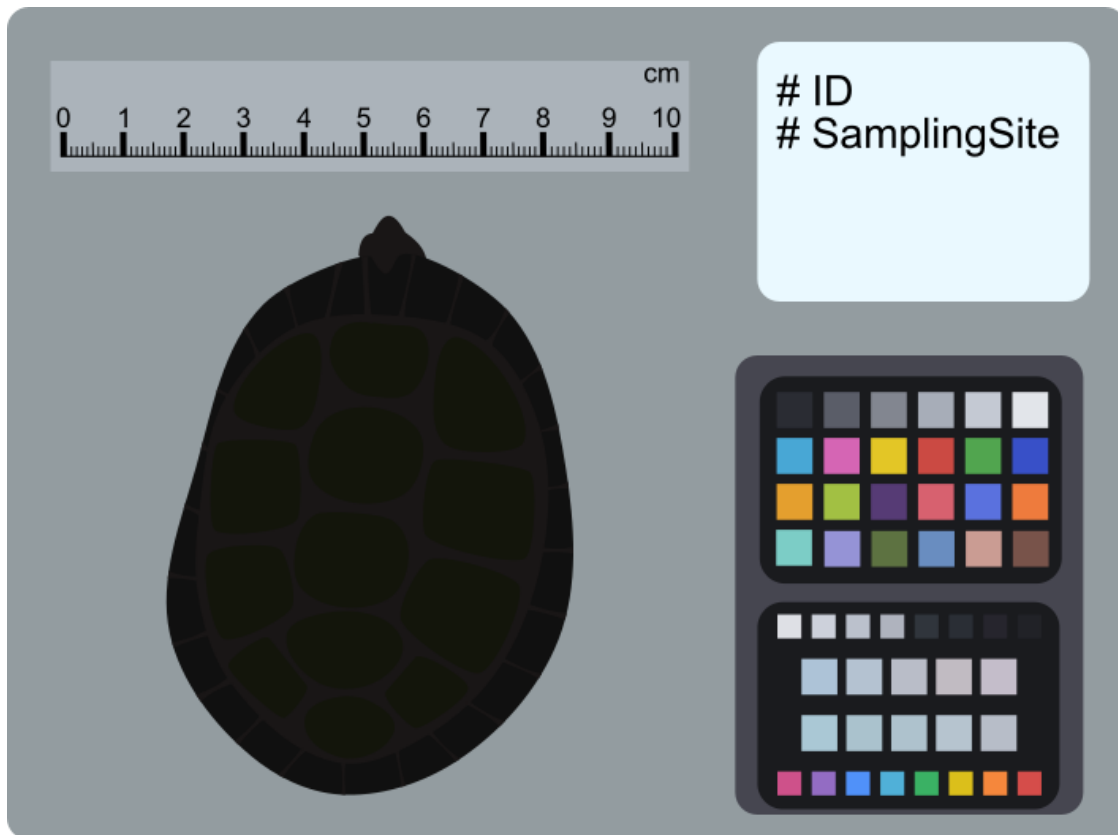


**Tip #5:** Take slightly underexposed pictures to avoid pixel saturation (see Stevens et al., 2007). Avoid direct sunlight; take your pictures in the shade or use a cover (e.g., umbrella).

**Tip #6:** Make sure you have access to the expected reflectance values (sRGB: Red (R), Green (G), Blue (B)) of the chart colours used. It is essential to correctly linearize your pictures because the expected grey reflectance values are necessary to create the linearization equations.

In our case, pictures were stored as .NEF and they all included an X-Rite ColorChecker Passport for which the grey reflectance values in sRGB are shown in the chart below (squares 19 to 24).

| No. | Colour name | | Expected reflectance value (sRGB) | | |
|---|---|---|---|---|---|
| | | | R | G | B |
| 1 | dark skin | | 115 | 82 | 68 |
| 2 | light skin | | 194 | 150 | 130 |
| 3 | blue sky | | 98 | 122 | 157 |
| 4 | foliage | | 87 | 108 | 67 |
| 5 | blue flower | | 133 | 128 | 177 |
| 6 | bluish green | | 103 | 189 | 170 |
| 7 | orange | | 214 | 126 | 44 |
| 8 | purplish blue | | 80 | 91 | 166 |
| 9 | moderate red | | 193 | 90 | 99 |
| 10 | purple | | 94 | 60 | 108 |
| 11 | yellow green | | 157 | 188 | 64 |
| 12 | orange yellow | | 224 | 163 | 46 |
| 13 | blue | | 56 | 61 | 150 |
| 14 | green | | 70 | 148 | 73 |
| 15 | red | | 175 | 54 | 60 |
| 16 | yellow | | 231 | 199 | 31 |
| 17 | magenta | | 187 | 86 | 149 |
| 18 | cyan | | 8 | 133 | 161 |
| 19 | white | | 243 | 243 | 242 |
| 20 | neutral 8 | | 200 | 200 | 200 |
| 21 | neutral 6.5 | | 160 | 160 | 160 |
| 22 | neutral 5 | | 122 | 122 | 121 |
| 23 | neutral 3.5 | | 85 | 85 | 85 |
| 24 | black | | 52 | 52 | 52 |

## 2. Extracting reflectance values with ImageJ

### 2.1 Preparing a spreadsheet file

To create linearization equations, you need to extract reflectance values from a subset of pictures that represents various ambient lighting conditions. If you have few pictures, you should use all of them. In

our case, we took multiple pictures for each turtle and, thus, we used the first picture taken of all individuals to cover all lighting conditions (N = 260 pictures). Before you start working with ImageJ, prepare a spreadsheet file similar to this one:

| | A | B | C | D | E | F | G | H | I | J | K |
|---|---|---|---|---|---|---|---|---|---|---|---|
| 1 | ID | No.Photo | RGB | Grey scale | Expected_sRGB | Square | Label | Area | Mean | Min | Max |
| 2 | 1 | 5 | R | Black | 52 | 1 | DSC_0522.NEF:3486-3375:Red | 0.122 | 17.355 | 2 | 40 |
| 3 | 1 | 5 | R | Neutral 3.5 | 85 | 2 | DSC_0522.NEF:3693-3369:Red | 0.129 | 36.574 | 22 | 49 |
| 4 | 1 | 5 | R | Neutral 5 | 122 | 3 | DSC_0522.NEF:3897-3360:Red | 0.122 | 58.94 | 48 | 69 |
| 5 | 1 | 5 | R | Neutral 6.5 | 160 | 4 | DSC_0522.NEF:4098-3336:Red | 0.144 | 86.193 | 75 | 98 |
| 6 | 1 | 5 | R | Neutral 8 | 200 | 5 | DSC_0522.NEF:4299-3324:Red | 0.096 | 111.026 | 102 | 119 |
| 7 | 1 | 5 | R | White | 243 | 6 | DSC_0522.NEF:4503-3306:Red | 0.136 | 140.177 | 129 | 150 |
| 8 | 1 | 5 | G | Black | 52 | 7 | DSC_0522.NEF:3486-3375:Green | 0.122 | 16.342 | 9 | 28 |
| 9 | 1 | 5 | G | Neutral 3.5 | 85 | 8 | DSC_0522.NEF:3693-3369:Green | 0.129 | 35.378 | 26 | 42 |
| 10 | 1 | 5 | G | Neutral 5 | 122 | 9 | DSC_0522.NEF:3897-3360:Green | 0.122 | 56.265 | 49 | 64 |
| 11 | 1 | 5 | G | Neutral 6.5 | 160 | 10 | DSC_0522.NEF:4098-3336:Green | 0.144 | 83.321 | 77 | 89 |
| 12 | 1 | 5 | G | Neutral 8 | 200 | 11 | DSC_0522.NEF:4299-3324:Green | 0.096 | 107.35 | 101 | 113 |
| 13 | 1 | 5 | G | White | 243 | 12 | DSC_0522.NEF:4503-3306:Green | 0.136 | 134.341 | 125 | 140 |
| 14 | 1 | 5 | B | Black | 52 | 13 | DSC_0522.NEF:3486-3375:Blue | 0.122 | 15.8 | 9 | 26 |
| 15 | 1 | 5 | B | Neutral 3.5 | 85 | 14 | DSC_0522.NEF:3693-3369:Blue | 0.129 | 34.38 | 26 | 41 |
| 16 | 1 | 5 | B | Neutral 5 | 121 | 15 | DSC_0522.NEF:3897-3360:Blue | 0.122 | 54.301 | 45 | 62 |
| 17 | 1 | 5 | B | Neutral 6.5 | 160 | 16 | DSC_0522.NEF:4098-3336:Blue | 0.144 | 80.024 | 73 | 86 |
| 18 | 1 | 5 | B | Neutral 8 | 200 | 17 | DSC_0522.NEF:4299-3324:Blue | 0.096 | 103.279 | 93 | 110 |
| 19 | 1 | 5 | B | White | 242 | 18 | DSC_0522.NEF:4503-3306:Blue | 0.136 | 128.618 | 116 | 135 |
| 20 | 2 | 13 | R | Black | 52 | 1 | DSC_0611.NEF:0582-1532:Red | 0.134 | 21.502 | 0 | 36 |

For each individual (ID), you need to have three rows per grey colour square from your colour chart for each picture you want to analyze. The number of grey colour squares can vary between colour charts. In our case, we had six grey colour squares giving us 18 rows per individual (column Square contains the number of each row). You will need to extract the reflectance value for each grey scale square from the colour chart (in our colour chart, we had six grey scales: Black, Neutral 3.5, Neutral 5, Neutral 6.5, Neutral 8, and White) for each colour channel (RGB: Red (R), Green (G), Blue (B)). Each grey scale square has a total of three expected reflectance value: one per colour channel (Expected_sRGB). Each row has a square number (Square) that represents the number of the region of interest that will later be created in ImageJ to calculate the reflectance value associated to each grey scale for each colour channel. All other columns (e.g., Label, Area, Mean, Min and Max) contain information that will be generated by ImageJ.

*2.2 Opening a .NEF picture in ImageJ*

All the steps that are performed in ImageJ are subject to slight variations due to the person performing the analyses. It is thus important to i) have the same person to make all the analyses in ImageJ or ii) quantify the variance between measurements that were performed by different persons in ImageJ (calculate repeatability).

🎬 You can see steps 2.2 and 2.3 in this video: https://youtu.be/kbqcvgtKjmw

In our case, all pictures were saved in .NEF format, which is the equivalent of .RAW file extension for Nikon cameras. Other companies may use other RAW extensions, but they should basically be the same. To open a .NEF picture in ImageJ, the DCRaw package is required (it can be found here: https://github.com/ij-plugins/ijp-dcraw; Installation instructions are provided on the same page). To install the package on your computer, you need to unzip the file and copy the executable document (ij-dcraw_.jar) in the *plugins* file of the *ImageJ* file from your computer.
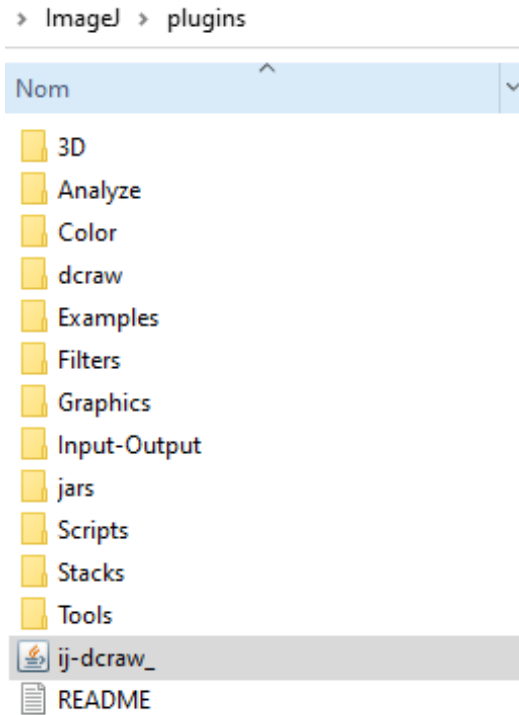
Once the package is installed, restart ImageJ and it will now be possible to open a picture by clicking on *Pluggins >> Input-Output >> DCRaw Reader* and then selecting the appropriate file. The following menu will appear, and you can see the options we used for our analyses:
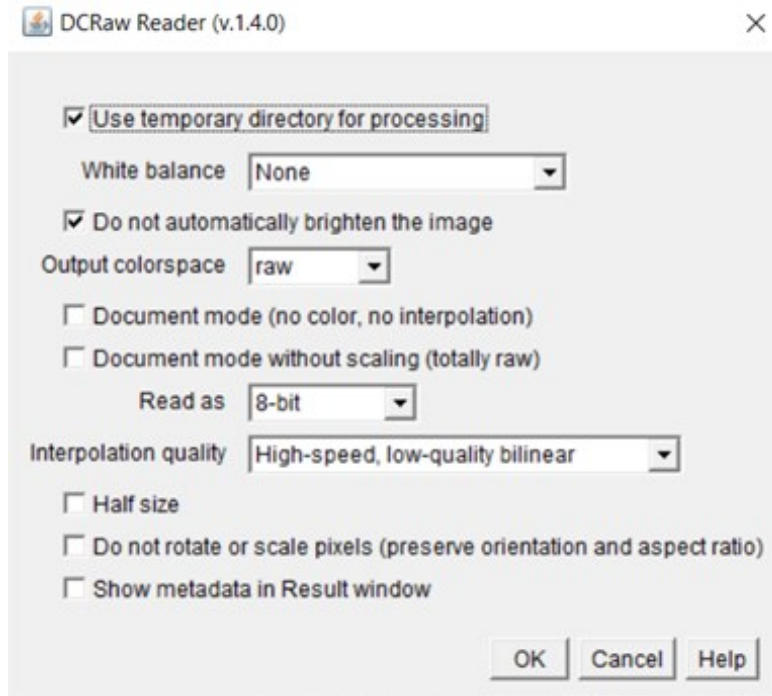
*2.3 Saving pictures in TIFF format*

Now save your pictures as .TIFF via *File >> Save as >> Tiff*. This will allow you to work on a picture that has the parameters you previously specified instead of working on a projection of a .RAW file for which you do not know what kind of transformations have been applied. The new .TIFF picture will be the one you will use as input in the following R scripts. Even if you only use a subset of pictures to obtain the linearization equations, you must do this step for all pictures that you want to use in your final analyses. The .TIFF picture may appear darker than the visualization, it is normal.

*2.4 Extracting RGB scores in ImageJ*

You can see step 2.4 in this video: https://youtu.be/8iDWLSDFgOo

Now that you have your .TIFF picture opened in ImageJ, the first step to extract RGB scores is to create selection squares (i.e., region of interest, ROI) over the colour chart's grey squares. To create multiple selections, open the *ROI Manager* by clicking on *Analyze >> Tools >> ROI Manager*. Make sure you

check the *Show All* and *Labels* options in the window before you begin.
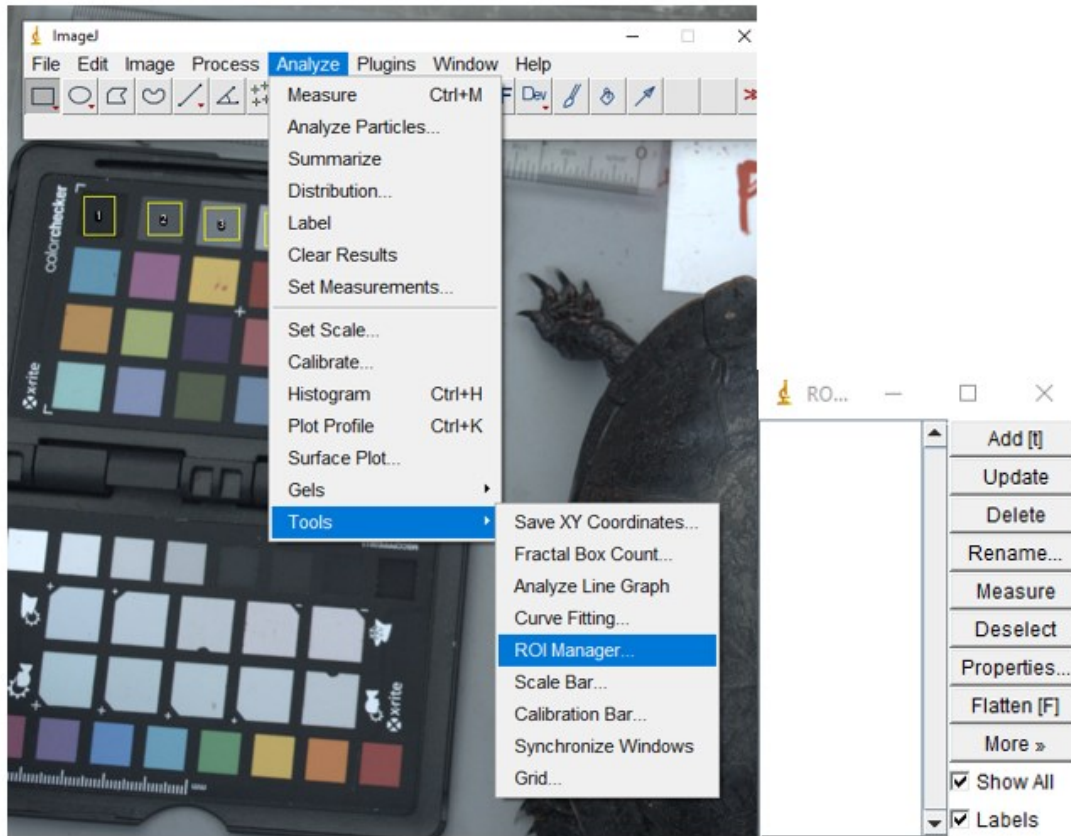


You can now draw a square over one of the chart's grey squares (make sure that your selection tool is the square one). To add it to the *ROI Manager*, simply press *t* or click *Add* in the *ROI Manager*. Your selection should now appear in the *ROI Manager* as shown below.
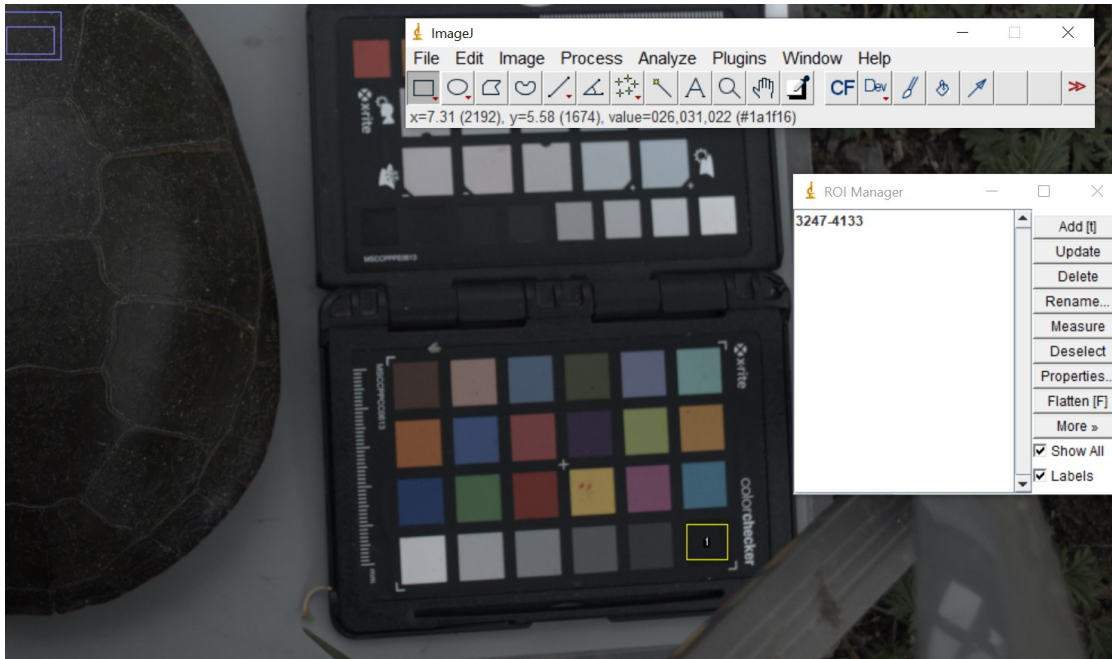
Do the same for all grey squares making sure that you only include the colour of interest (no black

borders) in each square, and that all squares are approximately the same size.
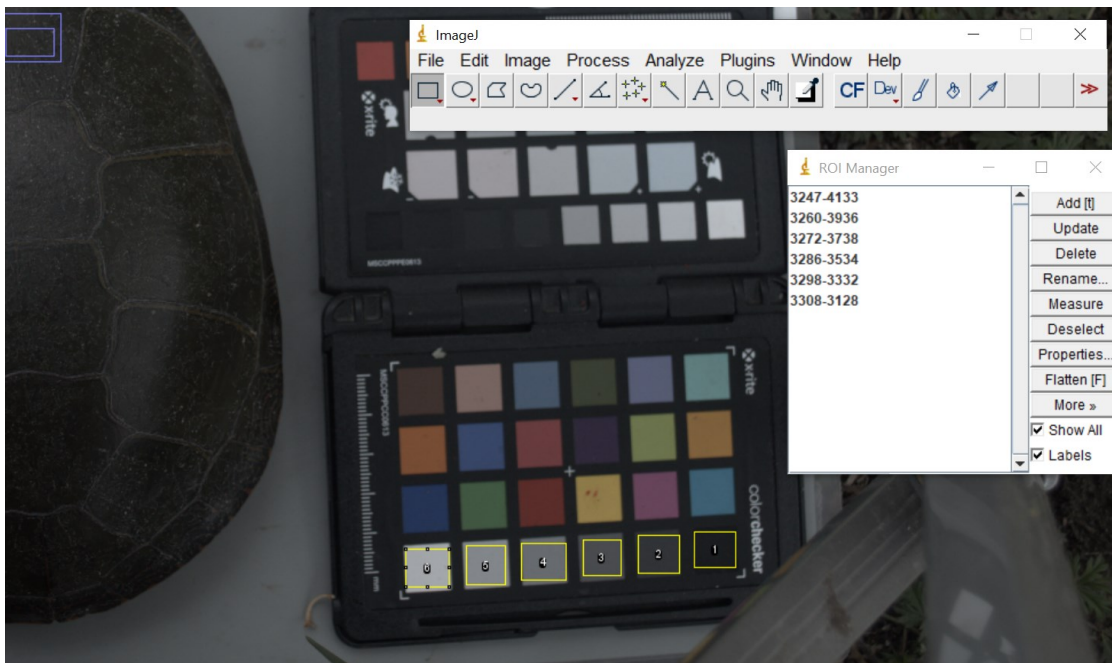


Because you need to extract the reflectance values for each of the three channels separately, you now

have to convert the image into a multi-channel stack. To do so, click on *Image >> Color >> Make Composite*.
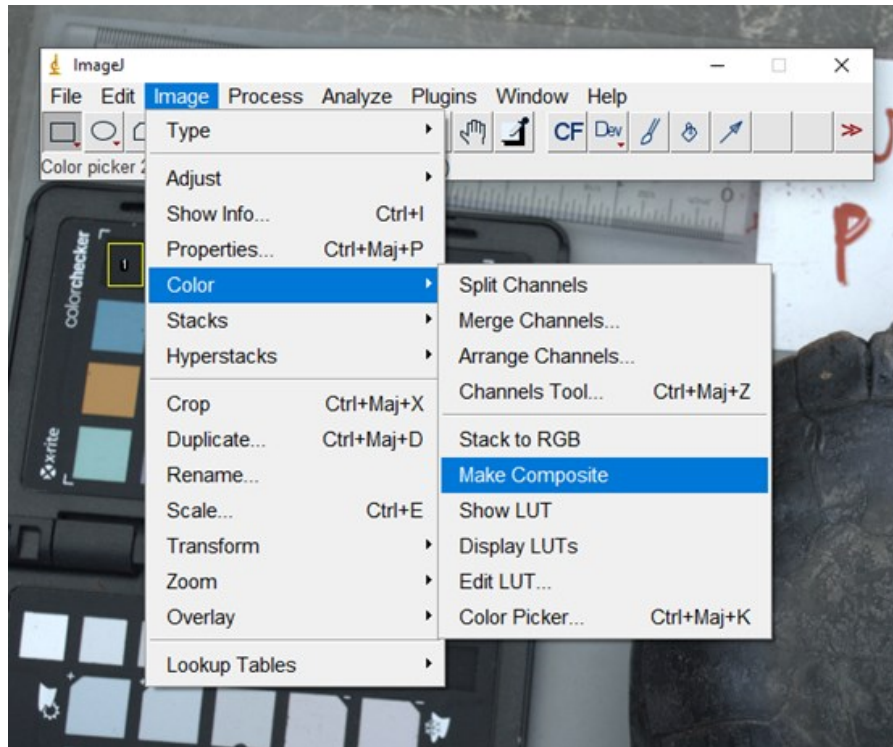


The picture should now be split in three. You can browse through the different channels by using the arrows on your keyboard or with the scrolling bar at the bottom of the picture. In the top left corner, you should be able to see which channel is represented (Red, Green or Blue). In the picture below, you can see that we are viewing the red channel (1/3 channel).

To get the reflectance values, select all the created ROI in the *ROI Manager* and click on *Measure* in the *ROI Manager* window. This will give you a mean reflectance value for all your squares for the channel that is displayed (and other values such as the area, the min and max reflectance values in the ROI, etc.). Do the same for each of the three colour channels by moving to the channel you want to analyze and click again on *Measure*. Finally, input all the measurements in your spreadsheet file.
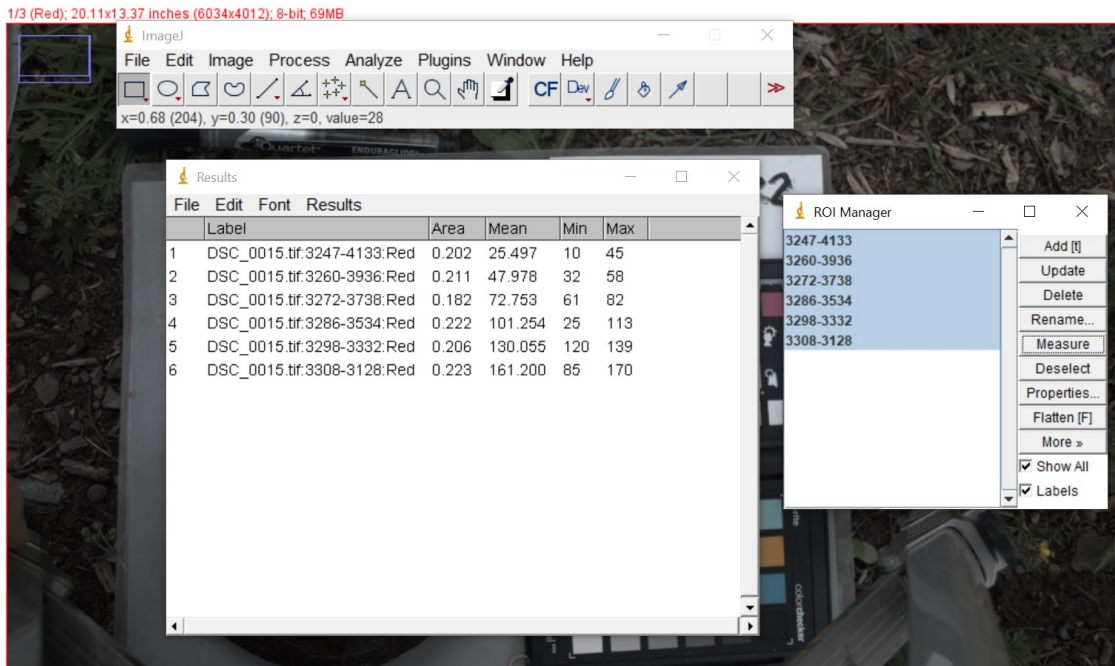
If the labels are not displayed properly, you can go in the *Results* window, click on *Results >> Set >> Measurements* and select *Display label >> OK*. You will need to measure your ROIs again to activate the labelling.
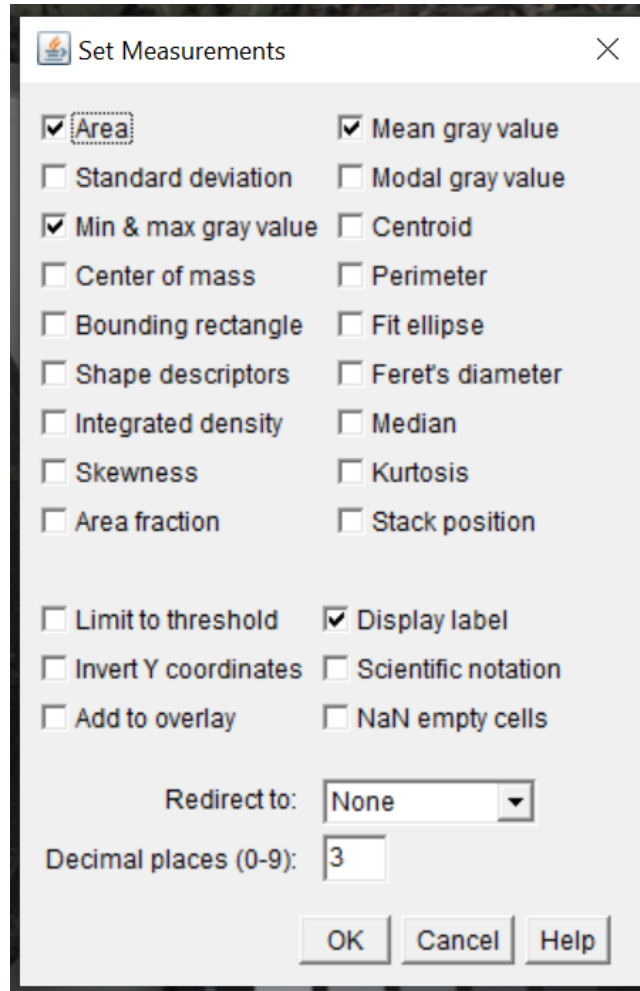
**Tip #1**: If you use labels, add this column to your spreadsheet file because they give information about the picture and the colour channel analyzed for each ROI. It is also possible to save a .CSV file with those results directly in ImageJ. You can also keep the measurements of a previous picture in ImageJ and copy the results to your spreadsheet after few pictures. You just need to keep the *ROI Manager* opened and calculate the reflectance values after a few pictures.

**Tip #2**: To be able to quickly fill the spreadsheet file, it is best to always select the different grey colour squares in the same order (i.e., always start and finish with the same ones). Make sure that the colour chart is always in the same position.

### 3. Creating linearization equations

As stated in Paterson & Blouin-Demers (2017), "To use photographs for the analysis of colour, a digital camera's three sensors (corresponding to red, green, and blue wavelengths) should respond linearly and equally to increases in light intensity". Contrary to Paterson & Blouin-Demers (2017), our observed reflectance values already appeared linearly related to expected reflectance values before any corrections because we used ImageJ's DCRAW package (Coffin, 2015; Troscianko & Stevens, 2015). The observed reflectance values, however, were always lower than the expected reflectance values. We thus simply needed to apply a linear correction with a normal lm() function in R to obtain a better fit. We used the following equations for each colour channel (i.e., camera's three sensors):

$$Q_r = a_1 + b_1 r \quad (1)$$

$$Q_g = a_2 + b_2 g \quad (2)$$

$$Q_b = a_3 + b_3 b \quad (3)$$

Where $Q$ is the expected reflectance values from the grey colour squares of the colour chart, $a$ and $b$ are constants (for each colour channel), and $r$, $g$, and $b$ are the observed reflectance values from each colour channel (red, green, and blue).

If the relationships had not been linear (as was the case for Paterson and Blouin-Demers (2017)), we could have used the following equations instead, using the nls() function in R:

$$Q_r = a_1 * (b_1^r) \quad (1)$$

$$Q_g = a_2 * \left(b_2^g\right) \quad (2)$$

$$Q_b = a_3 * \left(b_3^b\right) \quad (3)$$

We used the reflectance values extracted in section 2 and the expected reflectance values from the colour chart to estimate *a* and *b* in each equation. Before going further, you need to check how your observed reflectance values are related to the expected reflectance values and, thus, determine the type of correction needed. Other equations could be used. Make sure to select the equations that are more appropriated to your data. This will be done in the following steps.

*3.1 Loading R packages*

**Note**: Here we present the packages we used in R. However, they might not all be required to conduct the analyses and some other packages might be equivalent to the ones we used. Each package needs to be installed with the function install.packages() prior to being loaded and attached in R with the function library() as shown below.

```
library(readxl)
library(Hmisc)
library(tidyverse)
library(rio)
library(ggplot2)
library(ggpubr)
```

*3.2 Setting the directory*

To be able to run these scripts, you need to set your directory by choosing the folder where your data are saved (e.g., spreadsheet file) with the function setwd() or by following this path: *Session >> Set Working Directory >> Choose Directory*.

To practice with the scripts, you can use the Excel file created in section 2.1.

*3.3 Importing data*

As a reminder, the spreadsheet contains all observed reflectance values extracted in ImageJ from the colour chart's grey squares for a subset of pictures representing various ambient lighting conditions. For

each picture, the reflectance values were extracted from each colour channel (Red, Green and Blue).

```r
# Create a vector with the format we want for each column in our xlsx file.
Color_coltypes <- c("text", "numeric", rep("text", 2), rep("numeric", 2), "text",
rep("numeric", 4))

Color <- read_excel("Data_Example.xlsx", sheet = 2, col_types = Color_coltypes)

str(Color)

## tibble [4,698 × 11] (S3: tbl_df/tbl/data.frame)
##  $ ID          : chr [1:4698] "1" "1" "1" "1" ...
##  $ No.Photo    : num [1:4698] 5 5 5 5 5 5 5 5 5 5 ...
##  $ RGB         : chr [1:4698] "R" "R" "R" "R" ...
##  $ Grey scale  : chr [1:4698] "Black" "Neutral 3.5" "Neutral 5" "Neutral 6.5"
## ...
##  $ Expected_sRGB: num [1:4698] 52 85 122 160 200 243 52 85 122 160 ...
##  $ Square      : num [1:4698] 1 2 3 4 5 6 7 8 9 10 ...
##  $ Label       : chr [1:4698] "DSC_0522.NEF:3486-3375:Red" "DSC_0522.NEF:3693
## -3369:Red" "DSC_0522.NEF:3897-3360:Red" "DSC_0522.NEF:4098-3336:Red" ...
##  $ Area        : num [1:4698] 0.122 0.129 0.122 0.144 0.096 0.136 0.122 0.129
## 0.122 0.144 ...
##  $ Mean        : num [1:4698] 17.4 36.6 58.9 86.2 111 ...
##  $ Min         : num [1:4698] 2 22 48 75 102 129 9 26 49 77 ...
##  $ Max         : num [1:4698] 40 49 69 98 119 150 28 42 64 89 ...
```

*3.4 Deleting overexposed/underexposed pictures*

You should exclude all overexposed pictures (i.e., picture with a reflectance of or near to 255) to calculate your linearization equations. In our case, we arbitrary chose a threshold of 254.5 to identify potentially problematic overexposed pictures.

```r
which(Color$Mean>=254.5)

## integer(0)
```

You can see here that we do not have any overexposed pictures. You also do not want underexposed pictures with a mean reflectance value very close to zero. You should remove them if it is the case. In our case, we verified if we had pictures with a mean reflectance value of 0.5 or less.

```r
which(Color$Mean<=0.5)
```

```
## integer(0)
```

Again, you can see here that we do not have any underexposed pictures. If you have over or underexposed pictures, you can use the codes below to delete those pictures.

```
## To delete overexposed pictures
Color <- subset(Color, Mean <= 254.5)
## To delete underexposed pictures
Color <- subset(Color, Mean >= 0.5)
```

*3.5 Transforming the reflectance values: Scaling between 0 and 1*

To create your linearization equations, you want your reflectance values to be relative to the highest value possible (i.e., 255). It will avoid you to work simultaneously on three different matrices by having only one picture in gray scale. After this transformation, all your values (the expected and the observed values) will be between 0 and 1.

```
Color$Expected_sRGB_01 <- Color$Expected_sRGB / 255 # Expected value according to
the colour chart
Color$Mean_01 <- Color$Mean / 255 # Observed mean reflectance value

summary(Color$Expected_sRGB_01) # Should be between 0 and 1

##    Min. 1st Qu.  Median    Mean 3rd Qu.    Max.
##  0.2039  0.3333  0.5529  0.5630  0.7843  0.9529

summary(Color$Mean_01) # Should be between 0 and 1

##    Min. 1st Qu.  Median    Mean 3rd Qu.    Max.
## 0.02316 0.17860 0.33293 0.34808 0.49797 0.94441
```

*3.6 Splitting data by colour channel*

You need to create one linearization equation per colour channel and, thus, you need to split your data per colour channel.

```
# Red channel
Color_R <- subset(Color, RGB == "R")
hist(Color_R$Mean_01, main = "Red channel", xlab = "Mean observed reflectance val
ues")
```

## Red channel



Mean observed reflectance values
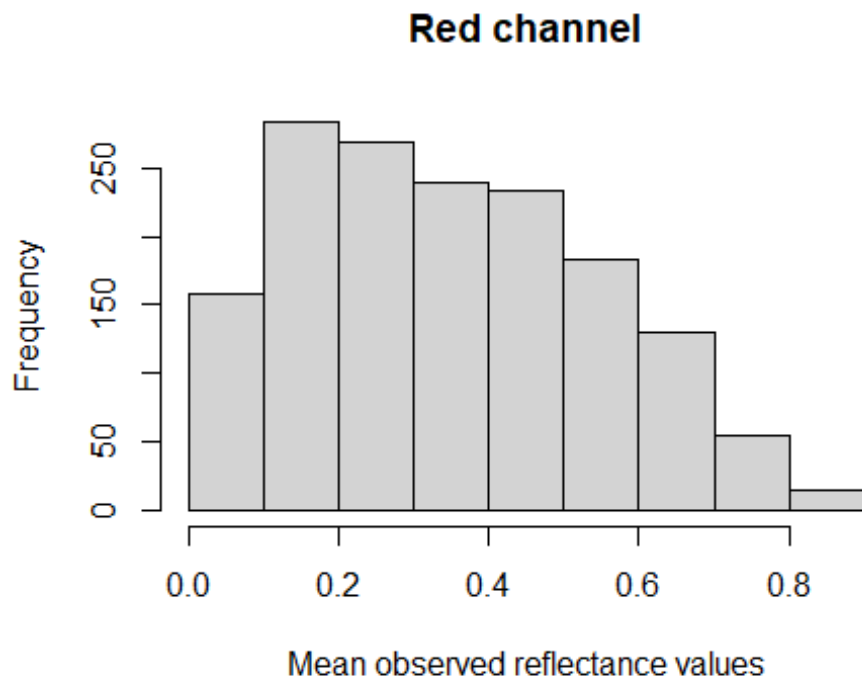
```r
# Green channel
Color_G <- subset(Color, RGB == "G")
hist(Color_G$Mean_01, main = "Green channel", xlab = "Mean observed reflectance values")
```

## Green channel
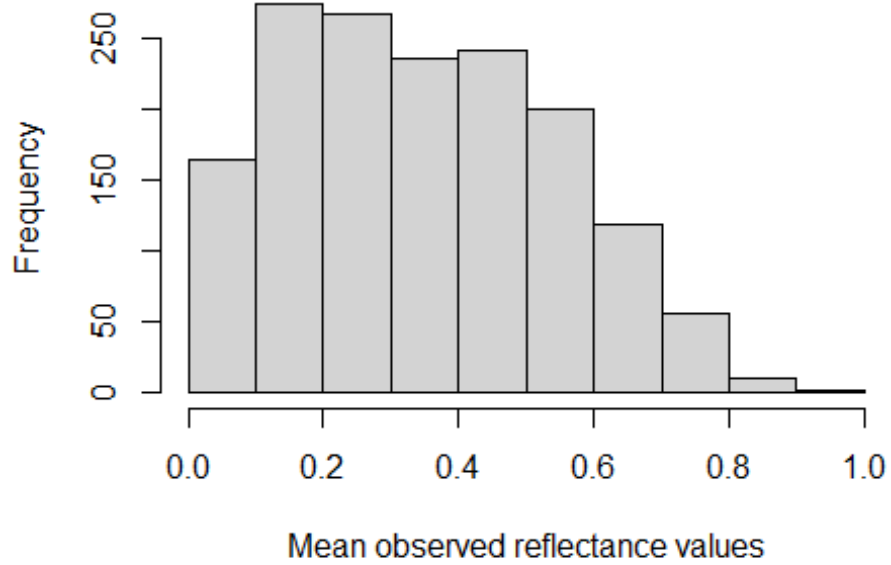


```r
# Blue channel
Color_B <- subset(Color, RGB == "B")
hist(Color_B$Mean_01, main = "Blue channel", xlab = "Mean observed reflectance va
lues")
```

## Blue channel
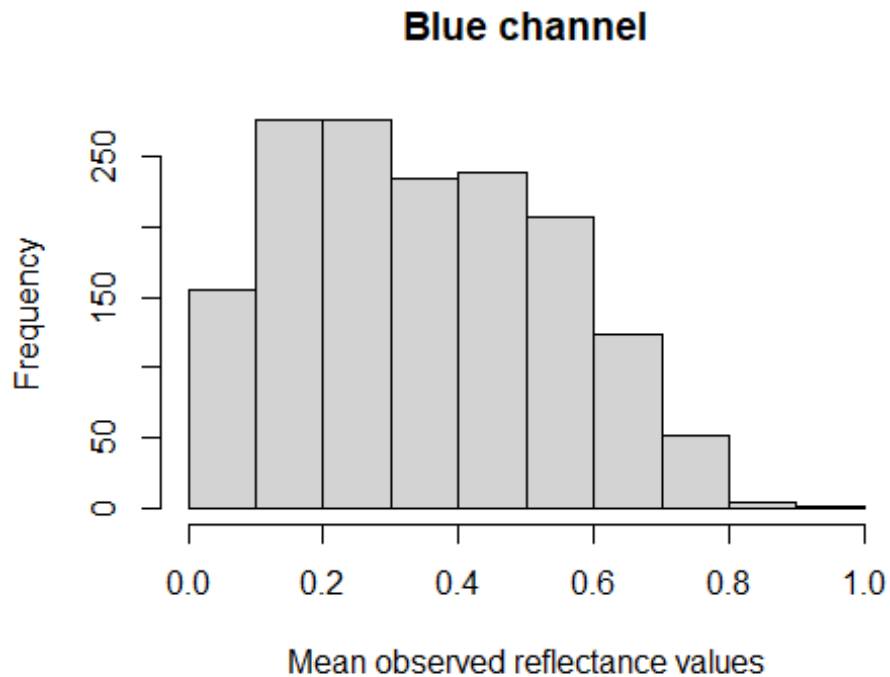


*3.7 Linearization equations*

Now, you can create a linear model for each colour channel and extract the slope and the intercept of each model to build your equations. In our case, we used the lm() function for our equations as mentioned earlier.

```
redlinear=lm(Expected_sRGB_01 ~ Mean_01, data = Color_R)
summary(redlinear)

##
## Call:
## lm(formula = Expected_sRGB_01 ~ Mean_01, data = Color_R)
##
## Residuals:
##      Min       1Q   Median       3Q      Max
## -0.27288 -0.06205 -0.01210  0.05449  0.43465
##
## Coefficients:
##              Estimate Std. Error t value Pr(>|t|)
## (Intercept) 0.141803   0.004648   30.51   <2e-16 ***
## Mean_01     1.213138   0.011629  104.32   <2e-16 ***
```

135

```
## ---
## Signif. codes:  0 '***' 0.001 '**' 0.01 '*' 0.05 '.' 0.1 ' ' 1
##
## Residual standard error: 0.0909 on 1564 degrees of freedom
## Multiple R-squared:  0.8744, Adjusted R-squared:  0.8743
## F-statistic: 1.088e+04 on 1 and 1564 DF,  p-value: < 2.2e-16
```

The intercept is **0.141803** and the slope is **1.213138** for the linearization equation of the red channel.

Now, you can linearize the mean observed reflectance values for the red channel with this equation that contains the constants that were extracted from the model.

```
r.2.linear <- 0.141803 + (Color_R$Mean_01*1.213138)
```

You can visualize the relationship between the linearized observed values and the expected reflectance values from the colour chart. If the linearization equation works well, the data are supposed to follow the black line (1:1).

```
plot(r.2.linear ~ Color_R$Expected_sRGB_01, main = "Red channel", xlab = "Expecte
d reflectance",ylab = "Linearized observed reflectance", xlim = c(0, 1), ylim = c
(0, 1.2))
abline(0,1)
```

## Red channel
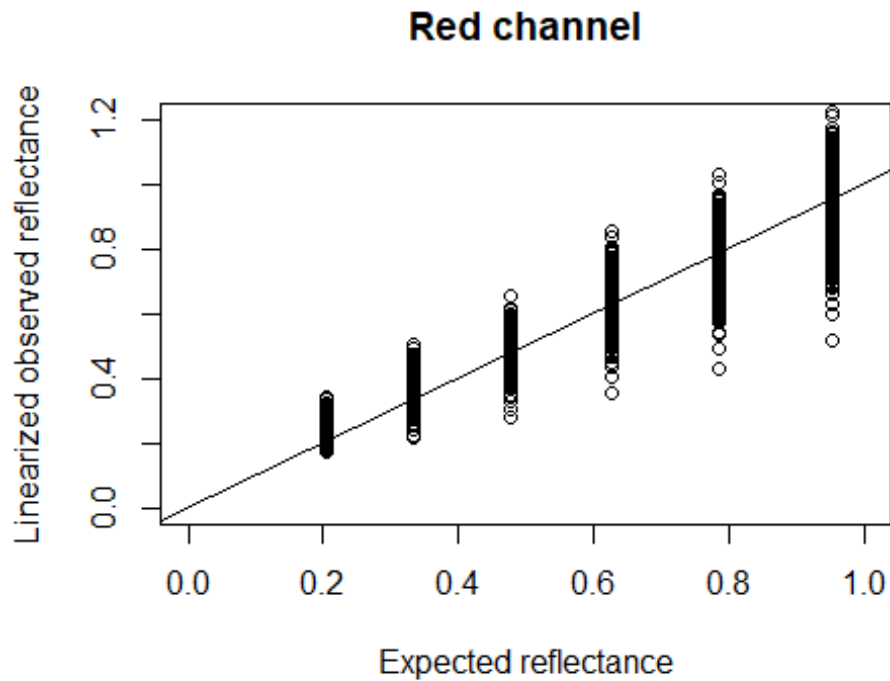


Repeat the same steps for the green and blue channels.

The intercept is **0.130617** and the slope is **1.242959** for the linearization equation of the green channel. Now, you can linearize the mean reflectance values for the green channel with this equation that contains the constants that were extracted from the model. In our case, the equations and plots for the green and blue channels were the following.

```
g.2.linear <- 0.130617 + (Color_G$Mean_01 * 1.242959)
```

## Green channel
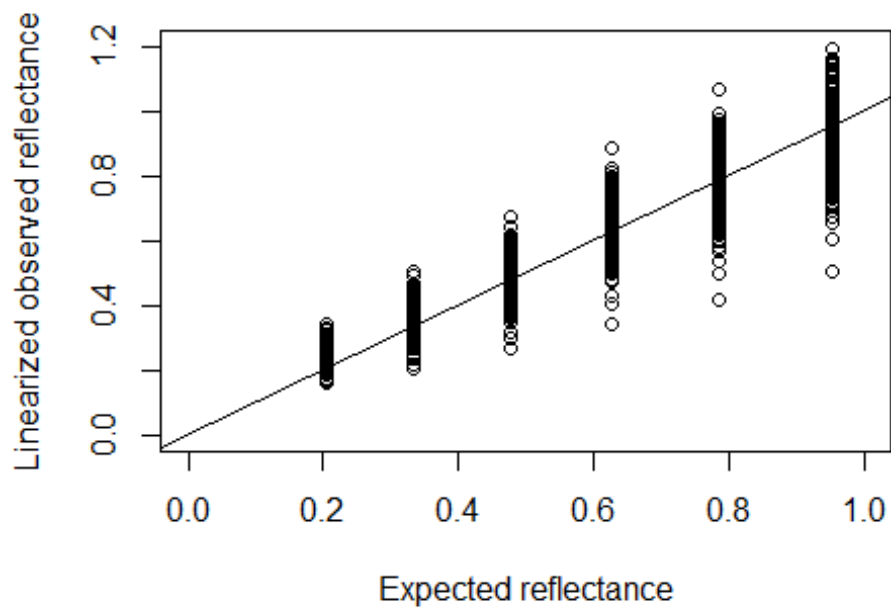


```
b.2.linear <- 0.118825 + (Color_B$Mean_01 * 1.271826)
```

## Blue channel
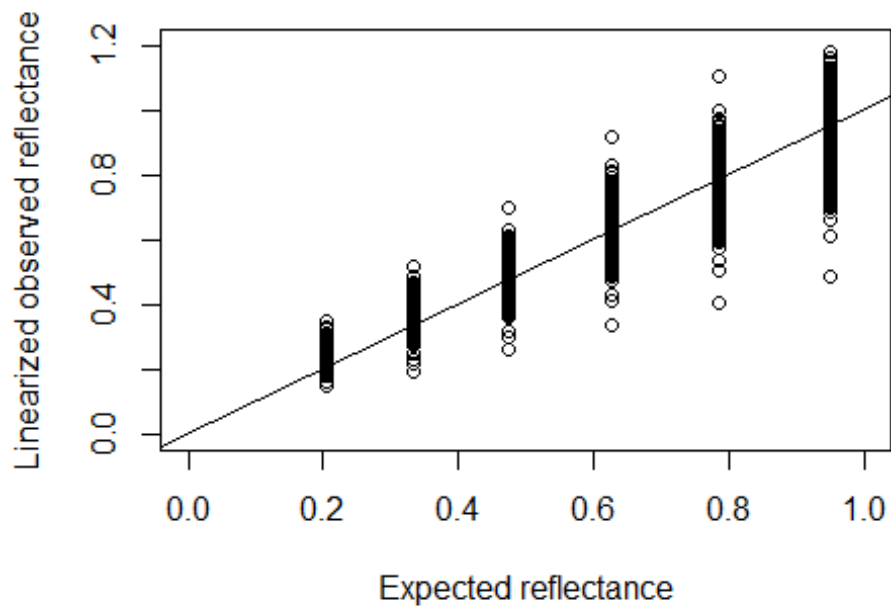
*Visualizing the three channels together before and after the linearization*

You can visualize the changes made by the linearization equations to the observed reflectance values

from the three channels.

```
# Plot of the relationship between the observed reflectance values with no linear
ization and the expected reflectance values.

graph.uncorrected <- ggplot() +
  geom_point(aes(x = Color_R$Expected_sRGB_01, y = Color_R$Mean_01), color = "red
", position = "jitter") +
  geom_point(aes(x = Color_B$Expected_sRGB_01, y = Color_B$Mean_01), color = "blu
e", position = "jitter") +
  geom_point(aes(x = Color_G$Expected_sRGB_01, y = Color_G$Mean_01), color = "gre
en", position = "jitter") +
  geom_abline(intercept = 0, slope = 1, color = "black") +
  ylab("Observed reflectance") + xlab("Expected reflectance") + labs(title = "Unc
orrected") + theme(plot.title = element_text(hjust = 0.5))


# Plot of the relationship between the corrected reflectance values with the line
arization equations and the expected reflectance values.

graph.corrected <- ggplot() +
  geom_point(aes(x = Color_R$Expected_sRGB_01, y = r.2.linear), color = "red", po
sition = "jitter") +
  geom_point(aes(x = Color_B$Expected_sRGB_01, y = b.2.linear), color = "blue", p
osition = "jitter") +
  geom_point(aes(x = Color_G$Expected_sRGB_01, y=g.2.linear), color = "green", po
sition = "jitter") +
  geom_abline(intercept = 0, slope = 1, color = "black") +
  ylab("Observed reflectance") + xlab("Expected reflectance") + labs(title = "Cor
rected") + theme(plot.title = element_text(hjust = 0.5))

ggarrange(graph.uncorrected, graph.corrected,
          ncol = 2, nrow = 1)
```
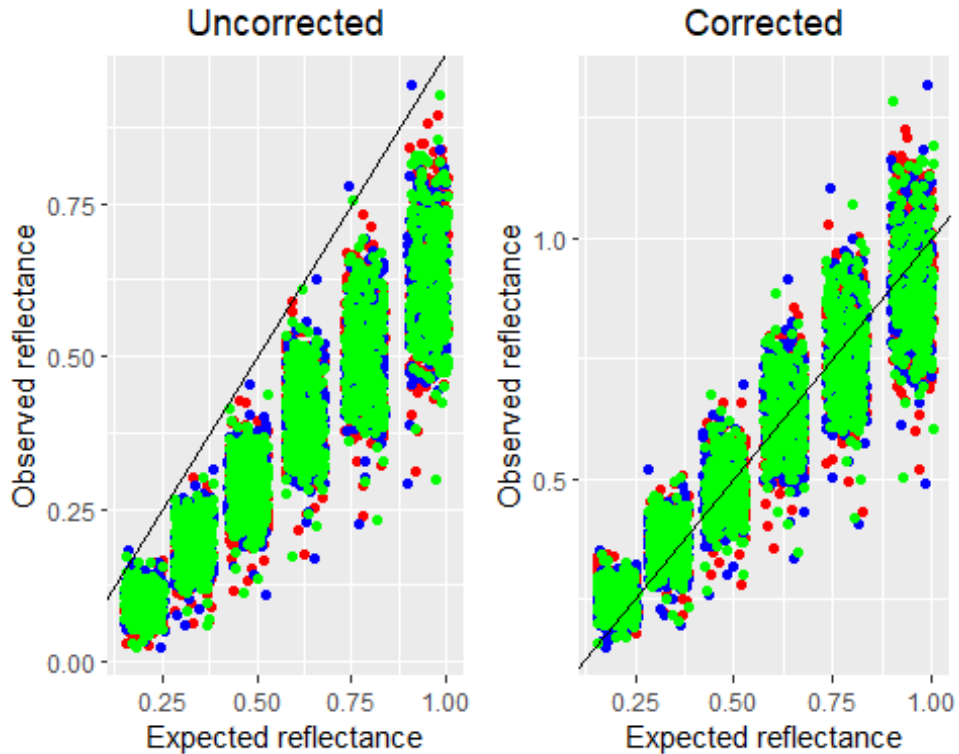
You can see that the corrected observed reflectance values for the three color channels (Red, Green and Blue) follow the reference line (1:1). This confirms that the linearization equations are working.

*3.8 Equalizing the channels*

In some cases, the linearization will also equalize the three colour channels (e.g., transformed R = transformed G = transformed B). You should thus confirm that linearized pixel scores of grey colour scales from the colour chart are equal in each channel using paired t-tests. If it is not the case, see the following paper: Stevens et al. (2007).

```
t.test(r.2.linear, g.2.linear, paired=TRUE)

##
##  Paired t-test
##
## data:  r.2.linear and g.2.linear
## t = -0.0011145, df = 1565, p-value = 0.9991
## alternative hypothesis: true mean difference is not equal to 0
## 95 percent confidence interval:
```

```
##  -0.0008726124  0.0008716213
## sample estimates:
## mean difference
##    -4.955514e-07

t.test(r.2.linear, b.2.linear, paired=TRUE)

##
##  Paired t-test
##
## data:  r.2.linear and b.2.linear
## t = 1.5925, df = 1565, p-value = 0.1115
## alternative hypothesis: true mean difference is not equal to 0
## 95 percent confidence interval:
##  -0.0003029215  0.0029174415
## sample estimates:
## mean difference
##      0.00130726

t.test(g.2.linear, b.2.linear, paired=TRUE)

##
##  Paired t-test
##
## data:  g.2.linear and b.2.linear
## t = 3.2623, df = 1565, p-value = 0.001129
## alternative hypothesis: true mean difference is not equal to 0
## 95 percent confidence interval:
##  0.0005214506 0.0020940605
## sample estimates:
## mean difference
##      0.001307756
```

You need to correct your p value according to the number of comparisons made (three in this case). alpha = 0.05/3 = **0.0167**. In our case, we only observed a significant difference between the green and blue channels. The mean difference, however, was very small (0.001). We thus concluded that the linearized pixel scores of the grey colour scales were equal in each colour channel (Red, Green and Blue).

4. Linearizing pictures

Now that the constants *a* and *b* are known, it is possible to linearize all your pictures (not just the

subsample of pictures previously used) with the equations created in section 3.7. In our case, our final dataset included two .TIFF pictures per individual, one representing the neck (showing both yellow and red) and one representing the top of the head (usually showing two yellow spots). Here is an example of a set of pictures for one turtle:



Before running this script, make sure that all your pictures are saved in .TIFF format and have the same properties. All steps in section 3 of this guide should have been completed.

*4.1 Loading R packages*

See note in section 3.1.

```
library(imageviewer)
library(magick)
library(rsvg)
library(beepr)
library(hexView)
library(tiff)
library(EBImage)
options(repos = BiocManager::repositories()) # You can use this setting to instal
l packages (e.g., EBImage) from other repositories than CRAN (e.g., BiocManager)
with the function install.packages().
```

The installation of EBImage should work if you follow these steps:

http://bioconductor.org/packages/devel/bioc/vignettes/EBImage/inst/doc/EBImage-

introduction.html#1_Getting_started. If you encounter difficulties for the installation, you can try

installing it with RStudio in administrator mode.

*4.2 Setting the directory*

To be able to run these scripts, you need to set your directory by choosing the folder where your pictures (in .TIFF) are saved with the function setwd() or by following this path: *Session >> Set Working Directory >> Choose Directory*.

*4.3 Creating a list of pictures*

You need to create a list of pictures to work on (put all pictures to be linearized in the appropriate directory). Subfolders are needed if there are several pictures to process or if you have limited computing power (e.g., R may run out of memory). In our case, we were able to process about 10 pictures at a time.

```
in.images<-list.files(path="images", pattern="DSC", full.names=FALSE, recursive=T
RUE)
in.images
## [1] "DSC_0022.tif" "DSC_0023.tif"
```

This step allows the creation of an object containing a list of all the pictures found in the selected subfolder (path = "path to the folder where a subset of pictures is located", and Recursive = TRUE allows access to the subfolders inside the directory selected). You do not need to write the entire path given that the directory is already set. The pattern argument indicates a common pattern of names in all pictures you want to open. In our case, we had a folder named *images* in our directory. All our pictures started with *DSC*, which was used as the pattern argument. This tutorial's subfolder only includes two pictures: DSC_0022 and DSC_0023. All steps in the following section will be performed on these two pictures.

143

*4.4 Converting pictures to arrays*

*Creating a function that formats pictures correctly*

When a picture is uploaded in R, the different colour channels are not automatically accessible. Instead, the picture is represented as one matrix. Since you need to apply your linearization equations to the three channels of your pictures (Red, Green and Blue), you need to access each colour channel's array. This function allows you to do so:

```r
Format.image <- function(y) {
  list_array <- list() # creates an empty list
  for (n in 1:length(y)) {
    image <- paste("Array", y[n], sep = "") # transforms the name of the pictures
    y2 <- image_read(y[n]) # read the .TIFF file
    print(dim(y2))
    #print(y2) # this step can be activated by deleting the (#). This step allows
you to see the picture in R-studio viewer (but it will take more time)
    print(image_info(y2))
    y_array <- as.integer(y2[[1]]) # converts to an array to be able to change th
e colour values
    y_array <- transpose(y_array)
    y_array <- y_array / 255 # To get grey values instead of colours
    print(y_array)
    list_array[[image]] <- y_array

  }
  return(list_array)
}
```

*Applying the previously created functions to the pictures*

```r
picture_list <- Format.image(in.images)
```

Make sure you can access the elements inside the list. In our case, we confirmed that the previous function worked by running the following code line, which looks at the reflectance values of picture #1 of our list between pixel rows 5 and 10, and pixel columns 10 and 20 for the third matrix (blue). The first matrix is the red channel, the second is the green channel and the third one is the blue channel.

```
picture_list[[1]][5:10, 10:20, 3]

##             [,1]      [,2]      [,3]      [,4]      [,5]      [,6]      [,7]
## [1,] 0.1490196 0.1490196 0.1490196 0.1411765 0.1333333 0.1333333 0.1372549
## [2,] 0.1529412 0.1529412 0.1490196 0.1411765 0.1333333 0.1372549 0.1372549
## [3,] 0.1529412 0.1529412 0.1490196 0.1450980 0.1372549 0.1372549 0.1372549
## [4,] 0.1529412 0.1529412 0.1490196 0.1450980 0.1450980 0.1372549 0.1333333
## [5,] 0.1490196 0.1490196 0.1490196 0.1450980 0.1450980 0.1411765 0.1372549
## [6,] 0.1450980 0.1450980 0.1490196 0.1450980 0.1450980 0.1450980 0.1450980
##             [,8]      [,9]     [,10]     [,11]
## [1,] 0.1450980 0.1568627 0.1568627 0.1607843
## [2,] 0.1529412 0.1686275 0.1607843 0.1490196
## [3,] 0.1490196 0.1607843 0.1529412 0.1490196
## [4,] 0.1411765 0.1490196 0.1490196 0.1490196
## [5,] 0.1411765 0.1411765 0.1372549 0.1333333
## [6,] 0.1372549 0.1333333 0.1254902 0.1176471
```

We also checked if we could see the dimensions of picture #1 in our list.

```
dim(picture_list[[1]])

## [1] 6034 4012    3
```

You can see the width (6034 pixels), the height (4012 pixels), and the three matrices (3: Red, Green, Blue) of picture #1.

You can also use the following function to see all reflectance values from all pixels of picture #1. The output is not shown here because it is too large.

```
picture_list[1]
```

*4.5 Applying the linearization equations*

Here are the equations we obtained in section 3.7:

```
fred = function(x) {0.141803 + (1.213138 * x)} # function to change RED pixel val
ues
fgreen = function(x) {0.130617 + (1.242959 * x)} # function to change GREEN pixel
values
fblue = function(x) {0.118825 + (1.271826 * x)} # function to change BLUE pixel v
alues
```

We created a function that will apply the different equations to their respective matrix. In other words,

the function will allow you to apply the linearization equation of the red channel to the red matrix, the green equation to the green matrix, and the blue equation to the blue matrix.

```
change.image <- function(x) {
  for(m in 1:length(x)){
    r <- apply(x[[m]][500:4500, 500:4000, 1], MARGIN = c(1, 2), FUN = fred) # app
ly the red linearization function to the red channel
    g <- apply(x[[m]][500:4500, 500:4000, 2], MARGIN = c(1, 2), FUN = fgreen) # a
pply the green linearization function to the green channel
    b <- apply(x[[m]][500:4500,500:4000, 3], MARGIN = c(1, 2), FUN = fblue) # app
ly the blue linearization function to the blue channel
    z <- Image(array(dim = c(nrow(r), ncol(r), 3),data = cbind(r, g, b))) # this
step allows to re-stack together the three matrices. The order of the three layer
s is important here: red, green and blue.
    colorMode(z) <- Color #set to colour mode
    writeImage(z, paste(names(x[m]), "_linearized", ".TIFF", sep="")) # save as a
new picture that will use the origin name, but will add "_linearized" at the end
and that will be saved in the .TIFF format.
  }
}
```

Here, the pictures from the picture list are in their original dimensions, and are cropped by the change.image() function. However, it could be a good idea to crop the pictures beforehand to reduce computing time, especially if the zone of interest is relatively small compared to the rest of the picture. In our case, we did not crop the pictures prior to running the script. The cropping was done via the change.image() function. Thus, the resulting pictures are linearized and only include the area located between pixel rows 500 and 4500, and between pixel columns 500 and 4000 for the three matrices. This helps reduce computing time. If you decide to crop your pictures this way, you need to make sure that all pictures still include the whole area of interest, as well as the ruler (or at least part of it). Now, you can apply the function to the list of pictures:

```
change.image(picture_list)
```

This step can take several minutes. In our case, the linearization of two pictures took about 5 minutes. Once it is done, the newly linearized pictures (named ArrayDSC_0022.tif_linearized and

ArrayDSC_0023.tif_linearized) should be saved in the directory selected at the beginning.

## 5. Rescaling pictures and selecting the area of interest

### 5.1 Rescaling pictures

Before going further, it is necessary to scale all pictures similarly. By doing this, you are ensuring that areas (in pixels) measured in one picture are comparable to that measured in other pictures. In ImageJ, you can scale the pictures previously linearized and cropped in section 4. In the following section, we used a different head picture compared to the previous section.

You can see the steps of section 5 in this video: https://youtu.be/IzjauL99_7Q

First, you need to measure a line of known length (i.e., a section of the ruler included in all pictures) with the straight-line tool.
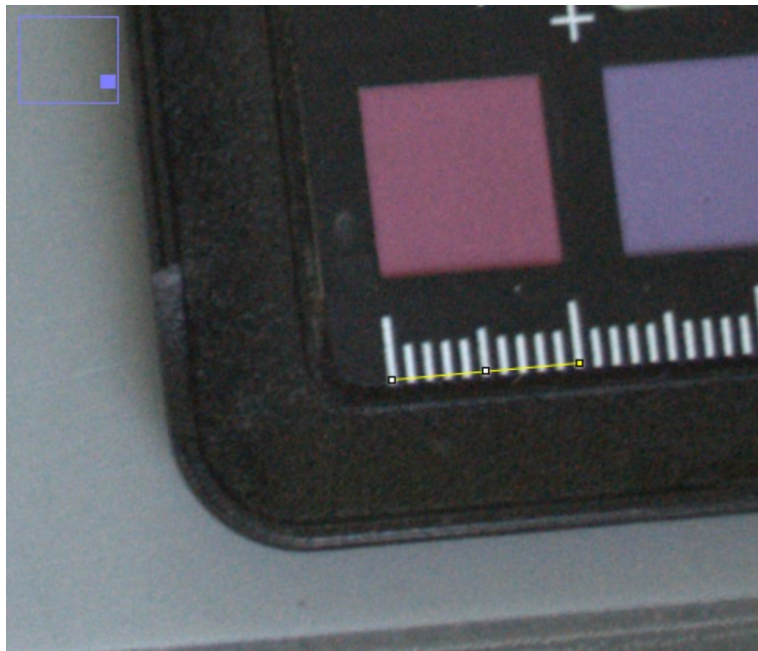


Then, in *Analyze >> Set Scale*, the measured distance should appear in the first box (i.e., *Distance in pixels*). The *Known distance* should be changed to the appropriate value. In our case, we used a known

distance of 1 cm. We thus changed *Known distance* to **1.00** and the *Unit of length* to **cm**.
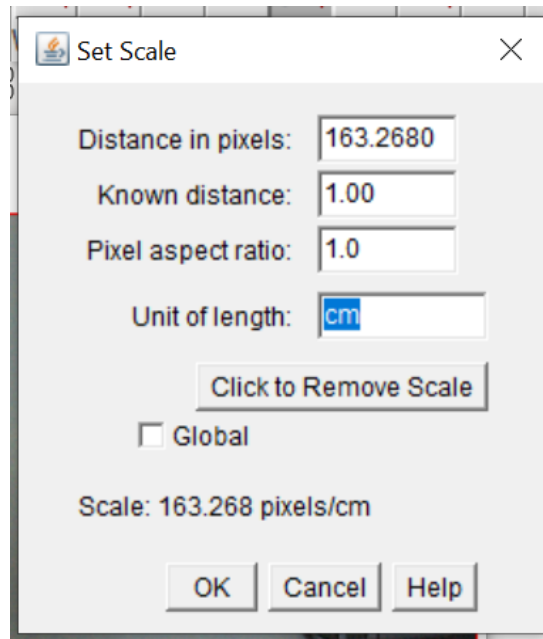


The scaling factor of the picture (i.e., Distance in pixels: 163.2680) needs to be noted in a new column of your spreadsheet file. It is also possible to create a new spreadsheet file with all the pictures that will be analyzed if you only analyzed a subset of your pictures to create the linearization equations. In our case, we added one column to enter the scaling factor (i.e., Scaling_factor_(pixels/cm)). We also added another column to compute the number of pixels in 10 cm (i.e., Number_of_pixels_in_10_cm). This column will later be used to uniformize the background size of all pictures (10 x 10 cm; see section *5.3 Resizing pictures on a 10 cm X 10 cm background*). This step is necessary because, to our knowledge, ImageJ only allows background rescaling in pixel units (and not in cm).

148

| | A | B | C | D | E | F | G | H | I | J | K | L | M |
|---|---|---|---|---|---|---|---|---|---|---|---|---|---|
| 1 | ID | No.Photo | RGB | Grey scale | Expected_sRGB | Square | Label | Area | Mean | Min | Max | Scaling_factor_(pixels/cm) | Number_of_pixels_in_10_cm |
| 2 | 1 | 5 | R | Black | 52 | 1 | DSC_0522.NEF:3486-3375:Red | 0.122 | 17.355 | 2 | 40 | 163.2680 | 1632.68 |
| 3 | 1 | 5 | R | Neutral 3.5 | 85 | 2 | DSC_0522.NEF:3693-3369:Red | 0.129 | 36.574 | 22 | 49 | 163.2680 | 1632.68 |
| 4 | 1 | 5 | R | Neutral 5 | 122 | 3 | DSC_0522.NEF:3897-3360:Red | 0.122 | 58.94 | 48 | 69 | 163.2680 | 1632.68 |
| 5 | 1 | 5 | R | Neutral 6.5 | 160 | 4 | DSC_0522.NEF:4098-3336:Red | 0.144 | 86.193 | 75 | 98 | 163.2680 | 1632.68 |
| 6 | 1 | 5 | R | Neutral 8 | 200 | 5 | DSC_0522.NEF:4299-3324:Red | 0.096 | 111.026 | 102 | 119 | 163.2680 | 1632.68 |
| 7 | 1 | 5 | R | White | 243 | 6 | DSC_0522.NEF:4503-3306:Red | 0.136 | 140.177 | 129 | 150 | 163.2680 | 1632.68 |
| 8 | 1 | 5 | G | Black | 52 | 7 | DSC_0522.NEF:3486-3375:Green | 0.122 | 16.342 | 9 | 28 | 163.2680 | 1632.68 |
| 9 | 1 | 5 | G | Neutral 3.5 | 85 | 8 | DSC_0522.NEF:3693-3369:Green | 0.129 | 35.378 | 26 | 42 | 163.2680 | 1632.68 |
| 10 | 1 | 5 | G | Neutral 5 | 122 | 9 | DSC_0522.NEF:3897-3360:Green | 0.122 | 56.265 | 49 | 64 | 163.2680 | 1632.68 |
| 11 | 1 | 5 | G | Neutral 6.5 | 160 | 10 | DSC_0522.NEF:4098-3336:Green | 0.144 | 83.321 | 77 | 89 | 163.2680 | 1632.68 |
| 12 | 1 | 5 | G | Neutral 8 | 200 | 11 | DSC_0522.NEF:4299-3324:Green | 0.096 | 107.35 | 101 | 113 | 163.2680 | 1632.68 |
| 13 | 1 | 5 | G | White | 243 | 12 | DSC_0522.NEF:4503-3306:Green | 0.136 | 134.341 | 125 | 140 | 163.2680 | 1632.68 |
| 14 | 1 | 5 | B | Black | 52 | 13 | DSC_0522.NEF:3486-3375:Blue | 0.122 | 15.8 | 9 | 26 | 163.2680 | 1632.68 |
| 15 | 1 | 5 | B | Neutral 3.5 | 85 | 14 | DSC_0522.NEF:3693-3369:Blue | 0.129 | 34.38 | 26 | 41 | 163.2680 | 1632.68 |
| 16 | 1 | 5 | B | Neutral 5 | 121 | 15 | DSC_0522.NEF:3897-3360:Blue | 0.122 | 54.301 | 45 | 62 | 163.2680 | 1632.68 |
| 17 | 1 | 5 | B | Neutral 6.5 | 160 | 16 | DSC_0522.NEF:4098-3336:Blue | 0.144 | 80.024 | 73 | 86 | 163.2680 | 1632.68 |
| 18 | 1 | 5 | B | Neutral 8 | 200 | 17 | DSC_0522.NEF:4299-3324:Blue | 0.096 | 103.279 | 93 | 110 | 163.2680 | 1632.68 |
| 19 | 1 | 5 | B | White | 242 | 18 | DSC_0522.NEF:4503-3306:Blue | 0.136 | 128.618 | 116 | 135 | 163.2680 | 1632.68 |
| 20 | 2 | 13 | R | Black | 52 | 1 | DSC_0611.NEF:0582-1532:Red | 0.134 | 21.502 | 0 | 36 | | |

**Note**: To determine how many pixels were needed on the background so that it would work with all pictures, we first used a subset of 50 pictures. This step confirmed that a background of 10 x 10 cm was sufficient to avoid cropping any important portion of our pictures. With the spreadsheet file, we then computed the number of pixels that corresponded to 10 cm (e.g., 163.268 pixels/cm * 10 cm = 1632.68). Thus, the size of your background will depend on the size of your area of interest and on the size variation of this area between individuals.

*5.2 Selecting the area of interest*

You can delimit the area of interest with the freehand selection tool. The selection can then be adjusted by selecting *Edit >> Selection >> Convex Hull*. You can create a new knot by pressing *Shift* and clicking on a knot. If you want to delete a knot, you can do so by pressing *Ctrl* and clicking on a knot. Here is an example of the area of interest, selected with the freehand selection tool and adjusted manually afterwards:
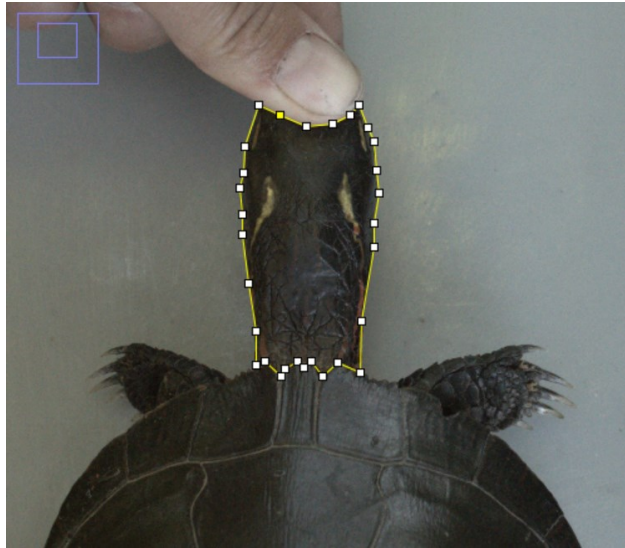
Then, you can erase everything outside of your selection by using *Edit >> Clear Outside*
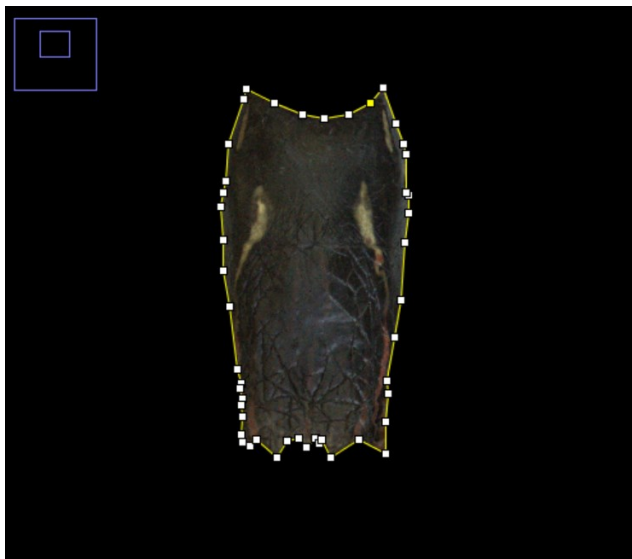


You can then crop the picture by selecting *Image >> Crop*.

*5.3 Resizing pictures on a 10 cm X 10 cm background*

Lastly, you can resize the black background to make it uniform between pictures by clicking on *Image >> Adjust >> Canvas size*. You will need to fill the width and height values with the ones you computed in the *Number_of_pixels_in_10_cm* column of your spreadsheet file for this specific picture. In our case, canvas width and height were changed to 1632.68 pixels.
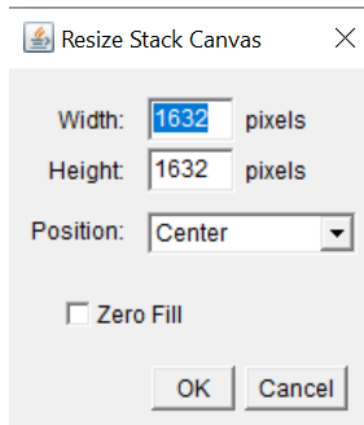
Now that the picture is scaled and resized, it should look like this:



The picture is ready to be used in the following steps. We recommend saving your modifications as a new picture with a name including as much information as possible. In our case, the following information was included in the picture's name:

− The individual's ID ;

− The first letter of Head or Neck (to indicate the region of interest in the picture) ;

- The mention that the picture was linearized, scaled and cropped, and that the background was uniformized to 10 cm.

**For example**, AB_H_linearized_scale_cut_10.tif, for the head picture of the turtle identified as **AB**.

6. Classifying pictures before standardization & binarization

By now, all your pictures are linearized, scaled, resized, and saved in the same folder on your computer. Before proceeding to the standardization/binarization, you need to group all your cropped and linearized pictures in different folders according to the area of interest that you want to analyze (if you have multiple areas). These folders will then be used in the following R scripts. In our case, all head pictures were grouped in one folder and all neck pictures in another. We suggested using the first letter of the region of interest (H for Head or N for Neck) in the picture file names and this is where it becomes useful. It allows us to sort all pictures automatically. This is especially useful when dealing with a lot of pictures. When choosing a letter to group picture categories, be cautious of not using a letter or character that appears elsewhere in the filename.

**Note**: This step is performed via the *Windows command processor* (also known as *command prompt*). An equivalent method should work under other operating systems such as Mac OS or Linux.

Open the command prompt by pressing the windows key (WIN) + R. Then, write *cmd* in the new window. **Be careful**: the command prompt is sensitive to caps lock and spaces.
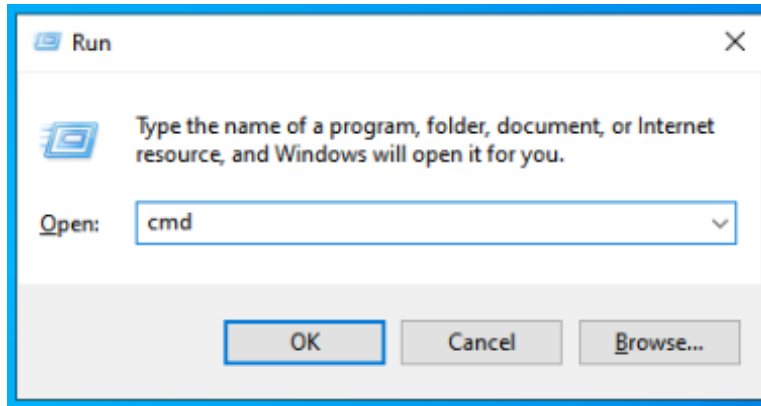
Now, specify the path of the directory where all the pictures are currently saved by using *cd* followed by a space and the directory path. Press enter.

**cd *Your_directory_path***

Then, to create new folders where you will send your pictures (in our case, we needed two new folders: one for the head pictures and one of the neck pictures), enter *md* followed by a space and the new folder's name. Separate each folder by a space and press enter.

**md Neck Head**

Finally, use the move command, followed by a space and the recurring pattern specified (in our case, _H_ or _N_) between two asterisks. Add a space and specify the name of the destination folder followed by "/" and press enter.

**move *_N_* Neck/**

**move *_H_* Head/**

```
C:\Users\Utilisateur>cd C:\Users\Utilisateur\Documents\Coloration

C:\Users\Utilisateur\Documents\Coloration>md Neck Head

C:\Users\Utilisateur\Documents\Coloration> move *_N_* Neck/

C:\Users\Utilisateur\Documents\Coloration>move *_H_* Head/
```

The pictures will now be sorted in their respective new folders according to the region of interest that you want to analyze.

7. Standardizing pictures before binarization

In most cases, you will need to create a new picture which is standardized. This step is required to remove absolute variation in pixel values (i.e., variations in brightness). For more information on this step see: Teasdale et al. (2013).

For each picture, the standardization is done on all three colour channels by dividing each pixel value by the total value from all colour channels (e.g., Standardized red = R/(R+G+B)). In our case, standardization made it too difficult to distinguish yellow from green during binarization. Thus, we did not standardize our pictures. If you need to standardize your pictures, you can follow the steps below.

*7.1 Loading R packages*

See note in section 3.1.

```
library(imageviewer)
library(magick)
library(rsvg)
library(beepr)
library(hexView)
library(tiff)
library(EBImage)
library(rio)
```

## 7.2 Setting the directory

To be able to run these scripts, you need to set your directory to the folder where you saved your linearized, scaled, and cropped head pictures in .TIFF format with the function setwd() or by following this path *Session >> Set Working Directory >> Choose Directory*.

## 7.3 Creating a list of pictures

```
in.images <- list.files(path = "images", pattern = "_H_", full.names = F, recursi
ve = F)
in.images

## [1] "ID_H_linearized_scale_cut_10.tif"
```

Here, again, you need to confirm that you can access the elements of the list.

```
length(in.images)

## [1] 1
```

In our case, we have one picture in our list.

## 7.4 Converting pictures to arrays

Like in section 4, we created a function that formats the pictures correctly (i.e., import, convert to an array) and lists them.

```
Format.image <- function(y) {
  list_array <- list() # creates an empty list
  for (n in 1:length(y)) {
    image <- paste("standardized_", y[n], sep = "") # creates a new picture name
where "standardized_" is added at the beginning of the name.
    print(image)
    y2 <- image_read(y[n]) # read .TIFF file
    #print(y2) # this is to see the picture in R-studio viewer (takes more time)
    print(image_info(y2))

    y_array <- as.integer(y2[[1]]) # converts to an array to be able to change th
e colour values
    y_array <- transpose(y_array)
    y_array <- y_array / 255
```

```
    #print(y_array)
    list_array[[image]] <- y_array
  }
  return(list_array)
}
```

You can apply the function to your list of pictures:

```
picture_list <- Format.image(in.images)

## [1] "standardized_ID_H_linearized_scale_cut_10.tif"
## # A tibble: 1 × 7
##   format width height colorspace matte filesize density
##   <chr>  <int>  <int> <chr>      <lgl>    <int> <chr>
## 1 TIFF    1381   1381 sRGB       FALSE 11443455 138x138
```

In our case, we can see that we have one picture of 1381 pixels (width) per 1381 pixels (height). Again,

you want to ensure you can access the reflectance values from the first picture. You also need to make

sure you select an area of your picture that is not black. In our case, we indicated that we wanted to see

the reflectance values between the pixel rows 670 and 675, and between the pixel columns 662 and 667

of the third colour channel (blue).

```
picture_list[[1]][670:675, 662:667, 3]

##          [,1]      [,2]      [,3]      [,4]      [,5]      [,6]
## [1,] 0.2549020 0.2470588 0.2392157 0.2274510 0.2117647 0.1921569
## [2,] 0.2549020 0.2392157 0.2392157 0.2352941 0.2196078 0.2000000
## [3,] 0.2470588 0.2392157 0.2352941 0.2352941 0.2117647 0.2000000
## [4,] 0.2431373 0.2352941 0.2352941 0.2274510 0.2117647 0.2000000
## [5,] 0.2392157 0.2274510 0.2274510 0.2274510 0.2196078 0.2078431
## [6,] 0.2352941 0.2235294 0.2235294 0.2235294 0.2235294 0.2235294
```

*7.5 Standardizing pictures*

We created a function that standardizes all three colour channels.

```
change.image <- function(x) {

    for(m in 1:length(x)){
    r <- x[[m]][, , 1] # name red layer
    g <- x[[m]][, , 2] # name green layer
    b <- x[[m]][, , 3] # name blue layer
```

```
    pr <- r / (r + g + b) # Standardize red channel
    pg <- g / (r + g + b) # Standardize green channel
    pb <- b / (r + g + b) # Standardize blue channel

    # When divisions by 0 occur, R outputs NaN, we need to replace those NaN by 0
(so that they are equal to the darkest pixel value)
    pr[is.na(pr)] <- 0
    pg[is.na(pg)] <- 0
    pb[is.na(pb)] <- 0

    z_norm <- Image(array(dim=c(nrow(pr), ncol(pr), 3), data=cbind(pr, pg, pb)))
# stack and convert to image. Order is important in the three layers. # this imag
e is now standardized (colours might seem weird because of the standardization)
    colorMode(z_norm) <- Color # set to colour mode
    writeImage(z_norm, paste(names(x[m]), "_norm", ".TIFF", sep="")) # save as ne
w image (with "_norm" added at the end) in 16bit TIFF format
  }
  }
change.image(picture_list)
```

The standardized version of our head picture looks like this:



## 8. Binarizing pictures

The binarization allows us to isolate the colour of interest (yellow in this case because we are focusing

158

on head pictures in this example) from all other colours present in our picture. It will give a score of 0 (black) to the colour of interest and a score of 1 (white) to the rest. Then, from the binarized pictures, it will compute the number of yellow pixels (black) and the number of pixels that are not considered yellow (white) allowing us to calculate the proportion of yellow pixels in the area of interest. The scripts can be adapted to any colour and area of interest.

*8.1 Loading R packages*

See note in section 3.1.

```
library(imageviewer)
library(magick)
library(rsvg)
library(beepr)
library(hexView)
library(tiff)
library(EBImage)
library(rio)
```

*8.2 Setting the directory*

To be able to run these scripts, you need to set your directory by choosing the folder where you saved your linearized, scaled, and cropped (and possibly standardized) pictures in .TIFF format with the function setwd() or by following this path *Session >> Set Working Directory >> Choose Directory*.

*8.3 Creating a list of pictures*

```
in.images <- list.files(path = "images", pattern = "_H_", full.names = F, recursive = F)
in.images
## [1] "ID_H_linearized_scale_cut_10.tif"
```

We can see that our file only included one picture named *ID_H_linearized_cut_10.tif*.

*8.4 Converting pictures to arrays*

Again, we created a function that formats our images correctly (import, convert to an array) and lists

them. This function is similar to the one in section 4.

```
Format.image <- function(y) {
  list_array <- list() # creates an empty list
  for (n in 1:length(y)) {
    image <- paste("10_", y[n], sep = "") # creates transformed names, you can re
place "10_" to something more meaningful for your own project.
    print(image)
    y2 <- image_read(y[n]) # read file
    #print(y2) # this is to see picture in R-studio viewer (takes more time)
    print(image_info(y2))

    y_array <- as.integer(y2[[1]]) # converts to an array to be able to change th
e colour values
    y_array <- transpose(y_array)
    y_array <- y_array / 255      #print(y_array)
    list_array[[image]] <- y_array
  }
  return(list_array)
}
```

Then, you can apply the function created to your initial list of pictures and create a new list of arrays for

all the pictures.

```
picture_list <- Format.image(in.images)

## [1] "10_ID_H_linearized_scale_cut_10.tif"
## # A tibble: 1 × 7
##   format width height colorspace matte filesize density
##   <chr>  <int>  <int> <chr>      <lgl>    <int> <chr>
## 1 TIFF    1381   1381 sRGB       FALSE 11443455 138x138
```

You can see that we had one picture of 1381 pixels (width) per 1381 pixels (height). Again, you need

to ensure you can access the reflectance values from the first picture. You also need to make sure you

select an area in your picture that is not black. In our case, we wanted to see the reflectance values

contained between the pixel rows 670 and 675, and between the pixel columns 662 and 667 on the third

colour channel (blue).

```
picture_list[[1]][670:675, 662:667, 3]
```

```
##              [,1]       [,2]       [,3]       [,4]       [,5]       [,6]
## [1,] 0.2549020 0.2470588 0.2392157 0.2274510 0.2117647 0.1921569
## [2,] 0.2549020 0.2392157 0.2392157 0.2352941 0.2196078 0.2000000
## [3,] 0.2470588 0.2392157 0.2352941 0.2352941 0.2117647 0.2000000
## [4,] 0.2431373 0.2352941 0.2352941 0.2274510 0.2117647 0.2000000
## [5,] 0.2392157 0.2274510 0.2274510 0.2274510 0.2196078 0.2078431
## [6,] 0.2352941 0.2235294 0.2235294 0.2235294 0.2235294 0.2235294
```

*8.5 Determining the colour threshold & binarizing the pictures*

We created a function that binarizes pictures according to the colour of interest. The function creates a

new picture where all pixels of our colour of interest are black and all other colours are white. In our

case, we wanted to compute the number of yellow pixels relative to the total number of pixels. We first

needed to determine which reflectance value corresponded to what we call *yellow* in our pictures (i.e.,

what our eyes see as yellow). We identified a threshold of reflectance value that is included in our

binarization function to determine which pixels are yellow. With this threshold, the function binarizes

our pictures for the colour of interest: the colour of interest (i.e., yellow) will have a score of 0 (black)

and the rest will have a score of 1 (white). To determine the threshold, we used the first part of the

function that isolates the yellow component of the pictures by substracting the blue channel from the

green channel. The equation to use to isolate the colour of interest will depend on the colour you want

to isolate. For each picture, a new picture is saved in the directory by adding *yellow_g-b* at the end of

the picture name. You can modify the new name as you wish. In our case, we performed this first step

on 50 pictures to select the optimal threshold to binarize our pictures according to the colour of interest.

```r
change.image<-function(x) {

  Prop_list_yellow_head <- NA # Creates an empty database to compile proportion o
f coloured pixels at the end

  for(m in 1:length(x)){
    pr <- x[[m]][, , 1] # name red channel
    pg <- x[[m]][, , 2] # name green channel
    pb <- x[[m]][, , 3] # name blue channel
```

```
    ## To isolate the yellow component: this part is specific to the colour you w
ant to isolate

    po_yellow <- pg - pb # To isolate yellow, we need to subtract the blue channe
l from the green channel.

    z.cropped.norm.o_yellow <- Image(array(dim = c(nrow(po_yellow), ncol(po_yello
w), 1), data = po_yellow))  # stack and convert to image. Order is important. Thi
s is to create a new picture with the yellow component isolated.

    writeImage(z.cropped.norm.o_yellow, paste(names(x[m]), "_yellow_g-b", ".TIFF"
,sep = "")) # save as a new picture in 16bit .TIFF format with "_yellow_g-b" adde
d at the end of the name in the directory selected at the beginning

  }

}
change.image(picture_list)
```

After running this function, you now have a picture that isolates the colour of interest and it should look

like this (what you see in white are the yellow areas):
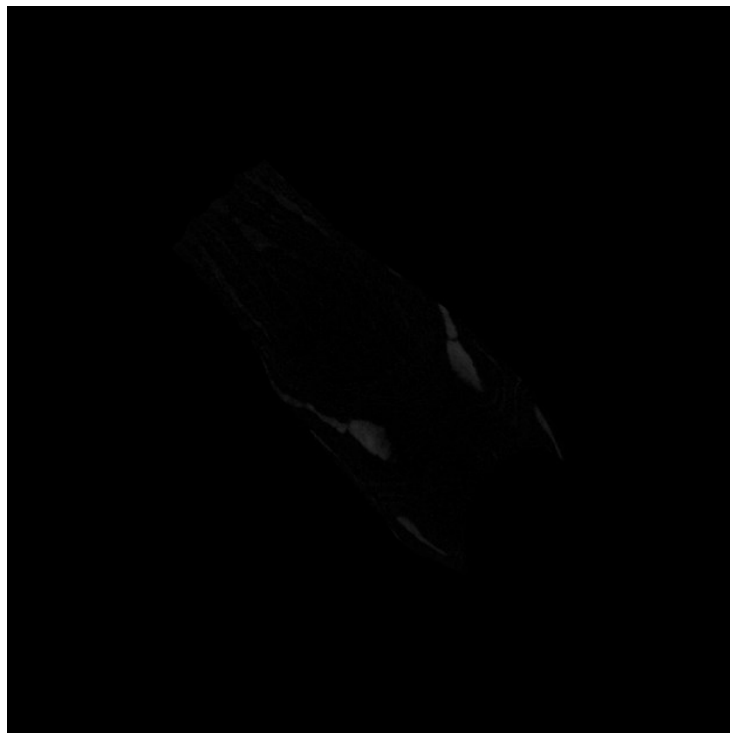
A subset of pictures must be used to determine the threshold that will be used to binarize your pictures. This can be done by opening the newly saved pictures with the colour of interest isolated in ImageJ and putting your cursor over a region of the colour of interest (yellow here) and noting the coordinates. Then, in R, you can find the reflectance value (between 0 and 1) that corresponds to the colour of interest. You can also use the version of the picture prior to the isolation of the colour of interest given that you will see the real colours and it can be easier to select the coordinates. Here, you can see our image representing the yellow component isolated from the other colours when we open it in ImageJ:
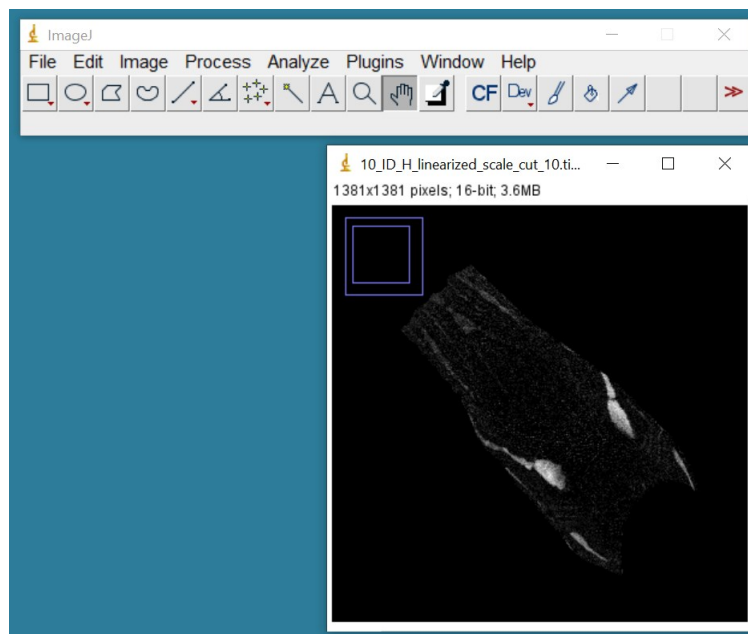


In our case, we opened the picture in ImageJ prior to the isolation of the yellow component to select the coordinates:
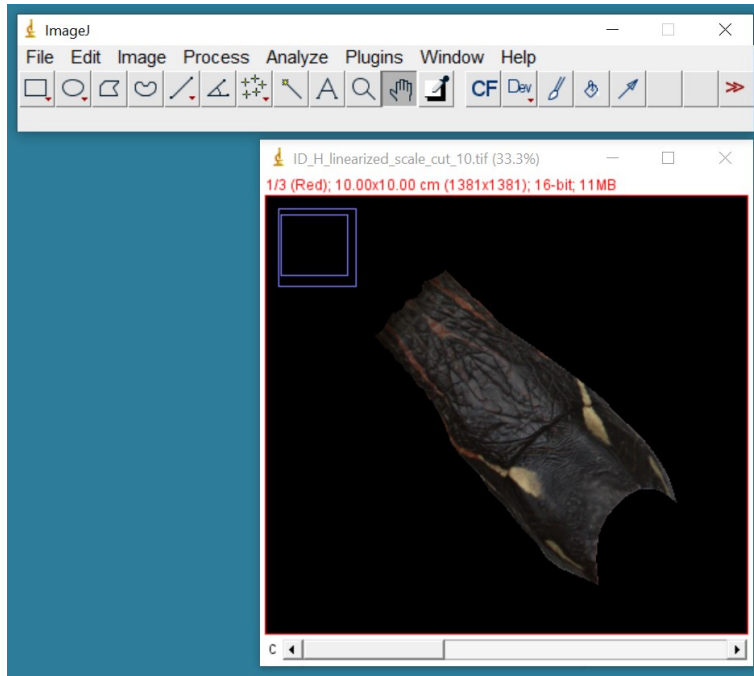
ImageJ gives you the coordinates of the pixel where you put your cursor. Move your cursor over a region

of your colour of interest to get its coordinates. In our case, we zoomed on a yellow spot of the head and

put our cursor over it (red arrow). We then noted the coordinates of the pixel (located in the red box) in

a spreadsheet file.
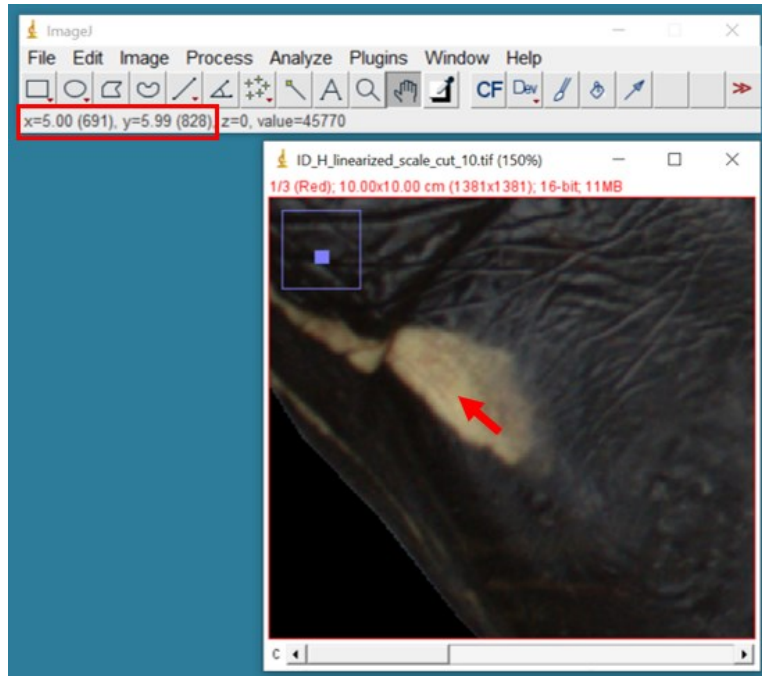
The coordinates of a yellow pixel in this picture were x = 691 and y = 828. You will need to do this for all your subset of pictures (one set of coordinates per colour of interest). You can then return in R to determine the reflectance values of these pixels. You can create a new spreadsheet file to i) keep all the coordinates obtained for each picture of the subset and ii) enter the reflectance values that you will later obtain in R.

|  | A | B | C | D | E |
|---|---|---|---|---|---|
| 1 | ID | CoordinateX | CoordinateY | Reflectance-value | |
| 2 | ID_H_linearized_cut_10 | 691 | 828 | | |
| 3 | | | | | |
| 4 | | | | | |
| 5 | | | | | |
| 6 | | | | | |

When all the coordinates are identified, you can return in R to a modified version of the previous function that will allow you to determine the reflectance values of the selected pixels coordinates.

**Be careful**: If you apply the function to your previous picture list (instead of applying it only to the

picture from which you got the coordinates), it will determine the reflectance value of the coordinates selected for all the pictures in the list. Since yellow areas of different pictures are not all at the same coordinates, this will lead to incorrect thresholds.

In this example, only one picture was included in our picture list, so we do not have to worry about this.

Here is the modified function, make sure to change the coordinates according to what you obtained in ImageJ:

```
change.image <- function(x) {

  Prop_list_yellow_head <- NA

  for(m in 1:length(x)){
    pr <- x[[m]][, , 1]
    pg <- x[[m]][, , 2]
    pb <- x[[m]][, , 3]

    po_yellow <- pg - pb

    z.cropped.norm.o_yellow <- Image(array(dim = c(nrow(po_yellow), ncol(po_yello
w), 1), data = po_yellow))
    writeImage(z.cropped.norm.o_yellow, paste(names(x[m]), "_yellow_g-b", ".TIFF"
, sep = ""))

    ## this is the section that you need to modify according the coordinates obta
ined in ImageJ to determine the reflectance value of this selected pixel. In our
case x = 691 and y = 828.

  print(c(z.cropped.norm.o_yellow[691, 828, 1], paste("Reflectance values - Yello
w pixel")))

    }
  return(Prop_list_yellow_head)
}
```

Now, you can run the new version of the function to have the reflectance value of the coordinates selected:

```
Reflectance_value_yellow <- change.image(picture_list)
```

```
## [1] "0.133333333333333"                    "Reflectance values - Yellow pixel"
```

You can see that the pixel selected (coordinates in ImageJ: x = 691 and y = 828) has a reflectance value

of **0.13**. The function can now be modified to binarize (black/white) the pictures according to this

reflectance threshold. For now, we will only show you how the function works and how a binarized

picture looks like based on the reflectance value that we just computed.

```r
change.image <- function(x) {

  Prop_list_yellow_head <- NA
  list_black_head <- NA
  list_white_head <- NA

  for(m in 1:length(x)){
    pr <- x[[m]][, , 1]
    pg <- x[[m]][, , 2]
    pb <- x[[m]][, , 3]

    po_yellow <- pg - pb

    z.cropped.norm.o_yellow <- Image(array(dim = c(nrow(po_yellow), ncol(po_yello
w), 1), data = po_yellow))

    #writeImage(z.cropped.norm.o_yellow, paste(names(x[m]), "_yellow_g-b", ".TIFF
", sep=""))

    ## You need to modify this function according to the reflectance value obtain
ed. In this example, our threshold is 0.13. Let us select only regions >0.13 for
yellow and create a new binarized picture to see the result.

    z.cropped.norm.o_yellow[which(z.cropped.norm.o_yellow[] <= 0.13)] <-1 # All y
ellow pixels will be black (0) and all other pixels will be white (1).
    z.cropped.norm.o_yellow[which(z.cropped.norm.o_yellow[] > 0.13 & z.cropped.no
rm.o_yellow[] != 1)] <-0

    White_yellow <- print(length(z.cropped.norm.o_yellow[which(z.cropped.norm.o_y
ellow[] == 1)])) # Number of pixels that are not considered yellow.
    Black_yellow <- print(length(z.cropped.norm.o_yellow[which(z.cropped.norm.o_y
ellow[] == 0)])) # Number of yellow pixels.
    Prop_yellow <- Black_yellow / (White_yellow + Black_yellow) # Proportion of y
ellow pixels.

    print(c(Prop_yellow, paste("Proportion of yellow pixels")))
```

```
    writeImage(z.cropped.norm.o_yellow, paste(names(x[m]), "yellow_0.13_g-b", ".T
IFF", sep = "")) # save as new picture in 16bit .TIFF with the "yellow_0.13_g-b"
at the end of the name.

    # Add the proportion of yellow pixels (and the count of black and white pixel
s) to the empty table created at the beginning of the function.

    Prop_list_yellow_head[[m]] <- Prop_yellow

    list_black_head[[m]] <- Black_yellow
    list_white_head[[m]] <- White_yellow

  }
  return_list <- list(Prop_list_yellow_head, list_black_head, list_white_head)

  return(return_list)
}

Proportion_list_head <- change.image(picture_list)

## [1] 1905941
## [1] 1220
## [1] "0.000639694289050584"        "Proportion of yellow pixels"
```

The output gives you the following information:

- The first row is the number of pixels that are not considered yellow according to the threshold selected (i.e., number of white pixels in the binarized picture).

- The second row is the number of yellow pixels according to the threshold selected (i.e., number of black pixels in the binarized picture).

- The third row is the proportion of yellow on the head.

Here is the picture binarized with this threshold:

168
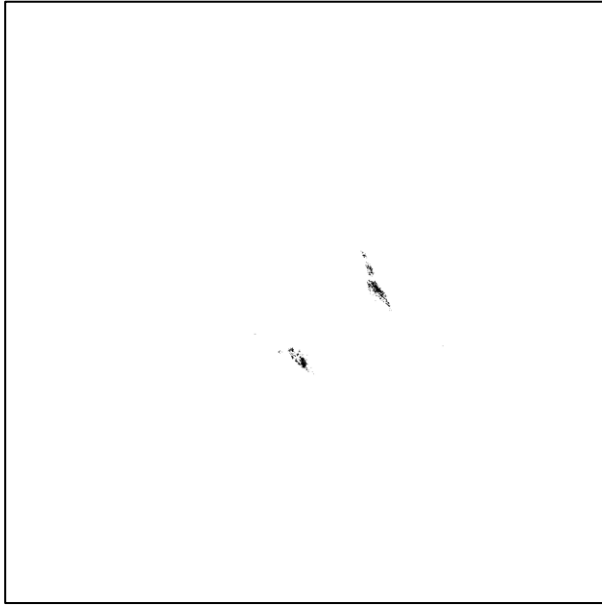
You can notice that the threshold selected here (0.13) is too restrictive (i.e., we are losing areas of the colour of interest (represented in black) according to the original picture). In other words, there should be more black pixels in the binarized picture since the area covered by yellow in the original picture is bigger than what we see in the binarized picture. By running the previous function with several pictures, you will find an optimal value allowing you to keep only the regions of interest, without losing too much of them. Some trial and error may be required. The black areas in the binarized pictures should only be present where your colour of interest is. You can try different thresholds on several pictures and select the one that keeps most areas of your colours of interest without including too much noise (i.e., areas that do not appear similar visually to your colour of interest).

In the following example, the first picture has a threshold of 0.01. This leads to most of the picture being black (not only the yellow patches), which is not restrictive enough. On the other hand, you do not want your threshold to be too restrictive, which would lead to losing your colour of interest (i.e., yellow patches (or parts of them) would be white while they should be black).

169
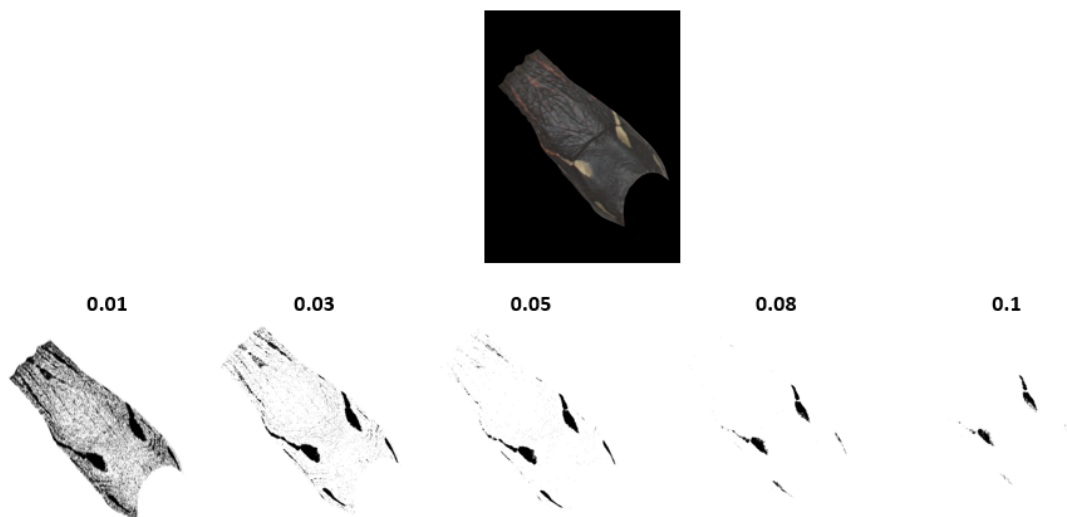
In our case, we used 50 pictures to determine visually the optimal threshold value to use. We selected a threshold of 0.08 for our shades of yellow. When the optimal threshold is selected, you can save the proportion of yellow pixels calculated for all your pictures in a database and export it to a spreadsheet file. We added a new column with the picture name alongside the proportion of yellow calculated. The number of black and white pixels used to calculate the proportion of yellow pixels is also available in the data frame.

```r
Proportion_list_head <- as.data.frame(Proportion_list_head)

Proportion_list_head["picture"] <- names(picture_list)

colnames(Proportion_list_head)[1] = "Proportion of yellow pixels (black/[black+white])"
colnames(Proportion_list_head)[2] = "Number of black pixels"
colnames(Proportion_list_head)[3] = "Number of white pixels"

Proportion_list_head

##   Proportion of yellow pixels (black/[black+white]) Number of black pixels
## 1                                       0.0006396943                   1220
##   Number of white pixels                         picture
## 1                1905941 10_ID_H_linearized_scale_cut_10.tif
```

```
export(Proportion_list_head, "Head_Picture.xlsx")
```

You should now have your colouration data extracted and ready for further analyses.

# Chapter 3

Exploring the effect of 195 years-old locks on species movement: Landscape genetics of painted turtles in the Rideau Canal, Canada

**Abstract**

Aquatic systems have been extensively altered by human structures (e.g., construction of dams/canals) and these have major impacts on the connectivity of wildlife populations through the loss and isolation of suitable habitats. Habitat loss and isolation affect gene flow and influence the persistence of populations in time and space by restricting movements. Isolation can result in higher inbreeding, lower genetic diversity, and greater genetic structure, which may render populations more vulnerable to environmental changes, and thus to extinction. Given the ubiquity and the persistence of dams and canals in space and time, it is crucial to understand their effects on the population genetics of aquatic species. Here, we documented the genetic diversity and structure of painted turtle (*Chrysemys picta*) populations in the Rideau Canal, Ontario, Canada. More specifically, we used 13 microsatellites to evaluate the influence of locks on genetic variation in 822 painted turtles from 22 sites evenly distributed along the 202-km canal. Overall, we found low, but significant, genetic differentiation suggesting that some dispersal is occurring throughout the canal. In addition, we showed that locks contribute to the genetic differentiation observed in the system. Clustering analysis revealed two distinct genetic groups whose boundary is associated with a series of six locks. Our results illustrate how artificial waterways, such as canal systems, can influence population genetic structure. We highlight the importance of adopting management plans that can mitigate the impacts of human infrastructure and preserve gene flow across the landscape to maintain viable populations.

## Introduction

Increase and expansion of human activities have led to the loss and isolation of natural habitats which, in turn, have resulted in the loss of biodiversity worldwide (Haddad et al., 2015; Su et al., 2021; WWF, 2018). Habitat loss and isolation have major impacts on the distribution, abundance and connectivity of wildlife populations that are often reflected in their population genetic diversity and structure (Fahrig, 2003; Schlaepfer et al., 2018). Alterations of natural habitats by human activities reduce the area and connectivity of suitable habitats for wildlife, restricting movements of individuals that are necessary to maintain gene flow (Fahrig, 2003; Lowe & Allendorf, 2010; Schlaepfer et al., 2018). By reducing population size and increasing genetic drift, loss of connectivity results in higher inbreeding and lower genetic diversity, leading to greater population genetic differentiation between isolated populations (Schmidt et al., 2020). A reduction of dispersal may also limit the exchange of alleles that are potentially important for individuals to adapt to their environment (Lenormand, 2002; Morjan & Rieseberg, 2004). In the long term, fitness of individuals from isolated populations can decrease and populations may become more vulnerable to environmental changes and, thus, to extinction (Leigh et al., 2019; Reed & Frankham, 2003; Willi et al., 2006). Therefore, to maintain gene flow and ensure the persistence of small and isolated populations in space and time, it is crucial to identify the factors that limit gene flow among these populations, especially in highly modified environments.

Freshwater habitats have been extensively altered by humans (e.g., construction of dams/canals) to sustain diverse economic activities (e.g., transportation, energy and water use) (Grill et al., 2015; Nilsson, 2005). Worldwide, water flow and connectivity of almost half of all rivers have been modified by dam construction (Grill et al., 2015). These alterations have drastically affected habitat quality and

connectivity for aquatic species and, thus, the ecological integrity of ecosystems (Barbarossa et al., 2020; Lin et al., 2020; Su et al., 2021). Reduction of the natural connectivity of ecosystems can impede the life cycles of freshwater species and represents a major cause of the decline of freshwater biodiversity worldwide (Carvajal-Quintero et al., 2017; Fuller et al., 2015; Jansson et al., 2000; Perkin & Gido, 2012). In comparison to dams, canals are more complex systems where both barriers (e.g., dams and locks) and new connections (e.g., excavated channels) are created (Lin et al., 2020). This duality makes it difficult to predict the long-term ecological effects of canals on aquatic ecosystems (Lin et al., 2020). The balance between possible negative and positive effects of canals on connectivity can also depend on their design and permeability (i.e., length and number of locks and dams), the original characteristics of the aquatic and surrounding terrestrial habitats, the intensity of changes made, and the management history of the canal (Lin et al., 2020). There is currently a lack of research on how genetic population structure of aquatic species is affected by artificial waterways, such as canal systems, especially at large spatial scales (Bergman et al., 2021; Koschorreck et al., 2020; Lin et al., 2020).

To determine how freshwater species are affected by anthropogenic changes, it is crucial to assess how their genetic structure is related to human-made barriers in these artificial systems (Selkoe et al., 2015). To do so, a landscape genetics approach can be used to determine the permeability to gene flow and the occurrence of genetic discontinuities in artificial waterways (Selkoe et al., 2015). In particular, by using landscape genetics modelling, one can quantify the relationship between genetic differentiation (e.g., genetic distance such as $F_{ST}$) and landscape features (e.g., number of barriers) (Row et al., 2017; Van Strien et al., 2012). Landscape genetics can also inform management decisions for vulnerable species by identifying areas of conservation concern (e.g., populations with low genetic diversity and high genetic structure, and identification of barriers responsible for the evolution of distinct genetic

groups; Holderegger & Wagner, 2008; Manel et al., 2003)

Turtles are among the most vulnerable taxa to anthropogenic changes (Böhm et al., 2013; Buhlmann et al., 2009; Gibbons et al., 2000) given their life-history traits (e.g., late sexual maturity, low juvenile survival) that make populations less resilient to reductions in adult survival (Brooks et al., 1991; Congdon et al., 1994; Midwood et al., 2015). In Canada, six out of 10 native freshwater turtles are considered at risk by the Committee on the Status of Endangered Wildlife in Canada (Species at risk public registry: www.canada.ca/en/environment-climate-change/services/species-risk-public-registry). Previous studies have evaluated the impact of landscape changes (e.g., expansion of road networks and agricultural/urban conversion of natural habitats) on genetic patterns of turtle populations (see Laporte et al., 2013; Reid et al., 2017; Reid & Peery, 2014; Willoughby et al., 2013 for examples). While some studies found no genetic effects of landscape changes (Laporte et al., 2013; Willoughby et al., 2013), others indicated that anthropogenic changes were associated with higher genetic differentiation and lower genetic diversity (Reid et al., 2017; Reid & Peery, 2014). To our knowledge, however, no study to date has assessed the effects of large-scale aquatic landscape alterations (e.g., constructions of canals) on genetic population structure of freshwater turtles (see Bennett et al. (2010) for a study at a small spatial scale).

In this study, we characterize the genetic diversity and genetic population structure of painted turtles (*Chrysemys picta*) in the Rideau Canal, Ontario, Canada. More specifically, we assess how landscape features, especially the presence of locks, are related to genetic differentiation throughout the system. We hypothesize that the construction of locks for the Rideau Canal has impeded movements of painted turtles and thus reduced gene flow between populations. Specifically, we predict that: i) the number of locks will be a better predictor of genetic structure than other landscape features (i.e.,

176

historical features of the landscape prior to canal construction and geographic distance) and ii) populations isolated by many locks will be more genetically distant than populations separated by few or no locks. Our study provides a rare example of how a canal system can influence the landscape genetics of a long-lived species.

The Rideau Canal is a slackwater canal located in southeastern Ontario, Canada, that connects the Ottawa River to Lake Ontario. This 202-km continuous waterway is a network of rivers, lakes, and excavated channels that were connected through the construction of 23 lockstations (45 locks), many of which were built with water-control dams (Legget, 1986). Construction started in 1826 and the canal officially opened in 1832. The main purpose of this canal was to provide a supply route for military activities to protect Canadian British colonies against the United States (Tulloch, 1981). Since its construction, however, the Rideau Canal has been mainly used for economic and recreational activities (Parks Canada, 2006). Given that the Rideau Canal is the oldest continuously operated canal in North America and that the effect of its construction on landscape connectivity remains completely unexplored, it is a valuable study system to evaluate the long-term effects of such constructions on genetic composition of turtle populations.

**Methods**

*Study species*

The painted turtle is a long-lived generalist species (i.e., generation time ~ 30-45 years; COSEWIC, 2018) widely distributed across North America that lives in various aquatic habitats (e.g., swamps, marshes, rivers and lakes; Ernst & Lovich, 2009). Painted turtles can disperse overland between wetlands and colonize new and artificial wetlands (Bowne, 2008; Dupuis-Desormeaux et al., 2018). Even if painted turtles are considered stable over their range by the IUCN (van Dijk, 2011),

populations in southeastern Ontario are considered of Special Concern by the Committee on the Status of Endangered Wildlife in Canada (COSEWIC, 2018).

*Study system and sample collection*

We sampled painted turtles at 22 sites distributed approximately every 10 km along the entire Rideau Canal in Ontario, Canada (Figure 3-1a, Table 3-1). There was wide variation in the number of locks between pairs of sites (range = 0–33, mean = 11.3, SE = 0.5). We sampled in suitable habitats for painted turtles characterized by shallow water, weak current, abundant aquatic vegetation, and presence of structures for basking (e.g., rocks and stumps).

We captured painted turtles with fyke nets between May and August in 2018–2020. We deployed fyke nets for one week at each site and checked them every 24 hours. We sampled some sites for more than one year to evaluate their temporal genetic stability (10/22 sites; Table 3-1; see *Genetic diversity and differentiation* section). Each painted turtle we captured was marked with the North American code (Nagle et al., 2017) to ensure unique sampling. We took blood samples from the coccygeal, jugular, or supracarapacial vein using a U-100 insulin syringe with 28 G x 12.7 mm microfine needle (BD Medical). We dried the blood samples on a qualitative P8 grade filter paper (Thermo Fisher Scientific) prior to DNA extraction.

*DNA extraction and amplification*

We extracted DNA from a $\geq$ 7-mm punch of a blood-soaked filter paper with an overnight proteinase K digestion followed by a salt extraction (Aljanabi & Martinez, 1997). We assessed extraction quality by running extraction products on 1% agarose gels (stained with ethidium bromide) and revealing the band under UV light. We then normalized each DNA sample to a final concentration of 10 ng/µl prior to PCR amplification. We genotyped all DNA samples using 15 microsatellite loci

previously described and tested on painted turtles (Supporting Information 1 – Table S3-1). We optimized PCR conditions by adapting original PCR protocols and by examining amplified products on 2% agarose gels (Supporting Information 1 – Table S3-2 and S3-3). All forward primers were labelled with a fluorescent dye (Supporting Information 1 – Table S3-1). We ran amplified products using three multiplexes with an AB3500 Genetic Analyzer and using GeneScan™ 600 LIZ as a size standard (Applied Biosystems). We scored all alleles twice manually with GeneMapper™ v.6 (Applied Biosystems). We assessed genotyping error rate for each locus from repeated genotyping of 38 painted turtles (= 4.6% of samples) that were sampled more than once between years.

*Genetic diversity and differentiation*

We obtained population genetic statistics using different packages in R 3.6.2 (R Core Team, 2019). We tested for deviations from Hardy-Weinberg equilibrium (HWE) for each locus, and for each combination of sampling sites and locus, using Chi-squared tests (Chisq) and exact tests based on 10,000 Monte Carlo (MC) permutations with the R package pegas (Paradis, 2010). We estimated the proportion of loci that deviated from HWE for each sampling site and estimated the proportion of sites out of HWE for each locus using a false discovery rate correction based on the significant deviations previously tested (based on MC and Chisq tests with and without Bonferroni correction; Benjamini & Yekutieli, 2001). We tested all loci for linkage disequilibrium with the R package poppr (Kamvar et al. 2014). We also assessed the frequency of null alleles for each locus with the R package PopGenReport (Adamack & Gruber, 2014). We excluded loci with i) a high frequency of null alleles (i.e., >10%), ii) a significant deviation from HWE across several sampling sites, or iii) a high genotyping error rate (i.e., >10%) from further analyses (see *Sample collection and genotyping* in *Results* section).

From the dataset with the remaining loci, we estimated observed and expected heterozygosity ($H_O$

and $H_E$), allelic richness ($A_R$) and inbreeding coefficients ($F_{IS}$) for each locus and sampling site using the R package diveRsity (Keenan et al., 2013). We then determined the number of private alleles ($P_A$) for each sampling site with the PopGenReport package (Adamack & Gruber, 2014). We also used the diveRsity package to calculate the global value of $F_{IS}$, $F_{ST}$, and $G_{ST}$ and the pairwise $F_{ST}$ (Weir & Cockerham, 1984) and $G_{ST}$ (Hedrick, 2005) values between each pair of sites. We estimated confidence intervals at 95% (95% CI) for $A_R$, $F_{IS}$, $F_{ST}$, and $G_{ST}$ with a bias-corrected bootstrapping method implemented in the DiveRsity package (10,000 bootstraps). We also estimated $H_O$, $H_E$, $A_R$, $F_{IS}$, and $F_{ST}$ values by grouping data according to the genetic cluster identified in the clustering analysis (see *Genetic clustering analysis* sections). We calculated the probability of identity (PI) and PI among siblings (PISibs) with the Excel extension of GenAlEx (Peakall & Smouse, 2012) to assess if our genetic parameters were biased by the sampling of close relatives. We performed a hierarchical AMOVA on data from 10 sites sampled in 2019 and 2020 (Table 3-1) by grouping sampling sites per year of sampling to determine the temporal stability of genetic diversity with the ade4 package (10,000 permutations; Thioulouse et al., 2018). We estimated the presence, degree, and direction of asymmetric gene flow among sampling sites using the relative migration network method developed by Sundqvist et al. (2016) and implemented in the diveRsity package. We calculated estimates of significant relative migration rates with $G_{ST}$ and Nm (i.e., effective number of migrants based on a statistic that incorporates information from Nei's $G_{ST}$ and Jost's D; (Alcala et al., 2014)) based on a bootstrap method with 50,000 replications.

*Genetic clustering analysis*

We used STRUCTURE v 2.3.4 (Pritchard et al., 2000) to estimate the most likely number of genetic clusters (K) in the system. We performed 10 runs for each number of potential clusters (K = 1–

22) by assuming an admixture model with correlated allele frequencies (length of burn-in period set to 100,000 repetitions; number of MCMC replicates: 250,000; sufficient for each run to converge). We evaluated the most likely number of clusters with two metrics: the mean log likelihood probability (LnP(K)) of the data for each K (Pritchard et al., 2000) and the delta K based on the rate of change in probability between successive K values (Evanno et al., 2005). We used CLUMPAK to compile and combine all runs for each K and to visualize the likelihood values (Kopelman et al., 2015). We then performed 10 additional runs with the selected most likely number of K applying the LOCPRIOR function that uses sampling sites as additional information in the analysis. The LOCPRIOR parameter provides a more definite distinction between clusters previously determined by the unsupervised model when population structure is relatively weak (Porras-Hurtado et al., 2013).

*Landscape genetic analyses*

We used maximum likelihood population effect models (MLPE models; Van Strien et al., 2012) with the R lme4 package (Bates et al., 2015) to assess how genetic differentiation was influenced by landscape features that could act as barriers to turtle movement. This approach allows to consider the non-independence of pairwise data by using a residual covariance structure with a mixed modelling approach (Clarke et al., 2002). We used pairwise $F_{ST}$ measures previously calculated between each pair of sampling sites as the genetic distance matrix and different types of landscape features as pairwise predictor matrices. We considered four landscape features that were calculated between each pair of sampling sites: i) the shortest aquatic distance (in meters) based on the geographic location of each sampling site, to represent a scenario of isolation by distance, ii) the number of locks, iii) the number of human-made constructions (e.g., mill dams) between 1783 (i.e., beginning of European settlement in the Rideau Canal region) and 1826 (i.e., beginning of Rideau Canal construction), and iv) the sum of

permeability values of historical features (i.e., waterfalls, rapids, and land barriers based on the work of Watson (2006)) previously located on the current path of the canal before any human-made alterations were made (Figure 3-2a; Supporting Information 2 of Chapter 3). We included the number of human-made constructions between 1783 and 1826, and historical features to disentangle the genetic effects of the canal construction from those of the original (prior to canal construction) landscape features. We also included the identity of sampling site pairs, used to calculate the genetic distance and landscape features matrices, in all models as a random effect.

We generated different combinations of permeability values for each historical feature (see Supporting Information 2 of Chapter 3) given that each feature may not have the same permeability to turtle movement. We compared the influence of each combination of permeability values on the genetic distance matrix by generating a set of univariate MLPE models. We used information criteria metrics (i.e., AICc) to identify the best model from the set of candidate models. We retained the combination of permeability values with the lowest AICc, among the set of candidate models, for further analyses (Supporting Information 2 of Chapter 3).

We fitted MLPE models for the different combinations of landscape features and the model with the lowest AICc (and ΔAICc < 2) was considered as the model that best fitted the genetic structure observed in the system (Supporting Information 1 – Table S3-4). Given that most landscape variables were highly correlated with each other ($r > 0.8$), we could not use them in the same model (Supporting Information 1 – Table S3-5). Following the results from STRUCTURE, we performed MLPE analyses separately for each genetic cluster identified to assess the role of landscape features on the genetic structure within each cluster (see *Genetic clustering analysis* in *Results* section). We verified model assumptions for each candidate model and calculated confidence intervals (95%) of estimates from the

best models. R codes used for MLPE models were adapted from codes available in R LandGenCourse package (Wagner, 2018) We obtained model predictions and built figures with the R ggeffects (Wickham, 2016) and ggplot2 packages (Lüdecke, 2018). We only present results from $F_{ST}$ pairwise values given that analyses conducted with pairwise $G_{ST}$ values and with Slatkin's linearized $F_{ST}$ ($F_{ST}/[1-F_{ST}]$) gave similar results (Supporting Information 1 – Table S3-6).

**Results**

*Sample collection and genotyping*

We collected blood samples from 822 painted turtles across the Rideau Canal (mean = 37 individuals/site, SE = 2.3; Figure 3-1a, Table 3-1). We excluded two microsatellites from the analyses (Supporting Information 1 – Table S3-1): GmuD87 had a high genotyping error rate (14%; Supporting Information 1 – Table S3-7), a high frequency of null alleles (11%; Supporting Information 1 – Table S3-8), and deviated from HWE in 14% of the sampling sites (Supporting Information 1 – Table S3-9); CpGT124 had a high genotyping error rate (18%; Supporting Information 1 – Table S3-7). We found no evidence of linkage disequilibrium among the 13 retained loci. PI and PIsibs were under 0.01 when a minimum of 2 loci and of 6 loci, respectively, were combined (Supporting Information 1 – Table S3-10). For the 13 retained loci, the missing data were 0.21% and the mean genotyping error rate was 2.3%.

*Genetic diversity and differentiation*

Population genetic statistics indicated a relatively high variability for the 13 retained loci (e.g., $H_O$ ranging from 0.28 to 0.93; see Supporting Information 1 – Table S3-1) and a homogenous genetic diversity between sampling sites with $A_R$ values ranging from 8.2 to 9.7 with overlapping 95% confidence intervals (Table 3-1). Overall, we found a low, but significant, genetic differentiation

183

throughout the canal ($F_{ST}$ = 0.007, 95% CI = 0.005 – 0.009) and a relatively low inbreeding level ($F_{IS}$ = 0.018, 95% CI = 0.009 – 0.027) (Table 3-1, Supporting Information 1 – Table S3-11).

The hierarchical AMOVA revealed that the majority of genetic variance occurred within samples (97.6%; $p < 0.001$) with the remaining variance partitioned between samples within sampling sites (1.6%; $p = 0.01$) and between sampling sites (0.8%; $p < 0.001$). We detected no significant genetic variance between years within sampling sites ($p = 0.31$) and no significant asymmetric migration rates between sampling sites.

*Genetic clustering analysis*

STRUCTURE analyses identified two genetic clusters throughout the Rideau Canal (Figure 3-1b, Supporting Information 1 – Table S3-12). The probability of having a single genetic cluster (K = 1), however, is close second (mean LnP(k) for K = 1: -43164.93; K = 2: -43159.16; Supporting Information 1 – Table S3-12). The split between the two clusters occurred between sites RR7 and RR8 (Figure 3-1a). We estimated that individuals from sites in the northern section of the canal (i.e., sites RR1, RR2, RR3, RR4, RR5, RR6 and RR7) had a likelihood of membership of 64% to cluster 1, while individuals from sites in the southern section (i.e., sites RR8, RR9, RR10, LR1, BR1, BR2, UP6, NB3, CL2, CL3, SA1, WF1, C1, RS1, CB1) had a likelihood of membership of 83% to cluster 2 (Figure 3-1b, 3-1c). Probability of assignment was stronger in the southern section of the canal where individuals from five sampling sites had a likelihood of membership over 90% to cluster 2 (i.e., UP6, CL2, CL3, C1, CB1; Figure 3-1b). A few sites were characterized by a lack of definitive assignment to a specific cluster (mean membership to each cluster ~ 50%, e.g., sites RR1, RR2, RR7, RR8, Figure 3-1b).

*Comparison between genetic clusters*

We found a pairwise $F_{ST}$ of 0.004 (95% CI = 0.002 – 0.005) between the two identified genetic

clusters. We observed a lower $A_R$ in the northern cluster ($A_R$ = 16.7, 95% CI = 16.2 – 17.0; N = 278) than in the southern cluster ($A_R$ = 18.4, 95% CI = 17.4 – 19.0; N = 544; Table 3-1). The mean number of $P_A$ per site was also lower in the northern cluster (mean = 1.43, SE = 0.30) than in the southern cluster (mean = 1.73, SE = 0.37; Table 3-1). On the other hand, $F_{IS}$ was 0.021 (95% CI = 0.007 – 0.033) in the southern cluster, while in the northern cluster the 95% CI overlapped with zero ($F_{IS}$ = 0.008, 95% CI = -0.012 – 0.024; Table 3-1). Finally, while we detected high relative migration rate among the two clusters ($G_{ST}$ and Nm: North to South = 0.84; South to North = 1.00), we found significant asymmetric gene flow only from the southern cluster to the northern cluster based on a bootstrap method with 50,000 replications.

*Landscape genetic analyses*

Across the Rideau Canal, the number of locks between pairs of sampling sites was the best predictor of the observed genetic structure (Table 3-2, Supporting Information 1 – Table S3-4). The genetic distance between pairs of sampling sites increased with the number of locks that separated them (Figure 3-2b, Table 3-2). In the northern cluster, historical features were the best predictors of the genetic differentiation observed; the presence of historical features increased the genetic distance between sites (Figure 3-2c, Table 3-2). In the southern cluster, models with historical features, number of locks, and geographic distance were the best models; the genetic distance increased with the presence of historical features, the number of locks, and the geographic distance between sites (Figure 3-2d, Table 3-2, Supporting Information 1 – Table S3-4 ).

## Discussion

Understanding how lasting human infrastructure can affect the genetic structure of aquatic wildlife is crucial to develop effective management plans for vulnerable species. This understanding is necessary

to reconcile the heritage and economic value of infrastructure, such as the Rideau Canal, and the maintenance of gene flow between freshwater species populations. The main goal of this study was to assess the impact of landscape features, especially the presence of locks, on the genetic structure of painted turtle populations. We found that, while locks seem partly permeable to turtle gene flow, the number of locks was still the best predictor of the genetic differentiation between sites in the Rideau Canal. To our knowledge, this is the first documentation that locks can potentially modulate gene flow in a long-lived species.

*Canal construction did not stop gene flow in the aquatic landscape*

We found weak genetic structure and homogeneous genetic diversity throughout the canal suggesting that locks are at least partly permeable to turtle gene flow and, thus, rendering this system much closer to panmixia than to complete isolation. Partial permeability to gene flow was also supported by the lack of definitive assignment to a specific cluster in clustering analysis for 50% of individuals (i.e., cluster assignment below 0.8) (Porras-Hurtado et al., 2013). A previous study by Reid et al. (2008) also detected weak genetic differentiation and low level of assignment of individuals to potential source populations for freshwater fishes in a canal system, suggesting that locks facilitated species movement. The use of a slackwater system (i.e., use of dams to flood the rapids rather than canal cuts to bypass them) in the Rideau Canal may have avoided major alterations to aquatic connectivity (Watson, 2006). By building locks "in the dry" (i.e., above pre-canal water level), only 10% of the length of the canal required alterations, such as excavated channels and locks, while the rest of the canal followed existing waterways or flooded lakes, which may have maintained gene flow in the system. It is also possible that the large population size (over 10,000 individuals in the Rideau Canal based on the Lincoln-Petersen index; see Supporting Information 1 – Table S3-13 and Supporting Information 1- Table S2-2 (Chapter

2)) and the limited time scale (in terms of number of painted turtle generations) since canal construction have limited our ability to detect a decline of genetic diversity and/or an increase in genetic structure (Frankham, 1996; Kuo & Janzen, 2004). As it was observed in previous studies, the detection of genetic isolation caused by recent anthropogenic changes can be hampered by long generation times (Hailer et al., 2006; Lippé et al., 2006; Su et al., 2018).

Terrestrial movements and dispersal at any life stage, such as female exploration to find nestling sites and post-hatching dispersal of juveniles, could also have contributed to the maintenance of gene flow throughout the system. Terrestrial movements of painted turtles are, however, typically short: female movements and nest sites further than 1 km from aquatic habitats are rare (Semlitsch & Bodie, 2003; Steen et al., 2012). Terrestrial dispersal (e.g., movements between ponds/wetlands) is usually shorter than 3 km (Bowne, 2002, 2008; Bowne & White, 2004), but longer movements are possible over longer time periods (e.g., 11.5 km straight-line distance over approximately 10 years; COSEWIC, 2018).

*A series of six locks may cause population isolation*

The clustering analysis revealed two genetic clusters within the canal. The boundary between genetic clusters occurred in the canal section with the highest number of locks per kilometer (i.e., 6 locks over 9.2 km; Supporting Information 1 – Table S3-14), suggesting that numerous locks in proximity can impede turtle gene flow. Previous studies in aquatic species have linked the presence of genetic clusters to permanent artificial barriers, such as dams (Fraik et al., 2021; Liu et al., 2020; Roberts et al., 2013). To our knowledge, however, our study is the first to suggest that several consecutive locks in proximity can have a similar impact on the genetic structure of an aquatic species.

We detected that gene flow between the two clusters was stronger from south to north, indicating

a possible source-sink dynamic in which the southern cluster may act as a source (Sundqvist et al., 2016). The possibility of source-sink dynamic is also supported by the lower genetic diversity (i.e., lower $A_R$ and $P_A$) in the northern cluster (Gustafson et al., 2019; Sundqvist et al., 2016). The direction of water flow is from south to north where the split between genetic clusters occurs and flow may have facilitated migration in this direction, as observed in other aquatic species (Alp et al., 2012; Jonsson, 1991; Junker et al., 2012). To our knowledge, however, there are no studies indicating a role for the direction of water flow in driving gene flow in freshwater turtles.

*Locks may act as barriers to movement*

We found that genetic differentiation of painted turtles in the canal increased with the number of locks and that the number of locks was a better predictor of genetic structure than other landscape features. Although recent anthropogenic changes do not always cause genetic isolation (Bennett et al., 2010; Su et al., 2018), our results suggest a relatively rapid effect of locks on genetic differentiation. Despite genetic differentiation possibly being underestimated because of the large population size, long generation time, and slow mutation rate of turtles (Avise et al., 1992; Shaffer et al., 2013), it was not sufficient to limit our detection capacity.

It is important to acknowledge the difficulty in disentangling the effects of individual landscape features given their interconnectedness. Locks were built to overcome navigational barriers. Thus, locks were usually built where waterfalls and rapids were located prior to canal construction (Watson, 2006; see Figure 3-2a). Therefore, we cannot exclude the possibility that the genetic structuring we observed along the canal may represent an effect of historical barriers that was exacerbated by the construction of locks.

Previous studies in migrating diadromous fishes showed that locks can impede their dispersal

across waterways by reducing the number of passages (Vergeynst et al., 2019; Verhelst et al., 2018). In the Rideau Canal, lock activity varies both temporally (May to October, mean = 8.6 lockages/day, May = 2.7, June = 6.4, July = 15.4, August = 15.6, September = 7.3, October = 3.3; Supporting Information 1 – Table S3-15) and spatially (min = 2.7 for Ottawa locks, max = 19.3 for Newboro lock; Supporting Information 1 – Table S3-15). Thus, lock passage can be particularly difficult at certain times of the turtle active season and at certain locations. Even if turtles are able to enter locks (see Bennett et al., 2010), the time window to pass through the locks can be short. Also, even if the timing is right, the use of locks could lead to disorientation, physical stress, injuries (e.g., impact by boat propellers; Bulté et al., 2010), and even mortality, as it was observed in migrating diadromous fishes (Vergeynst et al., 2019; Verhelst et al., 2018). Finally, if lock water filling is in the opposite direction to turtle movement, it can reduce the ability of turtles to disperse in the desired direction. Therefore, considering all these factors together, the probability to disperse through locks in the aquatic landscape can be low, especially where there is a close succession of locks.

The weaker effect of locks when we analysed the northern and southern clusters separately suggests an important role for the series of six locks on the overall genetic effect of locks we observed in the system. In the southern cluster, we were unable to distinguish the effect of locks from that of other landscape features, while in the northern cluster the best predictor of genetic structure was the historical features. In addition, the northern section of the canal contains the longest continuous section without locks (41 km without locks in the 69 km of the northern section; mean across the canal = 8 km), suggesting again that numerous locks in proximity impede more gene flow compared to distanced locks.

*What can be done to maintain gene flow in the system?*

Given the low genetic differentiation and the homogenous genetic diversity observed in painted

turtles in the Rideau Canal, turtles in this system appear resilient to the effects of locks. The detection of two genetic clusters within the canal, however, calls to consider conservation and management actions to maintain aquatic connectivity between the southern and the northern clusters and to ensure the maintenance of gene flow. Increased connectivity could be achieved by modifying the structure or operation of the locks between sites RR7 and RR8. For example, building wildlife passages adapted for turtles (e.g., curved concrete ramp with a variety of textures: logs, rocks, and heterogeneous aquatic vegetation, resting pools along the ramp with refuges, low water flow and limited vertical drop, as it was designed for the Gympie weir biopassage, Australia; see Sutherland, 2017) on the lands around the locks and changing the timing of lock operations (e.g., leave lock valves or doors opened as often as possible) could facilitate turtle dispersal and, thus, increase gene flow. The positive impact of any potential change to canal management on turtle movement, however, needs to be carefully weighed against the increased risk of invasion by non-native species (Lin et al., 2020), such as the red-eared slider (*Trachemys scripta*) already detected in southeastern Ontario (Seburn, 2015; Spear et al., 2018).

**Conclusion**

Overall, our study showed that locks are partly permeable to gene flow between painted turtle populations and can lead to genetic discontinuities where they are numerous and in proximity. Therefore, the effect of locks on the genetic integrity of aquatic species should be considered in conservation management plans. To our knowledge, our study is the first in the Rideau Canal, or any other similar canal system, to show how the construction of a canal can influence the genetic structure of a freshwater turtle. There is a need for additional studies on other aquatic species in the Rideau Canal and comparable canal systems, such as the Trent-Severn Waterway (386 km; connecting Lake Ontario to Georgian Bay in Canada; see Bennett et al. (2010) for a partial study) and the Erie Canal (843 km;

connecting Lake Erie to Hudson River in the USA) for a more comprehensive understanding of the long-term effects of artificial waterways on the connectivity between populations of long-lived freshwater species.

## Data availability

All R codes used for this study are available in the Zenodo Digital Repository: https://doi.org/10.5281/zenodo.5826150

# Tables

**Table 3-1** Population genetic statistics for each of the 22 sampling sites (Site) of the Rideau Canal, Canada: Number of painted turtles sampled (N), the number of private alleles ($P_A$), observed heterozygosity ($H_O$), expected heterozygosity ($H_E$), allelic richness ($A_R$) and inbreeding coefficient ($F_{IS}$) averaged over all loci with 95% confidence intervals [95% CI]. Mean value $\pm$ SE for overall $P_A$, $A_R$, $H_O$, $H_E$. *Sites used for the hierarchical AMOVA

| Site | Sampling year | N | $P_A$ | $A_R$ [95% CI] | $H_O$ | $H_E$ | $F_{IS}$ [95% CI] |
|---|---|---|---|---|---|---|---|
| RR1* | 2019 and 2020 | 27 | 2 | 8.15 [7.23 – 8.92] | 0.721 | 0.737 | 0.026 [-0.071 – 0.089] |
| RR2 | 2020 | 29 | 2 | 8.89 [8.00 – 9.69] | 0.759 | 0.745 | 0.002 [-0.076 – 0.045] |
| RR3* | 2019 and 2020 | 33 | 1 | 9.20 [8.23 – 10.08] | 0.774 | 0.752 | -0.044 [-0.106 – -0.014] |
| RR4 | 2019 | 32 | 2 | 8.86 [8.00 – 9.62] | 0.765 | 0.736 | -0.042 [-0.108 – -0.008] |
| RR5 | 2019 | 43 | 0 | 9.19 [8.39 – 9.92] | 0.719 | 0.74 | 0.017 [-0.040 – 0.051] |
| RR6* | 2019 and 2020 | 60 | 2 | 9.56 [8.69 – 10.39] | 0.765 | 0.75 | -0.029 [-0.068 – -0.006] |
| RR7* | 2019 and 2020 | 54 | 1 | 9.45 [8.54 – 10.31] | 0.719 | 0.739 | 0.014 [-0.031 – 0.041] |
| **Northern cluster** | – | 278 | 12 | 16.65 [16.15 – 17.08] | 0.745 | 0.756 | 0.008 [-0.012 – 0.024] |
| RR8 | 2019 | 35 | 0 | 9.43 [8.46 – 10.31] | 0.731 | 0.757 | 0.029 [-0.043 – 0.074] |
| RR9* | 2019 and 2020 | 34 | 0 | 8.87 [7.92 – 9.69] | 0.726 | 0.745 | 0.03 [-0.034 – 0.063] |
| RR10 | 2019 | 31 | 0 | 8.86 [7.92 – 9.69] | 0.759 | 0.744 | -0.028 [-0.094 – 0.004] |
| LR1 | 2019 | 47 | 2 | 9.48 [8.54 – 10.31] | 0.738 | 0.733 | -0.019 [-0.066 – 0.008] |
| BR1* | 2019 and 2020 | 54 | 1 | 9.18 [8.23 – 10.00] | 0.712 | 0.727 | 0.024 [-0.029 – 0.059] |
| BR2 | 2020 | 25 | 0 | 8.79 [7.85 – 9.62] | 0.711 | 0.739 | 0.077 [-0.045 – 0.126] |
| UP6 | 2018 and 2019 | 48 | 1 | 9.57 [8.54 – 10.46] | 0.759 | 0.761 | -0.009 [-0.061 – 0.023] |
| NB3 | 2018 | 36 | 4 | 9.35 [8.31 – 10.31] | 0.718 | 0.744 | 0.029 [-0.043 – 0.076] |
| CL2 | 2018 and 2020 | 43 | 3 | 9.65 [8.69 – 10.54] | 0.744 | 0.745 | -0.014 [-0.071 – 0.022] |
| CL3 | 2018 | 22 | 3 | 8.22 [7.31 – 9.00] | 0.721 | 0.728 | 0.006 [-0.085 – 0.046] |
| SA1 | 2018 and 2019 | 27 | 1 | 9.15 [8.15 – 10.08] | 0.707 | 0.713 | 0.000 [-0.062 – 0.029] |
| WF1* | 2019 and 2020 | 35 | 3 | 8.70 [7.69 – 9.62] | 0.716 | 0.721 | 0.006 [-0.058 – 0.043] |
| C1* | 2019 and 2020 | 26 | 2 | 8.98 [8.08 – 9.77] | 0.751 | 0.759 | 0.008 [-0.071 – 0.048] |
| RS1* | 2019 and 2020 | 29 | 2 | 8.88 [8.00 – 9.69] | 0.772 | 0.741 | -0.058 [-0.121 – -0.025] |
| CB1* | 2019 and 2020 | 52 | 4 | 9.44 [8.54 – 10.23] | 0.75 | 0.752 | -0.003 [-0.056 – 0.029] |
| **Southern cluster** | – | 544 | 50 | 18.37 [17.37 – 19.00] | 0.735 | 0.755 | 0.021 [0.007 – 0.033] |
| **Overall** | 2018 to 2020 | 822 | 1.63 ± 0.27 | 9.08 ± 0.09 | 0.738 ± 0.005 | 0.741 ± 0.003 | 0.018 [0.009 – 0.027] |

**Table 3-2** Summary statistics for the best MLPE (maximum likelihood population effect) models selected for each section of the Rideau Canal: the entire system, northern cluster (RR1, RR2, RR3, RR4, RR5, RR6, RR7), southern cluster (RR8, RR9, RR10, LR1, BR1, BR2, UP6, NB3, CL2, CL3, SA1, WF1, C1, RS1, CB1). In these models, pairwise $F_{ST}$ values were used as a response matrix and different landscape features as predictor matrices. For each model, we provide the estimates, the standard error (SE), t value, and 95% confidence intervals [95% CI]

| Variables | Estimate | SE | t value | 95% CI |
|---|---|---|---|---|
| **Entire system** | | | | |
| Number of locks | 0.000226 | 0.000026 | 8.85 | [0.000176 – 0.000277] |
| | | | | |
| **Northern cluster** | | | | |
| Historical features | 0.000334 | 0.000042 | 7.97 | [0.000252 – 0.000427] |
| | | | | |
| **Southern cluster** | | | | |
| Number of locks | 0.000218 | 0.000067 | 3.23 | [0.000086 – 0.000350] |
| Historical features | 0.000011 | 0.000004 | 3.13 | [0.000004 – 0.000018] |
| Geographic distance | 0.000884 | 0.000306 | 2.89 | [0.000284 – 0.001483] |
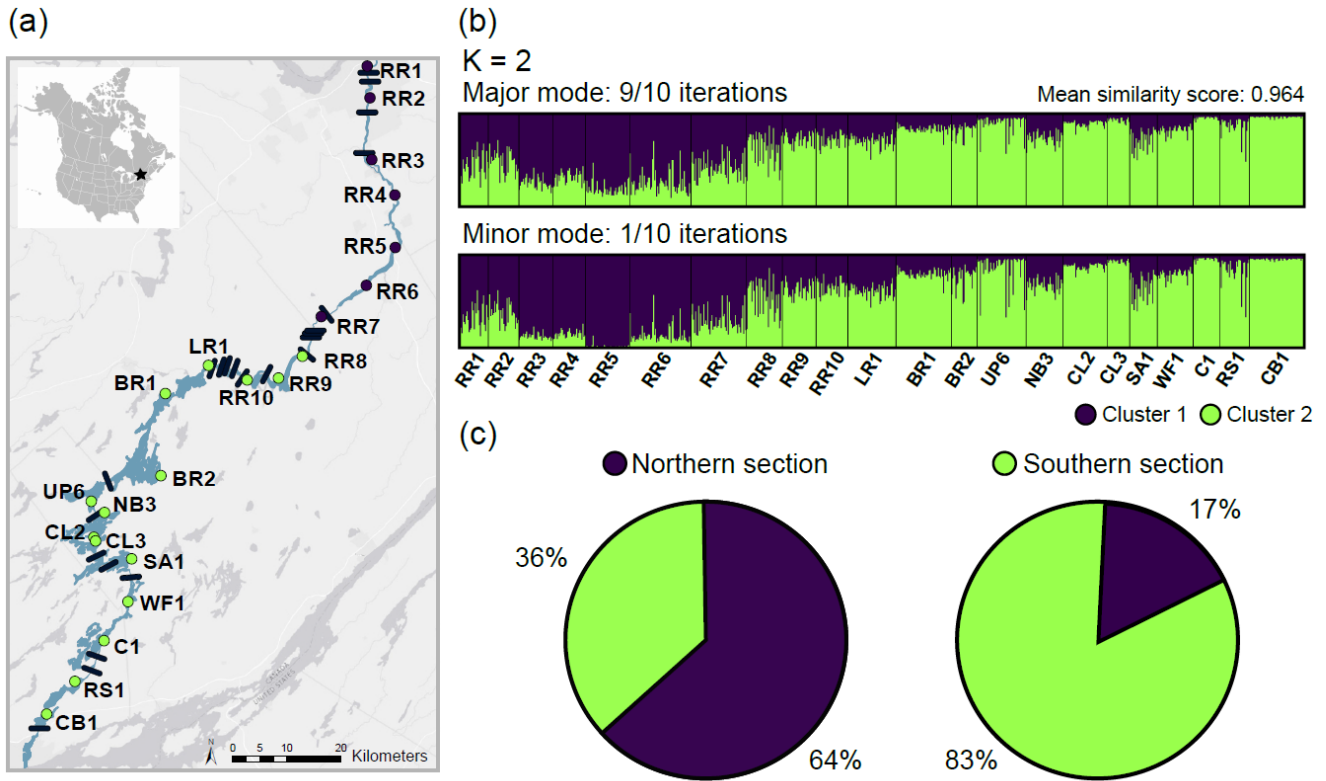
**Figure 3-1** (a) Map of the Rideau Canal, Ontario, Canada and the 22 sites (dots) sampled from 2018 to 2020: Dark dots (purple) represent the sampling sites of the northern cluster, light dots (green) represent the sampling sites of the southern cluster. Solid bars (dark blue) along the waterway indicate the location of the lockstations. The map was built using ArcGIS® software by Esri (www.esri.com). (b) Major and minor modes obtained from STRUCTURE analyses using K = 2 with the LOCPRIOR function for 822 painted turtles (*Chrysemys picta*) sampled throughout the canal. Vertical lines show the proportional membership for individuals to each cluster. Figures were generated with CLUMPAK (Kopelman et al., 2015). (c) Percentage of membership to each cluster identified by STRUCTURE for each section of the canal, based on cluster assignment of individuals

195
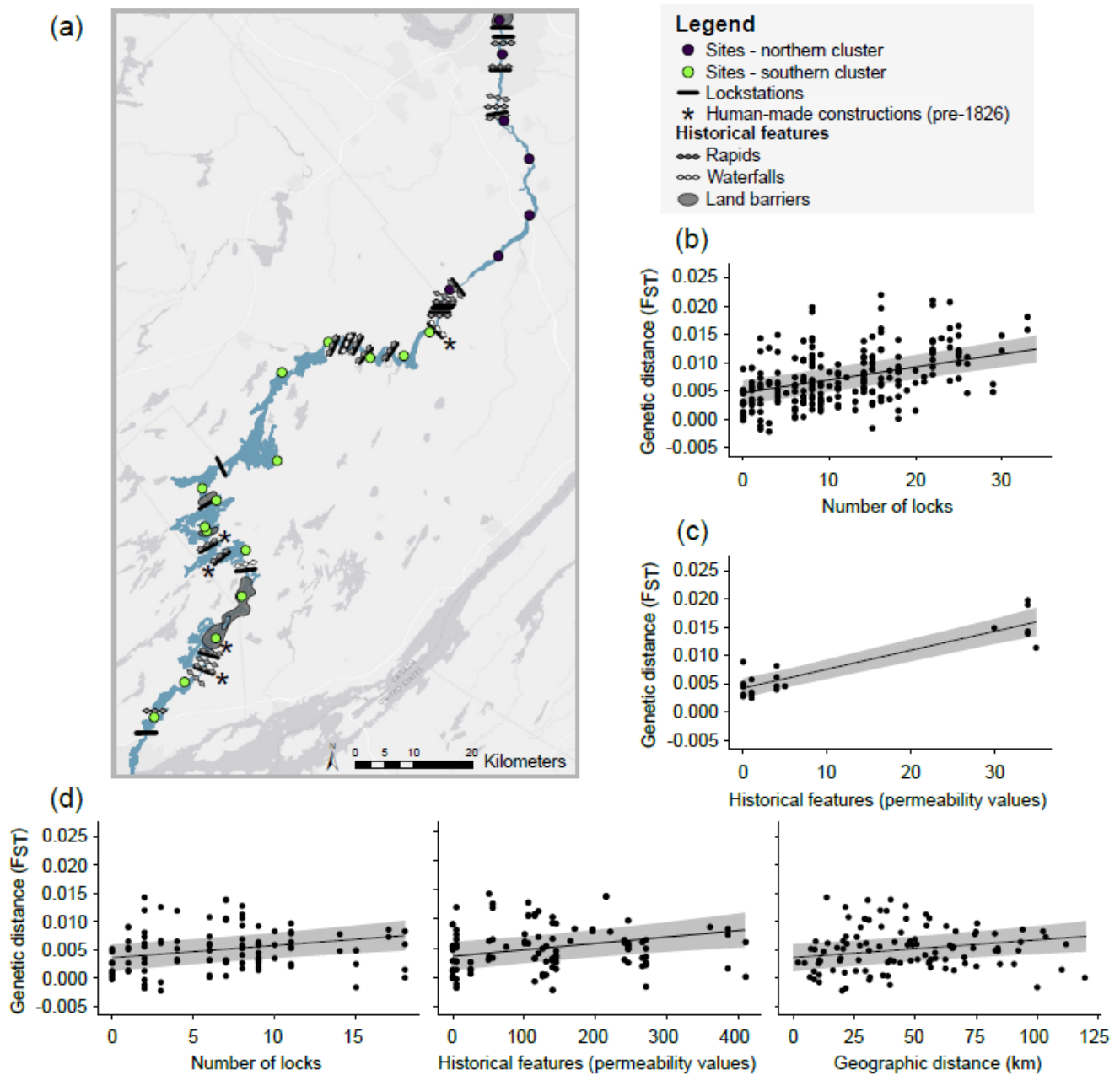
**Figure 3-2** (a) Map of the Rideau Canal, Ontario, Canada with the locations of lockstations (solid black bars), human-made constructions prior to Rideau Canal construction (e.g., mill dams; asterisks), and historical features (rapids: gray diamond bars; waterfalls: white diamond bars; land barriers: gray zones) in relation to sampling sites (dots). Dark dots (purple) represent the sampling sites from the northern cluster, light dots (green) represent the sampling sites from the southern cluster. (b-d) Relationship

between the genetic distance (pairwise $F_{ST}$) and landscape features in painted turtles (*Chrysemys picta*) from the best selected MLPE (maximum likelihood population effect) models of each section of the Rideau Canal: (b) entire system, (c) northern cluster, (d) southern cluster. Black dots are observed genetic distances. Grey areas represent the 95% confidence intervals of predictions (black line)

# Supplementary information for Chapter 3

*Supporting Information 1 – Table S3-1 to S3-15*

**Table S3-1** Microsatellite characteristics of the 15 microsatellite loci used for painted turtle population genetic analyses: Number of painted turtles genotyped per microsatellite (N), number of alleles identified (No. of alleles), fluorescent dye used, repeat structure of the locus, primer sequence, size range in number of base pairs (bp), annealing temperature of the PCR cycling protocol ($T_a$), expected heterozygosity ($H_E$), observed heterozygosity ($H_O$), access number to Genebank, and the reference to the original paper. Overall values of No. of alleles, $H_E$ and $H_O$ represent mean ± standard error. Loci were divided in 3 multiplexes for analysis. *microsatellite removed from final analysis

| Locus | N | No. of alleles | Fluorescent dye | Repeat structure | Primer sequence (5' to 3') | Size range (bp) | $T_a$ (°C) | $H_E$ | $H_O$ | No. Genebank | Reference |
|---|---|---|---|---|---|---|---|---|---|---|---|
| **MPX1** | | | | | | | | | | | |
| CP3 | 819 | 25 | FAM | Dinucleotide | ATCTTTAAGTCTGTGAACTTCAGGG CTGTCTCATGCAAAGCTGGTAG | 129-192 | 52 | 0.65 | 0.83 | — | Pearse et al., 2001 |
| CpGT124* | 807 | 54 | VIC | $(GT)_{31}(GC)_5$ | TCGGGGAGCACACTATACC CTCAGCCCCAAAATGAAC | 152-242 | 59-51 | 0.92 | 0.90 | GQ902944 | da Silva et al., 2010 |
| TerpSH3 | 820 | 17 | FAM | $(CAAA)_{14}$ | TCCCCCAATGCACAC CTGCCCAATCCATTTAGA | 164-313 | 59-51 | 0.84 | 0.78 | AY156711 | Hauswaldt & Glenn, 2003 |
| TerpSH2 | 821 | 26 | PET | $(AGAT)_{12}$ | TGGCCAGCAGGAGTAATG CTATTAGGGCAGAGACGAG | 135-233 | 59-51 | 0.91 | 0.89 | AY156710 | Hauswaldt & Glenn, 2003 |
| TerpSH5 | 822 | 26 | NED | $(CTAT)_{12}$ | TTGCTGCTATATGCTTAAT CCTCCCTGCCTATTGA | 129-210 | 59-51 | 0.91 | 0.83 | AY156713 | Hauswaldt & Glenn, 2003 |
| **MPX2** | | | | | | | | | | | |
| GmuD21 | 822 | 15 | FAM | $(ATCT)_{15}$ | GCAGTTAGGCATTACTCAACATC AGGGTATGAATACAGGGGTGTC | 139-204 | 58 | 0.65 | 0.65 | AF517236 | King & Julian, 2004 |
| GmuD79 | 820 | 18 | PET | $(ATCT)_{10}$ | GCCCTGTTCCATTCTTATTCTG ATCCCCTTAGTCGTCTCTTTTC | 165-217 | 58 | 0.90 | 0.90 | AF517243 | King & Julian, 2004 |
| GmuD87* | 810 | 27 | NED | $(ATCT)_{22}$ | AAACCCTAAGACATCAGACAGG CAAATCCAGTACCCAGAAAGTC | 207-298 | 58 | 0.93 | 0.74 | AF517244 | King & Julian, 2004 |
| GmuD70 | 820 | 71 | VIC | $(ATCT)_8$ | AGTGTAGTCATGGCATAGAGAGG ATCAAATTCTTCCAACCCTACC | 170-488 | 58 | 0.97 | 0.93 | AF517242 | King & Julian, 2004 |
| BTGA3 | 820 | 9 | VIC | $(GA)_{11}$ | CCTAGATTTTGTCTGGCTATTA TATCTCAGTAATAATCCCCTTAG | 98-116 | 48 | 0.76 | 0.75 | AY335792 | Libants et al., 2004 |

| | | | | | MPX3 | | | | | | | |
|---|---|---|---|---|---|---|---|---|---|---|---|---|
| BTCA5 | 821 | 3 | FAM | $(GA)_{11}$ | GCTGCTTAGCACAACTCATAA CTTTTGTATTTAATCCATGATGAA | 134-138 | 46 | 0.38 | 0.38 | AY335788 | Libants et al., 2004 |
| CP2 | 820 | 23 | FAM | Dinucleotide | CTCTAAGGGTTGCACTTCTCAAA GAGGTGGCATCAAAACATCAT | 171-248 | 52 | 0.86 | 0.83 | — | Pearse et al., 2001 |
| BTCA9 | 819 | 4 | VIC | $(CA)_9$ | TACTCAAGATTTGAAGCAGATACA GGCTTGATTCTACTGTCACTTAC | 132-145 | 46 | 0.27 | 0.28 | AY335790 | Libants et al., 2004 |
| BTCA7 | 820 | 7 | PET | $(CA)_{12}$ | TGGAATTAGATGTTTTGCAGTT TCATTTCTGTTTTCCACACTG | 148-170 | 48 | 0.71 | 0.72 | AY335789 | Libants et al., 2004 |
| CpGT108 | 820 | 36 | VIC | $(CA)_4CT(CA)_{11}$ | CCTAGAAAGTAAGAACCAATTTCAG CCACCAACAGAAGGAAGTTAGTG | 200-290 | 59-51 | 0.85 | 0.83 | GQ902943 | da Silva et al., 2010 |
| Overall | — | 21.5±4.9 | — | — | — | — | — | 0.75±0.06 | 0.73±0.05 | — | — |

200

**Table S3-2** PCR components and protocol reactions of the 15 microsatellite loci used for painted turtle population genetic analyses. ABI: Applied Biosystems. BSA: Albumin bovine serum

| | | MPX1 | | | | | | | | | |
| --- | --- | --- | --- | --- | --- | --- | --- | --- | --- | --- | --- |
| | | CP3 | | TerpSH2 | | TerpSH3 | | CpGT124 | | TerpSH5 | |
| Components | Stock solution concentration | per reaction | for 10 µl | per reaction | for 10 µl | per reaction | for 10 µl | per reaction | for 10 µl | per reaction | for 10 µl |
| $H_2O$dd | — | — | 4.7 µl | — | 4.44 µl | — | 4.41 µl | — | 2.71 µl | — | 4.49 µl |
| $MgCl_2$ ABI | 25 mM | 1.5 mM | 0.6 µl | 2 mM | 0.8 µl | 2 mM | 0.8 µl | 2.5 mM | 1 µl | 2 mM | 0.8 µl |
| dNTPs | 1 mM | 0.1 mM | 1 µl | 0.15 mM | 1.5 µl | 0.15 mM | 1.5 µl | 0.2 mM | 2 µl | 0.15 mM | 1.5 µl |
| Gold Buffer ABI | 10X (150 mM Tris HCl; 500 mM KCl) | 1X | 1 µl | 1X | 1 µl | 1X | 1 µl | 1X | 1 µl | 1X | 1 µl |
| BSA | 8 mg/ml | 0.4 mg/ml | 0.5 µl | 0.2 mg/ml | 0.25 µl | 0.2 mg/ml | 0.25 µl | 0.4 mg/ml | 0.5 µl | 0.2 mg/ml | 0.25 µl |
| R primer | 10 mM | 0.5 mM | 0.5 µl | 0.4 mM | 0.4 µl | 0.4 mM | 0.4 µl | 0.8 mM | 0.8 µl | 0.4 mM | 0.4 µl |
| F primer | 10 mM | 0.5 mM | 0.5 µl | 0.4 mM | 0.4 µl | 0.4 mM | 0.4 µl | 0.8 mM | 0.8 µl | 0.4 mM | 0.4 µl |
| Taq ABI | 5 U/µl | 0.1 U/µl | 0.2 µl | 0.105 U/µl | 0.21 µl | 0.12 U/µl | 0.24 µl | 0.095 U/µl | 0.19 µl | 0.08 U/µl | 0.16 µl |
| ADN | 10 ng/µl | 10 ng | 1 µl | 10 ng | 1 µl | 10 ng | 1 µl | 10 ng | 1 µl | 10 ng | 1 µl |

| | | MPX2 | | | | | | | | | |
| --- | --- | --- | --- | --- | --- | --- | --- | --- | --- | --- | --- |
| | | BTGA3 | | GmuD21 | | GmuD79 | | GmuD70 | | GmuD87 | |
| Components | Stock solution concentration | per reaction | for 10 µl | per reaction | for 10 µl | per reaction | for 10 µl | per reaction | for 10 µl | per reaction | for 10 µl |
| $H_2O$dd | — | — | 4.03 µl | — | 3.1 µl | — | 3.1 µl | — | 3.1 µl | — | 3.1 µl |
| $MgCl_2$ ABI | 25 mM | 2.5 mM | 1 µl | 2 mM | 0.8 µl | 2 mM | 0.8 µl | 2 mM | 0.8 µl | 2 mM | 0.8 µl |
| dNTPs | 1 mM | 0.16 mM | 1.6 µl | 0.25 mM | 2.5 µl | 0.25 mM | 2.5 µl | 0.25 mM | 2.5 µl | 0.25 mM | 2.5 µl |
| Gold Buffer ABI | 10X (150 mM Tris HCl; 500 mM KCl) | 1X | 1 µl | 1X | 1 µl | 1X | 1 µl | 1X | 1 µl | 1X | 1 µl |
| BSA | 8 mg/ml | 0.2 mg/ml | 0.25 µl | 0.4 mg/ml | 0.5 µl | 0.4 mg/ml | 0.5 µl | 0.4 mg/ml | 0.5 µl | 0.4 mg/ml | 0.5 µl |
| R primer | 10 mM | 0.5 mM | 0.5 µl | 0.5 mM | 0.5 µl | 0.5 mM | 0.5 µl | 0.5 mM | 0.5 µl | 0.5 mM | 0.5 µl |
| F primer | 10 mM | 0.5 mM | 0.5 µl | 0.5 mM | 0.5 µl | 0.5 mM | 0.5 µl | 0.5 mM | 0.5 µl | 0.5 mM | 0.5 µl |
| Taq ABI | 5 U/µl | 0.06 U/µl | 0.12 µl | 0.05 U/µl | 0.1 µl | 0.05 U/µl | 0.1 µl | 0.05 U/µl | 0.1 µl | 0.05 U/µl | 0.1 µl |
| ADN | 10 ng/µl | 10 ng | 1 µl | 10 ng | 1 µl | 10 ng | 1 µl | 10 ng | 1 µl | 10 ng | 1 µl |

| Components | Stock solution concentration | MPX3 | | | | | | | | | |
|---|---|---|---|---|---|---|---|---|---|---|---|
| | | BTCA5 | | BTCA7 | | CpGT108 | | BTCA9 | | CP2 | |
| | | per reaction | for 10 μl | per reaction | for 10 μl | per reaction | for 10 μl | per reaction | for 10 μl | per reaction | for 10 μl |
| $H_2Odd$ | — | — | 4 μl | — | 3.97 μl | — | 2.7 μl | — | 4 μl | — | 4.6 μl |
| $MgCl_2$ ABI | 25 mM | 2.5 mM | 1 μl | 2.5 mM | 1 μl | 2.5 mM | 1 μl | 2.5 mM | 1 μl | 1.5 mM | 0.6 μl |
| dNTPs | 1 mM | 0.16 mM | 1.6 μl | 0.16 mM | 1.6 μl | 0.2 mM | 2 μl | 0.16 mM | 1.6 μl | 0.1 mM | 1 μl |
| Gold Buffer ABI | 10X (150 mM Tris HCl; 500 mM KCl) | 1X | 1 μl | 1X | 1 μl | 1X | 1 μl | 1X | 1 μl | 1X | 1 μl |
| BSA | 8 mg/ml | 0.2 mg/ml | 0.25 μl | 0.2 mg/ml | 0.25 μl | 0.4 mg/ml | 0.5 μl | 0.2 mg/ml | 0.25 μl | 0.4 mg/ml | 0.5 μl |
| R primer | 10 mM | 0.5 mM | 0.5 μl | 0.5 mM | 0.5 μl | 0.8 mM | 0.8 μl | 0.5 mM | 0.5 μl | 0.5 mM | 0.5 μl |
| F primer | 10 mM | 0.5 mM | 0.5 μl | 0.5 mM | 0.5 μl | 0.8 mM | 0.8 μl | 0.5 mM | 0.5 μl | 0.5 mM | 0.5 μl |
| Taq ABI | 5 U/μl | 0.075 U/μl | 0.15 μl | 0.09 U/μl | 0.18 μl | 0.1 U/μl | 0.2 μl | 0.075 U/μl | 0.15 μl | 0.15 U/μl | 0.3 μl |
| ADN | 10 ng/μl | 10 ng | 1 μl | 10 ng | 1 μl | 10 ng | 1 μl | 10 ng | 1 μl | 10 ng | 1 μl |

**Table S3-3** PCR cycling protocol of the 15 microsatellite loci used for painted turtle population genetic analyses. The PCR cycling protocol for TerpSH2, TerpSH3 and TerpSH5 is a touchdown PCR protocol where there are several steps of cycles with different annealing temperatures

| Locus | Temperature and Time | | | | |
|---|---|---|---|---|---|
| **GmuD21, GmuD79, GmuD70, GmuD87** | Denaturation | **35 cycles** | | | Extension |
| | | Denaturation | Annealing | Extension | |
| | 2 min at 94°C | 45 s at 94°C | 45 s at 58°C | 1.5 min at 72°C | 5 min at 72 °C |
| **CP2, CP3** | Denaturation | **30 cycles** | | | Extension |
| | | Denaturation | Annealing | Extension | |
| | 2 min at 94°C | 50 s at 94°C | 50 s at 52°C | 50 s at 72°C | — |
| **CpGT108, CpGT124** | Denaturation | **30 cycles** | | | Extension |
| | | Denaturation | Annealing | Extension | |
| | 10 min at 95°C | 30 s at 95°C | 30 s at [59-51°C] decrease by 1°C per cycle and the remaining cycles at 51°C | 1 min at 72°C | 1 min at 72°C |
| **BTCA5, BTCA9** | Denaturation | **30 cycles** | | | Extension |
| | | Denaturation | Annealing | Extension | |
| | 2 min at 94°C | 1 min at 94°C | 1 min at 46°C | 1 min at 72°C | — |
| **BTCA7, BTGA3** | Denaturation | **30 cycles** | | | Extension |
| | | Denaturation | Annealing | Extension | |
| | 2 min at 94°C | 1 min at 94°C | 1 min at 48°C | 1 min at 72°C | — |
| **TerpSH2, TerpSH3, TerpSH5** | Denaturation | **Step 1: 5 cycles** | | | Extension |
| | | Denaturation | Annealing | Extension | |
| | | 20 s at 96°C | 30 s at 60°C | 1 min at 72°C | |
| | — | **Step 2: 30 cycles** | | | — |

203

| Denaturation | Annealing | Extension |
|---|---|---|
| 30 s at 96°C | 30 s at 60°C decrease by 0.5 °C per cycle | 1 min at 72°C |
| **Step 3: 10 cycles** | | |
| Denaturation | Annealing | Extension |
| 30 s at 96°C | 30 s at 50.5°C | 1 min at 72°C |
| **Step 4: 20 cycles** | | |
| Denaturation | Annealing | Extension |
| 30 s at 96°C | 30 s at 50°C | 1 min at 72°C |

**Table S3-4** Model selection summary with information criteria metrics of MLPE models using genetic distance ($F_{ST}$) as response variable and different landscape features as predictors for three different sections of the canal: Entire system, northern cluster and southern cluster. Four landscape features that were calculated between each pair of sampling sites were used in these models: 1) the shortest aquatic distance (Geo), 2) the number of locks (Lock), 3) the number of human-made constructions (e.g., mill dams) between 1783 (i.e., beginning of European settlement in the Rideau region) and 1826 (i.e., official beginning of Rideau Canal construction) (Post1783), and 4) the historical features (i.e., waterfalls, rapids and land barriers) previously located on the current path of the canal before any human-made alterations were made on the original landscape (Hist; codes in Supporting Information 2 of Chapter 3). *Top models ($\Delta$AICc < 2)

| Landscape features | k | AIC | AICc | ΔAICc |
|---|---|---|---|---|
| Entire system | | | | |
| Lock* | 4 | -2015.65 | -2014.72 | 0 |
| Lock + Post1783 | 5 | -2013.89 | -2012.46 | 2.26 |
| Hist 8 | 4 | -2013.29 | -2012.36 | 2.36 |
| Hist 8 + Post1783 | 5 | -2011.66 | -2010.23 | 4.49 |
| Geo | 4 | -2002.4 | -2001.47 | 13.25 |
| Geo + Post1783 | 5 | -2000.91 | -1999.48 | 15.24 |
| Post1783 | 4 | -1978.5 | -1977.57 | 37.15 |
| Null | 3 | -1949.84 | -1949.29 | 65.43 |
| Northern cluster | | | | |
| Hist 6* | 4 | -189.31 | -188.38 | 0 |
| Hist 7* | 4 | -188.91 | -187.98 | 0.40 |
| Lock | 4 | -174.17 | -173.24 | 15.13 |
| Null | 3 | -171.91 | -171.36 | 17.01 |
| Hist 8 | 4 | -171.90 | -170.97 | 17.40 |
| Geo | 4 | -169.98 | -169.05 | 19.32 |
| Southern cluster | | | | |
| Lock* | 4 | -911.15 | -910.22 | 0 |
| Hist 8* | 4 | -910.26 | -909.33 | 0.90 |
| Hist 7* | 4 | -910.09 | -909.16 | 1.06 |
| Hist 3* | 4 | -909.99 | -909.06 | 1.17 |
| Geo* | 4 | -909.26 | -908.33 | 1.90 |
| Lock + Post1783 | 5 | -909.38 | -907.96 | 2.27 |
| Hist 3 + Post1783 | 5 | -908.98 | -907.55 | 2.68 |
| Hist 8 + Post1783 | 5 | -908.88 | -907.45 | 2.78 |
| Hist 7 + Post1783 | 5 | -908.72 | -907.30 | 2.93 |
| Geo + Post1783 | 5 | -907.30 | -905.87 | 4.36 |
| Post1783 | 4 | -905.10 | -904.19 | 6.03 |
| null | 3 | -903.62 | -903.07 | 7.15 |

**Table S3-5** Pearson coefficient correlations between 1) landscape features and 2) different combinations of resistance values for historical landscape features for the entire system. For the landscape features table, Hist 4 was used for historical features (see Supporting Information 2 of Chapter 3)

1) Landscape features

| | Historical features | Construction 1783-1826 | Geographic distance |
|---|---|---|---|
| Number of locks | 0.99 | 0.64 | 0.95 |
| Historical features | — | 0.69 | 0.93 |
| Construction 1783-1826 | — | — | 0.62 |

2) Historical landscape features (see Supporting Information 2 of Chapter 3 for the codes)

| | Binary additive | Hist 1 | Hist 2 | Hist 3 | Hist 4 | Hist 5 | Hist 6 | Hist 7 | Hist 8 | Hist 9 |
|---|---|---|---|---|---|---|---|---|---|---|
| Binary | 0.39 | 0.38 | 0.32 | 0.37 | 0.38 | 0.38 | 0.30 | 0.35 | 0.38 | 0.38 |
| Binary additive | — | 0.99 | 0.89 | 0.97 | 0.96 | 0.94 | 0.85 | 0.94 | 0.97 | 0.96 |
| Hist 1 | — | — | 0.88 | 0.96 | 0.97 | 0.97 | 0.85 | 0.94 | 0.98 | 0.98 |
| Hist 2 | — | — | — | 0.95 | 0.75 | 0.73 | 1 | 0.97 | 0.78 | 0.77 |
| Hist 3 | — | — | — | — | 0.91 | 0.88 | 0.93 | 0.99 | 0.92 | 0.91 |
| Hist 4 | — | — | — | — | — | 0.99 | 0.71 | 0.87 | 1 | 1 |
| Hist 5 | — | — | — | — | — | — | 0.69 | 0.83 | 0.99 | 1 |
| Hist 6 | — | — | — | — | — | — | — | 0.96 | 0.75 | 0.74 |
| Hist 7 | — | — | — | — | — | — | — | — | 0.88 | 0.87 |
| Hist 8 | — | — | — | — | — | — | — | — | — | 1 |

**Table S3-6** Model selection with information criteria metrics of MLPE models using genetic distance (pairwise $G_{ST}$ values) as response variable and different landscape features as predictors for three different sections of the canal: Entire system, northern cluster and southern cluster. Four landscape features that were calculated between each pair of sampling sites were used in these models: 1) the shortest aquatic distance (Geo), 2) the number of locks (Lock), 3) the number of human-made constructions (e.g., mill dams) between 1783 (i.e., beginning of European settlement in the Rideau region) and 1826 (i.e., official beginning of Rideau Canal construction) (Post1783), and 4) the historical features (i.e., waterfalls, rapids and land barriers) previously located on the current path of the canal before any human-made alterations were made on the original landscape (Hist; see Supporting Information 2 of Chapter 3 for the codes). Summary statistics available for the best MLPE models ($\Delta$AICc < 2)

| Models | Estimate | 95% CI | k | AIC | AICc | ΔAICc |
|---|---|---|---|---|---|---|
| | | Entire system | | | | |
| Lock* | 0.0008 | 0.0006 — 0.001 | 4 | -1432.24 | -1431.31 | 0 |
| Lock + Post1783 | — | — | 5 | -1430.54 | -1429.11 | 2.20 |
| Hist 8 | — | — | 4 | -1429.62 | -1428.69 | 2.62 |
| Hist 8 + Post1783 | — | — | 5 | -1428.04 | -1426.61 | 4.70 |
| Geo | — | — | 4 | -1419.25 | -1418.32 | 13.00 |
| Geo + Post1783 | — | — | 5 | -1417.67 | -1416.24 | 15.07 |
| Post1783 | — | — | 4 | -1394.46 | -1393.53 | 37.79 |
| Null | — | — | 3 | -1365.93 | -1365.38 | 65.93 |
| | | Northern section | | | | |
| Hist 6* | 0.0012 | 0.0009 — 0.0015 | 4 | -135.27 | -134.34 | 0 |
| Hist 7* | 0.0014 | 0.0011— 0.0018 | 4 | -134.88 | -133.95 | 0.40 |
| Lock | — | — | 4 | -119.45 | -118.52 | 15.83 |
| Null | — | — | 3 | -117.31 | -116.76 | 17.58 |
| Hist8 | — | — | 4 | -117.13 | -116.20 | 18.15 |
| Geo | — | — | 4 | -115.42 | -114.49 | 19.86 |
| | | Southern section | | | | |
| Lock* | 0.0007 | 0.0003 — 0.001 | 4 | -648.88 | -647.95 | 0 |
| Hist 8* | 0.00003 | 0.00001 — 0.00006 | 4 | -647.71 | -646.78 | 1.17 |
| Hist 7* | 0.00006 | 0.00002 — 0.0001 | 4 | -647.61 | -646.68 | 1.26 |
| Hist 3* | 0.0002 | 0.00007 — 0.0003 | 4 | -647.51 | -646.58 | 1.37 |
| Geo* | 0.003 | 0.001 — 0.005 | 4 | -647.14 | -646.21 | 1.74 |
| Lock + Post1783 | — | — | 5 | -647.26 | -645.83 | 2.12 |
| Hist 3 + Post1783 | — | — | 5 | -646.83 | -645.40 | 2.55 |
| Hist 8 + Post1783 | — | — | 5 | -646.53 | -645.10 | 2.84 |
| Hist 7 + Post1783 | — | — | 5 | -646.50 | -645.07 | 2.88 |
| Geo + Post1783 | — | — | 5 | -645.14 | -643.71 | 4.24 |
| Post1783 | — | — | 4 | -642.29 | -641.36 | 6.59 |
| Null | — | — | 3 | -641.09 | -640.54 | 7.40 |

**Table S3-7** Genotyping error rate (Error rate) for each locus: number of error (Error number) on the total number of alleles (Total alleles) successfully genotyped

| Locus | Error number | Total alleles | Error rate |
|---|---|---|---|
| GmuD21 | 0 | 76 | 0 |
| GmuD79 | 0 | 76 | 0 |
| GmuD87 | 11 | 76 | 0.14 |
| GmuD70 | 2 | 76 | 0.03 |
| BTGA3 | 1 | 76 | 0.01 |
| BTCA5 | 0 | 76 | 0 |
| CP2 | 4 | 76 | 0.05 |
| BTCA9 | 0 | 76 | 0 |
| BTCA7 | 0 | 76 | 0 |
| CpGT108 | 1 | 76 | 0.01 |
| CP3 | 6 | 76 | 0.08 |
| TerpSH3 | 2 | 76 | 0.03 |
| CpGT124 | 13 | 74 | 0.18 |
| TerpSH2 | 5 | 74 | 0.07 |
| TerpSH5 | 2 | 76 | 0.03 |
| | | Global rate | 0.04 |

**Table S3-8** Observed frequency of null alleles for each locus with the 95% confidence intervals (95% CI). Frequency estimated with the Brookfield (1996) method

| Locus | Observed frequency | 95% CI |
|---|---|---|
| GmuD21 | 0 | [-0.02 — 0.02] |
| GmuD79 | 0 | [-0.01 — 0.01] |
| GmuD87 | 0.11 | [0.09 — 0.13] |
| GmuD70 | 0.02 | [0.01 — 0.03] |
| BGTA3 | 0 | [-0.02 — 0.02] |
| BTCA5 | 0 | [-0.02 — 0.02] |
| CP2 | 0.01 | [0 — 0.03] |
| BTCA9 | -0.01 | [-0.02 — 0.01] |
| BTCA7 | -0.01 | [-0.02 — 0.01] |
| CpGT108 | 0.01 | [0 — 0.03] |
| CP3 | 0 | [-0.01 — 0.02] |
| TerpSH3 | 0.03 | [0.02 — 0.05] |
| CpGT124 | 0.01 | [0 — 0.02] |
| TerpSH2 | 0.01 | [0 — 0.02] |
| TerpSH5 | 0.04 | [0.03 — 0.05] |

**Table S3-9** The significant proportion (according to a $p < 0.05$) of loci out of Hardy-Weinberg equilibrium (HWE) for each population and the proportion of populations out of HWE for each locus based on the chi-squared test statistic (Chisq) and Monte Carlo permutations (MC; 10,000 permutations). BF: significant proportion adjusted with a Bonferroni correction. fdr: significant proportion adjusted with a false discovery rate correction based on Benjamini and Yekutieli (2001)

| | Proportion of loci out of HWE for each population | | | | | | | |
|---|---|---|---|---|---|---|---|---|
| Site | Chisq | MC | Chisq.fdr | MC.fdr | Chisq.BF | MC.BF | Chisq.BF.fdr | MC.BF.fdr |
| BR1 | 0.07 | 0.07 | 0.07 | 0 | 0.07 | 0 | 0.07 | 0 |
| BR2 | 0.20 | 0.20 | 0.13 | 0 | 0 | 0 | 0 | 0 |
| C1 | 0.07 | 0.13 | 0.07 | 0 | 0 | 0 | 0 | 0 |
| CB1 | 0.20 | 0.27 | 0.13 | 0.07 | 0.13 | 0 | 0.13 | 0 |
| CL2 | 0.13 | 0.20 | 0.13 | 0.07 | 0.07 | 0 | 0 | 0 |
| CL3 | 0.20 | 0.07 | 0 | 0 | 0 | 0 | 0 | 0 |
| LR1 | 0.13 | 0.07 | 0.07 | 0.07 | 0 | 0 | 0 | 0 |
| NB3 | 0.33 | 0.13 | 0.27 | 0.07 | 0.07 | 0 | 0 | 0 |
| RR1 | 0.20 | 0.27 | 0.07 | 0.07 | 0 | 0 | 0 | 0 |
| RR10 | 0.07 | 0.13 | 0.07 | 0.07 | 0 | 0.07 | 0 | 0 |
| RR2 | 0.13 | 0.13 | 0.07 | 0.07 | 0 | 0 | 0 | 0 |
| RR3 | 0.20 | 0.13 | 0.13 | 0.07 | 0.07 | 0 | 0 | 0 |
| RR4 | 0.07 | 0.07 | 0.07 | 0 | 0 | 0 | 0 | 0 |
| RR5 | 0.27 | 0.13 | 0.27 | 0.13 | 0.07 | 0.13 | 0.07 | 0.13 |
| RR6 | 0.07 | 0.07 | 0.07 | 0.07 | 0.07 | 0 | 0.07 | 0 |
| RR7 | 0.33 | 0.40 | 0.33 | 0.27 | 0.20 | 0.13 | 0.13 | 0.13 |
| RR8 | 0.20 | 0.13 | 0.07 | 0.13 | 0 | 0 | 0 | 0 |
| RR9 | 0.07 | 0.07 | 0.07 | 0 | 0.07 | 0 | 0 | 0 |
| RS1 | 0.07 | 0.07 | 0.07 | 0 | 0.07 | 0 | 0 | 0 |
| SA1 | 0.07 | 0 | 0 | 0 | 0 | 0 | 0 | 0 |
| UP6 | 0.33 | 0.13 | 0.20 | 0.07 | 0.13 | 0.07 | 0.13 | 0.07 |
| WF1 | 0.13 | 0.07 | 0.07 | 0 | 0.07 | 0 | 0.07 | 0 |

| Proportion of populations out of HWE for each locus | | | | | | | |
|---|---|---|---|---|---|---|---|
| Locus | Chisq | MC | Chisq.fdr | MC.fdr | Chisq.BF | MC.BF | Chisq.BF.fdr | MC.BF.fdr |
| GmuD21 | 0.14 | 0.09 | 0.09 | 0 | 0.09 | 0 | 0.09 | 0 |
| GmuD79 | 0 | 0 | 0 | 0 | 0 | 0 | 0 | 0 |
| GmuD87 | 0.32 | 0.73 | 0.23 | 0.45 | 0.14 | 0.14 | 0.14 | 0.14 |
| GmuD70 | 0.23 | 0.23 | 0.14 | 0.09 | 0.05 | 0 | 0.05 | 0 |
| BGTA3 | 0.18 | 0.14 | 0.06 | 0 | 0.05 | 0 | 0.05 | 0 |
| BTCA5 | 0 | 0 | 0 | 0 | 0 | 0 | 0 | 0 |
| CP2 | 0.23 | 0.14 | 0.18 | 0.06 | 0.09 | 0 | 0.05 | 0 |
| BTCA9 | 0.06 | 0 | 0.06 | 0 | 0 | 0 | 0 | 0 |
| BTCA7 | 0 | 0 | 0 | 0 | 0 | 0 | 0 | 0 |
| CpGT108 | 0.32 | 0 | 0.27 | 0 | 0.05 | 0 | 0 | 0 |
| CP3 | 0.06 | 0.06 | 0 | 0 | 0 | 0 | 0 | 0 |
| TerpSH3 | 0.18 | 0.14 | 0.18 | 0.09 | 0.09 | 0.05 | 0.05 | 0.05 |
| CpGT124 | 0.23 | 0.14 | 0.09 | 0.09 | 0 | 0.05 | 0 | 0.05 |
| TerpSH2 | 0.09 | 0.06 | 0.06 | 0 | 0 | 0 | 0 | 0 |
| TerpSH5 | 0.41 | 0.32 | 0.32 | 0.06 | 0.18 | 0.05 | 0.05 | 0 |

**Table S3-10** Probability of identity (PI) and probability of identity among siblings (PIsibs) according to the number of locus combinations with the 13 remained loci. N = number of individuals sampled per site

| | | | | | | | Probability of identity (PI) | | | | | | | |
|---|---|---|---|---|---|---|---|---|---|---|---|---|---|---|
| Site | N | 1 locus | 2 loci | 3 loci | 4 loci | 5 loci | 6 loci | 7 loci | 8 loci | 9 loci | 10 loci | 11 loci | 12 loci | 13 loci |
| BR1 | 54 | 0.223 | 0.006 | < 0.001 | < 0.001 | < 0.001 | < 0.001 | < 0.001 | < 0.001 | < 0.001 | < 0.001 | < 0.001 | < 0.001 | < 0.001 |
| BR2 | 25 | 0.176 | 0.004 | < 0.001 | < 0.001 | < 0.001 | < 0.001 | < 0.001 | < 0.001 | < 0.001 | < 0.001 | < 0.001 | < 0.001 | < 0.001 |
| C1 | 26 | 0.208 | 0.004 | < 0.001 | < 0.001 | < 0.001 | < 0.001 | < 0.001 | < 0.001 | < 0.001 | < 0.001 | < 0.001 | < 0.001 | < 0.001 |
| CB1 | 52 | 0.208 | 0.004 | < 0.001 | < 0.001 | < 0.001 | < 0.001 | < 0.001 | < 0.001 | < 0.001 | < 0.001 | < 0.001 | < 0.001 | < 0.001 |
| CL2 | 43 | 0.13 | 0.003 | < 0.001 | < 0.001 | < 0.001 | < 0.001 | < 0.001 | < 0.001 | < 0.001 | < 0.001 | < 0.001 | < 0.001 | < 0.001 |
| CL3 | 22 | 0.193 | 0.006 | < 0.001 | < 0.001 | < 0.001 | < 0.001 | < 0.001 | < 0.001 | < 0.001 | < 0.001 | < 0.001 | < 0.001 | < 0.001 |
| LR1 | 47 | 0.178 | 0.004 | < 0.001 | < 0.001 | < 0.001 | < 0.001 | < 0.001 | < 0.001 | < 0.001 | < 0.001 | < 0.001 | < 0.001 | < 0.001 |
| NB3 | 36 | 0.172 | 0.004 | < 0.001 | < 0.001 | < 0.001 | < 0.001 | < 0.001 | < 0.001 | < 0.001 | < 0.001 | < 0.001 | < 0.001 | < 0.001 |
| RR1 | 27 | 0.182 | 0.004 | < 0.001 | < 0.001 | < 0.001 | < 0.001 | < 0.001 | < 0.001 | < 0.001 | < 0.001 | < 0.001 | < 0.001 | < 0.001 |
| RR10 | 31 | 0.250 | 0.007 | < 0.001 | < 0.001 | < 0.001 | < 0.001 | < 0.001 | < 0.001 | < 0.001 | < 0.001 | < 0.001 | < 0.001 | < 0.001 |
| RR2 | 29 | 0.181 | 0.005 | < 0.001 | < 0.001 | < 0.001 | < 0.001 | < 0.001 | < 0.001 | < 0.001 | < 0.001 | < 0.001 | < 0.001 | < 0.001 |
| RR3 | 33 | 0.144 | 0.004 | < 0.001 | < 0.001 | < 0.001 | < 0.001 | < 0.001 | < 0.001 | < 0.001 | < 0.001 | < 0.001 | < 0.001 | < 0.001 |
| RR4 | 32 | 0.221 | 0.007 | < 0.001 | < 0.001 | < 0.001 | < 0.001 | < 0.001 | < 0.001 | < 0.001 | < 0.001 | < 0.001 | < 0.001 | < 0.001 |
| RR5 | 43 | 0.207 | 0.004 | < 0.001 | < 0.001 | < 0.001 | < 0.001 | < 0.001 | < 0.001 | < 0.001 | < 0.001 | < 0.001 | < 0.001 | < 0.001 |
| RR6 | 60 | 0.184 | 0.005 | < 0.001 | < 0.001 | < 0.001 | < 0.001 | < 0.001 | < 0.001 | < 0.001 | < 0.001 | < 0.001 | < 0.001 | < 0.001 |
| RR7 | 54 | 0.176 | 0.005 | < 0.001 | < 0.001 | < 0.001 | < 0.001 | < 0.001 | < 0.001 | < 0.001 | < 0.001 | < 0.001 | < 0.001 | < 0.001 |
| RR8 | 35 | 0.224 | 0.007 | < 0.001 | < 0.001 | < 0.001 | < 0.001 | < 0.001 | < 0.001 | < 0.001 | < 0.001 | < 0.001 | < 0.001 | < 0.001 |
| RR9 | 34 | 0.098 | 0.004 | < 0.001 | < 0.001 | < 0.001 | < 0.001 | < 0.001 | < 0.001 | < 0.001 | < 0.001 | < 0.001 | < 0.001 | < 0.001 |
| RS1 | 29 | 0.214 | 0.005 | < 0.001 | < 0.001 | < 0.001 | < 0.001 | < 0.001 | < 0.001 | < 0.001 | < 0.001 | < 0.001 | < 0.001 | < 0.001 |
| SA1 | 27 | 0.240 | 0.006 | < 0.001 | < 0.001 | < 0.001 | < 0.001 | < 0.001 | < 0.001 | < 0.001 | < 0.001 | < 0.001 | < 0.001 | < 0.001 |
| UP6 | 48 | 0.216 | 0.003 | < 0.001 | < 0.001 | < 0.001 | < 0.001 | < 0.001 | < 0.001 | < 0.001 | < 0.001 | < 0.001 | < 0.001 | < 0.001 |
| WF1 | 35 | 0.299 | 0.008 | < 0.001 | < 0.001 | < 0.001 | < 0.001 | < 0.001 | < 0.001 | < 0.001 | < 0.001 | < 0.001 | < 0.001 | < 0.001 |

**Probability of identity among siblings (PIsibs)**

| Site | N | 1 locus | 2 loci | 3 loci | 4 loci | 5 loci | 6 loci | 7 loci | 8 loci | 9 loci | 10 loci | 11 loci | 12 loci | 13 loci |
|------|---|---------|--------|--------|--------|--------|--------|--------|--------|--------|---------|---------|---------|---------|
| BR1 | 54 | 0.506 | 0.162 | 0.044 | 0.018 | 0.011 | < 0.001 | < 0.001 | < 0.001 | < 0.001 | < 0.001 | < 0.001 | < 0.001 | < 0.001 |
| BR2 | 25 | 0.467 | 0.145 | 0.041 | 0.017 | 0.010 | < 0.001 | < 0.001 | < 0.001 | < 0.001 | < 0.001 | < 0.001 | < 0.001 | < 0.001 |
| C1 | 26 | 0.488 | 0.149 | 0.041 | 0.017 | 0.011 | < 0.001 | < 0.001 | < 0.001 | < 0.001 | < 0.001 | < 0.001 | < 0.001 | < 0.001 |
| CB1 | 52 | 0.488 | 0.151 | 0.041 | 0.016 | 0.010 | < 0.001 | < 0.001 | < 0.001 | < 0.001 | < 0.001 | < 0.001 | < 0.001 | < 0.001 |
| CL2 | 43 | 0.435 | 0.134 | 0.037 | 0.014 | 0.010 | < 0.001 | < 0.001 | < 0.001 | < 0.001 | < 0.001 | < 0.001 | < 0.001 | < 0.001 |
| CL3 | 22 | 0.484 | 0.156 | 0.045 | 0.018 | 0.013 | < 0.001 | < 0.001 | < 0.001 | < 0.001 | < 0.001 | < 0.001 | < 0.001 | < 0.001 |
| LR1 | 47 | 0.467 | 0.144 | 0.039 | 0.016 | 0.011 | < 0.001 | < 0.001 | < 0.001 | < 0.001 | < 0.001 | < 0.001 | < 0.001 | < 0.001 |
| NB3 | 36 | 0.465 | 0.146 | 0.039 | 0.016 | 0.011 | < 0.001 | < 0.001 | < 0.001 | < 0.001 | < 0.001 | < 0.001 | < 0.001 | < 0.001 |
| RR1 | 27 | 0.469 | 0.145 | 0.042 | 0.017 | 0.012 | < 0.001 | < 0.001 | < 0.001 | < 0.001 | < 0.001 | < 0.001 | < 0.001 | < 0.001 |
| RR10 | 31 | 0.523 | 0.167 | 0.046 | 0.018 | 0.012 | < 0.001 | < 0.001 | < 0.001 | < 0.001 | < 0.001 | < 0.001 | < 0.001 | < 0.001 |
| RR2 | 29 | 0.466 | 0.149 | 0.041 | 0.016 | 0.011 | < 0.001 | < 0.001 | < 0.001 | < 0.001 | < 0.001 | < 0.001 | < 0.001 | < 0.001 |
| RR3 | 33 | 0.442 | 0.139 | 0.040 | 0.017 | 0.011 | < 0.001 | < 0.001 | < 0.001 | < 0.001 | < 0.001 | < 0.001 | < 0.001 | < 0.001 |
| RR4 | 32 | 0.510 | 0.166 | 0.046 | 0.019 | 0.014 | < 0.001 | < 0.001 | < 0.001 | < 0.001 | < 0.001 | < 0.001 | < 0.001 | < 0.001 |
| RR5 | 43 | 0.489 | 0.150 | 0.041 | 0.018 | 0.011 | < 0.001 | < 0.001 | < 0.001 | < 0.001 | < 0.001 | < 0.001 | < 0.001 | < 0.001 |
| RR6 | 60 | 0.479 | 0.153 | 0.042 | 0.016 | 0.010 | < 0.001 | < 0.001 | < 0.001 | < 0.001 | < 0.001 | < 0.001 | < 0.001 | < 0.001 |
| RR7 | 54 | 0.470 | 0.148 | 0.040 | 0.016 | 0.011 | < 0.001 | < 0.001 | < 0.001 | < 0.001 | < 0.001 | < 0.001 | < 0.001 | < 0.001 |
| RR8 | 35 | 0.500 | 0.161 | 0.044 | 0.017 | 0.011 | < 0.001 | < 0.001 | < 0.001 | < 0.001 | < 0.001 | < 0.001 | < 0.001 | < 0.001 |
| RR9 | 34 | 0.400 | 0.133 | 0.037 | 0.014 | 0.010 | < 0.001 | < 0.001 | < 0.001 | < 0.001 | < 0.001 | < 0.001 | < 0.001 | < 0.001 |
| RS1 | 29 | 0.501 | 0.158 | 0.045 | 0.017 | 0.012 | < 0.001 | < 0.001 | < 0.001 | < 0.001 | < 0.001 | < 0.001 | < 0.001 | < 0.001 |
| SA1 | 27 | 0.521 | 0.164 | 0.045 | 0.020 | 0.016 | < 0.001 | < 0.001 | < 0.001 | < 0.001 | < 0.001 | < 0.001 | < 0.001 | < 0.001 |
| UP6 | 48 | 0.493 | 0.147 | 0.040 | 0.017 | 0.011 | < 0.001 | < 0.001 | < 0.001 | < 0.001 | < 0.001 | < 0.001 | < 0.001 | < 0.001 |
| WF1 | 35 | 0.548 | 0.176 | 0.050 | 0.021 | 0.016 | < 0.001 | < 0.001 | < 0.001 | < 0.001 | < 0.001 | < 0.001 | < 0.001 | < 0.001 |

**Table S3-11** Pairwise $F_{ST}$ (Lower panel) and $G_{ST}$ (Upper panel; Hedrick (2005)) values between each pair of sampling sites. Values in bold are significant (95% confidence intervals do not overlap with zero)

| Site | BR1 | BR2 | C1 | CB1 | CL2 | CL3 | LR1 | NB3 | RR1 | RR10 | RR2 |
|---|---|---|---|---|---|---|---|---|---|---|---|
| BR1 | — | 0.0051 | 0.0198 | 0.0094 | 0.0198 | **0.0415** | 0.0160 | 0.0003 | **0.0728** | **0.0377** | **0.0307** |
| BR2 | 0.0010 | — | 0.0132 | 0.0090 | 0.0064 | 0.0291 | 0.0055 | -0.0032 | **0.0754** | 0.0133 | 0.0164 |
| C1 | 0.0053 | 0.0027 | — | -0.0073 | 0.0017 | 0.0206 | 0.0196 | 0.0044 | **0.0476** | 0.0187 | 0.0184 |
| CB1 | 0.0025 | 0.0021 | -0.0022 | — | 0.0125 | 0.0226 | 0.0228 | 0.0082 | **0.0585** | 0.0271 | 0.0179 |
| CL2 | 0.0056 | 0.0013 | 0.0002 | 0.0033 | — | 0.0112 | 0.0096 | 0.0020 | **0.0587** | 0.0149 | 0.0233 |
| CL3 | **0.0120** | 0.0073 | 0.0049 | 0.0060 | 0.0028 | — | 0.0282 | 0.0212 | **0.0751** | 0.0410 | 0.0315 |
| LR1 | 0.0047 | 0.0013 | 0.0053 | 0.0064 | 0.0027 | 0.0081 | — | -0.003 | **0.0488** | 0.0111 | 0.0237 |
| NB3 | -0.0003 | -0.0018 | 0.0005 | 0.0019 | 0.0002 | 0.0052 | -0.0012 | — | **0.0480** | 0.0262 | 0.0071 |
| RR1 | **0.0210** | **0.0202** | 0.0121 | **0.0158** | **0.0161** | **0.0207** | **0.0139** | 0.0127 | — | **0.0714** | **0.0549** |
| RR10 | **0.0108** | 0.0032 | 0.0048 | 0.0073 | 0.0041 | 0.0113 | 0.0032 | 0.0069 | **0.0196** | — | 0.0268 |
| RR2 | 0.0087 | 0.0040 | 0.0046 | 0.0048 | 0.0064 | 0.0086 | 0.0068 | 0.0015 | 0.0149 | 0.0074 | — |
| RR3 | **0.0110** | 0.0067 | 0.0092 | 0.0072 | 0.0060 | **0.0154** | 0.0063 | 0.0038 | **0.0198** | 0.0060 | 0.0082 |
| RR4 | **0.0121** | 0.0083 | **0.0116** | **0.0118** | 0.0072 | **0.0160** | **0.0109** | 0.0032 | **0.0190** | 0.0099 | 0.0040 |
| RR5 | **0.0138** | 0.0071 | 0.0079 | **0.0118** | **0.0124** | **0.0220** | **0.0100** | 0.0063 | **0.0143** | 0.0069 | 0.0062 |
| RR6 | **0.0078** | 0.0055 | **0.0105** | **0.0099** | **0.0062** | **0.0122** | 0.0055 | 0.0039 | **0.0139** | 0.0037 | 0.0046 |
| RR7 | 0.0049 | 0.0031 | 0.0075 | 0.0068 | 0.0048 | **0.0146** | 0.0016 | 0.0029 | **0.0114** | 0.0039 | 0.0046 |
| RR8 | 0.0028 | 0.0029 | -0.0016 | 0.0001 | 0.0037 | 0.0026 | 0.0032 | 0.0014 | 0.0109 | 0.0014 | 0.0040 |
| RR9 | **0.0103** | 0.0031 | 0.0049 | 0.0060 | 0.0033 | 0.0092 | 0.0031 | 0.0045 | 0.0111 | 0.0012 | 0.0056 |
| RS1 | **0.0097** | 0.0055 | -0.0007 | 0.0006 | 0.0064 | 0.0030 | 0.0053 | 0.0059 | **0.0181** | 0.0086 | 0.0062 |
| SA1 | 0.0065 | 0.0119 | 0.0052 | **0.0139** | 0.0062 | 0.0143 | 0.0033 | 0.0035 | 0.0110 | 0.0083 | 0.0123 |
| UP6 | **0.0090** | 0.0054 | 0.0004 | 0.0035 | 0.0051 | 0.0065 | **0.0091** | 0.0027 | **0.0143** | **0.0105** | 0.0051 |
| WF1 | **0.0106** | 0.0128 | 0.0026 | 0.0062 | 0.0061 | 0.0074 | 0.0058 | 0.0058 | **0.0148** | 0.0078 | 0.0098 |

| Site | RR3 | RR4 | RR5 | RR6 | RR7 | RR8 | RR9 | RS1 | SA1 | UP6 | WF1 |
|---|---|---|---|---|---|---|---|---|---|---|---|
| BR1 | **0.0385** | **0.0411** | **0.0478** | **0.0270** | 0.0174 | 0.0112 | **0.0365** | **0.0334** | 0.0224 | **0.0325** | **0.0356** |
| BR2 | 0.0257 | 0.0298 | 0.0274 | 0.0203 | 0.0132 | 0.0142 | 0.0142 | 0.0205 | 0.0428 | 0.0218 | **0.0455** |
| C1 | **0.0357** | **0.0428** | 0.0310 | **0.0392** | 0.0289 | -0.0037 | 0.0206 | -0.0024 | 0.0201 | 0.0025 | 0.0103 |
| CB1 | **0.0267** | **0.0424** | **0.0433** | **0.0362** | **0.0249** | 0.0015 | 0.0228 | 0.0023 | **0.0489** | 0.0135 | 0.0222 |
| CL2 | 0.0220 | 0.0251 | **0.0450** | **0.0222** | 0.0179 | 0.0150 | 0.0131 | 0.0227 | 0.0221 | 0.0196 | 0.0215 |
| CL3 | **0.0561** | **0.0553** | **0.0790** | **0.0435** | **0.0527** | 0.0126 | 0.0353 | 0.0107 | **0.0493** | 0.0253 | 0.0260 |
| LR1 | 0.0221 | **0.0371** | **0.0351** | 0.0191 | 0.0062 | 0.0122 | 0.0117 | 0.0179 | 0.0117 | **0.0330** | 0.0197 |
| NB3 | 0.0147 | 0.0120 | 0.0243 | 0.0147 | 0.0118 | 0.0077 | 0.0185 | 0.0221 | 0.0143 | 0.0114 | 0.0213 |
| RR1 | **0.0731** | **0.0673** | **0.0524** | **0.0501** | **0.0415** | **0.0427** | 0.0421 | **0.0649** | 0.0392 | **0.0545** | **0.0515** |
| RR10 | 0.0214 | **0.0343** | 0.0254 | 0.0131 | 0.0148 | 0.0065 | 0.0054 | 0.0301 | 0.0289 | **0.0399** | 0.0270 |
| RR2 | 0.0299 | 0.0134 | 0.0232 | 0.0165 | 0.0174 | 0.0163 | 0.0217 | 0.0215 | **0.0426** | 0.0196 | **0.0339** |
| RR3 | — | 0.0103 | 0.0185 | 0.0159 | 0.0120 | 0.0156 | 0.0250 | **0.0438** | **0.0489** | **0.0336** | **0.0485** |
| RR4 | 0.0031 | — | **0.0318** | 0.0173 | 0.0207 | 0.0264 | 0.0247 | **0.0571** | 0.0309 | **0.0327** | **0.0454** |
| RR5 | 0.0049 | 0.0089 | — | 0.0104 | 0.0135 | 0.0203 | **0.0390** | **0.0529** | 0.0388 | **0.0370** | **0.0414** |
| RR6 | 0.0045 | 0.0050 | 0.0028 | — | 0.0091 | 0.0153 | **0.0275** | **0.0393** | **0.0291** | **0.0377** | **0.0422** |
| RR7 | 0.0032 | 0.0058 | 0.0035 | 0.0025 | — | 0.0070 | 0.0081 | **0.0501** | 0.0134 | **0.0373** | 0.0234 |
| RR8 | 0.0039 | 0.0070 | 0.0050 | 0.0040 | 0.0015 | — | 0.0018 | 0.0063 | 0.0299 | 0.0079 | 0.0106 |
| RR9 | 0.0066 | 0.0068 | **0.0104** | **0.0075** | 0.0019 | -0.0002 | — | 0.0305 | 0.0301 | **0.0359** | 0.0182 |
| RS1 | **0.0122** | **0.0165** | **0.0148** | **0.0111** | **0.0140** | 0.0015 | 0.0083 | — | **0.0468** | 0.0219 | 0.0223 |
| SA1 | **0.0140** | 0.0093 | 0.0110 | 0.0084 | 0.0035 | 0.0079 | 0.0082 | **0.0138** | — | **0.0457** | 0.0107 |
| UP6 | **0.0088** | **0.0089** | **0.0098** | 0.0101 | **0.0100** | 0.0017 | **0.0093** | 0.0059 | **0.0126** | — | **0.0379** |
| WF1 | 0.0139 | **0.0136** | **0.0119** | **0.0122** | 0.0066 | 0.0025 | 0.0049 | 0.0066 | 0.0030 | **0.0105** | — |

**Table S3-12** Mean log likelihood probability (Mean LnP(K)) for each K (K=1–22) and the delta K based on the rate of changes in probability between successive K values. 10 runs were performed for each K

| K | Mean LnP(K) | delta K |
|---|---|---|
| 1 | -43164.93 | — |
| 2 | -43159.16 | 71.69 |
| 3 | -45032.68 | 1.58 |
| 4 | -45955.50 | 1.40 |
| 5 | -44737.40 | 2.22 |
| 6 | -45059.55 | 1.68 |
| 7 | -46429.89 | 0.55 |
| 8 | -46475.46 | 1.16 |
| 9 | -48258.63 | 0.30 |
| 10 | -49227.85 | 0.26 |
| 11 | -49774.33 | 0.31 |
| 12 | -49651.82 | 0.61 |
| 13 | -50489.30 | 0.54 |
| 14 | -52299.12 | 0.51 |
| 15 | -52952.60 | 0.44 |
| 16 | -52249.89 | 0.80 |
| 17 | -53696.34 | 0.65 |
| 18 | -52733.71 | 0.78 |
| 19 | -53374.62 | 0.03 |
| 20 | -54098.24 | 6.51 |
| 21 | -78818.30 | 0.61 |
| 22 | -54472.73 | — |

**Table S3-13** Estimation of the population size (N) of painted turtles of the Rideau Canal Waterway based on the Lincoln-Petersen Index (N=(M*C)/R). We used data from sampling sites where we had data from sampling sessions in different years. Three sampling sites (i.e., BR1, RS1, and SA1) were excluded from the calculation of total mean density because we had no recaptures which prevented us from estimating the population size. M = the number of individuals captured and marked during the first sampling session (M - Year: year of the first sampling session). C = Number of individuals captured during the second sampling session (C - Year: year of the second sampling session). R = Number of individuals captured in the second sampling session that were marked during the first sampling session. Calculation of density is based on mean painted turtle home range area found in the literature (203,800 m$^2$; see Supporting Information 1 – Table S2-2 (Chapter2)).

| Site | M | M - Year | C | C - Year | R | N | Variance | Density (turtle/m$^2$) |
|---|---|---|---|---|---|---|---|---|
| RR1 | 21 | 2019 | 20 | 2020 | 15 | 28 | 3.18 | 0.000137 |
| RR3 | 11 | 2019 | 9 | 2020 | 4 | 24.75 | 28.00 | 0.000121 |
| RR6 | 22 | 2019 | 42 | 2020 | 3 | 308 | 9160.61 | 0.001511 |
| RR7 | 29 | 2019 | 27 | 2020 | 2 | 391.50 | 15750.00 | 0.001921 |
| RR9 | 13 | 2019 | 24 | 2020 | 3 | 104 | 918.75 | 0.000510 |
| BR1 | 13 | 2019 | 40 | 2020 | 0 | NA | NA | NA |
| WF1 | 7 | 2019 | 29 | 2020 | 1 | 203 | 3360.00 | 0.000996 |
| C1 | 12 | 2019 | 15 | 2020 | 1 | 180 | 2669.33 | 0.000883 |
| RS1 | 16 | 2019 | 13 | 2020 | 0 | NA | NA | NA |
| CB1 | 16 | 2019 | 38 | 2020 | 2 | 304 | 9282.00 | 0.001492 |
| UP6 | 10 | 2018 | 40 | 2019 | 2 | 200 | 3808.44 | 0.000981 |
| CL2 | 24 | 2018 | 21 | 2020 | 2 | 252 | 6386.11 | 0.001237 |
| SA1 | 7 | 2018 | 20 | 2019 | 0 | NA | NA | NA |
| | | | | | | | Mean density | 0.000979 |

**Table S3-13** (*continued*)

Mean density (turtle/m$^2$) = 0.000979

Rideau Canal area (m$^2$) = 195,194,686.74

Proportion of Rideau Canal consisting of suitable habitat for painted turtles = 20% (38,999,898.40 m$^2$)

Approximate population size = 38,180.90

Minimum density (turtle/m$^2$) = 0.00012

Minimum population size = 4,679.99

Maximum density (turtle/m$^2$) = 0.00192

Maximum population size =74,879.80

**References for Lincoln-Petersen index:**

Lincoln, F.C. (1930). Calculating waterfowl abundance on the basis of banding returns. Washington: U.S. Department of Agriculture, pp. 1-8. Circular, no. 118.

Petersen, C.G.J. (1896). The yearly immigration of young plaice into Limfjord from the German sea. Report of the Danish Biological Station, vol. 6, pp. 1-48.

**Table S3-14** Number of locks per kilometer (locks/km) for each Rideau Canal section between sampling sites from Ottawa River (RR1) to Ontario Lake (CB1)

| Section | locks/km |
|---------|----------|
| RR1-RR2 | 0.56 |
| RR2-RR3 | 0.32 |
| RR3-RR4 | 0 |
| RR4-RR5 | 0 |
| RR5-RR6 | 0 |
| RR6-RR7 | 0.01 |
| RR7-RR8 | 0.65 |
| RR8-RR9 | 0 |
| RR9-RR10 | 0.12 |
| RR10-LR1 | 0.56 |
| LR1-BR1 | 0 |
| BR1-BR2 | 0 |
| BR2-UP6 | 0.06 |
| UP6-NB3 | 0.22 |
| NB3-CL2 | 0 |
| CL2-CL3 | 0 |
| CL3-SA1 | 0.15 |
| SA1-WF1 | 0.36 |
| WF1-C1 | 0 |
| C1-RS1 | 0.28 |
| RS1-CB1 | 0 |

**Table S3-15** Mean daily number of lockages for each lockstation in the Rideau Canal Waterway between 2018 and 2020. Lockstations are in order from Ottawa River (Ottawa) to Ontario Lake (Kingston)

| | May | | | | June | | | | July | | | |
|---|---|---|---|---|---|---|---|---|---|---|---|---|
| Lockstations | 2018 | 2019 | 2020 | Mean | 2018 | 2019 | 2020 | Mean | 2018 | 2019 | 2020 | Mean |
| Ottawa locks | 1.64 | 0.07 | 0 | 0.57 | NA | 2.23 | 1.13 | 1.68 | 5.65 | 5.26 | 4.26 | 5.05 |
| Hartwells | 2.71 | 1.60 | 0 | 1.44 | NA | 4.50 | 2.77 | 3.63 | 10.94 | 10.81 | 7.65 | 9.80 |
| Hogs Back | 2.36 | 2.73 | 0 | 1.70 | NA | 7.27 | 2.83 | 5.05 | 11.58 | 17.03 | 7.90 | 12.17 |
| Black Rapids | 3.07 | 1.20 | 0 | 1.42 | NA | 5.53 | 5.67 | 5.60 | 12.61 | 11.55 | 12.97 | 12.38 |
| Long Island | 3.21 | 1.67 | 0 | 1.63 | NA | 5.40 | 3.03 | 4.22 | 10.16 | 10.13 | 7.32 | 9.20 |
| Burritts Rapids | 4.07 | 3.87 | 0 | 2.65 | NA | 8.63 | 4.93 | 6.78 | 17.23 | 18.48 | 15.52 | 17.07 |
| Nicholsons | 3.36 | 2.73 | 0 | 2.03 | NA | 7.50 | 3.43 | 5.47 | 16.77 | 16.42 | 13.61 | 15.60 |
| Clowes | 3.36 | 2.73 | 0 | 2.03 | NA | 7.87 | 3.53 | 5.70 | 17.16 | 16.58 | 13.71 | 15.82 |
| Merrickville | 3.57 | 3.20 | 0 | 2.26 | NA | 6.80 | 3.67 | 5.23 | 11.84 | 14.32 | 10.97 | 12.38 |
| **Northern cluster** | 3.04 | 2.20 | 0 | 1.75 | NA | 6.19 | 3.44 | 4.82 | 12.66 | 13.40 | 10.43 | 12.16 |
| Kilmarnock | 3.64 | 4.93 | 0 | 2.86 | NA | 7.73 | 3.57 | 5.65 | 17.03 | 10.68 | 14.84 | 14.18 |
| Edmonds | 4.36 | 5.40 | 0 | 3.25 | NA | 8.03 | 3.37 | 5.70 | 15.00 | 15.87 | 13.42 | 14.76 |
| Old Slys | 4.07 | 4.13 | 0 | 2.73 | NA | 6.40 | 2.57 | 4.48 | 15.35 | 14.16 | 11.68 | 13.73 |
| Combined | 0 | 5.60 | 0 | 1.87 | NA | 8.47 | 4.20 | 6.33 | 18.26 | 17.68 | 14.55 | 16.83 |
| Detached | 5.86 | 5.73 | 0 | 3.86 | NA | 8.77 | 6.40 | 7.58 | 19.29 | 18.29 | 16.26 | 17.95 |
| Poonamalie | 6.64 | 7.07 | 0 | 4.57 | NA | 10.93 | 7.13 | 9.03 | 20.87 | 20.81 | 20.23 | 20.63 |
| Narrows | 13.57 | 9.87 | 0 | 7.81 | NA | 18.73 | 16.57 | 17.65 | 30.23 | 32.97 | 30.68 | 31.29 |
| Newboro | 10.43 | 9.53 | 0 | 6.65 | NA | 21.57 | 12.73 | 17.15 | 36.32 | 35.77 | 31.10 | 34.40 |
| Chaffeys | 9.29 | 7.73 | 0 | 5.67 | NA | 16.20 | 7.43 | 11.82 | 26.42 | 26.71 | 20.74 | 24.62 |
| Davis | 7.50 | 7.27 | 0 | 4.92 | NA | 14.83 | 5.73 | 10.28 | 26.29 | 27.06 | 19.48 | 24.28 |
| Jones Falls | 2.93 | 3.13 | 0 | 2.02 | NA | 5.97 | 1.13 | 3.55 | 9.48 | 10.68 | 9.68 | 9.95 |
| Upper Brewers | 4.00 | 2.73 | 0 | 2.24 | NA | 8,00 | 1.73 | 4.87 | 15.55 | 15.81 | 12.71 | 14.69 |
| Lower Brewers | 3.43 | 3.13 | 0 | 2.19 | NA | 7.40 | 1.40 | 4.40 | 14.71 | 15.48 | 12.29 | 14.16 |
| Kingston Mills | 2.57 | 1.60 | 0 | 1.39 | NA | 6.17 | 1.17 | 3.67 | 12.00 | 11.16 | 8.61 | 10.59 |
| **Southern cluster** | 5.59 | 5.56 | 0 | 3.72 | NA | 10.66 | 5.37 | 8.01 | 19.77 | 19.51 | 16.88 | 18.72 |
| Mean | 4.32 | 3.88 | 0 | 2.73 | NA | 8.42 | 4.40 | 6.42 | 16.22 | 16.45 | 13.65 | 15.44 |

| Lockstations | August | | | | September | | | | October | | | | Mean |
|---|---|---|---|---|---|---|---|---|---|---|---|---|---|
| | 2018 | 2019 | 2020 | Mean | 2018 | 2019 | 2020 | Mean | 2018 | 2019 | 2020 | Mean | Mean |
| Ottawa locks | 5.87 | 5.87 | 4.61 | 5.45 | 2.37 | 2.33 | 1.80 | 2.17 | 1.00 | 1.00 | 1.00 | 1.00 | 2.71 |
| Hartwells | 11.32 | 11.48 | 9.39 | 10.73 | 4.40 | 4.47 | 4.03 | 4.30 | 1.75 | 1.50 | 1.75 | 1.67 | 5.36 |
| Hogs Back | 11.35 | 16.52 | 9.94 | 12.60 | 4.77 | 7.00 | 4.27 | 5.34 | 1.63 | 2.14 | 1.67 | 1.81 | 6.53 |
| Black Rapids | 12.26 | 11.45 | 15.23 | 12.98 | 5.33 | 5.07 | 7.60 | 6.00 | 2.13 | 1.00 | 3.67 | 2.26 | 6.84 |
| Long Island | 9.90 | 10.10 | 8.39 | 9.46 | 3.97 | 4.73 | 3.83 | 4.18 | 0.25 | 2.07 | 1.92 | 1.41 | 5.06 |
| Burritts Rapids | 17.58 | 18.03 | 15.84 | 17.15 | 6.40 | 6.80 | 6.00 | 6.40 | 1.38 | 2.36 | 3.50 | 2.41 | 8.86 |
| Nicholsons | 15.84 | 16.26 | 13.90 | 15.33 | 7.03 | 5.87 | 6.27 | 6.39 | 2.13 | 2.29 | 2.25 | 2.22 | 7.98 |
| Clowes | 16.26 | 16.97 | 14.26 | 15.83 | 7.17 | 5.87 | 6.27 | 6.43 | 2.13 | 2.79 | 2.25 | 2.39 | 8.17 |
| Merrickville | 11.10 | 14.19 | 11.87 | 12.39 | 5.13 | 5.53 | 6.13 | 5.60 | 2.00 | 3.00 | 3.00 | 2.67 | 6.84 |
| **Northern cluster** | 12.39 | 13.43 | 11.49 | 12.44 | 5.17 | 5.30 | 5.13 | 5.20 | 1.60 | 2.02 | 2.33 | 1.98 | 6.48 |
| Kilmarnock | 16.71 | 18.52 | 15.42 | 16.88 | 7.37 | 8.67 | 6.50 | 7.51 | 3.75 | 3.57 | 3.83 | 3.72 | 8.63 |
| Edmonds | 14.26 | 16.39 | 14.19 | 14.95 | 6.60 | 7.13 | 6.23 | 6.66 | 3.50 | 4.14 | 4.50 | 4.05 | 8.38 |
| Old Slys | 14.52 | 15.26 | 12.94 | 14.24 | 6.87 | 6.33 | 5.77 | 6.32 | 3.38 | 2.43 | 3.42 | 3.07 | 7.60 |
| Combined | 18.97 | 20.58 | 16.84 | 18.80 | 8.07 | 8.53 | 8.20 | 8.27 | 5.75 | 4.71 | 5.83 | 5.43 | 9.78 |
| Detached | 17.71 | 18.58 | 18.42 | 18.24 | 9.30 | 9.27 | 9.63 | 9.40 | 4.38 | 4.71 | 7.42 | 5.50 | 10.59 |
| Poonamalie | 20.97 | 22.65 | 22.35 | 21.99 | 12.23 | 11.23 | 11.90 | 11.79 | 4.75 | 5.50 | 9.67 | 6.64 | 12.64 |
| Narrows | 30.16 | 32.06 | 30.55 | 30.92 | 16.80 | 16.13 | 17.00 | 16.64 | 10.63 | 9.64 | 12.00 | 10.76 | 19.27 |
| Newboro | 35.00 | 34.10 | 29.26 | 32.78 | 18.87 | 17.70 | 15.07 | 17.21 | 6.25 | 6.36 | 8.17 | 6.92 | 19.31 |
| Chaffeys | 23.71 | 26.84 | 20.87 | 23.81 | 13.37 | 13.27 | 11.27 | 12.63 | 4.50 | 5.57 | 4.33 | 4.80 | 14.01 |
| Davis | 22.87 | 26.65 | 19.52 | 23.01 | 13.30 | 12.70 | 11.00 | 12.33 | 5.88 | 6.14 | 5.00 | 5.67 | 13.60 |
| Jones Falls | 8.77 | 10.87 | 8.81 | 9.48 | 5.83 | 5.50 | 4.57 | 5.30 | 2.75 | 2.36 | 1.50 | 2.20 | 5.53 |
| Upper Brewers | 15.48 | 15.65 | 12.74 | 14.62 | 7.73 | 6.80 | 6.27 | 6.93 | 3.50 | 2.14 | 2.00 | 2.55 | 7.81 |
| Lower Brewers | 14.97 | 15.32 | 12.16 | 14.15 | 7.20 | 6.57 | 6.27 | 6.68 | 2.75 | 2.14 | 1.75 | 2.21 | 7.47 |
| Kingston Mills | 11.52 | 10.84 | 8.84 | 10.40 | 5.30 | 4.80 | 4.40 | 4.83 | 2.63 | 2.00 | 1.33 | 1.99 | 5.58 |
| **Southern cluster** | 18.97 | 20.31 | 17.35 | 18.88 | 9.92 | 9.62 | 8.86 | 9.46 | 4.60 | 4.39 | 5.05 | 4.68 | 10.73 |
| Mean | 15.68 | 16.87 | 14.42 | 15.66 | 7.54 | 7.46 | 7.00 | 7.33 | 3.10 | 3.20 | 3.69 | 3.33 | 8.60 |

*Supporting Information 2 – Selection of permeability values for the historical features*

## 1. Context and problem

Based on the work of Watson (2006), we identified the positions of historical features such as rapids, waterfalls, and land barriers located on the path of the Rideau Canal before any human-made alterations (Figure S3-1).
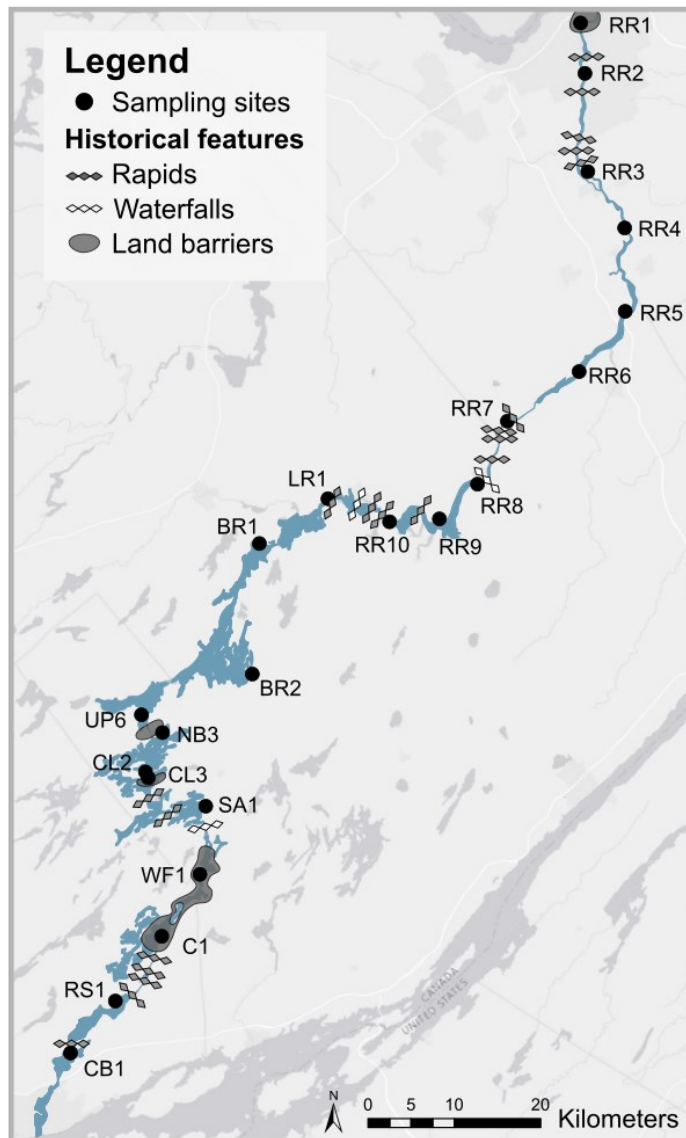
**Figure S3-1** Map of the Rideau Canal, Ontario, Canada (light blue) with the locations of the historical features (rapids: gray diamond bars; waterfalls: white diamond bars; land barriers: gray zones) in relation to sampling sites (black dots).

Our objective was to build a distance matrix from the historical features, similar to the lock matrix that calculated the number of locks between each pair of sites. In the latter case, the same value was given to each lock (i.e., 1) because all locks in the system are identical and should have the same level of permeability. In contrast, we expected that rapids, waterfalls, and land barriers in the landscape prior to canal construction would not have the same level of permeability to turtle movement. Therefore, although the exact levels of permeability of these landscape features to turtle movement are unknown, we could not give the same permeability value to each historical feature. An additional challenge was that we worked in a linear system that does not allow to compute resistance distances from a varied landscape surface (e.g., raster map). To our knowledge, no studies previously assessed how rapids and waterfalls affect turtle dispersal or gene flow.

2. Conception of combinations of permeability values

We built multiple scenarios using different permeability values for each historical feature by altering the level of difficulty to cross and, in some cases, by adjusting the permeability values according to the feature length (Table S3-16; see Figure S3-2 for an example of permeability values used for each feature on the map of the Rideau Canal). We did not use large differences in permeability values because we considered the historical features to be similar barriers to movement, but with slight differences. For each combination, we built a distance matrix that consisted of the sum of permeability values of the historical features between each pair of sites (Table S3-17; see red numbers on Figure S3-2).

**Table S3-16** Combinations of permeability values for each historical landscape features. *Models with permeability values adjusted for the length of the feature: same value for the waterfalls because all waterfalls had a similar length (between 1100 and 1600 m; including the rapids generally just upstream) and similar total drop (rapids and waterfalls together) between 8 and 20 m.

| Models | Rapids | Waterfalls | Land barriers |
|---|---|---|---|
| Hist 1 (Additive) | 1 | 1 | 1 |
| Hist 2 | 1 | 5 | 10 |
| Hist 3 | 1 | 10 | 5 |
| Hist 4 | 5 | 10 | 1 |
| Hist 5 | 10 | 5 | 1 |
| Hist 6* | 1: <1000 m; 5: 1000-2000 m | 10 | 15 to 35: +5 for each 1000 m |
| Hist 7* | 1: <1000 m; 5: 1000-2000 m | 35 | 10 to 30: +5 for each 1000 m |
| Hist 8* | 25: <1000 m; 30: 1000-2000 m | 35 | 1 to 20: +5 for each 1000 m |
| Hist 9* | 30: <1000 m; 35: 1000-2000 m | 25 | 1 to 20: +5 for each 1000 m |
| Binary | 1: if there is at least one barrier between the pair of sites; 0: no barrier | | |
| Binary additive | Additive model based on the binary score between each pair of sites. | | |

**Table S3-17** Example of a distance matrix of historical features based on the combination from the *Hist 4* model (see Table S3-16) with a sub-sample of four sampling sites.

| Sites | RR1 | RR2 | RR3 | RR4 |
|---|---|---|---|---|
| RR1 | — | 6 | 26 | 26 |
| RR2 | 6 | — | 20 | 20 |
| RR3 | 26 | 20 | — | 0 |
| RR4 | 26 | 20 | 0 | — |
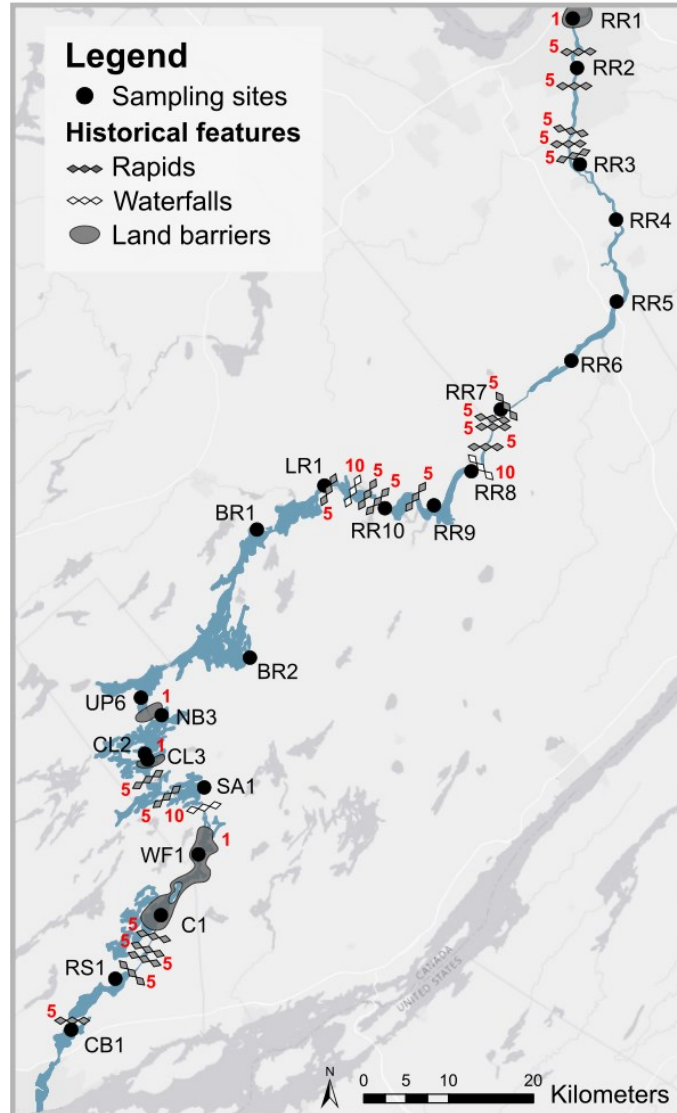
**Figure S3-2** Map of the Rideau Canal, Ontario, Canada (light blue) with the location of historical features (rapids: gray diamond bars; waterfalls: white diamond bars; land barriers: gray zones) in relation to sampling sites (black dots). The permeability values (in red) of each historical feature based on the *Hist 4* model (Table S3-16) used to build the distance matrix are shown beside each historical feature.

3. Selection of the permeability values for the historical features

We built a univariate maximum likelihood population effect (MLPE) model for each distance

matrix of historical features based on each model of permeability levels as predictor variable (Table S3-16), with $F_{ST}$ pairwise measures between each pair of sampling sites as the genetic distance matrix (response variable), and the identity of sampling site pairs as a random effect. We used the combination of permeability levels from the model with the best fit based on information criteria metrics (i.e., AICc) as the distance matrix of historical features for further analyses (see Table S3-18). We made this selection with the sampling sites from the entire system, with sites from the northern cluster (i.e., RR1, RR2, RR3. RR4. RR5, RR6, RR7 sites; Figure S3-1), and with sites from the southern cluster (i.e., RR8, RR9, RR10, LR1, BR1, BR2, UP6, NB3, CL2, CL3, SA1, WF1, C1, RS1, CB1; Figure S3-1)

**Table S3-18** Model selection summary with information criteria metrics of MLPE models using genetic distance ($F_{ST}$) as the response variable and different combinations of permeability values for historical landscape features as predictors for three sections of the canal: entire system, northern cluster, and southern cluster.

| Models | k | AIC | AICc | ΔAICc |
|---|---|---|---|---|
| **Entire system** | | | | |
| Hist 8 | 4 | -2013.29 | -2012.36 | 0 |
| Hist 4 | 4 | -2012.41 | -2011.48 | 0.89 |
| Hist 9 | 4 | -2011.99 | -2011.06 | 1.30 |
| Hist 1 | 4 | -2011.71 | -2010.78 | 1.58 |
| Hist 3 | 4 | -2011.39 | -2010.46 | 1.91 |
| Hist 7 | 4 | -2011.21 | -2010.28 | 2.09 |
| Hist 5 | 4 | -2010.07 | -2009.14 | 3.23 |
| Binary additive | 4 | -2010.05 | -2009.12 | 3.24 |
| Hist 2 | 4 | -1995.39 | -1994.46 | 17.90 |
| Hist 6 | 4 | -1993.88 | -1992.95 | 19.41 |
| Binary | 4 | -1965.79 | -1964.86 | 47.50 |
| Null | 3 | -1949.84 | -1949.29 | 63.07 |
| **Northern cluster** | | | | |
| Hist 6 | 4 | -189.31 | -188.38 | 0 |
| Hist 7 | 4 | -188.91 | -187.98 | 0.40 |
| Hist 2 | 4 | -184.31 | -183.38 | 4.99 |
| Hist 3 | 4 | -177.77 | -176.84 | 11.53 |
| Binary additive | 4 | -172.49 | -171.56 | 16.82 |
| Null | 3 | -171.91 | -171.36 | 17.01 |
| Binary | 4 | -172.19 | -171.26 | 17.12 |
| Hist 1 | 4 | -172.17 | -171.24 | 17.13 |
| Hist 8 | 4 | -171.90 | -170.97 | 17.40 |
| Hist 9 | 4 | -171.84 | -170.91 | 17.47 |
| Hist 4 | 4 | -171.66 | -170.73 | 17.65 |
| Hist 5 | 4 | -171.60 | -170.67 | 17.71 |
| **Southern cluster** | | | | |
| Hist 8 | 4 | -910.26 | -909.33 | 0 |
| Hist 7 | 4 | -910.09 | -909.16 | 0.17 |
| Hist 3 | 4 | -909.99 | -909.06 | 0.27 |
| Hist 4 | 4 | -909.90 | -908.97 | 0.36 |
| Hist 9 | 4 | -909.50 | -908.57 | 0.76 |
| Hist 1 | 4 | -909.43 | -908.50 | 0.83 |

| | | | | |
|---|---|---|---|---|
| Hist 5 | 4 | -908.82 | -907.89 | 1.43 |
| Hist 6 | 4 | -908.68 | -907.74 | 1.58 |
| Hist 2 | 4 | -908.59 | -907.66 | 1.67 |
| Binary additive | 4 | -908.33 | -907.40 | 1.93 |
| Null | 3 | -903.62 | -903.07 | 6.26 |
| Binary | 4 | -903.33 | -902.40 | 6.93 |

# General Conclusion

Overall, I found that human activities and human-made barriers impacted different components of the biology of painted turtles, from influencing their propensity to take risks, to inducing physiological changes and causing genetic substructuring. These findings indicate that human-induced perturbations and environmental changes have consequences on animals at different time scales: behavioural and physiological changes are generally the initial response to human activity reflecting the short-term and prolonged effects, especially when the perturbations persist over time, while genetic structuring caused by human-made barriers, which take more time to be detected, reflect long-term effects (Buchanan, 2000; Landguth et al., 2010). By observing variations in turtle physiological responsiveness according to their propensity to take risks, my thesis also highlights the importance of considering that biological processes are intertwined and should not be evaluated separately. Finally, my thesis provides information that could contribute to better protect species that are vulnerable to the growing pressures caused by humans, such as turtles, where the research is increasing but is still limited. I summarize the findings of my thesis in Figure 4-1.

In chapter one, I reported that painted turtles are consistent in their propensity to take risks which is related to the levels of recreational boating occurring in their environment. Painted turtles in proximity to lockstations with more daily vessel crossings used more active defensive behaviours indicating that these spatial differences in risk taking propensity potentially allow painted turtles to co-exist with human presence and to persist in disturbed landscapes. By documenting the consistency of risk-taking behaviours within painted turtles and associating spatial variation in risk-taking propensity to human disturbance, I bridged a gap in the literature and brought the field of behavioural research in turtles, a group of conservation concern, a step forward.

In chapter two, I found no changes in physiological response according to the levels of recreational boating, but turtles sampled during the first year of COVID-19 restrictions had lower H/L ratios illustrating how limiting human outdoor activities has the potential to reduce human pressures on wildlife. In addition, physiological responsiveness is influenced by individual risk-taking propensity where risk-prone males, but not females, exhibited higher H/L ratios than risk-averse males indicating a potential additional cost of taking risks when exposed to challenging conditions. I also observed that males and females exhibited different colour patterns, which indicates sexual colour dimorphism in painted turtles. However, these differences in colouration were not related to any physiological and behavioural processes indicating that colour patterns may not signal fitness-related information, but potentially share information used in mate and species recognition or facilitate crypsis. By evaluating the impact of human disturbance on the relationships between colouration, risk-taking behaviour, and physiological response in painted turtles with structural equation modelling, I generated new knowledge using a hypothesis-driven approach, which is different compared to other approaches that focus on each causal relationship individually.

In chapter three, I found that the number of locks was the best predictor of the genetic differentiation detected among painted turtle groups of the Rideau Canal. By being partially permeable to gene flow, the locks have the potential to dictate the population genetic structure of turtles, especially where they are numerous and clustered in space. With this study, I provide a rare example of how canal systems can influence the genetic population structure of a long-lived species at large spatial scales, which could set the baseline and open the door for other studies in artificial waterways.
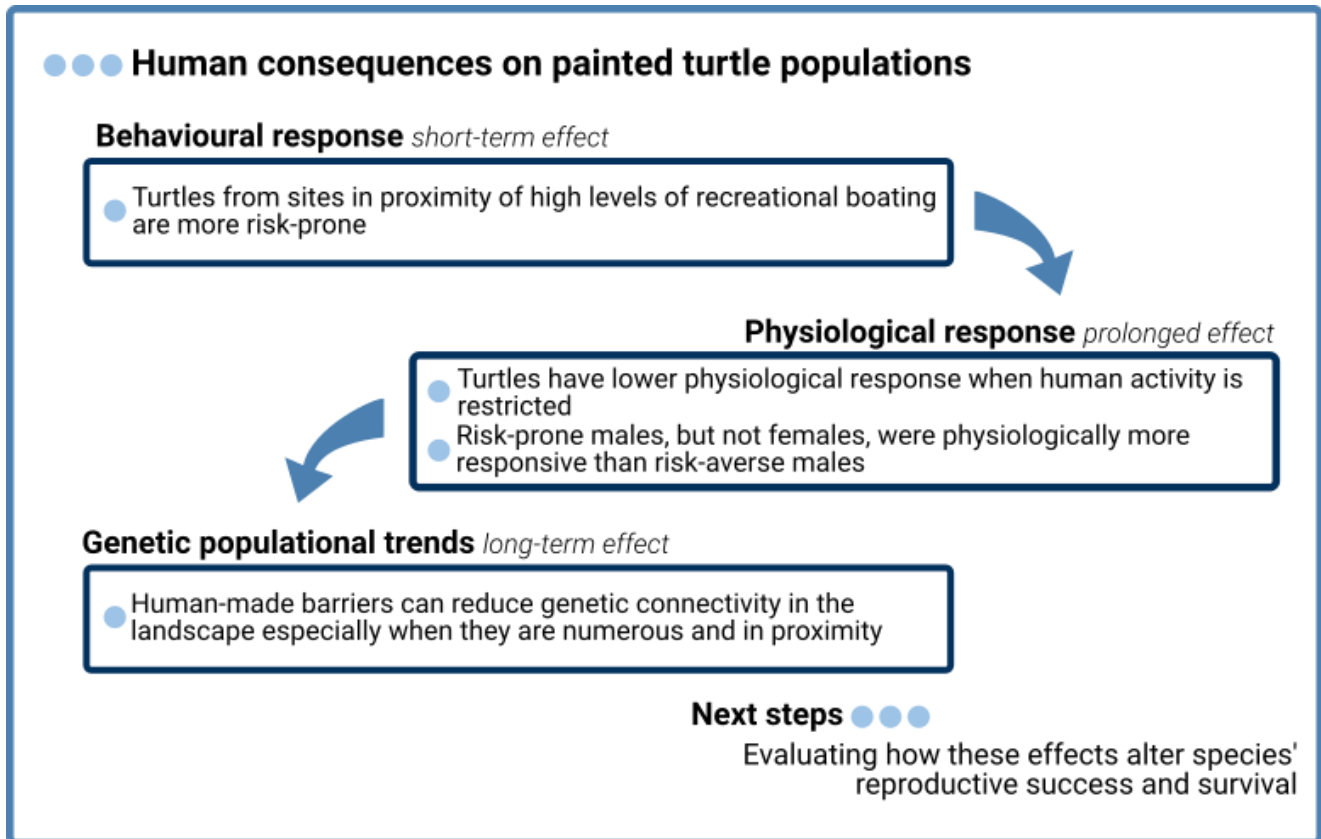
**Figure 4-1** Summary of the findings of my thesis evaluating the consequences of human activities and human-made barriers on different components of painted turtle's biology: the behaviour, the physiology and the population genetic structure within the Rideau Canal.

## Conservation implications

Beside generating fundamental knowledge on the consequences of human disturbance on animal populations, my thesis provides information that could be used to guide management decisions. My findings are relevant to other species which are impacted by human activities, and especially for half of the turtle species that are currently facing high risks of extinction (Stanford et al., 2020). My thesis highlights the importance of integrating different disciplines in the management of conservation issues, despite the additional challenges of using such an approach. By knowing how animals behaviourally respond to human disturbance, behaviour can be monitored where specific behavioural changes can

trigger immediate conservation interventions (Cooke et al., 2014). For instance, more frequent risk-averse behaviours (e.g., lower flight distance) or habitat use changes in areas highly disturbed by human activities could indicate that animals are sensitive to human presence and specific measures could be applied to attenuate the consequences (Blumstein, 2016; Rebelo & Rainho, 2009). However, it would be necessary to determine the consequence of these changes on species' persistence before triggering interventions (see *Next steps* section of the general discussion). In addition, long-term monitoring of physiological biomarkers, such as H/L ratio, can be used to record the physiological state of wildlife populations and then be utilised by conservation practitioners to flag rapidly potential population declines (Cooke & O'Connor, 2010; Walls & Gabor, 2019). Genetic analyses can be used to prioritize conservation actions by identifying specific areas that need to be protected to maintain gene flow in the landscape, such as areas already used as dispersal corridors by animals or areas where gene flow is restricted by the presence of barriers (Shaffer et al., 2015). To build the ultimate conservation tool kit, there is a need to adjust conservation actions by merging the knowledge generated by multiple disciplines, given that each one has weaknesses that can be compensated by the strength of others (Cooke et al., 2014; Walls & Gabor, 2019). For instance, animal behaviour can be relatively easily measured and monitored in a population, but it does not provide direct information on their health condition, but that can be estimated using physiological biomarkers (Cooke et al., 2014). Finally, merging disciplines can help to better understand the consequences of human disturbance by uncovering possible interactions between different components of species' biology and, thus, avoid the implantation of poorly adapted management plans (Walls & Gabor, 2019).

In the next decades, Parks Canada will invest billions of dollars to modernize the Rideau Canal infrastructure, giving them the opportunity to consider the results of this thesis to improve or conserve

the health of turtle populations and other aquatic species living in the canal. Thus, there is a great opportunity to integrate the findings of my thesis to develop efficient management policies, while maintaining the recreational use of the Rideau Canal. Several conservation strategies, such as the creation of freshwater sanctuaries, the limitation of vessel speed, and the restoration of connectivity using wildlife passages, have already proven to be efficient to reduce human pressures on aquatic wildlife and could be implemented in the Rideau Canal (Conn & Silber, 2013; Mcrae et al., 2012; Zolderdo et al., 2023).

## Next steps

One of the main limitations of my thesis is that I did not evaluate how the behavioural/physiological changes and the genetic discontinuities occurring in this system are related to any fitness-related activities, survival and/or population-level processes, which limit the capacity to fully evaluate the conservation issues that turtles are potentially facing (Cooke & O'Connor, 2010). Several studies showed that high physiological stress response and limited gene flow caused by human activities can have important fitness consequences and threaten animal populations (Acevedo-Whitehouse & Duffus, 2009; Reed & Frankham, 2003), thus a logical next step would be to assess these potential consequences in the study system. In particular, the quantification of important population-level parameters (e.g., population growth rates, effective population size) should be prioritized since changes in these parameters clearly affect population persistence (Anthony & Blumstein, 2000). For instance, I found that risk-prone painted turtles are more frequent in areas with higher levels of boat activity which seem to allow them to persist in a human-altered landscape, but identifying how this behavioural response is related to population-level parameters will allow to determine if being risk-prone is maladaptive and how it could potentially threaten population persistence. Making links between

235

the biological changes observed and population-level processes will be necessary to obtain a more complete portrait of possible conservation problems.

# Literature Cited

Abell, A. J. (2000). Costs of reproduction in male lizards, *Sceloporus virgatus*. *Oikos*, *88*, 630–640. https://doi.org/10.1034/j.1600-0706.2000.880320.x

Abràmoff, M. D., Magalhães, P. J., & Ram, S. J. (2004). Image processing with ImageJ. *Biophotonics International*, *11*, 36–42.

Acevedo-Whitehouse, K., & Duffus, A. L. J. (2009). Effects of environmental change on wildlife health. *Philosophical Transactions of the Royal Society B: Biological Sciences*, *364*, 3429–3438. https://doi.org/10.1098/rstb.2009.0128

Adamack A.T., & Gruber B. (2014). PopGenReport: Simplifying basic population genetic analyses in R. *Methods in Ecology and Evolution*, *5*, 384–387. https://doi.org/10.1111/2041-210X.12158

Aguilera, E., & Amat, J. A. (2007). Carotenoids, immune response and the expression of sexual ornaments in male greenfinches (*Carduelis chloris*). *Naturwissenschaften*, *94*, 895–902. https://doi.org/10.1007/s00114-007-0268-5

Alcala, N., Goudet, J., & Vuilleumier, S. (2014). On the transition of genetic differentiation from isolation to panmixia: What we can learn from $G_{ST}$ and D. *Theoretical Population Biology*, *93*, 75–84. https://doi.org/10.1016/j.tpb.2014.02.003

Aldridge, R. D., & Brown, W. S. (1995). Male reproductive cycle, age at maturity, and cost of reproduction in the timber rattlesnake (*Crotalus horridus*). *Journal of Herpetology*, *29*, 399–407. https://doi.org/10.2307/1564990

Aljanabi, S. M., & Martinez, I. (1997). Universal and rapid salt-extraction of high quality genomic DNA for PCR-based techniques. *Nucleic Acids Research*, *25*, 4692–4693.

https://doi.org/10.1093/nar/25.22.4692

Allard, S., Fuller, G., Torgerson-White, L., Starking, M. D., & Yoder-Nowak, T. (2019). Personality in zoo-hatched blanding's turtles affects behavior and survival after reintroduction into the wild. *Frontiers in Psychology*, *10*, 2324. https://doi.org/10.3389/fpsyg.2019.02324

Alp, M., Keller, I., Westram, A. M., & Robinson, C. T. (2012). How river structure and biological traits influence gene flow: A population genetic study of two stream invertebrates with differing dispersal abilities. *Freshwater Biology*, *57*, 969–981. https://doi.org/10.1111/j.1365-2427.2012.02758.x

Anderson, C., Wong, S. C., Fuller, A., Zigelsky, K., & Earley, R. L. (2015). Carotenoid-based coloration is associated with predation risk, competition, and breeding status in female convict cichlids (*Amatitlania siquia*) under field conditions. *Environmental Biology of Fishes*, *98*, 1005–1013. https://doi.org/10.1007/s10641-014-0333-9

Anthony, L. L., & Blumstein, D. T. (2000). Integrating behaviour into wildlife conservation: The multiple ways that behaviour can reduce $N_e$. *Biological Conservation*, *95*, 303–315. https://doi.org/10.1016/S0006-3207(00)00037-9

Arhonditsis, G. B., Stow, C. A., Steinberg, L. J., Kenney, M. A., Lathrop, R. C., McBride, S. J., & Reckhow, K. H. (2006). Exploring ecological patterns with structural equation modeling and Bayesian analysis. *Ecological Modelling*, *192*, 385–409. https://doi.org/10.1016/j.ecolmodel.2005.07.028

Arikan, H., & Çiçek, K. (2014). Haematology of amphibians and reptiles: A review. *North-Western Journal of Zoology*, *10*, 190–209.

Avise, J. C., Bowen, B. W., Lamb, T., Meylan, A. B., & Bermingham, E. (1992). Mitochondrial DNA evolution at a turtle's pace: Evidence for low genetic variability and reduced microevolutionary rate in the testudines. *Molecular Biology and Evolution*, *9*, 457–473. https://doi.org/10.1093/oxfordjournals.molbev.a040735

Banning Anthonysamy, W. J. (2012). *Spatial ecology, habitat use, genetic diversity, and reproductive success: measures of connectivity of a sympatric freshwater turtle assemblage in a fragmented landscape*. [Ph.D. Thesis, University of Illinois]. Proquest Dissertations Publishing. https://login.proxy.bib.uottawa.ca/login?url=https://www.proquest.com/dissertations-theses/spatial-ecology-habitat-use-genetic-diversity/docview/1419470696/se-2

Barbarossa, V., Schmitt, R. J. P., Huijbregts, M. A. J., Zarfl, C., King, H., & Schipper, A. M. (2020). Impacts of current and future large dams on the geographic range connectivity of freshwater fish worldwide. *Proceedings of the National Academy of Sciences of the United States of America*, *117*, 3648–3655. https://doi.org/10.1073/pnas.1912776117

Barnosky, A. D., Hadly, E. A., Bascompte, J., Berlow, E. L., Brown, J. H., Fortelius, M., Getz, W. M., Harte, J., Hastings, A., Marquet, P. A., Martinez, N. D., Mooers, A., Roopnarine, P., Vermeij, G., Williams, J. W., Gillespie, R., Kitzes, J., Marshall, C., Matzke, N., … Smith, A. B. (2012). Approaching a state shift in Earth's biosphere. *Nature*, *486*, 52–58. https://doi.org/10.1038/nature11018

Bartoń, K. (2020). *MuMIn: Multi-Model Inference*. R package version 1.43.17. https://CRAN.R-project.org/package=MuMIn

Bates, D., Maechler, M., Bolker, B., & Walker, S. (2015). Fitting linear mixed-effects models using lme4. *Journal of Statistical Software*, *67*, 1–48. https://doi.org/10.18637/jss.v067.i01

Bejder, L., Samuels, A., Whitehead, H., Finn, H., & Allen, S. (2009). Impact assessment research: use and misuse of habituation, sensitisation and tolerance in describing wildlife responses to anthropogenic stimuli. *Marine Ecology Progress Series*, *395*, 177–185. https://doi.org/10.3354/meps07979

Bell, A. M., Hankison, S. J., & Laskowski, K. L. (2009). The repeatability of behaviour: A meta-analysis. *Animal Behaviour*, *77*, 771–783. https://doi.org/10.1016/j.anbehav.2008.12.022

Benjamini, Y., & Yekutieli, D. (2001). The control of the false discovery rate in multiple testing under dependency. *The Annals of Statistics*, *29*, 1165–1188. https://10.1214/aos/1013699998

Bennett, A. M., Keevil, M., & Litzgus, J. D. (2010). Spatial ecology and population genetics of northern map turtles (*Graptemys geographica*) in fragmented and continuous habitats in Canada. *Chelonian Conservation and Biology*, *9*, 185–195. https://doi.org/10.2744/CCB-0824.1

Berg, M. L., Knott, B., Ribot, R. F. H., Buchanan, K. L., & Bennett, A. T. D. (2019). Do glucocorticoids or carotenoids mediate plumage coloration in parrots? An experiment in *Platycercus elegans*. *General and Comparative Endocrinology*, *280*, 82–90. https://doi.org/10.1016/j.ygcen.2019.04.014

Bergman, J. N., Beaudoin, C., Mistry, I., Turcotte, A., Vis, C., Minelga, V., Neigel, K., Lin, H.-Y., Bennett, J. R., Young, N., Rennie, C., Trottier, L. L., Abrams, A. E. I., Beaupre, P., Glassman, D., Blouin-Demers, D., Garant, D., Vermaire, J. C., Smol, J. P., & Cooke, S. J. (2021). Historical, contemporary, and future perspectives on a coupled social-ecological system in a changing world: Canada's historic Rideau Canal. *Environmental Reviews*, *30*, 72–87. https://doi.org/10.1139/er-2021-0026

Biro, P. A., & Stamps, J. A. (2008). Are animal personality traits linked to life-history productivity? *Trends in Ecology and Evolution*, *23*, 361–368. https://doi.org/10.1016/j.tree.2008.04.003

Blount, J. D., Metcalfe, N. B., Birkhead, T. R., & Surai, P. F. (2003). Carotenoid modulation of immune function and sexual attractiveness in Zebra Finches. *Science*, *300*, 125–126. https://doi.org/10.1126/science.1082142

Böhm, M., Collen, B., Baillie, J. E. M., Bowles, P., Chanson, J., Cox, N., Hammerson, G., Hoffmann, M., Livingstone, S. R., Ram, M., Rhodin, A. G. J., Stuart, S. N., van Dijk, P. P., Young, B. E., Afuang, L. E., Aghasyan, A., García, A., Aguilar, C., Ajtic, R., … Zug, G. (2013). The conservation status of the world's reptiles. *Biological Conservation*, *157*, 372–385. https://doi.org/10.1016/j.biocon.2012.07.015

Bowne D. R. (2002). *Linking individual behaviour to population processes at the landscape level*. [Ph.D. Thesis, University of Virginia]. Proquest Dissertations Publishing. https://login.proxy.bib.uottawa.ca/login?url=https://www.proquest.com/dissertations-theses/linking-individual-behavior-population-processes/docview/305528413/se-2

Bowne, D. R. (2008). Terrestrial activity of *Chrysemys picta* in northern Virginia. *Copeia*, *2008*, 306–310. https://doi.org/10.1643/CE-06-224

Bowne, D. R., & White, H. R. (2004). Searching strategy of the painted turtle *Chrysemys picta* across spatial scales. *Animal Behaviour*, *68*, 1401–1409. https://doi.org/10.1016/j.anbehav.2004.01.018

Breck, S. W., Poessel, S. A., Mahoney, P., & Young, J. K. (2019). The intrepid urban coyote: A comparison of bold and exploratory behavior in coyotes from urban and rural environments. *Scientific Reports*, *9*, 2104. https://doi.org/10.1038/s41598-019-38543-5

Briggs, C., & Bain, B. J. (2017). Basic Haematological Techniques. In B. J. Bain, I. Bates, & M. A.

    Laffan (Eds.), *Dacie and Lewis Practical Haematology* (pp. 18–49). Elsevier.

    https://doi.org/10.1016/B978-0-7020-6696-2.00003-5

Brookfield, J. F. Y. (1996). A simple new method for estimating null allele frequency from

    heterozygote deficiency. *Molecular Ecology*, *5*, 453–455. https://doi.org/10.1111/j.1365-

    294X.1996.tb00336.x

Brooks, R. J., Brown, G. P., & Galbraith, D. A. (1991). Effects of a sudden increase in natural

    mortality of adults on a population of the common snapping turtle (*Chelydra serpentina*).

    *Canadian Journal of Zoology*, *69*, 1314–1320. https://doi.org/10.1139/z91-185

Buchanan, K. L. (2000). Stress and the evolution of condition-dependent signals. *Trends in Ecology*

    *and Evolution*, *15*, 156–160. https://doi.org/10.1016/S0169-5347(99)01812-1

Buhlmann, K. A., Akre, T. S. B., Iverson, J. B., Karapatakis, D., Mittermeier, R. A., Georges, A.,

    Rhodin, A. G. J., Van Dijk, P. P., & Gibbons, J. W. (2009). A global analysis of tortoise and

    freshwater turtle distributions with identification of priority conservation areas. *Chelonian*

    *Conservation and Biology*, *8*, 116–149. https://doi.org/10.2744/CCB-0774.1

Bulté, G., & Blouin-Demers, G. (2010). Estimating the energetic significance of basking behaviour in

    a temperate-zone turtle. *Ecoscience, 17,* 387–393. https://doi.org/10.2980/17-4-3377

Bulté, G., Carrière, M.-A., & Blouin-demers, G. (2010). Impact of recreational power boating on two

    populations of nothern map turtles. *Aquatic Conservation: Marine and Freshwater Ecosystems*,

    *20*, 31–38. https://doi.org/10.1002/aqc

Bulté, G., Germain, R. R., O'Connor, C. M., & Blouin-Demers, G. (2013).  Sexual dichromatism in

the northern map turtle, *Graptemys geographica*. *Chelonian Conservation and Biology*, *12*, 187–192. https://doi.org/10.2744/ccb-0995a.1

Bulté, G., Léveillée, M. B., Blouin-Demers, G., Cooke, S. J., & Bertram, S. M. (2020). Observations on the short-term effects of motorboat disturbance on the use of basking sites by female northern map turtles. *Chelonian Conservation and Biology*, *19*, 302–304. https://doi.org/10.2744/CCB-1418.1

Bürkner, P.-C. (2017). brms: An R package for Bayesian multilevel models using Stan. *Journal of Statistical Software*, *80*, 1–28. https://doi.org/10.18637/jss.v080.i01

Campbell, T. W. (2015). Peripherical blood of reptiles. In T. W. Campbell (Ed.), *Exotic Animal Hematology and Cytology* (pp. 67–87). John Wiley & Sons. https://doi.org/10.1002/9781118993705.ch3

Čapkun-Huot, C., Fyson, V. K., & Blouin-Demers, G. (2021). Landscape composition predicts the local abundance of painted turtles (*Chrysemys picta*). *Herpetology Notes*, *14*, 215–223.

Carbillet, J., Rey, B., Lavabre, T., Chaval, Y., Merlet, J., Débias, F., Régis, C., Pardonnet, S., Duhayer, J., Gaillard, J. M., Hewison, A. J. M., Lemaître, J. F., Pellerin, M., Rannou, B., Verheyden, H., & Gilot-Fromont, E. (2019). The neutrophil to lymphocyte ratio indexes individual variation in the behavioural stress response of wild roe deer across fluctuating environmental conditions. *Behavioral Ecology and Sociobiology*, *73*, 144. https://doi.org/10.1007/s00265-019-2755-z

Carbó-Ramírez, P., & Zuria, I. (2017). Leukocyte profile and body condition of the house finch (*Haemorhous mexicanus*) in two sites with different levels of urbanization in central Mexico.

*Ornitología Neotropical*, *28*, 1–10. https://doi.org/10.58843/ornneo.v28i0.218

Carere, C., Caramaschi, D., & Fawcett, T. W. (2010). Covariation between personalities and

individual differences in coping with stress: Converging evidence and hypotheses. *Current*

*Zoology*, *56*, 728–740. https://doi.org/10.1093/czoolo/56.6.728

Carlson, B. E., & Tetzlaff, S. J. (2020). Long-term behavioral repeatability in wild adult and captive

juvenile turtles (*Terrapene carolina*): Implications for personality development. *Ethology*, *126*,

668–678. https://doi.org/10.1111/eth.13024

Carter, A. W., Paitz, R. T., McGhee, K. E., & Bowden, R. M. (2016). Turtle hatchlings show

behavioral types that are robust to developmental manipulations. *Physiology and Behavior*, *155*,

46–55. https://doi.org/10.1016/j.physbeh.2015.11.034

Carvajal-Quintero, J. D., Januchowski-Hartley, S. R., Maldonado-Ocampo, J. A., Jézéquel, C.,

Delgado, J., & Tedesco, P. A. (2017). Damming fragments species' ranges and heightens

extinction risk. *Conservation Letters*, *10*, 708–716. https://doi.org/10.1111/conl.12336

Caspi, T., Johnson, J. R., Lambert, M. R., Schell, C. J., & Sih, A. (2022). Behavioral plasticity can

facilitate evolution in urban environments. *Trends in Ecology and Evolution*, *37*, 1092–1103.

https://doi.org/10.1016/j.tree.2022.08.002

Ceballos, G., Ehrlich, P. R., Barnosky, A. D., García, A., Pringle, R. M., & Palmer, T. M. (2015).

Accelerated modern human-induced species losses: Entering the sixth mass exctinction. *Science*

*Advances*, *1*, e1400253. https://doi.org/10.1126/sciadv.1400253

Ciuti, S., Northrup, J. M., Muhly, T. B., Simi, S., Musiani, M., Pitt, J. A., & Boyce, M. S. (2012).

Effects of humans on behaviour of wildlife exceed those of natural predators in a landscape of

fear. *PLoS ONE*, *7*, e50611. https://doi.org/10.1371/journal.pone.0050611

Clarke, G. L. (1939). Light as a limiting factor for aquatic animals and plants. *The American Biology Teacher*, *1*, 150–154.

Clarke, R. T., Rothery, P., & Raybould, A. F. (2002). Confidence limits for regression relationships between distance matrices: Estimating gene flow with distance. *Journal of Agricultural, Biological, and Environmental Statistics*, *7*, 361–372. https://doi.org/10.1198/108571102320

Coffin, D. (2015). *IJ Plugins: ij-dcraw - Reader for digital camera raw images*. https://ij-plugins.sourceforge.net/plugins/dcraw/

Coico, R., & Sunshine, G. (2015). *Immunology - A short course*. Wiley-Blackwell.

Cole, E. F., & Quinn, J. L. (2014). Shy birds play it safe: Personality in captivity predicts risk responsiveness during reproduction in the wild. *Biology Letters*, *10*, 20140178. https://doi.org/10.1098/rsbl.2014.0178

Congdon, J. D., Dunham, A. E., & Van Loben Sels, R. C. (1994). Demographics of common snapping turtles (*Chelydra serpentina*): Implications for conservation and management of long-lived organisms. *Integrative and Comparative Biology*, *34*, 397–408. https://doi.org/10.1093/icb/34.3.397

Congdon, J. D., Nagle, R. D., Kinney, O. M., Van Loben Sels, R. C., Quinter, T., & Tinkle, D. W. (2003). Testing hypotheses of aging in long-lived painted turtles (*Chrysemys picta*). *Experimental Gerontology*, *38*, 765–772. https://doi.org/10.1016/S0531-5565(03)00106-2

Conn, P. B., & Silber, G. K. (2013). Vessel speed restrictions reduce risk of collision-related mortality for North Atlantic right whales. *Ecosphere*, *4*, 43. https://doi.org/10.1890/ES13-00004.1

Cooke, S. J., Blumstein, D. T., Buchholz, R., Caro, T., Fernández-Juricic, E., Franklin, C. E.,

    Metcalfe, J., O'Connor, C. M., St. Clair, C. C., Sutherland, W. J., & Wikelski, M. (2014).

    Physiology, behavior, and conservation. *Physiological and Biochemical Zoology*, *87*, 1–14.

    https://doi.org/10.1086/671165

Cooke, S. J., & O'Connor, C. M. (2010). Making conservation physiology relevant to policy makers

    and conservation practitioners. *Conservation Letters*, *3*, 159–166. https://doi.org/10.1111/j.1755-

    263X.2010.00109.x

COSEWIC. (2018). *COSEWIC assessment and status report on the Midland painted turtle Chrysemys*

    *picta marginata and the Eastern painted turtle Chrysemys picta picta in Canada*. Committee on

    the Status of Endangered Wildlife in Canada. https://www.registrelep-

    sararegistry.gc.ca/virtual_sara/files/cosewic/srMidlandPaintedTurtleEasternPaintedTurtle2018e.p

    df.

Cote, J., Clobert, J., Brodin, T., Fogarty, S., & Sih, A. (2010). Personality-dependent dispersal:

    Characterization, ontogeny and consequences for spatially structured populations. *Philosophical*

    *Transactions of the Royal Society B: Biological Sciences*, *365*, 4065–4076.

    https://doi.org/10.1098/rstb.2010.0176

Courtois, È., Garant, D., Pelletier, F., & Bélisle, M. (2021). Nonideal nest box selection by tree

    swallows breeding in farmlands: Evidence for an ecological trap? *Ecology and Evolution*, *11*,

    16296–16313. https://doi.org/10.1002/ece3.8323

Crawley, M. J. (2007). *The R Book*. John Wiley and Sons.

Cuthill, I. C., Allen, W. L., Arbuckle, K., Caspers, B., Chaplin, G., Hauber, M. E., Hill, G. E.,

Jablonski, N. G., Jiggins, C. D., Kelber, A., Mappes, J., Marshall, J., Merrill, R., Osorio, D., Prum, R., Roberts, N. W., Roulin, A., Rowland, H. M., Sherratt, T. N., … Caro, T. (2017). The biology of color. Science, 357, eaan0221. https://doi.org/10.1126/science.aan0221

Dantzer, B., Fletcher, Q. E., Boonstra, R., & Sheriff, M. J. (2014). Measures of physiological stress: A transparent or opaque window into the status, management and conservation of species? *Conservation Physiology*, *2*, cou023. https://doi.org/10.1093/conphys/cou023

da Silva, A. G., Williams, K. E., Kirk, S. L., Bishop, C. A., Hodges, K. E., & Russello, M. A. (2010). Isolation and characterization of microsatellite loci in two species-at-risk in British Columbia: great basin spadefoot (*Spea intermontana*) and western painted turtle (*Chrysemys picta bellii*). *Conservation Genetics Resources*, *2*, 37–40. https://doi.org/10.1007/s12686-009-9136-2

Davis, A. K., & Maney, D. L. (2018). The use of glucocorticoid hormones or leucocyte profiles to measure stress in vertebrates : What's the difference? *Methods in Ecology and Evolution*, *9*, 1556–1568. https://doi.org/10.1111/2041-210X.13020

Davis, A. K., Maney, D. L., & Maerz, J. C. (2008). The use of leukocyte profiles to measure stress in vertebrates: A review for ecologists. *Functional Ecology*, *22*, 760–772. https://doi.org/10.1111/j.1365-2435.2008.01467.x

DeCatanzaro, R., & Chow-Fraser, P. (2010). Relationship of road density and marsh condition to turtle assemblage characteristics in the Laurentian Great Lakes. *Journal of Great Lakes Research*, *36*, 357–365. https://doi.org/10.1016/j.jglr.2010.02.003

Dhabhar, F. S. (2002). A hassle a day may keep the pathogens away: The fight-or-flight stress response and the augmentation of immune function. *Integrative and Comparative Biology*, *42*,

556–564. https://doi.org/10.1093/icb/icp045

Dingemanse, N. J., Both, C., Drent, P. J., & Tinbergen, J. M. (2004). Fitness consequences of avian personalities in a fluctuating environment. *Proceedings of the Royal Society B: Biological Sciences*, *271*, 847–852. https://doi.org/10.1098/rspb.2004.2680

Dingemanse, N. J., & Wolf, M. (2010). Recent models for adaptive personality differences: A review. *Philosophical Transactions of the Royal Society B: Biological Sciences*, *365*, 3947–3958. https://doi.org/10.1098/rstb.2010.0221

Dirzo, R., Young, H. S., Galetti, M., Ceballos, G., Isaac, N. J. B., & Collen, B. (2014). Defaunation in the Anthropocene. *Science*, *345*, 401–406. https://doi.org/10.1126/science.1251817

Dugatkin, L. A., & Alfieri, M. S. (2003). Boldness, behavioral inhibition and learning. *Ethology Ecology & Evolution*, *15*, 43–49. https://doi.org/10.1080/08927014.2003.9522689

Dupuis-Desormeaux, M., Davy, C., Lathrop, A., Followes, E., Ramesbottom, A., Chreston, A., & MacDonald, S. E. (2018). Colonization and usage of an artificial urban wetland complex by freshwater turtles. *PeerJ*, *6*, e5423. https://doi.org/10.7717/peerj.5423

Dyer, J. R. G., Croft, D. P., Morrell, L. J., & Krause, J. (2009). Shoal composition determines foraging success in the guppy. *Behavioral Ecology*, *20*, 165–171. https://doi.org/10.1093/beheco/arn129

Eisenhauer, N., Bowker, M. A., Grace, J. B., & Powell, J. R. (2015). From patterns to causal understanding: Structural equation modeling (SEM) in soil ecology. *Pedobiologia*, *58*, 65–72. https://doi.org/10.1016/j.pedobi.2015.03.002

Ernst, C. H., & Lovich, J. E. (2009). *Turtles of the United States and Canada*. The Johns Hopkins University Press.

ESRI. (2019). *ArcGIS Desktop*. Release 10.7.1. Environmental Systems Research Institute (ESRI). https://www.esri.com/en-us/arcgis/products/arcgis-desktop/overview

ESRI. (2021). *Word Imagery* [Basemap]. Environmental Systems Research Institute (ESRI). https://www.arcgis.com/home/item.html?id=10df2279f9684e4a9f6a7f08febac2a9

Evanno, G., Regnaut, S., & Goudet, J. (2005). Detecting the number of clusters of individuals using the software STRUCTURE: A simulation study. *Molecular Ecology*, *14*, 2611–2620. https://doi.org/10.1111/j.1365-294X.2005.02553.x

Fahrig, L. (2003). Effects of habitat fragmentation on biodiversity. *Annual Review of Ecology, Evolution, and Systematics*, *34*, 487–515. https://doi.org/10.1146/annurev.ecolsys.34.011802.132419

Faivre, B., Grégoire, A., Préault, M., Cézilly, F., & Sorci, G. (2003). Immune activation rapidly mirrored in a secondary sexual trait. *Science*, *300*, 103. https://doi.org/10.1126/science.1081802

Fan, Y., Chen, J., Shirkey, G., John, R., Wu, S. R., Park, H., & Shao, C. (2016). Applications of structural equation modeling (SEM) in ecological studies: An updated review. *Ecological Processes*, *5*: 19. https://doi.org/10.1186/s13717-016-0063-3

Fokidis, H. B., Greiner, E. C., & Deviche, P. (2008). Interspecific variation in avian blood parasites and haematology associated with urbanization in a desert habitat. *Journal of Avian Biology*, *39*, 300–310. https://doi.org/10.1111/j.0908-8857.2008.04248.x

Foley, J. A., Defries, R., Asner, G. P., Barford, C., Bonan, G., Carpenter, S. R., Chapin, F. S., Coe, M. T., Daily, G. C., Gibbs, H. K., Helkowski, J. H., Holloway, T., Howard, E. A., Kucharik, C. J., Monfreda, C., Patz, J. A., Prentice, I. C., Ramankutty, N., & Snyder, P. K. (2005). Global

consequences of land use. *Science*, *309*, 570–574.

Fraik, A. K., McMillan, J. R., Liermann, M., Bennett, T., McHenry, M. L., McKinney, G. J., Wells, A. H., Winans, G., Kelley, J. L., Pess, G. R., & Nichols, K. M. (2021). The impacts of dam construction and removal on the genetics of recovering steelhead (*Oncorhynchus mykiss*) populations across the Elwha river watershed. *Genes*, *12*, 89. https://doi.org/10.3390/genes12010089

Frankham, R. (1996). Relationship of genetic variation to population size in wildlife. *Conservation Biology*, *10*, 1500–1508. https://doi.org/10.1046/j.1523-1739.1996.10061500.x

Fuller, M. R., Doyle, M. W., & Strayer, D. L. (2015). Causes and consequences of habitat fragmentation in river networks. *Annals of the New York Academy of Sciences*, *1355*, 31–51. https://doi.org/10.1111/nyas.12853.

Fyson, V. K., & Blouin-Demers, G. (2021). Effects of landscape composition on wetland occupancy by blanding's turtles (*Emydoidea blandingii*) as determined by environmental DNA and visual surveys. *Canadian Journal of Zoology*, *99*, 672–680. https://doi.org/10.1139/cjz-2021-0004

Gabry, J., & Veen, D. (2022). *shinystan: Interactive visual and numerical diagnostics and posterior analysis for Bayesian models*. R package version 2.6.0, https://CRAN.R-project.org/package=shinystan.

Gaynor, K. M., Hojnowski, C. E., Carter, N. H., & Brashares, J. S. (2018). The influence of human disturbance on wildlife nocturnality. *Science*, *360*, 1232–1235. https://doi.org/10.1126/science.aar7121

Gelman, A., Carlin, J. B., Stern, H. S., Dunson, D. B., Vehtari, A., & Rubin, D. B. (2022). *Bayesian*

*data analysis*. CRC Press. https://doi.org/10.4135/9781071812082.n42

Germano, J. M., Nafus, M. G., Perry, J. A., Hall, D. B., & Swaisgood, R. R. (2017). Predicting translocation outcomes with personality for desert tortoises. *Behavioral Ecology*, *28*, 1075–1084. https://doi.org/10.1093/beheco/arx064

Gibbons, J. W. (1968). Reproductive potential, activity, and cycles in the painted turtle, *Chrysemys Picta*. *Ecology*, *49*, 399–409. https://doi.org/10.2307/1934106

Gibbons, J. W. (1987). Why do turtles live so long? *BioScience*, *37*, 262–269. https://doi.org/10.2307/1310589

Gibbons, J. W., Greene, J. L., & Congdon, J. D. (1990). Temporal and spatial movement patterns of sliders and other turtles. In J. W. Gibbons (Ed.), *Life History and Ecology of the Slider Turtle* (pp. 201–2015). Smithsonian Institution.

Gibbons, J. W., Scott, D. E., Ryan, T. J., Buhlmann, K. A., Tuberville, T. D., Metts, B. S., Greene, J. L., Mills, T., Leiden, Y., Poppy, S., & Winne, C. T. (2000). The global decline of reptiles, Déjà vu Amphibians. *BioScience*, *50*, 653–666. https://doi.org/10.1641/0006-3568(2000)050[0653:TGDORD]2.0.CO;2

Goodrich, B., Gabry, J., Ali, I., & Brilleman, S. (2022). *rstanarm: Bayesian applied regression modeling via Stan*. R package version 2.21.3 https://mc-stan.org/rstanarm

Goodwin, T. W. (1980). *The Biochemistry of the Carotenoids, Volume 1: Plants*. Chapman and Hall. https://doi.org/10.1042/bst0090484

Goodwin, T. W. (1984). *The Biochemistry of Carotenoids. Volume 2: Animals.* Chapman and Hall. https://doi.org/10.1007/BF00226367

Gottdenker, N. L., & Jacobson, E. R. (1995). Effect of venipuncture sites on hematologic and clinical

biochemical values in desert tortoises *Gopherus agassizii*. *American Journal of Veterinary*

*Research*, *56*, 19–21.

Greene, H. W. (1988). Antipredator mechanisms in reptiles. In C. Gans & R. B. Huey (Eds.), *Biology*

*of the reptilian* (pp. 1–152). Branta Books.

Griffin, L. P., Brownscombe, J. W., Gagné, T. O., Wilson, A. D. M., Cooke, S. J., & Danylchuk, A. J.

(2017). Individual-level behavioral responses of immature green turtles to snorkeler disturbance.

*Oecologia*, *183*, 909–917. https://doi.org/10.1007/s00442-016-3804-1

Grill, G., Lehner, B., Lumsdon, A. E., MacDonald, G. K., Zarfl, C., & Reidy Liermann, C. (2015). An

index-based framework for assessing patterns and trends in river fragmentation and flow

regulation by global dams at multiple scales. *Environmental Research Letters*, *10*, 015001.

https://doi.org/10.1088/1748-9326/10/1/015001

Gustafson, K. D., Gagne, R. B., Vickers, T. W., Riley, S. P. D., Wilmers, C. C., Bleich, V. C., Pierce,

B. M., Kenyon, M., Drazenovich, T. L., Sikich, J. A., Boyce, W. M., & Ernest, H. B. (2019).

Genetic source–sink dynamics among naturally structured and anthropogenically fragmented

puma populations. *Conservation Genetics*, *20*, 215–227. https://doi.org/10.1007/s10592-018-

1125-0

Haddad, N. M., Brudvig, L. A., Clobert, J., Davies, K. F., Gonzalez, A., Holt, R. D., Lovejoy, T. E.,

Sexton, J. O., Austin, M. P., Collins, C. D., Cook, W. M., Damschen, E. I., Ewers, R. M., Foster,

B. L., Jenkins, C. N., King, A. J., Laurance, W. F., Levey, D. J., Margules, C. R., … Townshend,

J. R. (2015). Habitat fragmentation and its lasting impact on Earth's ecosystems. *Science*

*Advances*, *1*, e1500052. https://doi.org/10.1126/sciadv.1500052

Hadfield, J. D. (2010). MCMC methods for multi-response generalized linear mixed models: The MCMCglmm R package. *Journal of Statistical Software*, *33*(2), 1–22. https://doi.org/10.18637/jss.v033.i02

Hailer, F., Helander, B., Folkestad, A. O., Ganusevich, S. A., Garstad, S., Hauff, P., Koren, C., Nygård, T., Volke, V., Vilà, C., & Ellegren, H. (2006). Bottlenecked but long-lived: High genetic diversity retained in white-tailed eagles upon recovery from population decline. *Biology Letters*, *2*, 316–319. https://doi.org/10.1098/rsbl.2006.0453

Hardman, S. I., & Dalesman, S. (2018). Repeatability and degree of territorial aggression differs among urban and rural great tits (*Parus major*). *Scientific Reports*, *8*, 5042. https://doi.org/10.1038/s41598-018-23463-7

Harms, C. A., Jinks, M. R., & Harms, R. V. (2016). Blood gas, lactate, and hematology effects of venipuncture timing and location after mist-net capture of mourning doves (*Zenaida macroura*), boat-tailed grackles (*Quiscalus major*), and house sparrows (*Passer domesticus*). *Journal of Wildlife Diseases*, *52*, S54–S64. https://doi.org/10.7589/52.2S.S54

Harrell, F. E. (2020). *Hmisc: Harrell Miscellaneous*. R package version 4.4-2. https://CRAN.R-project.org/package=Hmisc

Hauswaldt, J. S., & Glenn, T. C. (2003). Microsatellite DNA loci from the Diamondback terrapin (*Malaclemys terrapin*). *Molecular Ecology Notes*, *3*, 174–176. https://doi.org/10.1046/j.1471-8286.2003.00388.x

Heatley, J. J., & Russell, K. E. (2018). Hematology. In S. J. Divers & J. Stahl, Scott (Eds.), *Reptile and Amphibian Medicine and Surgery* (pp. 301–318). Elsevier.

Hedrick, P. W. (2005). A standardized genetic differentiation measure. *Evolution*, *59*, 1633–1638. https://doi.org/10.1111/j.0014-3820.2005.tb01814.x

Hevia, G. D., Bertellotti, M., Gibson, D., & D'amico, V. L. (2023). Does human disturbance affect physiological traits of two-banded plovers nesting on an urban beach? *Avian Conservation and Ecology*, *18*, 2. https://doi.org/10.5751/ACE-02365-180102

Hill, G. E. (1992). Proximate basis of variation in carotenoid pigmentation in male house finches. *The Auk*, *109*, 1–12. https://doi.org/10.2307/4088262

Hill, G. E. (1996). Redness as a measure of the production cost of ornamental coloration. *Ethology Ecology and Evolution*, *8*, 157–175. https://doi.org/10.1080/08927014.1996.9522926

Holderegger, R., & Wagner, H. H. (2008). Landscape Genetics. *BioScience*, *58*, 199–207. https://doi.org/10.1016/B978-0-12-384719-5.00386-5

Holtmann, B., Lagisz, M., & Nakagawa, S. (2017). Metabolic rates, and not hormone levels, are a likely mediator of between-individual differences in behaviour: A meta-analysis. *Functional Ecology*, *31*, 685–696. https://doi.org/10.1111/1365-2435.12779

Holtmann, B., Santos, E. S. A., Lara, C. E., & Nakagawa, S. (2017). Personality-matching habitat choice rather than behavioural plasticity, is a likely driver of phenotype-environment covariance. *Proceedings of the Royal Society B: Biological Sciences*, *284*, 20170943. https://doi.org/10.1098/rspb.2017.0943

Ibáñez, A., López, P., & Martín, J. (2012). Discrimination of conspecifics' chemicals may allow spanish terrapins to find better partners and avoid competitors. *Animal Behaviour*, *83*, 1107–1113. https://doi.org/10.1016/j.anbehav.2012.02.001

Ibáñez, A., Martín, J., Gazzola, A., & Pellitteri-Rosa, D. (2018). Freshwater turtles reveal personality traits in their antipredatory behaviour. *Behavioural Processes*, *157*, 142–147. https://doi.org/10.1016/j.beproc.2018.08.011

Ibáñez, A., Marzal, A., López, P., & Martín, J. (2013a). Boldness and body size of male spanish terrapins affect their responses to chemical cues of familiar and unfamiliar males. *Behavioral Ecology and Sociobiology*, *67*, 541–548. https://doi.org/10.1007/s00265-012-1473-6

Ibáñez, A., Marzal, A., López, P., & Martín, J. (2013b). Sexually dichromatic coloration reflects size and immunocompetence in female spanish terrapins, *Mauremys leprosa*. *Naturwissenschaften*, *100*, 1137–1147. https://doi.org/10.1109/ICIT.2017.7915458

Ibáñez, A., Marzal, A., López, P., & Martín, J. (2015). Reproductive state affects hiding behaviour under risk of predation but not exploratory activity of female Spanish terrapins. *Behavioural Processes*, *111*, 90–96. https://doi.org/10.1016/j.beproc.2014.12.004

Ibáñez, A., Polo-Cavia, N., López, P., & Martín, J. (2014). Honest sexual signaling in turtles: experimental evidence of a trade-off between immune response and coloration in red-eared sliders *Trachemys scripta elegans*. *Naturwissenschaften*, *101*, 803–811. https://doi.org/10.1007/s00114-014-1219-6

Jacob, S., Bestion, E., Legrand, D., Clobert, J., & Cote, J. (2015). Habitat matching and spatial heterogeneity of phenotypes: implications for metapopulation and metacommunity functioning. *Evolutionary Ecology*, *29*, 851–871. https://doi.org/10.1007/s10682-015-9776-5

Jaeger, C. P., & Cobb, V. A. (2012). Comparative spatial ecologies of female painted turtles (*Chrysemys picta*) and red-eared sliders (*Trachemys scripta*) at Reelfoot Lake, Tennessee.

*Chelonian Conservation and Biology*, *11*, 59–67. https://doi.org/10.2744/CCB-0949.1

Jain-Schlaepfer, S. M. R., Blouin-Demers, G., Cooke, S. J., & Bulté, G. (2017). Do boating and

basking mix? The effect of basking disturbances by motorboats on the body temperature and

energy budget of the northern map turtle. *Aquatic Conservation: Marine and Freshwater*

*Ecosystems*, *27*, 547–558. https://doi.org/10.1002/aqc.2693

Jansson, R., Nilsson, C., & Renöfält, B. (2000). Fragmentation of riparian floras in rivers with

multiple dams. *Ecology*, *81*, 899–903. https://doi.org/10.1890/0012-

9658(2000)081[0899:FORFIR]2.0.CO;2

Javanbakht, H., Vaissi, S., & Parto, P. (2013). The morphological characterization of the blood cells in

the three species of turtle and tortoise in Iran. *Research in Zoology*, *3*, 38–44.

https://doi.org/10.5923/j.zoology.20130301.06

Jonsson, N. (1991). Influence of water flow, water temperature and light on fish migration in rivers.

*Nordic Journal of Freshwater Ressources*, *66*, 20–35.

Judson, J. M. (2021). Selection and population demography shape evolution of two long-lived

ectotherms. [Ph.D. Thesis, Iowa State University]. ProQuest Dissertations Publishing.

https://login.proxy.bib.uottawa.ca/login?url=https://www.proquest.com/dissertations-

theses/selection-population-demography-shape-evolution/docview/2553803321/se-2

Junker, J., Peter, A., Wagner, C. E., Mwaiko, S., Germann, B., Seehausen, O., & Keller, I. (2012).

River fragmentation increases localized population genetic structure and enhances asymmetry of

dispersal in bullhead (*Cottus gobio*). *Conservation* Genetics, *13*, 545–556.

https://doi.org/10.1007/s10592-011-0306-x

Kamvar Z. N., Tabima J. F., Grünwald N. J. (2014). Poppr: an R package for genetic analysis of populations with clonal, partially clonal, and/or sexual reproduction. *PeerJ*, *2*, e281. https://doi.org/10.7717/peerj.281

Kashon, E. A. F., & Carlson, B. E. (2018). Consistently bolder turtles maintain higher body temperatures in the field but may experience greater predation risk. *Behavioral Ecology and Sociobiology*, *72*, 9. https://doi.org/10.1007/s00265-017-2428-8

Kassab, A., Shousha, S., & Fargani, A. (2009). Morphology of blood cells , liver and spleen of the desert tortoise (*Testudo graeca*). *The Open Anatomy Journal*, *1*, 1–10. https://doi.org/10.2174/1877609400901010001

Keenan K., McGinnity P., Cross T. F., Crozier, W. W., & Prodöhl, P. A. (2013). diveRsity: An R package for the estimation of population genetics parameters and their associated errors. *Methods in Ecology and Evolution*, *4*, 782–788. https://doi.org/10.1111/2041-210X.12067

Kennedy, C. M., Oakleaf, J. R., Theobald, D. M., Baruch-Mordo, S., & Kiesecker, J. (2019). Managing the middle: A shift in conservation priorities based on the global human modification gradient. *Global Change Biology*, *25*, 811–826. https://doi.org/10.1111/gcb.14549

Kettel, E. F., Gentle, L. K., Quinn, J. L., & Yarnell, R. W. (2018). The breeding performance of raptors in urban landscapes: A review and meta-analysis. *Journal of Ornithology*, *159*, 1–18. https://doi.org/10.1007/s10336-017-1497-9

King, T. L., & Julian, S. E. (2004). Conservation of microsatellite DNA flanking sequence across 13 Emydid genera assayed with novel bog turtle (*Glyptemys muhlenbergii*) loci. *Conservation Genetics*, *5*, 719–725. https://doi.org/10.1007/s10592-004-1854-0

Koolhaas, J. M., Korte, S. M., De Boer, S. F., Van Der Vegt, B. J., Van Reenen, C. G. ., Hopster, J. M., De Jong, I. C., Ruis, M. A. W., & Blokhuis, H. J. (1999). Coping styles in animals: Current status in behavior and stress-physiology. *Neuroscience and Biobehavioral Reviews*, *23*, 925–935. https://doi.org/10.1016/S0149-7634(99)00026-3

Kopelman, N. M., Mayzel, J., Jakobsson, M., Rosenberg, N. A., & Mayrose, I. (2015). Clumpak: A program for identifying clustering modes and packaging population structure inferences across K. *Molecular Ecology Resources*, *15*, 1179–1191. https://doi.org/10.1111/1755-0998.12387

Koschorreck, M., Downing, A. S., Hejzlar, J., Marcé, R., Laas, A., Arndt, W. G., Keller, P. S., Smolders, A. J. P., van Dijk, G., & Kosten, S. (2020). Hidden treasures: Human-made aquatic ecosystems harbour unexplored opportunities. *Ambio*, *49*, 531–540. https://doi.org/10.1007/s13280-019-01199-6

Kuo, C.-H., & Janzen, F. J. (2004). Genetic effects of a persistent bottleneck on a natural population of ornate box turtles (*Terrapene ornata*). *Conservation Genetics*, *5*, 425–437. https://doi.org/10.1023/B:COGE.0000041020.54140.45

Landguth, E. L., Cushman, S. A., Schwartz, M. K., McKelvey, K. S., Murphy, M., & Luikart, G. (2010). Quantifying the lag time to detect barriers in landscape genetics. *Molecular Ecology*, *19*, 4179–4191. https://doi.org/10.1111/j.1365-294X.2010.04808.x

Laporte, M., Silva Beaudry, C. O., & Angers, B. (2013). Effects of road proximity on genetic diversity and reproductive success of the painted turtle (*Chrysemys picta*). *Conservation Genetics*, *14*, 21–30. https://doi.org/10.1007/s10592-012-0419-x

Larson, C. L., Reed, S. E., Merenlender, A. M., & Crooks, K. R. (2016). Effects of recreation on

animals revealed as widespread through a global systematic review. *PLoS ONE*, *11*, e0167259. https://doi.org/10.1371/journal.pone.0167259

Legget, R. F. (1986). *Rideau Waterway* (Vol. 3). University of Toronto Press.

Leigh, D. M., Hendry, A. P., Vázquez-Domínguez, E., & Friesen, V. L. (2019). Estimated six per cent loss of genetic variation in wild populations since the industrial revolution. *Evolutionary Applications*, *12*, 1505–1512. https://doi.org/10.1111/eva.12810

Lenormand, T. (2002). Gene flow and the limits to natural selection. *Trends in Ecology and Evolution*, *17*, 183–189. https://doi.org/10.1111/j.1365-2184.1976.tb01248.x

Lentfer, T. L., Pendl, H., Gebhardt-Henrich, S. G., Fröhlich, E. K. F., & Von Borell, E. (2015). H/L ratio as a measurement of stress in laying hens - methodology and reliability. *British Poultry Science*, *56*, 157–163. https://doi.org/10.1080/00071668.2015.1008993

Lessells, C. M., & Boag, P. T. (1987). Unrepeatable repeatabilities: A common mistake. *The Auk*, *104*, 116–121.

Libants, S., Kamarainen, A. M., Scribner, K. T., & Congdon, J. D. (2004). Isolation and cross-species amplification of seven microsatellite loci from *Emydoidea blandingii*. *Molecular Ecology Notes*, *4*, 300–302. https://doi.org/10.1111/j.1471-8286.2004.00650.x

Lin, H. Y., Cooke, S. J., Wolter, C., Young, N., & Bennett, J. R. (2020). On the conservation value of historic canals for aquatic ecosystems. *Biological Conservation*, *251*, 108764. https://doi.org/10.1016/j.biocon.2020.108764

Lindeman, P. V. (1999). Aggressive interactions during basking among four species of emydid turtles. *Journal of Herpetology*, *33*, 214–219. https://doi.org/10.2307/1565717

Lippé, C., Dumont, P., & Bernatchez, L. (2006). High genetic diversity and no inbreeding in the endangered copper redhorse, *Moxostoma hubbsi* (Catostomidae, Pisces): The positive sides of a long generation time. *Molecular Ecology*, *15*, 1769–1780. https://doi.org/10.1111/j.1365-294X.2006.02902.x

Liu, X., Wu, R., Chen, X., Zhou, Y., Yang, L., Ouyang, S., & Wu, X. (2020). Effects of dams and their environmental impacts on the genetic diversity and connectivity of freshwater mussel populations in Poyang Lake Basin, China. *Freshwater Biology*, *65*, 264–277. https://doi.org/10.1111/fwb.13419

Liu, Y., Davy, C. M., Shi, H.-T., & Murphy, R. W. (2013). Six in the half-shell: a review of the functions and evolution of courtship behavior in freshwater turtles. *Chelonian Conservation and Biology*, *12*, 84–100. https://doi.org/10.2744/CCB-1037.1

Loiseau, C., Fellous, S., Haussy, C., Chastel, O., & Sorci, G. (2008). Condition-dependent effects of corticosterone on a carotenoid-based begging signal in house sparrows. *Hormones and Behavior*, *53*, 266–273. https://doi.org/10.1016/j.yhbeh.2007.10.006

Lovich, J. (1988). Aggressive basking behavior in eastern painted turtles (*Chrysemys picta picta*). *Herpetologica*, *44*, 197–202.

Lovich, J. E., Ennen, J. R., Agha, M., & Gibbons, J. W. (2018). Where have all the turtles gone, and why does it matter? *BioScience*, *68*, 771–781. https://doi.org/10.1093/biosci/biy095

Lowe, W. H., & Allendorf, F. W. (2010). What can genetics tell us about population connectivity? *Molecular Ecology*, *19*, 3038–3051. https://doi.org/10.1111/j.1365-294X.2010.04688.x

Lowry, H., Lill, A., & Wong, B. B. M. (2013). Behavioural responses of wildlife to urban

environments. *Biological Reviews*, *88*, 537–549. https://doi.org/10.1111/brv.12012

Lüdecke D. (2018). ggeffects: Tidy data frames of marginal effects from regression models. *Journal of Open Source Software*, *3*, 772.

Lyons, J., Mastromonaco, G., Edwards, D. B., & Schulte-Hostedde, A. I. (2017). Fat and happy in the city: Eastern chipmunks in urban environments. *Behavioral Ecology*, *28*, 1464–1471. https://doi.org/10.1093/beheco/arx109

Mafli, A., Wakamatsu, K., & Roulin, A. (2011). Melanin-based coloration predicts aggressiveness and boldness in captive eastern Hermann's tortoises. *Animal Behaviour*, *81*, 859–863. https://doi.org/10.1016/j.anbehav.2011.01.025

Maia, J. P., James Harris, D., Carranza, S., & Gómez-Díaz, E. (2014). A comparison of multiple methods for estimating parasitemia of hemogregarine hemoparasites (apicomplexa: Adeleorina) and its application for studying infection in natural populations. *PLoS ONE*, *9*, e95010. https://doi.org/10.1371/journal.pone.0095010

Manel, S., Schwartz, M. K., Luikart, G., & Taberlet, P. (2003). Landscape genetics: Combining landscape ecology and population genetics. *Trends in Ecology and Evolution*, *18*, 189–197. https://doi.org/10.1016/S0169-5347(03)00008-9

Martin, A. E., Collins, S. J., Crowe, S., Girard, J., Naujokaitis-Lewis, I., Smith, A. C., Lindsay, K., Mitchell, S., & Fahrig, L. (2020). Effects of farmland heterogeneity on biodiversity are similar to - or even larger than - the effects of farming practices. *Agriculture, Ecosystems and Environment*, *288*, 106698. https://doi.org/10.1016/j.agee.2019.106698

Martin, J. G. A., & Réale, D. (2008). Animal temperament and human disturbance: Implications for

the response of wildlife to tourism. *Behavioural Processes*, *77*, 66–72.

https://doi.org/10.1016/j.beproc.2007.06.004

Martin, L. B. (2009). Stress and immunity in wild vertebrates: Timing is everything. *General and Comparative Endocrinology*, *163*, 70–76. https://doi.org/10.1016/j.ygcen.2009.03.008

Martínez-Padilla, J., Mougeot, F., García, J. T., Arroyo, B., & Bortolotti, G. R. (2013). Feather corticosterone levels and carotenoid-based coloration in common buzzard (*Buteo buteo*) nestlings. *Journal of Raptor Research*, *47*, 161–173. https://doi.org/10.3356/JRR-12-41.1

McBlain, M., Jones, K. A., & Shannon, G. (2020). Sleeping eurasian oystercatchers adjust their vigilance in response to the behaviour of neighbours, human disturbance and environmental conditions. *Journal of Zoology*, *312*, 75–84. https://doi.org/10.1111/jzo.12812

McCauley, D. J., Pinsky, M. L., Palumbi, S. R., Estes, J. A., Joyce, F. H., & Warner, R. R. (2015). Marine defaunation: Animal loss in the global ocean. *Science*, *347*, 1255641. https://doi.org/10.1126/science.1255641

McDougall, P. T., Réale, D., Sol, D., & Reader, S. M. (2006). Wildlife conservation and animal temperament: Causes and consequences of evolutionary change for captive, reintroduced, and wild populations. *Animal Conservation*, *9*, 39–48. https://doi.org/10.1111/j.1469-1795.2005.00004.x

Mcgraw, K. J. (2005). The antioxidant function of many animal pigments: Are there consistent health benefits of sexually selected colourants? *Animal Behaviour*, *69*, 757–764. https://doi.org/10.1016/j.anbehav.2004.06.022

Mcrae, B. H., Hall, S. A., Beier, P., & Theobald, D. M. (2012). Where to restore ecological

connectivity? Detecting barriers and quantifying restoration benefits. *PloS ONE*, *7*, e52604.

https://doi.org/10.1371/journal.pone.0052604

Midwood, J. D., Cairns, N. A., Stoot, L. J., Cooke, S. J., & Blouin-Demers, G. (2015). Bycatch

mortality can cause extirpation in four freshwater turtle species. *Aquatic Conservation: Marine and Freshwater Ecosystems*, *25*, 71–80. https://doi.org/10.1002/aqc.2475

Miranda, A. C., Schielzeth, H., Sonntag, T., & Partecke, J. (2013). Urbanization and its effects on

personality traits: A result of microevolution or phenotypic plasticity? *Global Change Biology*, *19*, 2634–2644. https://doi.org/10.1111/gcb.12258

Moldowan, P. D., Brooks, R. J., & Litzgus, J. D. (2020a). Demographics of injuries indicate sexual

coercion in a population of painted turtles (*Chrysemys picta*). *Canadian Journal of Zoology*, *98*, 269–278. https://doi.org/10.1139/cjz-2019-0238

Moldowan, P. D., Brooks, R. J., & Litzgus, J. D. (2020b). Sex, shells, and weaponry: coercive

reproductive tactics in the painted turtle, *Chrysemys picta*. *Behavioral Ecology and Sociobiology*, *74*, 142. https://doi.org/10.1007/s00265-020-02926-w

Møller, A. P. (2008). Flight distance of urban birds, predation, and selection for urban life. *Behavioral Ecology and Sociobiology*, *63*, 63–75. https://doi.org/10.1007/s00265-008-0636-y

Montgomery, R. A., Raupp, J., & Parkhurst, M. (2021). Animal behavioral responses to the COVID-

19 quietus. *Trends in Ecology and Evolution*, *36*, 184–186.

https://doi.org/10.1016/j.tree.2020.12.008

Moore, M. J. C., & Seigel, R. A. (2006). No place to nest or bask: Effects of human disturbance on the

nesting and basking habits of yellow-blotched map turtles (*Graptemys flavimaculata*). *Biological*

*Conservation*, *130*, 386–393. https://doi.org/10.1016/j.biocon.2006.01.001

Morjan, C. L., & Rieseberg, L. H. (2004). How species evolve collectively: Implications of gene flow and selection for the spread of advantageous alleles. *Molecular Ecology*, *13*, 1341–1356. https://doi.org/10.1111/j.1365-294X.2004.02164.x

Morreale, S. J., Gibbons, J. W., & Congdon, J. D. (1984). Significance of activity and movement in the yellow-bellied slider turtle (*Pseudemys scripta*). *Canadian Journal of Zoology*, *62*, 1038–1042. https://doi.org/10.1139/z84-148

Mouchet, A., & Dingemanse, N. J. (2021). A quantitative genetics approach to validate lab- versus field-based behavior in novel environments. *Behavioral Ecology*, *32*, 903–911. https://doi.org/10.1093/beheco/arab059

Mueller, J. C., Partecke, J., Hatchwell, B. J., Gaston, K. J., & Evans, K. L. (2013). Candidate gene polymorphisms for behavioural adaptations during urbanization in blackbirds. *Molecular Ecology*, *22*, 3629–3637. https://doi.org/10.1111/mec.12288

Mumm, L. E., Winter, J. M., Andersson, K. E., Glowacki, G. A., Adamovicz, L. A., & Allender, M. C. (2019). Hematology and plasma biochemistries in the blanding's turtle (*Emydoidea blandingii*) in Lake County, Illinois. *PLoS ONE*, *14*, e0225130. https://doi.org/10.1371/journal.pone.0225130

Muposhi, V. K., Gandiwa, E., Makuza, S. M., & Bartels, P. (2017). Ecological, physiological, genetic trade-offs and socio-economic implications of trophy hunting as a conservation tool: A narrative review. *Journal of Animal and Plant Sciences*, *27*, 1–14.

Muth, C., Oravecz, Z., & Gabry, J. (2018). User-friendly Bayesian regression modeling: A tutorial

with rstanarm and shinystan. *The Quantitative Methods for Psychology*, *14*, 99–119. https://doi.org/10.20982/tqmp.14.2.p099

Nagle, R. D., Kinney, O. M., Gibbons, J. W., & Congdon, J. D. (2017). A simple and reliable system for marking hard-shelled turtles: the North American code. *Herpetological Review*, *48*, 327–330.

Nakagawa, S., & Schielzeth, H. (2010). Repeatability for Gaussian and non-Gaussian data: A practical guide for biologists. *Biological Reviews*, *85*, 935–956. https://doi.org/10.1111/j.1469-185X.2010.00141.x

Nardini, G., Leopardi, S., & Bielli, M. (2013). Clinical hematology in reptilian species. *Veterinary Clinics of North America - Exotic Animal Practice*, *16*, 1–30. https://doi.org/10.1016/j.cvex.2012.09.001

Nickel, B. A., Suraci, J. P., Allen, M. L., & Wilmers, C. C. (2020). Human presence and human footprint have non-equivalent effects on wildlife spatiotemporal habitat use. *Biological Conservation*, *241*, 108383. https://doi.org/10.1016/j.biocon.2019.108383

Nilsson, C. (2005). Fragmentation and flow regulation of the world's large river systems. *Science*, *308*, 405–408. https://doi.org/10.1126/science.1107887

Olsson, M., & Madsen, T. (1998). Sexual selection and sperm competition in reptiles. In T. Birkhead & A. Møller (Eds.), *Sperm Competition and Sexual Selection* (pp. 503–577). Academic Press. https://doi.org/10.1016/b978-012100543-6/50038-6

OMNRF. (2019). *Southern Ontario Land Resource Information System (SOLRIS) 3.0.* Ontario Ministry of Natural Resources and Forestry (OMNRF). https://geohub.lio.gov.on.ca/documents/0279f65b82314121b5b5ec93d76bc6ba/about

Palacios, M. G., Amico, V. L. D., & Bertellotti, M. (2018). Ecotourism effects on health and immunity of magellanic penguins at two reproductive colonies with disparate touristic regimes and population trends. *Conservation Physiology*, *6*, coy060. https://doi.org/10.1093/conphys/coy060

Paradis, E. (2010). Pegas: An R package for population genetics with an integrated–modular approach. *Bioinformatics*, *26*, 419–420. https://doi.org/10.1093/bioinformatics/btp696

Parks Canada (2006). *Nomination of the Rideau Canal by the Government of Canada, 2006 for the Inscription on the Word Heritage List.* https://whc.unesco.org/uploads/nominations/1221.pdf

Pascual, J., & Senar, J. C. (2014). Antipredator behavioural compensation of proactive personality trait in male Eurasian siskins. *Animal Behaviour*, *90*, 297–303. https://doi.org/10.1016/j.anbehav.2014.02.002

Paterson, J. E., & Blouin-Demers, G. (2017). Distinguishing discrete polymorphism from continuous variation in throat colour of tree lizards, *Urosaurus ornatus*. *Biological Journal of the Linnean Society*, *121*, 72–81. https://doi.org/10.1093/biolinnean/blw024

Paterson, J. E., & Blouin-Demers, G. (2020). High tolerance of two parasites in ornate tree lizards reduces the fitness costs of parasitism. *Journal of Zoology*, *312*, 102–110. https://doi.org/10.1111/jzo.12795

Peakall, R., & Smouse, P. E. (2012). GenAlEx 6.5: genetic analysis in Excel. Population genetic software for teaching and research-an update. *Bioinformatics*, *28*, 2537–2539. https://doi.org/10.1093/bioinformatics/bts460

Pearse, D. E., Janzen, F. J., & Avise, J. C. (2001). Genetic markers substantiate long-term storage and utilization of sperm by female painted turtles. *Heredity*, *86*, 378–384.

https://doi.org/10.1046/j.1365-2540.2001.00841.x

Pérez-Rodríguez, L., & Viñuela, J. (2008). Carotenoid-based bill and eye ring coloration as honest signals of condition: An experimental test in the red-legged partridge (*Alectoris rufa*). *Naturwissenschaften*, *95*, 821–830. https://doi.org/10.1007/s00114-008-0389-5

Perkin, J. S., & Gido, K. B. (2012). Fragmentation alters stream fish community structure in dendritic ecological networks. *Ecological Applications*, *22*, 2176–2187. https://doi.org/10.1890/12-0318.1

Perpiñán, D. (2017). Chelonian haematology 1. Collection and handling of samples. *In Practice*, *39*, 194–202. https://doi.org/10.1136/inp.j1692

Pich, J. M., Belden, A. J., & Carlson, B. E. (2019). Individual variation in boldness in turtles is consistent across assay conditions and behavioural measures. *Behaviour*, *156*, 1039–1056. https://doi.org/10.1163/1568539X-00003555

Polich, R. L., & Barazowski, M. (2016). Flight initiation distance in a freshwater turtle, *Chrysemys picta*. *Chelonian Conservation and Biology*, *15*, 214–218. https://doi.org/10.2744/CCB-1164.1

Polo-Cavia, N., López, P., & Martín, J. (2013). Head coloration reflects health state in the red-eared slider *Trachemys scripta elegans*. *Behavioral Ecology and Sociobiology*, *67*, 153–162. https://doi.org/10.1007/s00265-012-1435-z

Porras-Hurtado, L., Ruiz, Y., Santos, C., Phillips, C., Carracedo, Á., & Lareu, M. V. (2013). An overview of STRUCTURE: Applications, parameter settings, and supporting software. *Frontiers in Genetics*, *4*, 98. https://doi.org/10.3389/fgene.2013.00098

Posit Team. (2022). *RStudio: Integrated Development Environment for R. Posit Software*, PBC, Boston, MA. http://www.posit.co/.

Prange, S., Gehrt, S. D., & Wiggers, E. P. (2003). Demographic factors contributing to high raccoon densities in urban landscapes. *Journal of Wildlife Management*, *67*, 324–333. https://doi.org/10.2307/3802774

Price, M. (2008). The impact of human disturbance on birds: A selective review. In D. Lunney, A. Munn, & W. Meikle (Eds.), *Too close for comfort: Conflicts in human wildlife encounters* (pp. 163–196). Royal Zoological Society of New South Wales.

Pritchard, J. K., Stephens, M., & Donnelly, P. (2000). Inference of population structure using multilocus genotype data. *Genetics*, *155*, 945–959.

Python Software Foundation. (2019). *Python Language Reference*. version 2.7.16. http://www.python.org.

R Core Team. (2019). *R: A language and environment for statistical computing*. R Foundation for Statistical Computing. https://www.R-project.org/

R Core Team (2022) *R: A language and environment for statistical computing.* R Foundation for Statistical Computing. https://www.R-project.org/

Réale, D., Garant, D., Humphries, M. M., Bergeron, P., Careau, V., & Montiglio, P. O. (2010). Personality and the emergence of the pace-of-life syndrome concept at the population level. *Philosophical Transactions of the Royal Society B: Biological Sciences*, *365*, 4051–4063. https://doi.org/10.1098/rstb.2010.0208

Réale, D., Martin, J., Coltman, D. W., Poissant, J., & Festa-Bianchet, M. (2009). Male personality, life-history strategies and reproductive success in a promiscuous mammal. *Journal of Evolutionary Biology*, *22*, 1599–1607. https://doi.org/10.1111/j.1420-9101.2009.01781.x

Réale, D., Reader, S. M., Sol, D., Mcdougall, P. T., & Dingemanse, N. J. (2007). Integrating animal temperament within ecology and evolution. *Biological Reviews*, *82*, 291–318. https://doi.org/10.1111/j.1469-185X.2007.00010.x

Rebelo, H., & Rainho, A. (2009). Bat conservation and large dams: Spatial changes in habitat use caused by Europe's largest reservoir. *Endangered Species Research*, *8*, 61–68. https://doi.org/10.3354/esr00100

Reed, D. H., & Frankham, R. (2003). Correlation between fitness and genetic diversity. *Conservation Biology*, *17*, 230–237. https://doi.org/10.1046/j.1523-1739.2003.01236.x

Reid, B. N., Mladenoff, D. J., & Peery, M. Z. (2017). Genetic effects of landscape, habitat preference and demography on three co-occurring turtle species. *Molecular Ecology*, *26*, 781–798. https://doi.org/10.1111/mec.13962

Reid, B. N., & Peery, M. Z. (2014). Land use patterns skew sex ratios, decrease genetic diversity and trump the effects of recent climate change in an endangered turtle. *Diversity and Distributions*, *20*, 1425–1437. https://doi.org/10.1111/ddi.12243

Reid, S. M., Wilson, C. C., Carl, L. M., & Zorn, T. G. (2008). Species traits influence the genetic consequences of river fragmentation on two co-occurring redhorse (Moxostoma) species. *Canadian Journal of Fisheries and Aquatic Sciences*, *65*, 1892–1904. https://doi.org/10.1139/F08-093

Roberts, J. H., Angermeier, P. L., & Hallerman, E. M. (2013). Distance, dams and drift: What structures populations of an endangered, benthic stream fish? *Freshwater Biology*, *58*, 2050–2064. https://doi.org/10.1111/fwb.12190

Rollinson, N., & Brooks, R. J. (2007). Proximate constraints on reproductive output in a northern population of painted turtles: An empirical test of the bet-hedging paradigm. *Canadian Journal of Zoology*, *85*, 177–184. https://doi.org/10.1139/Z07-002

Roth, T. C., Rosier, M., Krochmal, A. R., & Clark, L. (2020). A multi-trait, field-based examination of personality in a semi-aquatic turtle. *Ethology*, *126*, 851–857. https://doi.org/10.1111/eth.13030

Row, J. R., Knick, S. T., Oyler-McCance, S. J., Lougheed, S. C., & Fedy, B. C. (2017). Developing approaches for linear mixed modeling in landscape genetics through landscape-directed dispersal simulations. *Ecology and Evolution*, *7*, 3751–3761. https://doi.org/10.1002/ece3.2825

Rowe, J. W. (2003). Activity and movements of midland painted turtles (*Chrysemys picta marginata*) living in a small marsh system on beaver island. *Journal of Herpetology*, *37*, 342–353.

Rowe, J. W., Bunce, C. F., & Clark, D. L. (2014). Spectral reflectance and substrate color-induced melanization in immature and adult midland painted turtles (*Chrysemys picta marginata*). *Amphibia Reptilia*, *35*, 149–159. https://doi.org/10.1163/15685381-00002934

Rowe, J. W., & Dalgarn, S. F. (2010). Home range size and daily movements of midland painted turtles (*Chrysemys Picta Marginata*) in relation to body size, sex, and weather patterns. *Herpetological Conservation and Biology*, *5*, 461–473.

Rowe, J. W., Gradel, J. R., Bunce, C. F., & Clark, D. L. (2012). Sexual dimorphism in size and shell shape, and dichromatism of spotted turtles (*Clemmys guttata*) in Southwestern Michigan. *Amphibia Reptilia*, *33*, 443–450. https://doi.org/10.1163/15685381-00002847

Rudin, F. S., Simmons, L. W., & Tomkins, J. L. (2018). Social cues affect quantitative genetic variation and covariation in animal personality traits. *Evolution*, *73*, 540–553.

https://doi.org/10.1111/evo.13661

Rudin, F. S., Tomkins, J. L., & Simmons, L. W. (2018). The effects of the social environment and physical disturbance on personality traits. *Animal Behaviour*, *138*, 109–121. https://doi.org/10.1016/j.anbehav.2018.02.013

Rutz, C., Loretto, M. C., Bates, A. E., Davidson, S. C., Duarte, C. M., Jetz, W., Johnson, M., Kato, A., Kays, R., Mueller, T., Primack, R. B., Ropert-Coudert, Y., Tucker, M. A., Wikelski, M., & Cagnacci, F. (2020). COVID-19 lockdown allows researchers to quantify the effects of human activity on wildlife. *Nature Ecology and Evolution*, *4*, 1156–1159. https://doi.org/10.1038/s41559-020-1237-z

Saba, V. S., & Spotila, J. R. (2003). Survival and behavior of freshwater turtles after rehabilitation from an oil spill. *Environmental Pollution*, *126*, 213–223. https://doi.org/10.1016/S0269-7491(03)00192-1

Sanchez, E., & Refsnider, J. M. (2017). Immune activity, but not physiological stress, differs between the sexes during the nesting season in painted turtles. *Journal of Herpetology*, *51*, 449–453. https://doi.org/10.1670/16-175

Sapolsky, R. M., Romero, L. M., & Munck, A. U. (2000). How do glucocorticoids influence stress responses? Integrating permissive, suppressive, stimulatory, and preparative actions. *Endocrine Reviews*, *21*, 55–89. https://doi.org/10.1210/er.21.1.55

Schlaepfer, D. R., Braschler, B., Rusterholz, H. P., & Baur, B. (2018). Genetic effects of anthropogenic habitat fragmentation on remnant animal and plant populations: a meta-analysis. *Ecosphere*, *9*, e02488. https://doi.org/10.1002/ecs2.2488

Schmidt, C., Domaratzki, M., Kinnumen, R. P., Bowman, J., & Garroway, C. J. (2020). Continent-wide effects of urbanization on bird and mammal genetic diversity. *Proceedings Royal Society B*, *287*, 20192497. https://doi.org/10.1101/2020.08.16.253104

Schweitzer, C., Motreuil, S., & Dechaume-Moncharmont, F. X. (2015). Coloration reflects behavioural types in the convict cichlid, *Amatitlania siquia*. *Animal Behaviour*, *105*, 201–209. https://doi.org/10.1016/j.anbehav.2015.04.024

Seburn, D. C. (2015). Distribution of the exotic pond slider (*Trachemys scripta*) in Ontario. *Canadian Field-Naturalist*, *129*, 342–348. https://doi.org/10.22621/cfn.v129i4.1756

Selkoe, K. A., Scribner, K. T., & Galindo, H. M. (2015). Waterscape genetics - Applications of landscape genetics to rivers, lakes, and seas. In N. Balkenhol, S. A. Cushman, A. T. Storfer & L. P. Waits (Eds.). *Landscape Genetics: Concepts, Methods, Applications* (pp. 220–246). Wiley Blackwell. https://doi.org/10.1002/9781118525258.ch13

Selman, W., Qualls, C., & Owen, J. C. (2013). Effects of human disturbance on the behavior and physiology of an imperiled freshwater turtle. *Journal of Wildlife Management*, *77*, 877–885. https://doi.org/10.1002/jwmg.538

Semlitsch, R. D., & Bodie, J. R. (2003). Biological criteria for buffer zones around wetlands and riparian habitats for amphibians and reptiles. *Conservation Biology*, *17*, 1219–1228. https://doi.org/10.1046/j.1523-1739.2003.02177.x

Shaffer, H. B., Minx, P., Warren, D. E., Shedlock, A. M., Thomson, R. C., Valenzuela, N., Abramyan, J., Amemiya, C. T., Badenhorst, D., Biggar, K. K., Borchert, G. M., Botka, C. W., Bowden, R. M., Braun, E. L., Bronikowski, A. M., Bruneau, B. G., Buck, L. T., Capel, B., Castoe, T. A., …

Wilson, R. K. (2013). The western painted turtle genome, a model for the evolution of extreme
physiological adaptations in a slowly evolving lineage. *Genome Biology*, *14*, R28.
https://doi.org/10.1186/gb-2013-14-3-r28

Shaffer, H. B., Gidiş, M., McCartney-Melstad, E., Neal, K. M., Oyamaguchi, H. M., Tellez, M., &
Toffelmier, E. M. (2015). Conservation genetics and genomics of amphibians and reptiles.
*Annual Review of Animal Biosciences*, *3*, 113–138. https://doi.org/10.1146/annurev-animal-
022114-110920

Sigma-Aldrich (2016). *Wright-Giemsa Stain modified, Procedure: Dip Method (Rapid)*
https://www.sigmaaldrich.com/deepweb/assets/sigmaaldrich/product/documents/348/803/wg.pdf

Sih, A. (2004). Behavioural syndromes: An integrative overview. *The Quarterly Review of Biology*,
*79*, 241–277. https://doi.org/10.1086/422893

Sih, A. (2013). Understanding variation in behavioural responses to human-induced rapid
environmental change: A conceptual overview. *Animal Behaviour*, *85*, 1077–1088.
https://doi.org/10.1016/j.anbehav.2013.02.017

Sih, A., Ferrari, M. C. O., & Harris, D. J. (2011). Evolution and behavioural responses to human-
induced rapid environmental change. *Evolutionary Applications*, *4*, 367–387.
https://doi.org/10.1111/j.1752-4571.2010.00166.x

Slavenko, A., Itescu, Y., Ihlow, F., & Meiri, S. (2016). Home is where the shell is: Predicting turtle
home range sizes. *Journal of Animal Ecology*, *85*, 106–114. https://doi.org/10.1111/1365-
2656.12446

Smith, B. R., & Blumstein, D. T. (2008). Fitness consequences of personality: A meta-analysis.

*Behavioral Ecology*, *19*, 448–455. https://doi.org/10.1093/beheco/arm144

Spalding, B. (2020). *Painted turtle (Chrysemys picta) home range and habitat use in a dam impoundment*. [Senior Honors Thesis]. Eastern Michigan University.

Spear, M. J., Elgin, A. K., & Grey, E. K. (2018). Current and projected distribution of the red-eared slider turtle, *Trachemys scripta elegans*, in the great lakes basin. *American Midland Naturalist*, *179*, 191–221. https://doi.org/10.1674/0003-0031-179.2.191

Spotswood, E. N., Beller, E. E., Grossinger, R., Grenier, J. L., Heller, N. E., & Aronson, M. F. (2021). The biological deserts fallacy: Cities in their landscapes contribute more than we think to regional biodiversity. *BioScience*, *71*, 148–160. https://doi.org/10.1093/biosci/biaa155

Sprau, P., & Dingemanse, N. J. (2017). An approach to distinguish between plasticity and non-random distributions of behavioral types along urban gradients in a wild passerine bird. *Frontiers in Ecology and Evolution*, *5*, 92. https://doi.org/10.3389/fevo.2017.00092

Stacy, N. I., Alleman, A. R., & Sayler, K. A. (2011). Diagnostic hematology of reptiles. *Clinics in Laboratory Medicine*, *31*, 87–108. https://doi.org/10.1016/j.cll.2010.10.006

Stan Development Team (2023). *RStan: the R interface to Stan*. R package version 2.26.13. https://mc-stan.org/

Stanford, C. B., Iverson, J. B., Rhodin, A. G. J., Paul van Dijk, P., Mittermeier, R. A., Kuchling, G., Berry, K. H., Bertolero, A., Bjorndal, K. A., Blanck, T. E. G., Buhlmann, K. A., Burke, R. L., Congdon, J. D., Diagne, T., Edwards, T., Eisemberg, C. C., Ennen, J. R., Forero-Medina, G., Frankel, M., … Walde, A. D. (2020). Turtles and tortoises are in trouble. *Current Biology*, *30*, R721–R735. https://doi.org/10.1016/j.cub.2020.04.088

Stearns, S. C. (1989). Trade-offs in life-history evolution. *Function Ecology*, *3*, 259–268. https://doi.org/10.2307/2389364

Steen, D. A., Gibbs, J. P., Buhlmann, K. A., Carr, J. L., Compton, B. W., Congdon, J. D., Doody, J. S., Godwin, J. C., Holcomb, K. L., Jackson, D. R., Janzen, F. J., Johnson, G., Jones, M. T., Lamer, J. T., Langen, T. A., Plummer, M. V., Rowe, J. W., Saumure, R. A., Tucker, J. K., & Wilson, D. S. (2012). Terrestrial habitat requirements of nesting freshwater turtles. *Biological Conservation*, *150*, 121–128. https://doi.org/10.1016/j.biocon.2012.03.012

Steffen, J. E., Learn, K. M., Drumheller, J. S., Boback, S. M., & McGraw, K. J. (2015). Carotenoid composition of colorful body stripes and patches in the painted turtle (*Chrysemys picta*) and red-eared slider (*Trachemys scripta*). *Chelonian Conservation and Biology*, *14*, 56–63. https://doi.org/10.2744/ccab-14-01-56-63.1

Steven, R., Pickering, C., & Castley, J. G. (2011). A review of the impacts of nature based recreation on birds. *Journal of Environmental Management*, *92*, 2287–2294. https://doi.org/10.1016/j.jenvman.2011.05.005

Stevens, M., Párraga, C. A., Cuthill, I. C., Partridge, J. C., & Troscianko, T. S. (2007). Using digital photography to study animal coloration. *Biological Journal of the Linnean Society*, *90*, 211–237. https://doi.org/10.1111/j.1095-8312.2007.00725.x

Stewart, K., Mitchell, M. A., Norton, T., & Krecek, R. C. (2012). Measuring the level of agreement in hematologic and biochemical values between blood sampling sites in leatherback sea turtles (*Dermochelys coriacea*). *Journal of Zoo and Wildlife Medicine*, *43*, 719–725. https://doi.org/10.1638/2011-0045R.1

Stoffel, M. A., Nakagawa, S., & Schielzeth, H. (2017). rptR: Repeatability estimation and variance decomposition by generalized linear mixed-effects models. *Methods in Ecology and Evolution*, *8*, 1639–1644. https://doi.org/10.1111/2041-210X.12797

Su, G., Logez, M., Xu, J., Tao, S., Villéger, S., & Brosse, S. (2021). Human impacts on global freshwater fish biodiversity. *Science*, *371*, 835–838. https://doi.org/10.1126/science.abd3369

Su, J., Yan, Y., Song, J., Li, J., Mao, J., Wang, N., Wang, W., & Du, F. K. (2018). Recent fragmentation may not alter genetic patterns in endangered long-lived species: Evidence from taxus cuspidata. *Frontiers in Plant Science*, *871*, 1571. https://doi.org/10.3389/fpls.2018.01571

Sundberg, J. (1995). Female yellowhammers (*Emberiza citrinella*) prefer yellower males: A laboratory experiment. *Behavioral Ecology and Sociobiology*, *37*, 275–282. https://doi.org/10.1007/BF00177407

Sundqvist, L., Keenan, K., Zackrisson, M., Prodöhl, P., & Kleinhans, D. (2016). Directional genetic differentiation and relative migration. *Ecology and Evolution*, *6*, 3461–3475. https://doi.org/10.1002/ece3.2096

Sutherland, H. (2017). Great expectations for biopassage innovation in design of a turtle passage at gympie weir. *The Australian National Committee on Large Dams Incorporated*. https://www.ancold.org.au/?product=2017-great-expectations-for-biopassage-innovation-in-design-of-a-turtle-passage-at-gympie-weir

Svobodová, J., Gabrielová, B., Synek, P., Marsik, P., Vaněk, T., Albrecht, T., & Vinkler, M. (2013). The health signalling of ornamental traits in the grey partridge (*Perdix perdix*). *Journal of Ornithology*, *154*, 717–725. https://doi.org/10.1007/s10336-013-0936-5

Tablado, Z., & Jenni, L. (2017). Determinants of uncertainty in wildlife responses to human disturbance. *Biological Reviews*, *92*, 216–233. https://doi.org/10.1111/brv.12224

Teasdale, L. C., Stevens, M., & Stuart-Fox, D. (2013). Discrete colour polymorphism in the tawny dragon lizard (*Ctenophorus decresii*) and differences in signal conspicuousness among morphs. *Journal of Evolutionary Biology*, *26*, 1035–1046. https://doi.org/10.1111/jeb.12115

Thioulouse, J., Dray, S., Dufour, A.-B., Siberchicot, A., Jombart, T., & Pavoine, S. (2018). *Multivariate analysis of ecological data with ade4*. Springer.

Tobias, J. A., & Pigot, A. L. (2019). Integrating behaviour and ecology into global biodiversity conservation strategies. *Philosophical Transactions of the Royal Society B: Biological Sciences*, *374*, 20190012. https://doi.org/10.1098/rstb.2019.0012

Troscianko, J., & Stevens, M. (2015). Image calibration and analysis toolbox - a free software suite for objectively measuring reflectance, colour and pattern. *Methods in Ecology and Evolution*, *6*, 1320–1331. https://doi.org/10.1111/2041-210X.12439

Tucker, M. A., Böhning-gaese, K., Fagan, W. F., Fryxell, J. M., Moorter, B. Van, Alberts, S. C., Ali, A. H., Allen, A. M., Attias, N., Avgar, T., Bartlam-Brooks, H., Bayarbaatar, B., Belant, J. L., Bertassoni, A., Beyer, D., Bidner, L., van Beest, F. M. Van, Blake, S., Blaum, N., … Muller, T. (2018). Moving in the Anthropocene: Global reductions in terrestrial mammalian movements. *Science*, *369*, 466–469. https://doi.org/10.1126/science.aam9712

Tulloch, J. (1981). *The Rideau Canal: Defence, transport, and recreation* (vol 50). National Historic Parks and Sites Branch. Parks Canada.

Tuomainen, U., & Candolin, U. (2011). Behavioural responses to human-induced environmental

change. *Biological Reviews*, *86*, 640–657. https://doi.org/10.1111/j.1469-185X.2010.00164.x

Turcotte, A., Garant, D., & Blouin-Demers, G. (2023). Effects of human disturbance on risk-taking behavior in painted turtles. *Ethology*, *00*, 1–15. https://doi.org/10.1111/eth.13377

van Dijk, P. P. (2011). *Chrysemys picta* (errata version published in 2016). *The IUCN Red List of Threatened Species, 2011*, e.T163467A97410447. https://dx.doi.org/10.2305/IUCN.UK.2011-1.RLTS.T163467A5608383.en

Van Strien, M. J., Keller, D., & Holderegger, R. (2012). A new analytical approach to landscape genetic modelling: Least-cost transect analysis and linear mixed models. *Molecular Ecology*, *21*, 4010–4023. https://doi.org/10.1111/j.1365-294X.2012.05687.x

Ventura, D. F., De Souza, J. M., Devoe, R. D., & Zana, Y. (1999). UV responses in the retina of the turtle. *Visual Neuroscience*, *16*, 191–204. https://doi.org/10.1017/S0952523899162011

Vergeynst, J., Pauwels, I., Baeyens, R., Coeck, J., Nopens, I., De Mulder, T., & Mouton, A. (2019). The impact of intermediate-head navigation locks on downstream fish passage. *River Research and Applications*, *35*, 224–235. https://doi.org/10.1002/rra.3403

Verhelst, P., Baeyens, R., Reubens, J., Benitez, J. P., Coeck, J., Goethals, P., Ovidio, M., Vergeynst, J., Moens, T., & Mouton, A. (2018). European silver eel (*Anguilla anguilla* L.) migration behaviour in a highly regulated shipping canal. *Fisheries Research*, *206*, 176–184. https://doi.org/10.1016/j.fishres.2018.05.013

Vincze, E., Papp, S., Preiszner, B., Seress, G., Bókony, V., & Liker, A. (2016). Habituation to human disturbance is faster in urban than rural house sparrows. *Behavioral Ecology*, *27*, 1304–1313. https://doi.org/10.1093/beheco/arw047

Wagner, H. (2020). *LandGenCourse: Interface for course "Landscape genetic data analysis with R"*. R package version 1.4.4

Walls, S. C., & Gabor, C. R. (2019). Integrating behavior and physiology into strategies for amphibian conservation. *Frontiers in Ecology and Evolution*, *7*, 234. https://doi.org/10.3389/fevo.2019.00234

Walthers, A. R., & Barber, C. A. (2020). Traffic noise as a potential stressor to offspring of an urban bird, the european starling. *Journal of Ornithology*, *161*, 459–467. https://doi.org/10.1007/s10336-019-01733-z

Wang, J. C., Yang, C.-C., Liang, W., & Shi, H.-T. (2013). Spectra analysis reveals the sexual dichromatism of red-eared slider turtle (*Trachemys scripta*). *Dongwuxue Yanjiu*, *34*, 475–478. https://doi.org/10.11813/j.issn.0254-5853.2013.5.0475

Watson, K. W. (2006). *Engineered Landscapes*. Ken W. Watson.

Webster, M. M., & Rutz, C. (2020). How STRANGE are your study animals? *Nature*, *582*, 337–340. https://doi.org/10.1038/d41586-020-01751-5

Weir B. S., & Cockerham, C. C. (1984). Estimating F-statistics for the analysis of population structure. *Evolution*, *38*, 1358–1370. https://doi.org/10.2307/2408641

Wickham, H. (2016). *ggplot2: Elegant graphics for data analysis*. Springer.

Wilkin, T. A., Garant, D., Gosler, A. G., & Sheldon, B. C. (2006). Density effects on life-history traits in a wild population of the great tit *Parus major*: Analyses of long-term data with GIS techniques. *Journal of Animal Ecology*, *75*, 604–615. https://doi.org/10.1111/j.1365-2656.2006.01078.x

Willi, Y., Van Buskirk, J., Hoffmann, A. A., Buskirk, J. Van, & Hoffmann, A. A. (2006). Limits to the

    adaptive potential of small populations. *Annual Review of Ecology, Evolution, and Systematics*,

    *37*, 433–458. https://doi.org/10.1146/annurev.ecolsys.37.091305.110145

Willoughby, J. R., Sundaram, M., Lewis, T. L., & Swanson, B. J. (2013). Population decline in a long-

    lived species: The wood turtle in Michigan. *Herpetologica*, *69*, 186–198.

    https://doi.org/10.1655/HERPETOLOGICA-D-12-00033R2

Wilson, D. S., Tracy, C. R., & Tracy, C. R. (2003). Estimating age of turtles from growth rings: A

    critical evaluation of the technique. *Herpetologica*, *59*, 178–194. https://doi.org/10.1655/0018-

    0831(2003)059[0178:EAOTFG]2.0.CO;2

Wingfield, J. C. (2013). Ecological processes and the ecology of stress: The impacts of abiotic

    environmental factors. *Functional Ecology*, *27*, 37–44. https://doi.org/10.1111/1365-2435.12039

Wingfield, J. C., Hunt, K., Breuner, C., Dunlap, K., Fowler, G. S., Freed, L., & Lepson, J. (1997).

    Environmental stress, field endocrinology, and conservation biology. In J. R. Clemmons & R.

    Buchholz (Eds.), *Behavioral approaches to conservation in the wild* (pp. 95–131). Cambridge

    University Press.

Wong, B. B. M., & Candolin, U. (2015). Behavioral responses to changing environments. *Behavioral*

    *Ecology*, *26*, 665–673. https://doi.org/10.1093/beheco/aru183

WWF (2018). *Living Planet Report 2018: Aiming higher*.

    https://c402277.ssl.cf1.rackcdn.com/publications/1187/files/original/LPR2018_Full_Report_Spre

    ads.pdf

WWF (2022). *Living Planet Report 2022: Building a nature-positive society*. https://wwf.ca/wp-

content/uploads/2022/10/lpr_2022_full_report_en.pdf

Zellmer, A. J., Wood, E. M., Surasinghe, T., Putman, B. J., Pauly, G. B., Magle, S. B., Lewis, J. S.,
Kay, C. A. M., & Fidino, M. (2020). What can we learn from wildlife sightings during the
COVID-19 global shutdown? *Ecosphere*, *11*, e03215. https://doi.org/10.1002/ecs2.3215

Zera, A. J., & Harshman, L. G. (2001). The physiology of life history trade-offs in animals. *Annual
Review of Ecology and Systematics*, *32*, 95–126.
https://doi.org/10.1146/annurev.ecolsys.32.081501.114006

Zolderdo, A. J., Abrams, A. E. I., Lawrence, M. J., Reid, C. H., Suski, C. D., Gilmour, K. M., &
Cooke, S. J. (2023). Freshwater protected areas can preserve high-performance phenotypes in
populations of a popular sportfish. *Conservation Physiology*, *11*, coad004.
https://doi.org/10.1093/conphys/coad004

Zuur, A. F., Ieno, E. N., Walker, N. J., Saveliev, A. A., & Smith, G. M. (2009). *Mixed effects models
and extensions in ecology with R*. Springer.